PHYSICOCHEMICAL STUDIES OF A NOVEL ADJUVANT AND CONJUGATE VACCINES

A thesis submitted to the

UNIVERSITY OF CAPE TOWN

In fulfilment of the requirements for the degree of

DOCTOR OF PHILOSOPHY

by

PRISCILLA DARLING NAA-AHIMAH MENSAH

(MSc)

Department of Chemistry

University of Cape Town

Rondebosch 7701

South Africa

February 2010

To my Parents Samuel and Lucy for being my inspiration

TABLE OF CONTENTS

CHAPTER 2: Description of physicochemical techniques for the characterisation of adjuvant and vaccine components

CHAPTER 3: Characterisation of Pheroid™ and raw materials by NMR spectroscopy and Coulter Counter analysis

ACKNOWLEDGEMENTS

I wish to express my heartfelt gratitude to the following people for their invaluable assistance during the course of this thesis:

Associate Professor Neil Ravenscroft for his patience, encouragement and supervision, and for introducing me to the fascinating field of vaccine research,

Dr Meredith Hearshaw for the HPAEC-PAD chromatograms and generous assistance in the lab, and for proofreading this thesis,

Anne Grobler and Awie Kotze (North West University) for supplying the Pheroid™ raw materials, formulations and N_2O saturated water,

The Biovac Institute for providing all the Hib conjugates, capsular polysaccharide (PRP), tetravalent and pentavalent vaccines,

Noel Hendricks and Pete Roberts for recording all the NMR spectra,

Other members of the Bioanalytical and Vaccine Research group, past and present, especially Ronica Ramsout and Tanith-Lea Curtin for their moral support and friendship,

My parents and the rest of my family and friends for being my pillars of support, and always encouraging me to give my best.

CONFERENCES

Poster, 2007 Keystone symposia conference: T1 *"Challenges of Global Vaccine Development"*, October 2007

"Characterisation and evaluation of PheroidTM: a novel fatty acid-based adjuvant"

ABSTRACT

South African children currently receive vaccines against Diphtheria, Tetanus, Pertussis (administered as DTP), Hepatitis B (HBV) and *Haemophilus influenzae* type b (Hib) at 6, 10 and 14 weeks. The use of combination vaccines provides a means of avoiding the logistical problems and costs associated with multiple injections of these different vaccines. A local vaccine manufacturer is in the process of developing a combined tetravalent DTP-HBV as well as a liquid pentavalent DTP-HBV-Hib vaccine. The Hib vaccine is a glycoconjugate in which *Haemophilus influenzae* type b capsular polysaccharide (polyribosylribitolphosphate or PRP) is conjugated to a carrier protein. The conjugate is immunogenic in infants who have a higher risk of infection while the polysaccharide vaccine is not. The compatibility of the Hib antigenic component in the presence of the other antigens and adjuvant presents a challenge. Aluminium containing adjuvants have been the most widely used adjuvants in human vaccines. Aluminium hydroxide has been found to catalyse the hydrolysis of PRP when added to Hib conjugate vaccines. Although this can be circumvented by the use of aluminium phosphate, there is a need for new adjuvants that elicit broader immune responses. This thesis presents a study of the size, structure and composition of a locally developed experimental adjuvant called Pheroid™ by use of NMR spectroscopy and Coulter Counter. NMR analysis of Pheroid™ formulations provided a structural fingerprint for the formulations and indicated the relative proportions of the major components present, whereas their particle size distribution was profiled using a Coulter Counter. The average size distribution was similar in the formulations tested including those that had been activated using nitrous oxide.

The primary focus of this thesis was the application of appropriate physicochemical procedures for evaluation of the locally manufactured Hib vaccine alone and when in combination with DTP-HBV-Hib. Investigating the stability and integrity of Hib conjugate vaccines requires determination of the total saccharide and unbound or free saccharide which is expressed as the percentage of free saccharide present. In the absence of a suitable Hib conjugate, model compounds such as human serum albumin (HSA), meningococcal group A polysaccharide (PsA) and the derived conjugate (Mn A-TT) were used to investigate three methods of free saccharide separation: solid phase extraction (SPE), acid precipitation using deoxycholate (DOC/HCl) and ultrafiltration (UF). At physiological pH, the binding capacity was low and so the SPE method was not investigated further. For Mn A-TT the DOC/HCl method generally gave lower free

saccharide values than the UF method; this was attributed to entrapment and co-precipitation of free saccharide by DOC/HCl. In contrast, washing steps in the UF method ensured good free saccharide recovery. A colorimetric assay for phosphorus and high performance anion exchange chromatography with pulsed amperometric detection (HPAEC-PAD) were investigated for saccharide quantification in Mn A-TT vaccines. The HPAEC-PAD method for the monomer (mannosamine-6-phosphate from acid hydrolysis) permitted higher specificity and sensitivity for the free saccharide analysis compared to the phosphate assay. The DOC/HCl and UF methods were compared by their application to Mn A-TT samples subjected to an accelerated stability study.

The free saccharide assay methods developed for Mn A-TT were applied to the analysis of Hib-TT vaccines. Quantification of Hib was performed using the phosphate and ribose colorimetric assays and HPAEC-PAD analysis of the ribitol component (released by acid hydrolysis). The HPAEC-PAD method proved to be sensitive and specific and with the use of an internal standard (sorbitol), potentially applicable to the analysis of Hib in both monovalent and combination vaccines. This was tested on a Hib pentavalent vaccine containing sucrose formulated with Pheroid™ or aluminium-containing adjuvant and subjected to a thermal stability study. Poor free saccharide extraction by phosphate in the Pheroid™- and aluminium hydroxide-adjuvanted vaccines as well as interference from the sucrose excipient complicated the analysis. In the control pentavalent vaccine and aluminium phosphate-adjuvanted vaccine, the finding that the free saccharide assay could detect increasing amounts of free saccharide generated showed the potential of this method for these formulations. The free saccharide assay was applied to aluminium phosphate-adjuvanted Hib pentavalent liquid vaccines formulated without sucrose. Similar free saccharide values were obtained for Hib in the pentavalent formulation as determined for the monovalent Hib-TT vaccines. These results confirmed that without interference from sucrose, the free saccharide assay can be used to measure low levels of free saccharide in Hib combination vaccines containing aluminium phosphate adjuvant. The present study established that the application of the DOC/HCl method to Hib vaccines can be greatly improved by using a high ionic strength buffer. The use of a 50 kDa UF membrane gave free saccharide values comparable to the 100 kDa membrane, yielded good free saccharide spike recovery and <5 % protein was detected in the filtrate. Preliminary experiments showed fucose to be a better internal standard compared to sorbitol for the quantification of ribitol in Hib vaccines.

ABBREVIATIONS

ADH	Adipic acid dihydrazide
ALH	Aluminium hydroxide adjuvant
ALP	Aluminium phosphate adjuvant
$CDCl_3$	Chloroform (deuterated)
COSY	Correlation spectroscopy
d_6-DMSO	Dimethyl sulfoxide (deuterated)
DOC/HCl	Deoxycholic acid/Hydrochloric acid
DTP-HBV	Diphtheria, Tetanus, Pertussis and Hepatitis B (combined tetravalent vaccine)
DTP-HBV-Hib	Diphtheria, Tetanus, Pertussis, Hepatitis B and *Haemophilus influenzae* type b (combined pentavalent vaccine)
g	Gram(s)
GC-FID	Gas chromatography with flame ionisation detector
Hib	*Haemophilus influenzae* type b
Hib-TT	*Haemophilus influenzae* type b conjugated to tetanus toxoid
HMBC	Heteronuclear multiple bond correlation
HPAEC-PAD	High performance anion exchange chromatography with pulsed amperometric detection
HPLC	High performance liquid chromatography
HPSEC-UV	High performance size exclusion chromatography with ultraviolet detection
HSA	Human serum albumin
HSQC	Heteronuclear single quantum correlations
M6P	Mannosamine-6-phosphate
Mn A-TT	Meningococcal group A capsular polysaccharide conjugated to tetanus toxoid
min	Minute(s)
M	Molar
ND	Not detected
PEG	Poly(ethylene) glycol
PRP	Polyribosylribitolphosphate

PRP-ADH	Polyribosylribitolphosphate activated with adipic acid dihydrazide	
PsA	Polysaccharide A (meningococcal group A capsular polysaccharide)	
SPE	Solid phase extraction	
TFA	Trifluoroacetic acid	
TT	Tetanus toxoid	
UF	Ultrafiltration	
NMR	s	singlet
	d	doublet
	t	triplet
	q	quartet
	m	unresolved multiplet
	b	broad

CHAPTER 1

INTRODUCTION

1.1 Introduction to currently available (paediatric) combination vaccines

Immunisation remains the most effective weapon against infectious diseases[1]. The smallpox vaccine which led to eradication of smallpox worldwide is one of the most acclaimed victories of medical science[2]. Paralytic poliomyelitis has disappeared from the Americas, Europe, Australia and many countries on other continents, and represents the next target for worldwide eradication[3]. The introduction of conjugate vaccines against *Haemophilus influenzae* type b (Hib)[4], *Streptococcus pneumoniae*[5] and *Neisseria meningitidis*[6] has significantly reduced the number of cases due to these pathogens.

The rapid development of new technologies has helped to overcome technological barriers that used to limit vaccine development[7]. Gene-based vaccines for example are a new approach to immunisation and immunotherapy, in which, rather than a live or inactivated organism (or subunit thereof), one or more genes that encode proteins of the pathogen are delivered. The goal of this approach is to generate immunity against diseases for which traditional vaccines and treatments have not worked and to improve vaccines[8]. Protein-based approaches have been applied to produce vaccines against *B. pertussis*[9], *S. pneumoniae*[10], non-typeable *H. Influenzae*[11], and some viruses such as hepatitis B (HBV)[12], hepatitis C (HCV)[13], human immunodeficiency virus (HIV)[14] and human papilloma virus (HPV)[15].

Progress in vaccine development has resulted in an increase in the number of vaccine preventable diseases[16, 17]. There are currently 20 vaccines recommended for routine immunisation by the World Health Organisation (WHO)[18]. It will thus be difficult to add any new vaccines to an already overcrowded immunisation calendar for young children[1]. A solution to this problem is the combination of antigens that induce immunity against several diseases, into a multivalent vaccine[1, 2, 16-19]. A combination vaccine may therefore consist of two or more live organisms, inactivated organisms or purified antigens combined by a manufacturer or mixed immediately before administration[20]. Combining vaccines in this way spares patients the discomfort of multiple injections and also reduces some logistic costs linked to factors such as fewer clinic visits, syringes

and needles and a reduced requirement for cold storage of vaccines[21, 22]. Furthermore, when vaccines are given separately, there is greater capacity for missed doses, so combined vaccines can also increase compliance and therefore the overall effectiveness of vaccination programmes[21].

Combined vaccines that have been used for many decades include DTP (triple vaccine against diphtheria, tetanus and pertussis), trivalent oral (OPV) and injectable (IPV) polio, MMR (measles, mumps and rubella), trivalent influenzae, polyvalent pneumococcal and meningococcal vaccines[1, 4]. In recent years, vaccine manufacturers have used DTP as the corner stone on which to build more polyvalent vaccines. Concerns over safety has prompted a shift from use of the classical whole cell pertussis vaccine to acellular vaccines composed of purified antigens from *B. pertussis* believed to be involved in immunity[23]. More recently combination vaccines have been developed which contain six valencies (diphtheria, tetanus, acellular pertussis, IPV, *Haemophilus influenzae* type b (Hib) and hepatitis B[24, 25]) or seven valencies (Prevnar is a pneumococcal conjugate vaccine containing the seven vaccine-serotypes of *Streptococcus pneumoniae* – 4, 6B, 9V, 14, 18C, 19F and 23F)[26] Developing such a combined vaccine poses a number of challenges that will be discussed in the following section.

1.2 Development of combination vaccines

The development of combination vaccines involves considerable research and expense to ensure efficacy and safety. Each combination vaccine must be evaluated in preclinical and clinical trials to ensure antigen compatibility, immunogenicity and acceptable reactogenicity[27]. Various scientific, regulatory, public health and manufacturer issues are involved in determining which vaccines are combined and evaluated[28]. It is important to take all these issues into account as early as possible in the development programme because they are interrelated and such planning will maximise the probability of developing the final vaccine product in the shortest period of time[16].

Vaccines are complex mixtures that contain not only viral or bacterial antigens but also other components such as preservatives, adjuvants, buffers, salts and stabilisers such as gelatine and alditols[29]. The incompatibility of any of these components would compromise the safety or effectiveness of the vaccine[4, 20]. For example, the components

of inactivated vaccines may adversely affect one or more components of the active components. This occurred when whole-cell pertussis vaccine and inactivated poliovirus vaccine were combined, resulting in a combination with decreased pertussis potency[20]. For multi-disease combinations, excipients from one vaccine component may adversely affect the stability of other components. For instance, an antigen not adsorbed to aluminium adjuvant may be mixed with an aluminium-adsorbed antigen and itself become adsorbed or conversely, thereby changing its immunological properties. An exchange of antigens from one type of aluminium adjuvant to another may also occur[16]. As an example of the interaction of a preservative with a vaccine antigen, Sawyer and co-workers reported that thiomersal, used to preserve the DTwP vaccine, is detrimental to the IPV component in a DTwP-IPV combination vaccine[30]. Thus, not only should the combination be characterised and its components assessed through a series of physicochemical, biochemical and biological assays, but the formulation should also be optimised for its component antigens and their excipients[16, 20].

In multi-disease combinations, vaccines may be manufactured at different sites by different companies under different protocols, so it may be necessary to review the conformity of procedures and documentation for assuring regulatory acceptability[16]. Preclinical animal trials must be conducted to determine the consequences of combination on potency and immunogenicity[20]. It is also necessary to demonstrate consistency at the level of both manufacturing and clinical trials[2, 20].

Prior to licensure, clinical studies are conducted to demonstrate the safety, immunogenicity and efficacy of a new vaccine with evaluation of simultaneous administration with other licensed vaccines[29]. For multi-disease combinations, this implies that the combination is at least as well tolerated as its component vaccines given separately[17, 21, 23, 31-36]. For example DTP-Hib (combined) vs. DTP + Hib (separate). Administration of the new vaccine simultaneously with other vaccines given to the same age-group is evaluated to assure that there is no interference with such vaccines[16]. The effectiveness of a biological product is defined as the clinically significant prevention of disease in a significant proportion of the target population, with proof of effectiveness consisting of controlled investigations[37].

For some antigens, studies of vaccine efficacy and immunogenicity have identified correlations between levels of antibody and protection from disease (called a serologic correlate)[27, 38]. Correlates of protection have been established by identifying an antibody level above which the majority of a population is protected from disease[37]. If a combination vaccine produces serologic results for a particular antigen that are significantly lower than those seen in the monovalent vaccine but are nonetheless greater than the level known to provide clinical protection throughout the period of risk, then the diminished immunogenicity would not alter the acceptability of the combination vaccine[38].

The regulatory process consists of a logical progression from preclinical testing through phase I, II and III studies, to post-licensure or phase IV studies[37]. During phase I, the initial safety and immunologic activity of a combination is evaluated in a small number of subjects which may not comprise the final target population. The sample size in phase II is increased to include several hundred individuals. In the case of new combination vaccines, phase II includes assessment of the immunogenicity of all antigens contained in the combination. It may also provide initial evaluation of the immune response to other vaccines administered in the same schedule as the combination[38]. These studies will be able to determine any common adverse events in the combination compared to monovalent vaccines[2]. In addition, phase II studies evaluate whether the immune response to any antigen in the combination vaccine is decreased before proceeding with large-scale pivotal safety and efficacy studies. Data collected to this point will be used to determine whether progression to larger phase III studies is justified. It will also form the basis for formulating safety and immunogenicity endpoints for pivotal studies. In phase III the sample size is generally larger – hundreds to several thousand subjects in multiple centres from different ethnic and geographic backgrounds. It enables acquisition of additional information on safety and effectiveness which if found to be satisfactory will lead to the vaccine being licensed[38]. Even after licensure clinical studies continue as manufacturers are usually asked to commit to completing specific post marketing or phase IV studies in large numbers of vaccine recipients[29]. These studies will provide additional assessment of rare adverse events or further assess the duration of vaccine-induced immunity[29].

Commercial companies usually coordinate and finance the developmental work and extensive clinical testing that is required before a combined vaccine can be approved for routine use[1]. The decision to develop any particular combined vaccine will therefore be influenced not only by its medical desirability and technical feasibility but also by the potential financial returns that the required investments in time and resources may bring to the company[1]. Despite the fact that an increasing number of diseases can be prevented by vaccination[39], the potential for disease control offered by vaccines is not being fully realised in the world[1, 40]. In the developing world, inadequacies in vaccine delivery, communication and transportation infrastructures are generally the most relevant problems[41]. Added to this is the fact that vaccine efficacy can vary markedly in different host populations perhaps due to nutritional inadequacies or prior contact with antigens contained within the vaccine[42]. In the developed world, there has been heightened parental concern about combination vaccines following reports by Wakefield and co-workers which suggested that MMR immunisation was associated with autism, inflammatory bowel disease and diabetes[43]. Their interpretation was based on the reports by parents or general practitioners of 12 children that symptoms were observed soon after MMR immunisation. Still, the article showed only a temporal association and no evidence of causation[44]. Since then, several agencies have established the safety of licensed MMR vaccines[45-48] and over 500 million children worldwide have received MMR vaccine since its licensure in 1971[49].

There is no doubt that developing a new combination vaccine presents unique challenges to both manufacturers and regulatory authorities, however, success is attainable if both parties cooperate.

1.3 Role of adjuvants in vaccines

Live attenuated vaccines such as those against measles, mumps and tuberculosis are very effective because they multiply in the body thereby inducing a large immune response. However, the disadvantage of these live attenuated vaccines is their potential to mutate back to the virulent form at any time. Such mutation would result in induction of the disease rather than in protection against it. For this reason, attenuated vaccines are not recommended for use in immunocompromised individuals. Many new vaccines or vaccine candidates are purified, subunit and synthetic vaccines which are poorly immunogenic and thus stimulate a lower level and shorter duration of immunity than that

elicited by live vaccines[50-52]. Thus, there is a need for immunomodulatory adjuvants that will render these vaccines sufficiently immunogenic.

Nearly 80 years ago the French scientist Ramon discovered helper substances, known as adjuvants, which when added to a vaccine, significantly increased the level of protection afforded by the vaccine[51]. In the years that followed, many adjuvant formulations have been developed among them mineral salts, emulsions, saponins, liposomes, microparticles, small molecules, nucleic acids and bacterial products[53-57]. Immunological adjuvants can be defined as compounds that bias the immune system toward Th1 or Th2 immunity and significantly enhance the immune response against an antigen[58].

The ideal adjuvant should fulfill all of the following requirements:

- Is non-toxic or has a negligible toxicity at the dose range for effective adjuvanticity
- Stimulates a strong humoral and/or T cell immune response
- Provides good immunological memory or long-term immunity
- Does not induce autoimmunity
- Is non-mutagenic, carcinogenic or teratogenic
- Is non-pyrogenic
- Is stable under broad ranges of storage time, temperature and pH[58].

As such, it will produce a protective immune response even with weak antigens such as polysaccharide-protein conjugates with lower doses of antigen and with fewer injections and will be effective in infants and young children, ideally at birth, and elicit high affinity antibodies. In reality, the above requirements are rarely met and thus, the availability of suitable adjuvants is limited. Currently, although aluminium-containing adjuvants are the most widely used adjuvants they do not meet all the above criteria and hence the motivation for finding better adjuvants[57, 58].

MF59 is a squalene-based oil-in-water emulsion that was licensed for a flu vaccine formulation (Fluad) a decade ago. More recently, AS03, another oil-in water emulsion, was approved as a component of a pre-pandemic H5N1 vaccine (Prepandrix). A

combination of two adjuvants, monophosphoryl lipid A (MPL) and aluminium hydroxide, namely AS04, was approved for use in HBV (Fendrix) and HPV (Cervarix) vaccines[55].

Adjuvants can be divided into three classes based on their properties. The first group of adjuvants, referred to as **vehicles**, consist of a two-phased system that can transport antigens from injection sites to lymphoid tissues and includes mineral oil emulsions (e.g. incomplete Freund's adjuvant), biodegradable oil emulsions (e.g. emulsions containing peanut oil or squalene), non-ionic block copolymer surfactants, liposomes and biodegradable polymer microspheres[58, 59]. **Carriers** are the second type of adjuvants. A carrier is a molecule which when bound to a second antigen, greatly intensifies the immune response to the latter[58]. Included in this category are bacterial toxoids, outer membrane proteins, fatty acids and live vectors[58, 59]. **Immunomodulators** are the third type of adjuvants. Immunomodulation is the ability of an adjuvant to modify the cytokine network and includes aluminium salts, saponin, muramyl di- and tripeptides, monophophoryl lipid A, *Bordetella pertussis* and cytokines, to mention a few[59]. Their mode of action is discussed in further detail in the following section.

1.4 Mode of adjuvant action

One mechanism by which adjuvants exert their effects is depot formation, where antigens and adjuvants are sequestered at the injection site and released over time to stimulated antigen-presenting cells (APCs), such as macrophages and dendritic cells (DCs)[58]. Short term depots are produced by aluminium salts and water-in-oil emulsions, where antigen is trapped at the injection site and therefore cannot be lost by liver clearance[60]. More recently, long term depots have been achieved using synthetic polymers such as polylactide-co-glycolide (PLG) to produce microspheres which degrade to yield a pulsed delivery[61, 62].

Targeting is the mechanism by which an adjuvant-antigen complex is delivered to antigen-presenting cells for processing – particulate adjuvants bind to antigens forming aggregates that are engulfed by APCs via endocytosis to form endosomes[53, 58]. Studies have demonstrated that particles of 1-10 μm can be delivered orally to optimise uptake of Peyer's patches[61]. More effective targeting is achieved using adjuvants with residues that are recognised by receptors on antigen-presenting cells. For example, the macrophage mannose receptor is an endocytic pattern-recognition receptor (PRR) that

binds compounds containing mannose (e.g. mannans), N-acetylglucosamine or fucose residues (e.g. some saponins) and sulfated oligosaccharides. Binding of these adjuvant-antigen complexes to pattern-recognition receptor initiates efficient receptor-mediated endocytosis and antigen processing[58].

1.4.1 Innate immunity

The immune system is divided into innate and adaptive components. The main distinction between the two lies in the mechanisms and receptors used for immune recognition (Fig 1). The adaptive component is organised into T cells and B cells. Each clonal receptor in both T and B cells is structurally unique and not encoded in the germ line. Binding of an antigen to its receptor triggers activation and proliferation of the cell. This process of clonal selection and expansion is essential for the generation of an effective immune response[63]. However, it takes 3-5 days for a sufficient number of clones to be produced and to differentiate into effector cells. In contrast, the effector mechanisms of innate immunity, which include antimicrobial peptides, phagocytes and the alternative complement pathway, are activated immediately after infection and rapidly control the replication of the infecting pathogen[63].

The strategy of the innate immune response is to focus on a few highly conserved structures present in large groups of microorganisms. These structures are known as Pathogen-Associated Molecular Patterns (PAMPs), and the receptors that recognise them are called Pattern Recognition Receptors (PRRs). For example, bacterial polysaccharide, peptidoglycans, lipoteichoic acid and bacterial DNA are bound by germline-encoded pattern recognition receptors [58, 63]. Structurally, pattern recognition receptors belong to several families of proteins. Leucine-rich repeat domains, calcium-dependent lectin domains and scavenger-receptor protein domains, for example, are often involved in pattern recognition[63]. These pattern recognition receptors can be (a) secreted molecules found in blood and lymph that are associated with complement and opsonisation, (b) surface receptors on phagocytic cells that are associated with endocytosis, or (c) toll-like receptors (TLRs), a family of receptors found on macrophages, dendritic cells and epithelial cells that have been conserved from insects to mammals[64]. Toll-like receptors are transmembrane proteins with an extracellular domain containing leucine-rich repeats that recognise conserved motifs on pathogens, and a cytoplasmic domain similar to the corresponding domain of the interleukin-1 (IL-1)

receptor[64, 65]. Toll-like receptors induce signalling pathways, leading to activation of the nuclear factor-κB (NF-κB) in antigen presenting cells, which results in the expression of various cytokine genes, production of co-stimulatory ligands B7-1 (CD80) and B7-2 (CD86), and activation of adaptive imunity[63, 65]. It is the initial response of the innate immune system, stimulated by pathogen-associated molecular patterns, that triggers and controls the adaptive immune system response[58]. The binding of pathogen-associated molecular patterns, such as lipopolysaccharide or bacterial CpG-DNA, initiating the activation of adaptive immunity, is indicative of their adjuvant effect acting via specific toll-like receptors. Indeed several natural or synthetic adjuvants, including monophosphoryl lipid A and lipoarabinomannan, that are bacterial cell-wall components, or the yeast polysaccharide glycan, are structurally closely related to different pathogen-associated molecular patterns[58, 66]. The receptors involved in the interplay of the innate and adaptive immune systems are shown in Fig 1.1.

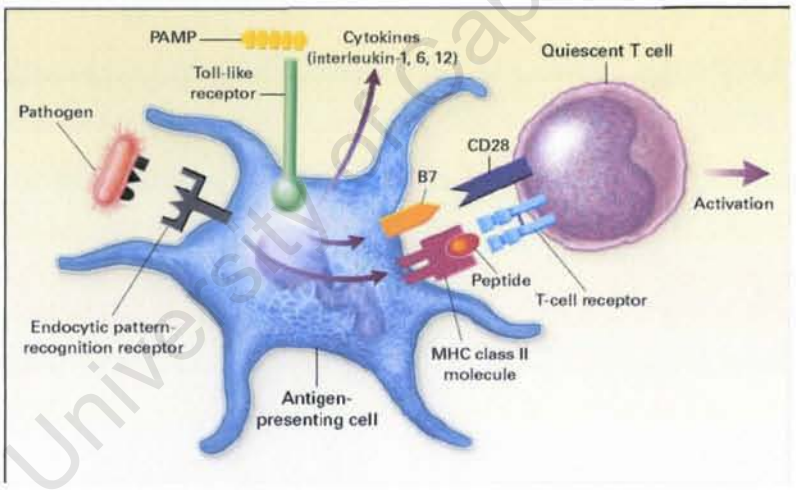

Fig 1.1: *Recognition of the pathogen-associated molecular pattern (PAMP) by pattern-recognition receptors, such as the toll-like receptors, generates signals that activate the adaptive immune system. Proteins derived from the microorganisms are processed in the lysosomes to generate antigenic peptides, which form a complex with major-histocompatibility-complex (MHC) class II molecules on the surface of antigen presenting cells. These peptides are recognized by T-cell receptors. In the case of the signaling class of pattern-recognition receptors, the recognition of pathogen-associated molecular patterns by toll-like receptors leads to the activation of signaling pathways that induce the expression of cytokines, chemokines, and costimulatory molecules. Therefore, pattern-recognition receptors have a role in the generation of both the peptide–MHC-molecule complex and the costimulation required for the activation of T cells*[63].

1.4.2 Adaptive immunity

Processing and presentation of protein antigens by antigen-presenting cells to T or B cells is dependent on whether the antigen is intracellular (endogenous) or extracellular (exogenous)[67]. Endogenous antigens (e.g. viral antigens produced or delivered into the cell cytosol) are degraded into small peptides which are transported into the endoplasmic reticulum (ER) and loaded onto the Major Histocompatibility Complex (MHC) class I, to form MHC-I-peptide complexes. These complexes are exported via the Golgi apparatus to the antigen-presenting cell surface for presentation and binding to CD8+ T cells, containing both T cell receptors (TCRs) and CD8 molecules that recognise both the MHC-I-peptide complexes and CD8 receptors on the antigen-presenting cell, respectively[58]. Exogenous antigens (e.g. bacteria) are taken up by antigen-presenting cells via endocytosis and degraded in the lysosomes into small peptides, bound by MHC class II molecules that are embedded in the lysosome membrane to form MHC-II-peptide complexes and delivered by exocytosis to the cell membrane for presentation to CD4+ T cells. Certain adjuvants such as amphipathic non-ionic block copolymers, bind to exogenous antigens, preserving their three-dimensional conformation (required for the production of neutralising antibodies) during the internalisation by antigen presenting cells[53, 68]. Depending on their size and the balance of hydrophilic (polyethylene) to lipophilic (polyoxypropylene) chains, block polymers can deliver exogenous antigens to the class I (cytoplasm) or class II (phagosomes) pathways for processing; they are effective antigen delivery systems that can be used with other adjuvants[52, 58].

1.4.3 T-cell activation

CD4+ and CD8+ T cells recognise antigens that are present on antigen-presenting cells as complexes with MHC class II or I, respectively. The process mediated by the T cell receptors leads to T cell activation and the production of effector cells that are capable of secreting cytokines[67]. Two signals are necessary for T cell activation, one is derived from the interaction of the T cell receptors with the antigen-MHC complex and the other is the co-stimulatory signal delivered by the B7-1 or B7-2 ligand, present on the antigen-presenting cells, to the CD28 receptor on T cells. Several studies indicate that B7-1 signals preferentially promote development of Th1 cells and B7-2 signals, Th2 cells[68-73]. This co-stimulatory signal provides an avenue for immune stimulation by adjuvants that can substitute for the B7-1 or B7-2 ligands[74]. Activated T cells produce two major types of effector cells: helper (Th) and cytotoxic (Tc) cells, derived from CD4 and CD8 cells,

respectively. CD4 cells interact with antigen-presenting cells carrying MHC-II-antigen complexes to yield Th1 or Th2 cells. This selection appears to depend on the origin of the activated dendritic cell that interacts with the CD4 cell. Th1 cells produce pro-inflammatory cytokines, such as interferon gamma, interleukin-2 and tumour necrosis factor β (TNF- β), and stimulates production of cytotoxic T lymphocytes (CTL). Th2 cells produce interleukin-4 and interleukin-10 cytokines that favour antibody production and class-switching, and also inhibit Th cells from entering the Th1 path[75]. Presentation by antigen-presenting cells of MHC-I-antigen complexes to CD8+ T cells results in activation of CD8 cells to produce cytotoxic T lymphocytes; following recognition of MHC-I-antigen complexes, cytotoxic T lymphocytes bind to target T cells and insert perforins into their cell membrane, delivering granzymes into the cell cytoplasm and initiating a process leading to cell apoptosis[58, 76].

For an adjuvant to be useful for induction of cytotoxic T lymphocytes, it must facilitate incorporation or persistence of an appropriate peptide into MHC-1. The most effective way to achieve this is for the adjuvant to interact in some way with cell membranes so that antigen associated with the adjuvant is deposited within the cytosol in a form suitable for normal processing in the proteosome[53]. An alternative mechanism for induction of cytotoxic T lymphocytes is by direct attachment of peptide to empty externally exposed MHC-1. In this instance, a water-in-oil (w/o) formulation is prepared in which the aqueous phase contains peptide and a universally recognised protein such as tetanus toxoid[77]. The water-in-oil emulsion creates a depot which, in addition to attracting dendritic cells, protects the peptide from proteolysis[53]. The tetanus toxoid will cause dendritic cells to migrate to lymphoid tissue and, while presenting tetanus-derived peptides, T-cells will be attracted, some of which will be cytotoxic T-cells (Tc) which recognise the original peptide derived from cytotoxic T lymphocytes[53]. The ability of adjuvants to preserve the conformational integrity of an antigen and present it to the appropriate antigen-presenting cells has three major benefits. Firstly it maximises the amount of conformationally relevant antibody, secondly it influences the affinity of the antibody and thirdly it can influence the duration of the immune response[78].

Understanding the different ways in which an adjuvant functions at a molecular level is important because if the pathogenesis of a disease is known, an adjuvant which can generate an appropriate protective immune response can be selected for vaccine

respectively. CD4 cells interact with antigen-presenting cells carrying MHC-II-antigen complexes to yield Th1 or Th2 cells. This selection appears to depend on the origin of the activated dendritic cell that interacts with the CD4 cell. Th1 cells produce pro-inflammatory cytokines, such as interferon gamma, interleukin-2 and tumour necrosis factor β (TNF- β), and stimulates production of cytotoxic T lymphocytes (CTL). Th2 cells produce interleukin-4 and interleukin-10 cytokines that favour antibody production and class-switching, and also inhibit Th cells from entering the Th1 path[75]. Presentation by antigen-presenting cells of MHC-I-antigen complexes to CD8+ T cells results in activation of CD8 cells to produce cytotoxic T lymphocytes; following recognition of MHC-I-antigen complexes, cytotoxic T lymphocytes bind to target T cells and insert perforins into their cell membrane, delivering granzymes into the cell cytoplasm and initiating a process leading to cell apoptosis[58, 76].

For an adjuvant to be useful for induction of cytotoxic T lymphocytes, it must facilitate incorporation or persistence of an appropriate peptide into MHC-1. The most effective way to achieve this is for the adjuvant to interact in some way with cell membranes so that antigen associated with the adjuvant is deposited within the cytosol in a form suitable for normal processing in the proteosome[53]. An alternative mechanism for induction of cytotoxic T lymphocytes is by direct attachment of peptide to empty externally exposed MHC-1. In this instance, a water-in-oil (w/o) formulation is prepared in which the aqueous phase contains peptide and a universally recognised protein such as tetanus toxoid[77]. The water-in-oil emulsion creates a depot which, in addition to attracting dendritic cells, protects the peptide from proteolysis[53]. The tetanus toxoid will cause dendritic cells to migrate to lymphoid tissue and, while presenting tetanus-derived peptides, T-cells will be attracted, some of which will be cytotoxic T-cells (Tc) which recognise the original peptide derived from cytotoxic T lymphocytes[53]. The ability of adjuvants to preserve the conformational integrity of an antigen and present it to the appropriate antigen-presenting cells has three major benefits. Firstly it maximises the amount of conformationally relevant antibody, secondly it influences the affinity of the antibody and thirdly it can influence the duration of the immune response[78].

Understanding the different ways in which an adjuvant functions at a molecular level is important because if the pathogenesis of a disease is known, an adjuvant which can generate an appropriate protective immune response can be selected for vaccine

formulation[53]. The following section focuses on aluminium adjuvants as well as alternative adjuvants currently being developed for use in human vaccines.

1.5 Adjuvants used in human vaccines

In recent years, researchers have gained a better understanding of the molecular basis for the action of adjuvants, the role of cytokines and different types of cells involved in the immune response. This has led to development of adjuvants which can selectively modulate the immune response and even selectively elicit T-cells only. This basic knowledge is important for developing suitable vaccines for emerging diseases such as AIDS and/or for new vaccine candidates against infectious agents, cancer, fertility, allergic and autoimmune diseases[57]. It is likely that because of their excellent track record of safety, aluminium adjuvants will continue to be used with current human vaccines. However, aluminium adjuvants cannot elicit cell-mediated immune responses such as cytotoxic T-cell responses and therefore there is a need for alternative adjuvants; particularly for diseases for which cell-mediated immune responses are important for prevention or cure[57]. Recently, several adjuvant formulations such as QS-21[79], MF-59[80], MPL-based adjuvants[81, 82], liposomes[83] and biodegradable polymer microspheres[84] and a strategy for making combination protein-polysaccharide conjugate vaccines have been described. Thus, it appears that the range of adjuvants accepted for human vaccines will expand in the years to come.

1.5.1 Aluminium compounds

The ability of aluminium compounds to act as an adjuvant was first reported by Glenny and co-workers in 1926[85]. These authors reported that the addition of potassium alum to diphtheria toxoid resulted in the formation of a precipitate. Injecting this precipitated diphtheria toxin into guinea pigs resulted in a higher antigenic response compared to the fluid toxoid[86, 87]. The range of aluminium compounds which have since been investigated for their adjuvant properties include aluminium chloride which has been used in antisera against cobra venom[88, 89]. Fujimaki and co-workers have investigated the role of aluminium silicate in inducing an IgE response[90]. Other aluminium-based adjuvant preparations which have been studied include gamma inulin complexes with aluminium hydroxide, known as Algammulin[91, 92] and aluminium monostearate[93, 94], used as a co-stabiliser in Adjuvant-65. Here, the aim of the aluminium compound is to allow formation of a water-in-oil emulsion between triglyceride oil and mannide monooleate.

CHAPTER 1

The most commonly used forms of aluminium adjuvant in vaccines include aluminium hydroxide, aluminium phosphate and alum ($KAl(SO_4)_2.12H_2O$)[87]. Aluminium hydroxide is a crystalline aluminiumoxyhydroxide that is positively charged at physiological pH. Aluminium phosphate is an amorphous aluminium hydroxyphosphate which is negatively charged at physiological pH[95]. Aluminium-based adjuvants were the first adjuvants to be approved for use in human vaccines[52].

Aluminium hydroxide and aluminium phosphate adjuvants are generally prepared by exposing aqueous solutions of aluminium ions to alkaline conditions under very controlled circumstances, which in the case of aluminium phosphate takes place in the presence of phosphate ions. Various soluble aluminium salts can be used for the production of these adjuvants, but the experimental conditions - temperature, concentration and even rate of addition of reagents – strongly influence the results[87]. Alhydrogel™ is a commercially available preparation which was chosen in 1988 as a research standard[87].

The original model proposed for aluminium hydroxide was based on a six-membered ring-structure, each member consisting of Al^{3+} surrounded by six coordinated water molecules in an octahedral shape[96]. The coordinated water molecules are oriented with the oxygen toward the aluminium ion. The high charge of Al^{3+} is believed to enhance the removal of protons, especially under alkaline conditions[96]. The alkaline conditions assist deprotonation leading to the initial formation of dimers by dihydroxyl bridges between octahedrons and later to the formation of the six-membered ring structure and even larger structures. In this process the ratio of aluminium to hydroxide approaches 1:3[97]. The above model is a generalised one that does not take into consideration the crystalline forms or inclusion of other ions. When inclusion of other ions originating from the salts used in the preparation was taken into consideration, aluminium hydroxide precipitated from aluminium chloride was described as $Al(OH)_{2.55}(Cl)_{0.45}$, existing as a polymer of ten fused six-membered rings. However, if precipitated from aluminium sulphate the adjuvant exists as $Al(OH)_{2.30}(SO_4)_{0.35}$ and is based on three fused six-membered rings[96].

Aluminium adjuvants have been used primarily in human vaccines for tetanus, diphtheria[98], pertussis[99-102] and poliomyelitis vaccines, some but not all Hib vaccines and

hepatitis A and hepatitis B virus vaccines[87]. Other vaccines containing aluminium include lyme disease, anthrax and rabies[103]. The immunostimulating effect of aluminium adjuvants has been attributed to the formation of a depot at the injection site from which the antigen is slowly released. In a Cynomolgus monkey model, alum was detected in the muscle up to 6 months after intra-muscular injection of a DT-TT vaccine and it was hypothesised that the alum-adsorbed antigen could also persist longer than if it was administered alone[104]. However, the depot effect has been questioned by Holt who demonstrated that the excision of the DT-alum treated site soon after subcutaneous vaccination did not change the immune response to the antigen[105]. Another study showed that ^{14}C-labelled TT is released very rapidly from the alum complex at the injection site[106]. Furthermore, it has been proposed that antigens adsorbed to alum are presented in a particulate multivalent from, which is more immunogenic and more efficiently internalised by antigen-presenting cells. *In vitro* experiments lent support to this model and showed that although dendritic cells can engulf antigens in solution through macropinocitosis, they are more efficient in internalising alum-adsorbed antigens through phagocytosis in a process dependent on the size of the aggregate[57, 104, 107-109]. Other suggested mechanisms of alum adjuvanticity include the activation of the complement cascade and the generation of a local inflammatory environment at the injection site characterised by the recruitment of blood cells[110, 111].

Recent studies on alum have demonstrated that besides antigen delivery functions, these classes of adjuvants can also activate innate immunity pathways *in vivo*, generating an immunocompetent environment at the injection site. The molecular target for alum pro-inflammatory activity has been identified as NOD-like receptor protein 3 (NLRP3)[55, 112]. Phagocytosis of alum crystals induced phagosomal swelling, destabilisation and rupture, finally resulting in the release of lysosomal proteins into the cytosol. Cathepsin B, a lysosomal protease, was shown to be involved in caspase 1 activation and interleukin-1β release in macrophages in response to alum and silica. These results suggested that phagosome destabilisation preceded the activation of the NLRP3 inflammasome[112].

A major advantage of aluminium adjuvants is the development of earlier, higher and longer-lasting immunity after primary immunisation compared to soluble vaccines[57]. In addition, there is a 70-year history of safe and effective use of aluminium salts in

vaccines which continue to save millions of lives annually[103]. The ability of the body to eliminate aluminium-containing adjuvants may contribute to the excellent safety record of these adjuvants[113]. Some adverse reactions have been reported with aluminium containing vaccines, but none of these reactions have been sufficiently frequent to arouse concern[98, 114-117].

There are certain instances where the use of aluminium adjuvants is not ideal. For example, aluminium adjuvants are ineffective when used with typhoid vaccines[118] and influenza haemagglutinin antigen[119]. Moreover, the the inability of aluminium adjuvants to elicit cell mediated immune responses, particularly cytotoxic T cell responses[53], may be a significant limitation for vaccines against intracellular parasites and viral infections such as human immunodeficiency virus (HIV)[57]. Studies on booster injections, conducted over a 10-year period, revealed that children who received aluminium-based vaccines were more prone to have local reactions such as redness, swelling and itching compared to those who received the unadsorbed vaccines for primary immunisation. This is because aluminium adjuvants increase the production of IgE antibodies and may promote IgE mediated allergic reactions[120]. Other limitations stem from the fact that as inducers of Th2 type responses, aluminium adjuvants are not likely to provide protection against diseases for which Th1 immunity and MHC class I restricted cytotoxic T cells are essential for protection e.g. with tuberculosis[121]. Studies have indicated that aluminium adjuvants are ineffective in raising high antibody titres against small-sized peptides[122]. It is possible that they cause the antigens to be proteolytically degraded more efficiently thus causing these peptides to lose their antigenicity[87]. In the case of foot-and-mouth disease aluminium adjuvants result in the partial degradation of epitopes due to adsorption[123]. Conjugation of the peptide to a carrier prior to adsorption helps overcome this problem[123]. Aluminium hydroxide when added to *Haemophilus influenzae* type b (Hib) conjugate vaccine has been found to result in catalytic depolymerisation of polyribosylribitolphosphate (PRP) which is the active ingredient in the vaccine[124]. There is thus a need for alternative adjuvants, especially for diseases in which cell-mediated immune responses are required for prevention or cure[125].

1.5.2 Calcium compounds

Calcium phosphate adjuvant was developed at the Pasteur Institute and is a viable alternative to aluminium adjuvants. In addition to having similar adjuvant properties to aluminium adjuvants, calcium phosphate has the added advantages of being a natural component of the body and of not increasing IgE production[125]. It is used to potentiate the immune response of vaccines in two ways[126]. Firstly, the depot mechanism allows the antigen to be adsorbed during the preparation of the vaccine and slowly released following injection. Secondly, it presents the adsorbed antigen to APCs as a particulate antigen[53]. The chemical structure of calcium phosphate has been investigated by X-ray diffraction, Fourier-transform infrared spectroscopy and thermal analysis[126]. The Ca/P molar ratio obtained identified commercial calcium phosphate adjuvant as a non-stoichiometric hydroxyapatite complex, $Ca_{10-x}(HPO_4)_x(PO_4)_{6-x}(OH)_{2-x}$, where x varies from 0 to 2[126]. At physiological pH, it is negatively charged and electrostatically adsorbs positively charged antigens. In addition, the presence of hydroxyls allows calcium phosphate adjuvant to adsorb phosphorylated antigens by ligand exchange with surface hydroxyls[126].

1.5.3 Oil emulsions

The first oil emulsion to be used as an adjuvant was Freund's complete adjuvant (FCA), which consisted of mineral (paraffin) oil mixed with killed Mycobacteria[54, 57]. Because of its toxicity, FCA was later replaced by Freund's incomplete adjuvant (FIA) which did not contain Mycobacteria and was formulated with the surfactant Arlacel A. In mice, FIA has been associated with side-effects such as local reactions at the injection site, oil-induced neoplasmas and Arlacel A induced carcinogenicity[55]. In humans, FIA has been used with influenza and killed poliomyelitis vaccines enhancing their immunogenicity[55, 127]. Despite the absence of tumour formation in 18 000 recipients of FIA-based influenza vaccine monitored for up to 18 years, further use of this adjuvant was discontinued due to carcinogenicity of Arlacel A in mice[57].

The unacceptable toxicity caused by Freund's adjuvant prompted researchers to pursue alternative approaches to the development of particulate adjuvants. One with exceptional results in recent years is MF59. The emulsion is made up of small (approximately 160 nm), uniform and stable microvesicles[128] and each oil droplet is surrounded by a monolayer of non-ionic detergents. The oil is squalene, a natural

component of cell membranes; found in human sebum (a skin surface lipid) and a naturally occurring hydrocarbon precursor of cholesterol. Squalene droplets are stabilised by addition of two non-ionic surfactants, a low hydrophilic-lipophilic balance (HBL) surfactant, Polysorbate 80 (Tween 80), which is widely used as an emulsifier in foods, cosmetics and pharmaceuticals, and sorbitan triolate (commonly called Span 85) (Fig 1.2). After manufacturing and filtration of the emulsion through a 0.22 µm, the mean particle size, composition and pH of MF59 remained unchanged compared to initial values for at least 3 years at 2-8 °C, providing an excellent stability profile. Another important feature was the low concentration of large droplets of MF59 which remained stable for the same period of time[128].

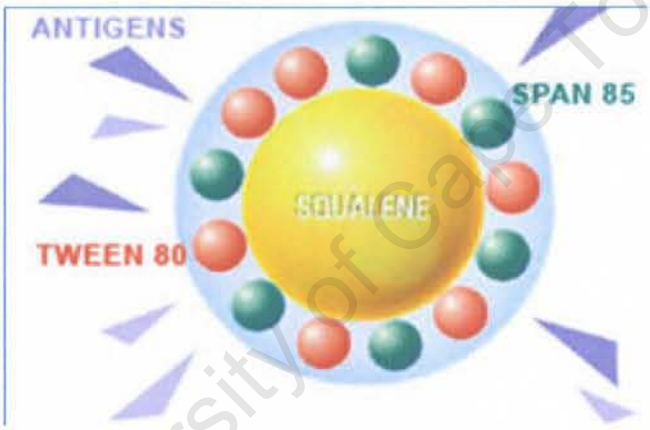

Figure 1.2: *MF59 adjuvant emulsion*[129].

The adjuvant properties of MF59 have been evaluated with several types of antigens including bacterial toxoids (e.g. tetanus toxoid and diphtheria toxoid), outer membrane vesicles (e.g. *Neisseria meningitidis*), polysaccharide conjugates (e.g. meningococcal C conjugate vaccines), recombinant antigens (e.g. hepatitis B surface antigen, meningococcal B, Herpes Simplex Virus [HSV]-2 gD2) and viral antigens (e.g. influenza antigens)[130-136]. In 1997, almost 70 years after the introduction of aluminium as adjuvant, MF59 became the first new adjuvant to be licensed for use in humans as part of an enhanced influenza vaccine (Fluad) for the elderly, and is now commercially available in 23 countries worldwide including 12 European Union countries[128].

The precise mechanism of MF59 adjuvanticity is still under investigation. Studies conducted with fluorescently labelled MF59 have shown that 4 hours after intramuscular administration, only 36 % of injected adjuvant was still present in the muscle and that the peak of localization in the corresponding lymph nodes was reached 2 days after injection. The presence of adjuvant did not influence the distribution of co-administered Herpes Simplex Virus [HSV]-2 gD2) antigen, which was cleared from the site of injection independently of MF59. Two days after intramuscular injection, MF59 localised in the draining lymph node was shown to be partially located in T cell areas within lymph node-resident cells that had the characteristics of antigen-presenting cells[128].

Administration of MF59 also induced a significant influx of macrophages at the site of injection, which was significantly suppressed in mice deficient for chemokines receptor 2[137-139]. Thus, it is likely that one of the effects of MF59 is to trigger the production of chemokines in cells resident at the injection site[138, 139]. Irrespective of its mechanism(s) of action, results obtained from mice studies strongly suggest that MF59 enhances functional and protective antibody responses[131-133] and/or induces a strong T cell response.

1.5.4 Monophosphoryl lipid A (MPL)

MPL is isolated from bacterial cell walls and is a detoxified form of lipid A derived from the lipopolysaccharide (LPS) of *Salmonella minnesota* R595 that has shown potential as a vaccine adjuvant[140-145]. Because of MPL's ability to activate monocytes and macrophages, vaccine antigens are more readily phagocytised, processed and presented[141]. These cells also release tumor necrosis factor α (TNF α), interleukin-1, and granulocyte-macrophage colony stimulating factor GM-CSF in response to MPL[143]. These monokines in turn lead to the recruitment and maturation of dendritic cells in the lymph nodes, where the dendritic cells can efficiently present antigen to T lymphocytes[143]. Thus, MPL assists the immune system in regulating Th1 and Th2 response[141, 142].

MPL can be formulated as an aqueous vehicle or an oil-in-water emulsion (o/w). The oil-in-water emulsion results in a more vigorous response for several reasons. Emulsions can cause tissue damage at the injection site leading to non-specific inflammation, attraction of macrophages and the inception of the immunological cascade[146]. Antigen

associated with oil droplets in an emulsion becomes more particulate, is more readily trapped in the lymph node and taken up by macrophages and dendritic cell, leading to enhanced antigen presentation[84]. The particulate nature of the antigen/oil droplet may also increase the presentation of the antigen by major histocompatibility complex (MHC) class I molecules resulting in cytotoxic T-lymphocyte (CTL) induction[147].

1.5.5 Saponin, Quil A, QS21 and immunostimulating complexes (ISCOMs)

Trends in modern vaccine development towards the use of highly purified recombinant proteins which are often poorly immunogenic when given alone or in combination with aluminium salts, have driven research on saponin adjuvants[148]. Saponin is derived from the bark of the *Quillaja saponaria* tree and has long been known as an immunostimulator (Fig 1.3)[57].

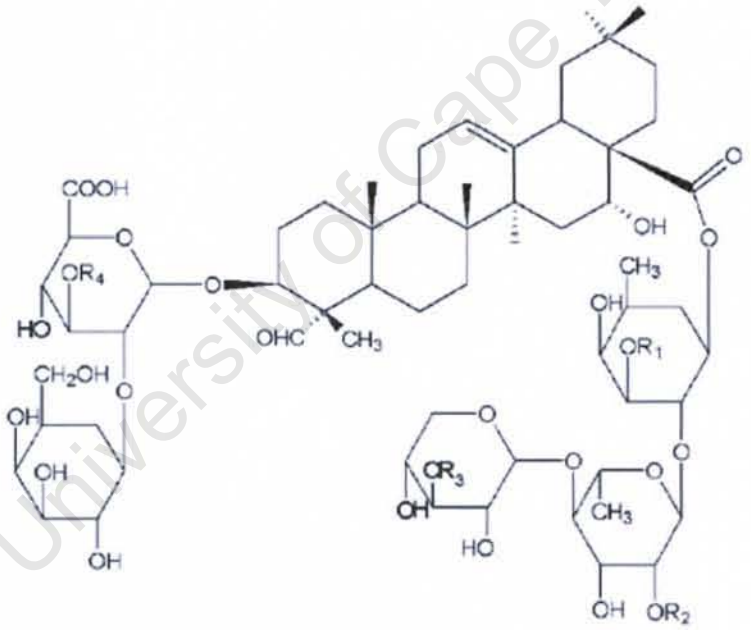

Figure 1.3: *Chemical structure of Quillaja saponins (R_1, R_2, R_3, and R_4 represent different substitution patterns of individual molecules)*[149].

The crude extract is not added to vaccines directly because it results in adverse side effects but is purified by HPLC to yield "Quil A" a very potent adjuvant with several unique features such as the ability to stimulate both the humoral and cellular branch of the immune system[79, 150]. Further analysis of Quil A by HPLC led to the discovery of

QS21 a potent water soluble adjuvant with minimal or reduced toxicity which can be used in vaccines with or without emulsion type formulations[57].

ISCOMs refer to non-covalently bound complexes of Quil A adjuvant and cholesterol. Amphipathic proteins together with an additional lipid (e.g. phospholipid) can be incorporated to form a highly immunogenic antigen complex[151]. If the ratio of Quil A to cholesterol is low, the micelles do not exist as individual particles[152]. Hydrophobic interactions cause aggregation and sheets of micelles to form i.e. a precipitate forms. The presence of phospholipid makes the micelles more fluid and permits the formation of spherical structures: empty ISCOMs consisting of about 14-ring like micelles[151]. Thus, the interior of ISCOMs has an open connection with its surroundings. It is for this reason that ISCOMs can only contain antigens if contact with the structure can be established and that ISCOM-matrix and antigen associate after mixing[152].

Quil A molecules have three distinct areas with respect to polarity: hydrophilic-hydrophobic-hydrophilic[153]. The hydrophilic region is part quillaic acid. It is thought that this three-block structure enables the formation of non-bilayer structures like ISCOMs[153]. Centrifugation and dialysis were the first two methods described in the literature for the preparation of ISCOMs. More recently, however, ISCOMs have been prepared by reversed-phased HPLC[154], by hydration of a cholesterol/phospholipid film with an aqueous solution of Quil A[151] or containing a mixture of two purified low toxicity Quillaja saponin fractions[155].

1.5.6 Liposomes

The classical view of a liposome is that it consists of a phospholipid bilayer structure to which cholesterol is often added to increase stability by increasing bilayer rigidity[152]. Liposomes can be prepared in two ways. Charged liposomes may be prepared by the incorporation of charged lipids. A second way of preparing liposomes is by detergent removal from a solution of mixed micelles[152, 156]. The efficient incorporation of antigen into the prepared liposomes is difficult and may require extensive optimisation experimentation in order to be achieved. The 'liposome' group can be broken down into liposomes[83], virosomes[157], transferosomes[158], archaeosomes[159], niosomes[160-162], cochleates[163] and proteosomes[164-166], depending on the source of the lipid.

Compared to ISCOMS, liposomes have enormous variation with respect to composition, size, physicochemical and immunological characteristics which permits flexible design in order to maximise functionality[57, 152]. This has led to the development of many liposome-like structures for antigen delivery[152]. Unlike ISCOMS, liposomal structures (with the exception of cochleates) contain an internal space separated from the environment. This allows the incorporation of hydrophilic antigens or adjuvants. Liposomes also differ from ISCOMS in that they have an inherent modest adjuvant activity[152].

1.5.7 Biodegradable polymer microspheres

Biodegradable polymer microspheres can be prepared from a variety of polymers such as poly (lactic-co-glycolic) acid (PLGA) and polyanhydrides[60, 84]. Microspheres made up of PLGA have the advantage of a long safety record from the use of PLGA as surgical sutures in humans[57] and in several commercial formulations, such as Lupron Depot (a drug commonly used in the treatment of uterine fibroids)[167]. Polyanhydrides have also been approved for use in humans and have been used to deliver proteins and model antigens[168].

Both PLGA[167] and polyanhydrides[169] are insoluble in water and must be dissolved in organic solvents such as methylene chloride or ethyl acetate to facilitate microsphere formation. The antigen is then mixed by homogenisation or sonication to form a fine dispersion of antigen in polymer/organic solvent (emulsion) [167, 169]. After immunisation, this emulsion forms a controlled release system which enhances the immune response by providing a long-term reservoir for the antigen[127, 170]. Such a controlled release system can provide a release of antigens for weeks to months, a time far exceeding the depot effect of aluminium salts or water-in-oil emulsions such as Freund's adjuvant[167] .

Microspheres less than 10 μm in diameter are readily ingested by macrophages and processed via the MHC class II pathway[171]. Recent studies have confirmed that encapsulation of antigen within particulates[172-174], or on their surface[175], can lead to antigen presentation by the MHC class I pathway as well. Additionally, microspheres are capable of protecting antigens from rapid destruction *in vivo* thus allowing presentation of the antigen in its native conformation to the immune cells[172-174]. Native antigen is important in order for B-cells to produce antibody with the highest affinity for the antigen being delivered. Antigen protection by encapsulation allows antigen delivery

via the oral route. The antigen is shielded from destruction by the low pH, of the stomach and the high levels of proteases and bile salts in the intestine[57, 167]. It has been established that a percentage of microspheres smaller than 10 µm in diameter are taken up from the intestine into the immune-inductive environment of the Peyer's patches where they can induce both mucosal and systemic immune responses[176, 177]. Finally, microspheres can deliver adjuvants or be made of polymers that break down into adjuvant-active molecules, thus providing long-term delivery of antigen associated with a vaccine adjuvant for further potentiation of the immune system[167].

1.5.8 Carrier proteins

Conjugation of nonimmunogenic antigens with immunogenic foreign protein carriers has been applied to induce immune responses against a variety of antigens, including bacterial polysaccharides, and have been approved for use in infants[176, 178, 179]. Invasive infections cause by *Haemophilus influenzae* type b (Hib), *Neisseria meningitidis* and *Streptococcus pneumoniae* have their highest incidence in early childhood[180]. After identifying that the polysaccharide capsule is an important determinant for virulence, vaccines containing the purified polysaccharide were developed and tested in humans and their immunogenicity and protective efficacy in adults was demonstrated. However, polysaccharide vaccines were not immunogenic in young children. This observation triggered the development of polysaccharide-protein conjugated vaccines that are immunogenic in infants[181]. Conjugate vaccines consisting of capsular polysaccharide of Hib bacteria covalently linked to a carrier protein (diphtheria, tetanus or pertussis toxoid, CRM_{197} protein or meningococcal outer membrane protein complex), have been demonstrated to be safe, immunogenic in infants, able to induce immunologic memory and protective against invasive Hib infections[180]. Commercially available meningococcal and pneumococcal multivalent vaccines are prepared in the same way as Hib conjugate vaccines. Protein-polysaccharide conjugates therefore have potential to be used for a safe and potent combined diphtheria-tetanus-acellular pertussis-Hib vaccine. Such a combination vaccine would simplify immunisation schedules, increase immunisation coverage and reduce the cost and stress of immunisation[32, 57].

1.5.9 Bacterial CpG DNA

Bacterial DNA contains unmethylated-CpG dinucleotides (uncommon in mammalian DNA), which in recent years has been found to induce powerful mucosal adjuvant

activity for systemic and mucosal immune responses[182, 183]. CpG DNA is most often administered in the form of synthetic oligodeoxynucleotides (CpG ODN) that are made with a nuclease-resistant phophorothioate backbone. CpG containing DNA binds to Toll-like receptor 9 (TLR-9) and stimulates B cells to proliferate, secrete immunoglobulin (Ig), interleukin-6 and interleukin-12, and induces protection from apoptosis[184-186]. In addition, it enhances expression of class II MHC and B7 co-stimulatory molecules[187, 188]. Furthermore, CpG DNA also directly activates monocytes, macrophages and dendritic cells to secrete various cytokines and chemokines, which can provide T-helper functions (Fig 1.4)[186, 188, 189].

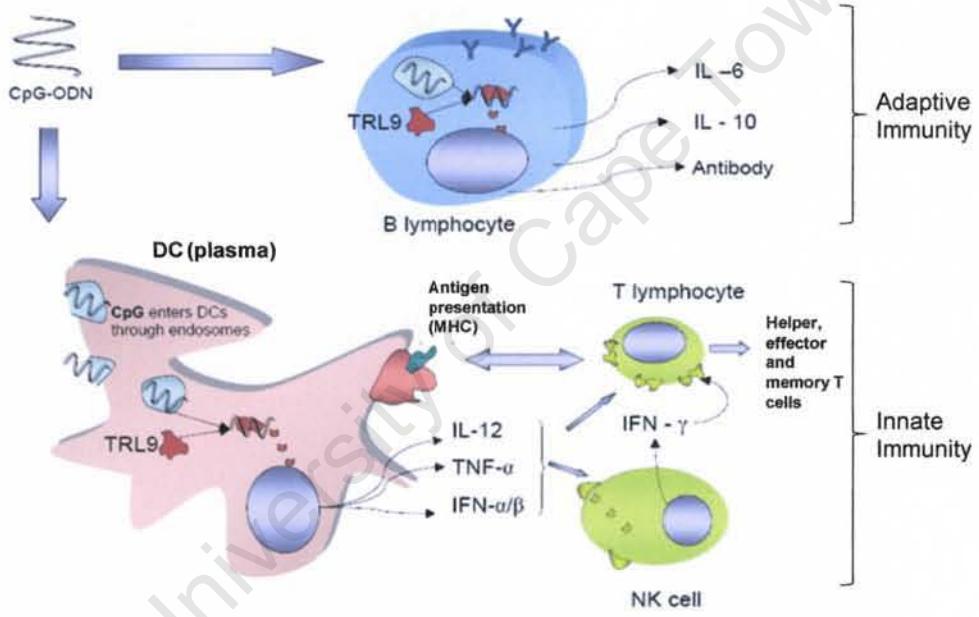

Figure 1.4: *Bacterial DNA and synthetic oligodeoxynucleotides containing CpG motifs (CpG-ODN) are strong activators of both adaptive and innate immunity*[190].

Immunisation of animals against a variety of antigens delivered parenterally (e.g. intramuscularly or subcutaneously) demonstrated that addition of CpG DNA induces more Th-1-like responses as indicated by strong cytotoxic T lymphocytes (CTL), high levels of IgG2a antibodies, and predominantly Th1 cytokines (e.g. interleukin-12, and IFN-γ but not interleukin -4 or interleukin -5)[187, 188, 191-194]. Oral administration of CpG ODN with tetanus toxoid demonstrated strong systemic responses with mucosal immunity induced at both local and distant sites[183]. T-helper subtypes induced were Th2

(IgG1, IgA) at mucosal sites, and Th1 systematically (CTLs, IgG2a). Intranasal administration with a hepatitis B surface antigen elicited similar results[182]. Human trials of CpG DNA have demonstrated its efficacy as an adjuvant for human use[195]. However, the development of CpG DNA vaccines faces several challenges[196]. Most importantly, results obtained from murine studies cannot be used to predict human immune responses because human and mouse immune cells are optimally stimulated by different CpG motifs[197], and major differences in TLR-9 distribution exists between species[198]. Moreover, CpG DNA is known to stimulate mild-transient inflammatory responses upon injection[198, 199].

1.5.10 Pheroid™

Pheroid™ (previously Emzaloid™) is a micro-emulsion formulated using plant and essential fatty acids emulsified in water saturated with nitrous oxide. Pheroid™ was first discovered when it was used as a basic formulation for the treatment of psoriasis. One of the basic ingredients of this first formulation was present in banana peel extract and was identified as essential fatty acids[200]. The fatty acid component consists of oleic, linoleic and linolenic fatty acid ethyl esters and PEG hydrogenated castor oil. Also included is the anti-oxidant dl-α-tocopherol[201]. A variety of Pheroid™ types can be formulated depending on the composition and method of manufacturing. The manufacturing process and the various types of Pheroid™ formed is shown in Fig 1.5.

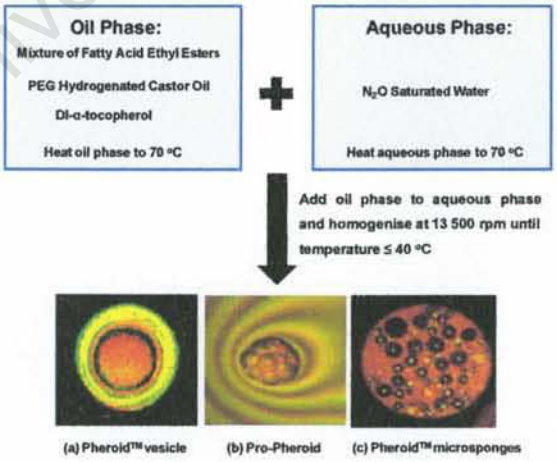

Figure 1.5: *A schematic representation of the Pheroid™ manufacturing process, as indicated by the supplier. Vesicle (a), pro-Propheroids (b) and microsponges are the three main types of Pheroid™[200].*

The size and shape of the vesicles can be reproducibly controlled (typically between 0.5-1.5 µm), whereas those of the microsponges usually ranges between 1.5-5 µm. The sizes of reservoirs or depots are determined by the amount of pro-Pheroids contained in the reservoirs[200]. The microsponges and depots support prolonged release according to a concentration gradient[201]. Pheroid™ can entrap, transport and deliver pharmacologically active compounds and other useful molecules. Depending upon the clinical indication, it can also act in synergism with such compounds or molecules resulting in an enhancement of therapeutic action. The Pheroid™ drug delivery system differs significantly from conventional macromolecular carriers, such as liposomal delivery systems. Table 1.1 provides a comparison of some of the differences and key of Pheroid™ over other lipid-based or liposomal drug delivery systems[201].

Table 1.1: Similarities and differences of lipid-based delivery systems and Pheroid™[201]

Lipid-based delivery systems	**Pheroid™ technology**
Contains of substances foreign to the body such as artificial polymers and lysolecithin[202].	Consists mainly of essential fatty acids, a natural and essential ingredient of the body[203].
Most if not all lipid-based delivery systems contain phospholipids and cholesterol[202, 204, 205].	Pheroid™ contains no cholesterol but the interior volume is nevertheless stably maintained.
Some liposomal formulations have been shown to elicit immune responses in man[202, 204].	Cytokine studies demonstrated that Pheroid™ elicited no immune responses in man.
Cytotoxicity and impaired cell integrity are common problems with substances that enter the body.	Pheroid™ causes no cytotoxicity because it is part of the natural biochemical pathways. Rather, it assists with cell maintenance[203].
Specific binding and uptake mechanisms by mammalian cells have not been described.	An affinity exists between Pheroid™ and cell membranes because it is comprised of fatty acids, thus ensuring penetration and delivery[203, 206, 207].

CHAPTER 1

A comparative study was undertaken in mice to investigate the efficacy of a commercially available rabies vaccine versus the vaccine formulated with Pheroid™. The rabies vaccine was prepared by inactivation of the virus. For the comparative animal study, different formulations of the virus were used, namely the inactivated virus, the inactivated virus with aluminium hydroxide adjuvant and the inactivated virus incorporated into Pheroid™. The Pheroid™-adjuvanted rabies vaccine showed a 9-fold increase in the antibody response over the unadjuvanted sample. This study was repeated four times with similar results[201].

A similar study was conducted using a commercially available hepatitis B vaccine and the vaccine formulated with Pheroid™. Non-recombinant hepatitis B vaccines are generally based on the use of the surface molecules of the virus as antigen. For the comparative animal studies, different formulations of this peptide-based vaccine were used (the peptide, the peptide with aluminium hydroxide adjuvant and the Pheroid™-entrapped peptide). The use of Pheroid™ as a delivery system led to more than a 10-fold increase in the efficacy of the peptide-based hepatitis B vaccine as measured by antibody response. Thus, Pheroid™ has a dual role in vaccinology, firstly as a delivery system for disease specific antigens, and secondly as an immuno-stimulatory adjuvant[201].

As part of the preclinical studies on Pheroid™, physicochemical techniques which had not previously been applied to the study of Pheroid™ were employed to characterise the composition and size of this novel adjuvant. Nuclear magnetic resonance (NMR) spectroscopy provides a window into the structure of organic molecules and ^{1}H- and ^{13}C-NMR spectra were used to profile the raw materials used to prepare Pheroid™ and to study the composition of Pheroid™ formulations. Coulter Counter analysis was used to investigate particle volume-size and particle number-size distributions of different Pheroid™ formulations in order to determine the average particle size of the emulsion.

1.6 Regulatory consideration of new adjuvants

Due to the limitations of currently available aduvants, greater emphasis by vaccine manufacturers is now being placed on the discovery, development and testing of new adjuvants for use with modern vaccines[80, 201]. In addition to being fully characterised for its chemical properties, all new biological products must undergo pre-clinical evaluation prior to being used in humans[80, 209]. Besides establishing their biological properties and evaluating their possible risk to the public, these pre-clinical trials form the basis for subsequent clinical trials from which safety and efficacy can be evaluated[210]. No adjuvant is licensed as a medicinal product, but only as a component of a particular vaccine; as such preclinical and appropriate toxicology studies are designed on a case-by-case basis to determine the safety profile of the adjuvant or adjuvant/vaccine combination[210]. Finally, clinical studies are performed on the adjuvant(s) alone and on its combination with the antigen(s) in order to determine that:

i. Inclusion of the adjuvant is justified.
ii. Potentiation of immune response occurs without undue increase in local and systemic reactions.
iii. The risk-benefit relation for a modified product is at least as favourable as for the existing product.

The various clinical scenarios to be considered for confirmatory clinical studies are summarised in Table 1.2.

Table 1.2: Requirements for the evaluation of new adjuvants in vaccines – clinical aspects[210]

Scenario	Expected study approach
• Changes to licensed vaccines • Removal of one or more adjuvants from a licensed vaccine (without replacement) or reduction in the adjuvant content in order to improve the safety profile	Studies to demonstrate: • Superiority for safety (if possible) • Non-inferiority for immune response(s)
• Addition of one or more novel or established adjuvant(s) to a licensed vaccine or increase in the amount of adjuvant(s) in order to enhance the immune response	Studies to demonstrate: • Superiority for immune responses to the antigen or to at least one of the antigens • Non-inferiority for responses to any antigen(s)
• Replacement of one or more adjuvant(s) in a licensed vaccine with one or more novel or established adjuvant(s)	If primary aim is to enhance immunogenicity, studies to demonstrate: • Superiority for immune response to the antigen or to at least one of the antigens • Non-inferiority for responses to any other antigen(s) If primary aim is to enhance safety, studies to demonstrate: • Superiority for safety (if possible) • Non-inferiority for immune response(s)

With the introduction of new technologies, regulators are faced with issues that cannot be easily addressed during development, pre-clinical and even clinical studies, using existing models and technologies. Currently, very little is known about the possible modes of action of existing and new adjuvants and even less is known about their possible interactions. It is difficult to generate useful comparative studies in current animal models to adequately provide information on the effectiveness of adjuvants[80, 210]. However, as knowledge of fundamental biological mechanisms increase and genetic engineering becomes applicable to a widening range of species, the construction of more appropriate animal models in which to evaluate new adjuvants is likely to improve the situation[210].

1.7 Conjugate Vaccines

Several bacterial pathogens, including *Haemophilus influenzae, Streptococcus pneumonia* and *Neisseria meningitidis*, possess a polysaccharide capsule which protects the bacterium from phagocytosis and complement-mediated lysis and is a potent virulence factor[211]. Vaccines which result in the production of antibodies have been shown to confer protection against these bacterial pathogens. The first generation vaccines against infectious diseases such as *Haemophilus influenzae* type b (Hib), *Streptococcus pneumonia* and *Neisseria meningitidis* were polysaccharide vaccines which elicited type-specific antibodies. Unfortunately, the polysaccharide vaccines were found to be poorly immunogenic in children less than 18-24 months of age, and this is the age of highest incidence of disease in non-immunised populations[212]. Pioneering studies by Landsteiner in 1924 demonstrated that whereas a small hapten was non-immunogenic, immunisation with the hapten linked to a protein antigen induced an antihapten antibody response[212]. In 1929 Avery and Goebel showed that by conjugating a bacterial polysaccharide to a carrier protein, a stronger antibody response to the carbohydrate moiety was obtained[213].

Two types of carrier protein are most commonly chosen for use in conjugate vaccines. The earliest and most widely used group have been bacterial toxoids, including tetanus and diphtheria toxoid. These proteins were already licensed for human use. Another popular carrier is CRM_{197}, a genetically toxoided variant of diphtheria toxin, as chemical toxoiding is not required and the vaccines are simpler to characterise and control, and there is less variability possible in carrier protein production. An alternative approach is to choose a carrier protein which will induce an immune response that complements the role of anti-saccharide antibodies[214]. For example, *Streptococcus pneumoniae* causes acute otitis media in childred under 2 years of age. The polyvalent pneumococcal capsular polysaccharide vaccine is not immunogenic in this age group, however conjugation of the *Streptococcus pneumoniae* capsular polysaccharide to a recombinant non-lipidated form of protein D from non-typeable *Haemophilus influenzae* reduces nasopharyngeal carriage of both *Streptococcus pneumoniae* vaccine serotypes and non-typeable *Haemophilus influenzae* in children under 2 years old[215, 216].

Polysaccharides require activation before attachment to the carrier protein. It may be necessary to also activate the carrier protein. The optimum means to activate the polysaccharide depends on its structure. For example, periodate oxidation of the Hib polysaccharide and meningococcal group C polysaccharide creates aldehydes at either end which are attached to the free amino groups of lysine residues in the carrier protein by reductive amination[217]. Both the Hib and the meningococcal group C polysaccharides are susceptible to mild acid hydrolysis, generating a protected aldehyde group at the reducing end. This reducing end can be activated, for example by reductive amination, and a linker attached which allows covalent attachment to the carrier protein – this approach has been used by Chiron Vaccines (now Novartis)[218]. The polysaccharide from *Salmonella typhi* and *Staphylococcus aureus*, in contrast, have few free hydroxyl groups and are extremely resistant to hydrolysis. These polysaccharides have been activated by the addition of bifunctional reagent to the uronic acid carboxyl group, which allows conjugation to a suitable activated carrier protein[219-221].

Treatment of a polysaccharide with cyanogen bromide or a cyanogen bromide analogue such as 1-cyano-4-dimethylaminopyridinium tetrafluoroborate (CDAP)[222], results in random activation of hydroxyl groups to which a bifunctional linker, such as adipic acid dihydrazide, can be attached[222]. This linker is then attached to asparagine or glutamate carboxyl groups on the carrier protein by treatment with a water-soluble carbodiimide[214]. Reaction of a carboxylate-containing capsular polysaccharide with an amine in the presence of carbodiimide is a means to attach a reactive group – such as a protected thiol – to the capsular polysaccharide. This can be conjugated to a complementary reactive groups pre-attached to the carrier protein to create the polysaccharide-protein complex[214]. Another conjugation chemistry that has been used involves partial de-N-acetylation of an N-acetylglucoseamine residue in the repeating unit of the capsular polysaccharide from *Streptococcus pneumonia* type 14. Treatment with nitrous acid leads to the formation of an anhydromannose residue with a free aldehyde group, suitable for conjugation by a lysine residue in an appropriate carrier protein[223, 224]. The effectiveness of this strategy depends on the nature and substitution pattern of the acetamido sugar[214]. These conjugation strategies are summarised in Table 1.3.

Table 1.3: Summary of conjugation chemistries[214]

Conjugation Chemistry	
1. Reductive amination:	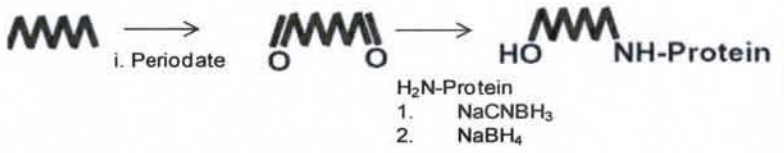
2. Active ester chemistry	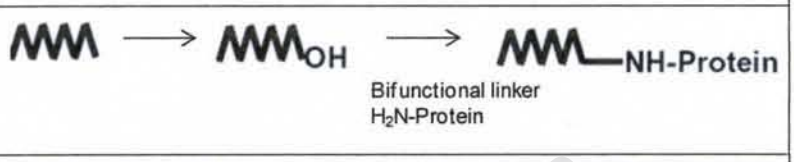
3. Random CNBr activation	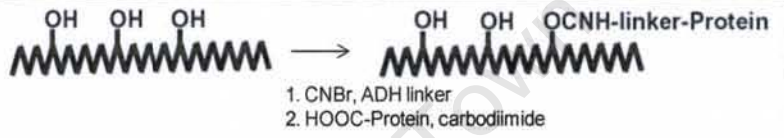
4. Disulphide chemistry	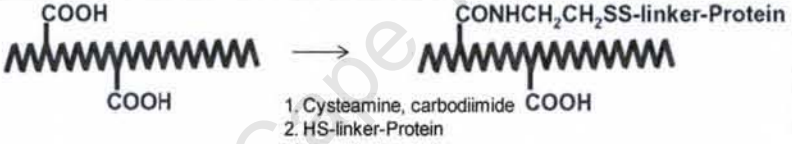

At present, there is a lack of good animal models for predicting the potency of conjugates in humans. Therefore, physicochemical methods such as chromatography, spectroscopy and hyphenated techniques are used by the vaccine industry and control agencies to test the quality of the vaccine intermediates and the final product[225]. These physicochemical methods will be discussed in further detail in chapters 2-5.

1.7.1 *Haemophilus influenzae*

Haemophilus influenzae type b (Hib) is a respiratory pathogen which causes several diseases in humans, the most common and most serious being meningitis and pneumonia, mainly in children under 5 years of age[180, 226]. Hib also causes epiglottitis, septicaemia, facial cellulitis, septic arthritis, osteomyelitis and pericarditis[48, 211]. The capsular polysaccharide is a polymer made of repeating units of -(PO_2H→3)-β-D-Rib*f*-(1→1)-D-Ribitol-5→ and plays an important role in the virulence of the organism[227].

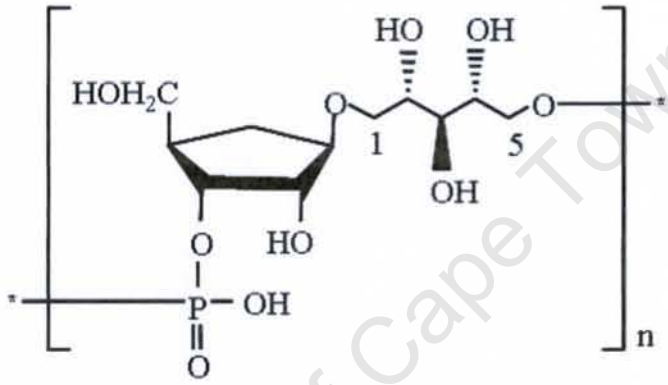

Figure 1.6: *Hib Polysaccharide repeating unit*
[-(PO_2H→3)-β-D-Rib*f*-(1→1)-D-Ribitol-5→]$_n$

Before the availability of vaccines, an estimated 20 000 to 25 000 people developed invasive Hib disease annually in the United States and until 1992 when conjugate vaccines were used for routine immunisation of infants, Hib was the most common cause of bacterial meningitis[228]. Population-based studies in other industrialised nations showed an incidence of Hib disease that is approximately one third to two thirds that in the United States. In Sweden[229-232], Finland[229, 233, 234], the Netherlands[235] and Australia[236], it was the most common cause of bacterial meningitis. It also ranked as the leading cause of bacterial meningitis in Canada, which has a disease incidence similar to that in the United States[237, 238]. An exceptionally high rate of invasive Hib disease has been reported among Aboriginal children in central Australia[237, 239, 240] and among Native Americans[241].

Although population-based data for developing countries are limited, Hib also appears to be ranked as the leading cause of bacterial meningitis in most of these countries[242-246].

Most studies in Africa show rates in meningitis and invasive disease similar to those in the United States, while data from South America and the Middle East demonstrate rates of disease similar to those found in Western Europe. A study in Niger reported a rate of Hib meningitis of over 200 cases per 100 000 infants less than a year old[247]. Hib disease is also prevalent in The Gambia[248, 249]. Many studies of hospitalised patients with presumed bacterial meningitis throughout Asia (Indonesia, Singapore[250], China[251], Hong Kong[252], the Philippines[253, 254], Taiwan[255], Thailand, India[256], Vietnam, Korea and Japan[257]) consistently show Hib to be the leading cause of bacterial meningitis in children[228].

The first vaccine against Hib consisted of the purified polysaccharide polyribosylribitolphosphate (PRP) alone; however it failed to induce protective antibodies in children under 18 months old. Immunogenicity against Hib could be improved dramatically by covalently linking PRP to a protein carrier[48]. Four Hib conjugates (PRP-D, PRP-T, HbOC and PRP-OMP) were licensed and have been used to immunise tens of millions of infants worldwide[180, 211]. These conjugates from different manufacturers differ in the size range of the polysaccharide, the identity of the protein carrier and the method of conjugation[228].

The mechanism by which glycoconjugates stimulate an immune response involves an initial binding of the conjugate to the surface immunoglobulin (sIg) of B cells with appropriate specificity for the saccharide hapten. This complex is internalised and the carrier protein degraded by proteolytic enzymes. Suitable peptides are transported to and displayed by MHC II complexes. The peptide-loaded MHC II complex is recognised by T cells, which then provide appropriate signals through direct interaction of cell surface proteins and through cytokine signalling processes, to induce maturation of the B cell into an antibody secreting plasma cell[258]. The T cell dependent response to a conjugate results in both serum IgG antibodies and memory B cells, even in infants. In general, immunogenicity of a polysaccharide-protein conjugate, in contrast to the native polysaccharide, does not depend on the size of the conjugated polysaccharide; conjugates prepared with either polysaccharides or oligosaccharides may have similar immunogenicity[259].

The generation of mucosal immune responses by Hib conjugate vaccines has been investigated in animal models. Bergguist and co-workers reported that intranasal immunisation of Hib vaccines gave rise to both mucosal and systemic anti-PRP antibody responses[260]. Similar results have been reported in more recent studies and support the rationale for Hib conjugate vaccines which can be administered to infants and young children via mucosal routes[261-262].

In populations where one of the Hib conjugates have been in use as a universal infant vaccine for several years, including the United States, United Kingdom, Finland, Iceland and Australia, a rapid sustained reduction of all Hib infections was observed[211, 263-267]. The WHO recommends that the Hib conjugate vaccine should be included in national immunisation programmes worldwide[48].

1.7.2 *Neisseria meningitidis*

Although there are several different bacteria that can cause meningitis, meningococcus is one of the most important because of its potential to cause epidemics[259, 268]. Meningitis caused by *Neisseria meningitidis* accounts for an estimated 171 000 deaths worldwide[269]. The meningococcus has both an outer and inner (cytoplasmic) cell membrane that is separated by a peptidoglycan cell wall. The outer membrane is surrounded by a polysaccharide capsule that is essential for pathogenicity as it confers resistance to phagocytosis[270, 271] and complement-mediated lysis and offers protection against environmental injuries. Although there are 12 serogroups, essentially all meningococcal disease is caused by serogroups A, B, C, W135 and Y[259]. The structures of their repeating units are shown below[272]:

Group A: →6)-α-D-ManpNAc(3OAc)-(1→OPO3→
Group B: →8)-α-D-Neu5Ac-(2→
Group C: →9)-α-D- Neu5Ac(7/8OAc)-(2→
Group W135: →6)-α-D-Galp-(1→4)-α-D- Neu5Ac(9OAc)-(2→
Group Y: →6)-α-D-Glcp-(1→4)-α-D- Neu5Ac(9OAc)-(2→

The relative importance of each serogroup varies with geographical region. At present, group A is a problem mainly in Africa[273] and Asia[274], and occasional outbreaks have been associated with population movements and overcrowding in other regions over the

past half century[275]. In industrialised nations, group B meningococci cause 30-70 % of cases of sporadic meningococcal disease[273, 276, 277] and have been responsible for pockets of persistently increased rates of disease[278-280]. Group C meningococcal disease affects individuals of all age groups, but the highest incidence is in children less than 5 years old, and especially among infants aged 3-12 months[276]. Group Y disease is uncommon in the United Kingdom, but accounts for up to 30 % of cases in the United States; rates of Y disease may also be on the increase in parts of Canada[277]. Occasional sporadic disease caused by W135 meningcocci had been largely ingnored until a recent large outbreak among pilgrims to the Hajj in 2000[281].

Epidemics caused by *N meningitidis* are usually characterised by a predominance of a single meningococcal genotype, higher incidence rates, and a shift of cases toward older age groups. For more than 100 years group A[282] and, to a lesser extent group C[283] strains have been responsible for recurrent epidemics in countries of the meningitis belt of sub-Saharan Africa[284]. These epidemics take place in regular cycles every 5-12 years, and last for two to three dry seasons, dying out during the intervening rainy season. These epidemics can be enormous, with up to 400-800 cases per 100 000. In 1996, in the largest epidemic ever recorded, there were more than 200 000 cases and 20 000 deaths[285].

Concurrent epidemics caused by group A and W135 have been associated with the Hajj pilgrims in Saudi Arabia, with 53 % of the cases caused by group W135. Additional cases of group W135 meningococcal disease arose concomitantly in countries outside of Saudi Arabia, including countries in the African meningitis belt[286, 287]. In 2002, a large W135 meningococcal outbreak was reported in Burkina Faso, with more than 8 000 cases[285].

Large outbreaks of group A disease occurred frequently in China and Mongolia during the 70s, and disease occasionally reached Nepal and India. Large outbreaks of group A disease were also recorded in Mongolia in the mid-90s. However, in the past 20 years, rates of disease in China have declined, coincident with introduction of meningococcal polysaccharide vaccine[288]. Rates also declined in Hong Kong, Nepal and India[275] in the absence of widespread vaccination. By contrast, with the abrupt onset and short duration of group A epidemics in sub-Saharan Africa, group B epidemics develop

gradually over several years and last up to a decade or more[289]. These epidemics have happened in Europe (Belgium, Iceland, Norway and Spain)[292-295], the United States and some middle income countries of the Americas (Brazil, Chile, Columbia Cuba)[296-299]. Since 1991 New Zealand has been experiencing an epidemic of group B meningococcal disease with incidence rates reaching ten times background incidence, and with much higher age-specific, area-specific and ethnic-specific rate. Without an efficient vaccine, the incidence rate still remains high[285]. It is still unclear why group B epidemics are so rare in Africa and other areas of the developing world[300, 301]. The polysaccharide capsule of serogroup B meningococcal is a homopolymer of sialic acid, which is chemically identical to polysaccharides found in human tissues during development[302]. Hence, the B capsule is seen by the immune system as a self antigen and is thus poorly immunogenic, even after conjugation to a protein carrier[303]. Consequently, conventional approaches to develop a vaccine for group B stains have been largely unsuccessful and various alternative strategies are being investigated[304].

Polysaccharide vaccines against serogroups A, C, W135, and Y have been available since the mid-1980s and are effective in children 5 years of age or older and adults. A tetravalent polysaccharide vaccine that provides protection against serogroups A, C, W135 and Y is also available but is not recommended for routine childhood vaccination because meningococcal polysaccharides, like most other bacterial polysaccharides, do not effectively stimulate the immune system in young children and are largely non-immunogenic in infants, who have the highest risk of sporadic disease[259, 305-308]. The exception is the group A meningococcal polysaccharide, which for reasons not well understood, is immunogenic in infants as young as 6 months of age, primed for a boosted response, and is effective when used in infants and toddlers in a two-dose immunization schedule[309].

As with Hib conjugate vaccines, serogroup A, C, W135 and Y meningococcal polysaccharides have been covalently linked to carrier proteins (such as diphtheria and tetanus toxoids, meningococcal outer membrane protein complex or protein D from non-typeable *Haemophilus influenzae*). These meningococcal conjugate vaccines induce a T cell dependent response, resulting in an improved immune response in infants, priming immunologic memory, and leading to a booster response to subsequent doses[308]. The first meningococcal conjugate vaccines to be licensed were against group

C (Meningtec, Menjugate and Neis Vac-C)[225, 259, 310]. A tetravalent conjugate vaccine against groups A, C, W135 and Y was licensed in the United States in 2005 for use in adolescents and adults[311]. Clinical studies assessing the immunogenicity of this vaccine in infants showed modest results, suggesting a need for alternative presentations, perhaps with the addition of adjuvants[312]. Nearly a decade ago the Meningitis Vaccine Project (MVP) was created as a partnership between PATH (Program for Appropriate Technology in Health) and the WHO with the goal of eliminating meningococcal group A epidemics in Africa through the development, licensure, introduction and widespread use of group A *N. meningitidis* conjugate vaccine. A phase I study of the vaccine in India has shown that it is safe and immunogenic. Phase II studies are currently underway in Mali and The Gambia[313].

1.7.3 Pneumococcal and other conjugate vaccines

Pneumococcal infections elicited by *Streptococcus pneumoniae* (which include pneumonia, otitis media, sinusitis, meningitis) are frequently occurring diseases that are associated with considerable morbidity even in developed countries[314]. Of the ninety-one different serotypes described, approximately 20 serotypes are responsible for more than 70 % of invasive pneumococcal disease in all age groups[315], and approximately 10 or 11 serotypes account for at least 70 % of invasive paediatric infections in all regions of the world[316]. In 2005, the WHO estimated that 1.6 million people a year die from pneumococcal disease, including up to 1 million children less than 5 years old[317].

The pneumococcal polysaccharide vaccine, PPV23, is licensed for use in adults (especially the elderly) and children over 2 years old who have certain underlying medical conditions, for the prevention of pneumococcal disease. It is a blend of 23 serotype-specific polysaccharides which account for 85-90 % of all cases of pneumococcal disease[214, 225, 315]. As a polysaccharide vaccine, it was poorly immunogenic in infants and children under 2 years of age and did not induce immune memory[315]. A prophylactic conjugate vaccine became available for this age group with the licensure of Prevenar in 2000[318]. This 7-valent pneumococcal conjugate vaccine contains the serotypes Pn 4, 6B, 9V, 14, 18C, 19F and 23F[214]: In contrast to the pure polysaccharide pneumococcal vaccine, the conjugate vaccine stimulates a robust T cell-dependent immune response that allows for generation of protective anti-pneumococcal antibody even in young infants[315].

The success of the Hib conjugates and the potential shown by the meningococcal and pneumococcal vaccines under development has inspired the application of this technology to other bacterial diseases[319]. Group B streptococcus (GBS) represent the leading cause of neonatal septicaemia and meningitis in industrialised countries. Capsular polysaccharides from GBS types Ia and Ib[320], type III[321], and types VI and VIII, conjugated to carrier proteins, have been shown to be effective in preclinical studies. Furthermore, tetanus toxoid-based conjugates of types Ia, Ib and II were immunogenic in humans[320, 322]. Similar attempts are underway to make immunogenic and safe vaccines against the Vi polysaccharide capsule of *Salmonella typhi*[323], *Escherichia coli*[324], *Shigella dysenteriae* type 1[325], *Shigella sonnei* and *Shigella flexneri* 2a[326] and *Vibrio cholerae*[327].

1.8 Aims and objectives

The aims of this thesis is to characterise an experimental adjuvant called Pheroid™ which has been developed in South Africa, to develop methods for analysis of the integrity of conjugate vaccines, to apply these methods to combination vaccines and to evaluate the effect of adjuvants on the stability and integrity of conjugate vaccines. The objectives of this thesis can be stated as follows:

- To investigate size, structure and composition of Pheroid™ using NMR spectroscopy and Coulter Counter;
- To investigate different methods of free saccharide separation and quantification of saccharide for meningococcal group A conjugate vaccine;
- To apply the methodology developed to evaluate the integrity of a Hib monovalent vaccine;
- To investigate methods for PRP and Hib-TT processing in the presence of Pheroid™ and aluminium-containing adjuvants;
- To investigate the applicability of the free saccharide assay to Hib pentavalent vaccine containing sucrose formulated with Pheroid™ or aluminium-containing adjuvant and subjected to a thermal stability study; and
- To apply the assay to an aluminium phosphate-adjuvanted pentavalent liquid vaccine formulated without sucrose.

1.9 References

1. Andre, F. E., Development and clinical application of new polyvalent combined paediatric vaccines. *Vaccine* 1999;**17**:1620-7.

2. Douglas, R. G. JR., The Jeremiah Metzger lecture, Vaccine prophylaxis today: its science application and politics. *Trans Am Clin Climatol Assoc* 1998;**109**:185-98.

3. Giudice, G. D., Vaccination strategies: an overview. *Vaccine* 2003;**21**:S2/83-8.

4. Peltola, H., Worldwide *Haemophilus influenzae* type b disease at the beginning of the 21st century: global analysis of the disease burden 25 years after the use of the polysaccharide vaccine and a decade after the advent of conjugates. *Clin Microbiol Rev* 2000;**13**:302-17.

5. Hsu, E. H., Shutt, K. A., et al., Effect of pneumococcal conjugate vaccine on pneumococcal meningitis. *N Engl J Med* 2009;**360**:244-56.

6. Balmer, P., Borrow, R., et al., Impact of meningococcal C conjugate vaccine in the UK. *J Med Microbiol* 2002;**51**:717-22.

7. Serruto D., Adu-Bobie, J., et al., Biotechnology and vaccines: application of functional genomics to *Neisseria Meningitidis* and other bacterial pathogens. *J Biotechnol* 2004;**113**:15-32.

8. Srivastava I. K., Lui M. A., Gene vaccines. *Ann Intern Med* 2003;**138**:550-59.

9. Pizza M., Covacci, A., et al., Mutants of pertusis toxin suitable for vaccine development. *Science* 1989;**246**:497-500.

10. Swiatlo E., Ware, D., Novel vaccine strategies with protein antigens of *Streptococcus pneumoniae*. *FEMS Immunol Med Microbiol* 2003;**38**:1-7.

11. McMichael J. C., Green, B. A., Vaccines for *Moraxella catarrhalis* and non-typeable *Haemophilus influenzae*. *Curr Opin Investig Drugs* 2003;**4**:953-958.

12. Andre, F. E., Hepatitis B virus and primary hepatocellular carcinoma: treatment of HBV carriers with Phyllanthus amarus. *Vaccine* 1990;**8**:S74-8.

13. Hsu H. H., Abrignani, S., et al., Prospects for a hepatitis C vaccine. *Clin Liver Dis* 1999;**3**:901-15.

14. Amara R. R., Robinson, H., L., A new generation of HIV vaccines. *Trends Mol Med* 2002;**8**:489-95.

15. Rohan T. E., Burk, R. D., et al., Toward a reduction of the global burden of cervical cancer. *Am J Obstet Gynecol* 2003;**189**:S37-9.

16. Ellis, R. W., Development of combination vaccines. *Vaccine* 1999;**17**:1635-42.

17. Capiau C., Poolman, J., et al., Development and clinical testing of multivalent vaccines based on a diphtheria-tetanus-acellular pertussis vaccine: difficulties encountered and lessons learned. *Vaccine* 2003;**21**:2273-87.

18. www.who.int/immunization/policy/immunization_routine_table1.pdf. Accessed 07 April 2009.

19. Fletcher M. A., Fabre, P., et al., Vaccines administered simultaneously: directions for new combination vaccines based on an historical review of the literature. *Int J Infect Dis* 2004;**8**:328-38.

20. Ebbert, G. B., Mascolo, E. D., Vaccine Manufacturing, In *Vaccines*, Plotkin, S. A. and Orenstein, W. A., Editors. 4th edn, 2004, Elsevier Inc: Philadelphia. pp. 53-67.

21. Arístegui, J. U. V., Coovadia, H., et al., Facilitating the WHO expanded programme of immunisation: the clinical profile of a combined diphtheria, tetanus, pertussis, hepatitis B and *Haemophilus influenzae* type b vaccine. *Int J Infect Dis* 2003;**7**:143-51.

22. Weniger, B. G., Chen, R. T., et al., Addressing the challenges to immunization practice with an economic algorithm for vaccine selection. *Vaccine* 1998;**16**:1885-97.

23. Mallet, E., Fabre, P., et al., Immunogenicity and safety of a new liquid hexavalent combined vaccine compared with separate administration of reference licensed vaccines in infants. *Pediatr Infect Dis J* 2000;**19**:1119-27.

24. Glyca, R., Glyca, V., et al., A new DTPa-HBV-IPV vaccine co-administered with Hib, compared to a commercially available DTPw-IPV/Hib vaccine co-administered with HBV, given at 6, 10 and 14 weeks following HBV at birth. *Vaccine* 2001;**19**:825-33.

25. Plotkin, S. A., Disease states and vaccines: selected cases (Part A), In *The Vaccine Book*, Bloom, B. R. and Lambert, P. H., Editors. 2003, Academic Press: New York. pp. 179-88.

26. http://www.prevnar.com/e01_vaccine__information.aspx. Accessed 20 August 2009.

27. Marcy, S., M., Pediatric combination vaccines: their impact on patients, providers, managed care organizations, and manufacturers. *Am J Manag Care* 2003;**9**:314-20.

28. Yeh SH, W. J., Strategies for development of combination vaccines. *Pediatr Infect Dis J* 2001;**20**:S5-9.

29. Baylor, N. W., Midthun, K., Regulation and testing of vaccines, In *Vaccines*, Plotkin, S. A. and Orenstein, W. A., Editors. 4th edition, 2004, Elsevier Inc: Philadelphia. pp. 1539-56.

30. Sawyer, L. A., McInnis, J., et al., Deleterious effect of thimerosal on the potency of inactivated poliovirus vaccine. *Vaccine* 1994;**12**:851-6.

31. Avdicova, M., Prikazsky, V., et al., Immunogenicity and reactogenicity of a novel hexavalent DTPa-HBV-IPV/Hib vaccine compared to separate concomitant injections of DTPa-IPV/Hib and HBV vaccines, when administered according to a 3, 5 and 11 month vaccination schedule. *Eur J Pediatr* 2002;**161**:581-7.

32. Elliman, D., Bedford, H., Safety and efficacy of combination vaccines. *BMJ* 2003;**326**:995-6.

33. Knutsson, N., Trollfors, B., et al., Immunogenicity and reactogenicity of diphtheria, tetanus and pertussis toxoids combined with inactivated polio vaccine, when administered concomitantly with or as a diluent for a Hib conjugate vaccine. *Vaccine* 2001;**19**:4396-403.

34. Poolman, J., Kaufhold, A., et al., Clinical relevance of lower Hib response in DTPa-based combination vaccines. *Vaccine* 2001;**19**:2280-5.

35. Riedemann, S., Reinhardt, G., et al., Immunogenicity and reactogenicity of combined versus separately administered DTPw-HBV and Hib vaccines given to healthy infants at 2, 4 and 6 months of age, with a booster at 18 months. *Int J Infect Dis* 2002;**6**:215-22.

36. Saenger, R., Maechler, G., et al., Booster vaccination with hexavalent DTPa-HBV-IPV/Hib vaccine in the second year of life is as safe as concomitant DTPa-IPV/Hib + HBV administered separately. *Vaccine* 2005;**23**:1135-43.

37. Ball L. K., Horne, A. D., et al., Evaluating the immune response to combination vaccines. *Clin Infect Dis* 2001;**33**:S299-305.

38. Decker, M. D., Edwards, K. M., et al., Combination vaccines, In *Vaccines*, Plotkin, S. A. and Orenstein, W. A., Editors. 4th edition, 2004, Elsevier Inc: Philadelphia. pp. 825-62.

39. Andre, F. E., Booy, R., et al., Vaccination greatly reduces disease, disability, death and inequity world. *Bull World Health Organ* 2008;**86**:140-6.

40. Andreae, M. C., Freed, G. L., et al., Safety concerns regarding combination vaccines: the experience in Japan. *Vaccine* 2004;**22**:3911-6.

41. Di Fabio, J. L., de Quadros, C., Considerations for combination vaccine development and use in the developing world. *Clin Infect Dis* 2001;**33 Suppl 4**:S340-5.

42. Hausdorff, W. P., Prospects for the use of new vaccines in developing countries: cost is not the only impediment. *Vaccine* 1996;**14**:1179-86.

43. Wakefield, A. J., Murch, S. H., et al., Ileal-lymphoid-nodular hyperplasia, non-specific colitis, and pervasive developmental disorder in children. *Lancet* 1998;**351**:637-41.

44. Chen, R. T., DeStefano, F., Vaccine adverse events: causal or coincidental? *Lancet* 1998;**351**:611-2.

45. Elliman, D. A., Bedford, H. E., MMR vaccine--worries are not justified. *Arch Dis Child* 2001;**85**:271-4.

46. Halsey, N. A., Hyman, S. L., Measles-mumps-rubella vaccine and autistic spectrum disorder: report from the New Challenges in Childhood Immunizations Conference convened in Oak Brook, Illinois, June 12-13, 2000. *Pediatrics* 2001;**107**:E84.

47. Miller, E., Andrews, N., et al., Bacterial infections, immune overload, and MMR vaccine. Measles, mumps, and rubella. *Arch Dis Child* 2003;**88**:222-3.

48. WHO Expert Committee on Biological Standardization. Forty-ninth report. *World Health Organ Tech Rep Ser* 2000;**897**:i-vi, 1-106.

49. Best, J. M., O'Shea, S., Disease states and vaccines: selected cases (Part C), In *The Vaccine Book*, Bloom, B. R. and Lambert, P. H., Editors. 2003, Academic Press: New York. pp. 197-209.

50. Ada, G., Progress towards achieving new vaccine and vaccination goals. *Intern Med J* 2003;**33**:297-304.

51. Schijns, V. E., Antigen delivery systems and immunostimulation. *Vet Immunol Immunopathol* 2002;**87**:195-8.

52. Hunter, R. L., Overview of vaccine adjuvants: present and future. *Vaccine* 2002;**20 Suppl 3**:S7-12.

53. Cox, J. C., Coulter, A. R., Adjuvants--a classification and review of their modes of action. *Vaccine* 1997;**15**:248-56.

54. Freund, J., The effect of paraffin oil and mycobacteria on antibody formation and sensitization; a review. *Am J Clin Pathol* 1951;**21**:645-56.

55. Tritto, E., Mosca, F., et al., Mechanism of action of licensed vaccine adjuvants. *Vaccine* 2009 (in press); doi:10.1016/j.vaccine.2009.01.084

56. Gupta, R. K., Relyveld, E. H., et al., Adjuvants--a balance between toxicity and adjuvanticity. *Vaccine* 1993;**11**:293-306.

57. Gupta, R. K., Siber, G. R., Adjuvants for human vaccines--current status, problems and future prospects. *Vaccine* 1995;**13**:1263-76.

58. Marciani DJ., Vaccine adjuvants: role and mechanisms of action in vaccine immunogenicity. *Drug Discov Today* 2003;**8**:934-43.

59. Alving, C. R., Design and selection of vaccine adjuvants: animal models and human trials. *Vaccine* 2002;**20 Suppl 3**:S56-64.

60. Dillon, S. B., Demuth, S. G., et al., Induction of protective class I MHC-restricted CTL in mice by a recombinant influenza vaccine in aluminium hydroxide adjuvant. *Vaccine* 1992;**10**:309-18.

61. Eldridge, J. H., Hammond, C. J., et al., Controlled vaccine release in the gut-associated lymphoid tissues. 1. Orally administered biodegradable microspheres target the Peyer's patches. *J Control Release* 1990;**11**:205-14.

62. Gupta, R. K., Singh, M., et al., Poly(lactide-co-glycolide) microparticles for the development of single-dose controlled-release vaccines. *Adv Drug Deliv Rev* 1998;**32**:225-46.

63. Medzhitov, R., Janeway, C., Innate immunity. *NEJM* 2000;**343**:338-344.

64. Akira, S., Takeda, K., et al., Toll-like receptors: critical proteins linking innate and acquired immunity. *Nat Immunol* 2001;**2**:675-80.

65. Hallman, M., Rämet, M., et al., Toll-like receptors as sensors of pathogens. *Pediatr Res* 2001;**50**:315-21.

66. Lien, E., Sellati, T. J., et al., Toll-like receptor-2 functions as a pattern recognition receptor for diverse bacterial products. *J Biol Chem* 1999;**274**:33419-25.

67. Parkin, J., Cohen, B., An overview of the immune system. *Lancet* 2001;**357**:1777-89.

68. Hathcock, K. S., Laszlo, G., et al., Comparative analysis of B7-1 and B7-2 costimulatory ligands: Expression and function. *J Exp Med* 1994;**180**:631-40.

69. Fleischer, J., Soeth, E., et al., Differential expression and function of CD80 (B7-1) and CD86 (B7-2) on human peripheral blood monocytes. *Immunology* 1996;**89**:592-8.

70. Chang, C. H., Furue, M., et al., B7-1 expression of Langerhans cells is up-regulated by proinflammatory cytokines, and is down-regulated by interferon-gamma or by interleukin-10. *Eur J Immunol* 1995;**25**:394-8.

71. Nabavi, N., Freeman, G. J., et al., Signalling through the MHC class II cytoplasmic domain is required for antigen presentation and induces B7 expression. *Nature* 1992;**360**:266-8

72. Krummel, M. F., Allison, J. P., CD28 and CTLA-4 have opposing effects on the response of T cells to stimulation. *J Exp Med* 1995;**182**:459-65.

73. Boussiotis, V. A., Freeman, G. J., et al., Activated human B lymphocytes express three CTLA-4 counterreceptors that costimulate T-cell activation. *Proc Natl Acad Sci USA* 1993;**90**:11059-63.

74. Rhodes, J., Covalent chemical events in immune induction: fundamental and therapeutic aspects. *Immunol Today* 1996;**17**:436-41.

75. Murphy, K. M., Reiner, S. L., The lineage decisions of helper T cells. *Nat Rev Immunol* 2002;**2**:933-44.

76. Edwards, K.M., Davis, et al., Anti-viral strategies of cytotoxic T lymphocytesare manifested through a variety of granule-bound pathways of apoptosis induction. *Immunol Cell Biol* 1999;**77**:76-89.

77. Scalzo, A. A., Elliott, S. L., et al., Induction of protective cytotoxic T cells to murine cytomegalovirus by using a nonapeptide and a human-compatible adjuvant (Montanide ISA 720). *J Virol* 1995;**69**:1306-9.

78. Baldon, C. M., *Pharmaceutical Chemistry*. 2007, New York: Wiley. pp. 95-119.

79. Kensil, C. R., Patel, U., et al., Separation and characterization of saponins with adjuvant activity from Quillaja saponaria Molina cortex. *J Immunol* 1991;**146**:431-7.

80. Vogel, F. R., Hem, S. L., Immunologic adjuvants, In *Vaccines*, Plotkin, S. A. and Orenstein, W. A., Editors. 4th edition, 2004, Elsevier Inc: Philadelphia. pp. 69-79.

81. Alving, C. R., Verma, J. N., et al., Liposomes containing lipid A as a potent non-toxic adjuvant. *Res Immunol* 1992;**143**:197-8.

82. Alving, C. R., Lipopolysaccharide, lipid A, and liposomes containing lipid A as immunologic adjuvants. *Immunobiology* 1993;**187**:430-46.

83. Kersten, G. F., Crommelin, D. J., Liposomes and ISCOMS as vaccine formulations. *Biochim Biophys Acta* 1995;**1241**:117-38.

84. Gupta, R. K., Chang, A. C., et al., Biodegradable polymer microspheres as vaccine adjuvants and delivery systems. *Dev Biol Stand* 1998;**92**:63-78.

85. Glenney, A. T., Pope, C. G., et al., XXIII-the antigenic value of toxoid precipitated by potassium alum. *J Pathol Bacteriol* 1926;**29**:38-9.

86. Baylor, N. W., Egan, W., et al., Aluminum salts in vaccines--US perspective. *Vaccine* 2002;**20 Suppl 3**:S18-23.

87. Lindblad, E. B., Aluminium adjuvants--in retrospect and prospect. *Vaccine* 2004;**22**:3658-68.

88. Kawamura, Y., Sawai, Y., Study on Indian cobra venom toxoid. *Snake* 1989;**21**:6-8.

89. Kawamura, Y., Sawai, Y., Study on the immunogenicity of purified toxoid of siamese cobra (Naja Naja koauthia) venom. *Snake* 1989;**21**:81-4.

90. Fujimaki, H., Ozawa, M., et al., Adjuvant effects of aluminum silicate on IgE and IgG1 antibody production in mice. *Int Arch Allergy Appl Immunol* 1984;**75**:351-6.

91. Cooper, P. D., Steele, E. J., Algammulin, a new vaccine adjuvant comprising gamma inulin particles containing alum: preparation and in vitro properties. *Vaccine* 1991;**9**:351-7.

92. Cooper, P. D., McComb, C., et al., The adjuvanticity of Algammulin, a new vaccine adjuvant. *Vaccine* 1991;**9**:408-15.

93. Hilleman, M. R., Woodhour, A. F., et al., Studies for safety of adjuvant 65. *Ann Allergy* 1972;**30**:477-83.

94. Woodhour, A. F., Metzgar, D. P., et al., New Metabolizable Immunologic Adjuvant for Human Use. I. Development and Animal Immune Response. *Proc Soc Exp Biol Med* 1964;**116**:516-23.

95. Burrell L. S., Schulze D., et al., Aluminium phosphate adjuvants prepared by precipitation at constant pH. Part I: composition and structure. *Vaccine* 2001;**19**:275-81.

96. Nail, S., L., White, J., L., et al., Structure of aluminium hydroxide gel. Part I. Initial precipitate. *J Pharm Sci* 1976;**65**:1188-91.

97. Hem, S. L., White, J. L., Characterisation of aluminium hydroxide for use as an adjuvant in parenteral vaccines. *J Parent Sci Techn* 1984;**38**:2-11.

98. Gupta, P., Saxena, S. N., et al., Effect of different concentrations of diphtheria toxoid & aluminum phosphate on potency of diphtheria component in DPT vaccines. *Indian J Med Res* 1990;**91**:171-3.

99. Denoel, P., Poolman, J., et al., Effects of adsorption of acellular pertussis antigens onto different aluminium salts on the protective activity in an intranasal murine model of *Bordetella pertussis* infection. *Vaccine* 2002;**20**:2551-5.

100. Krantz, I., Sekura, R., et al., Immunogenicity and safety of a pertussis vaccine composed of pertussis toxin inactivated by hydrogen peroxide, in 18- to 23-month-old children. *J Pediatr* 1990;**116**:539-43.

101. Redhead, K., Riley, A., et al., The effect of adsorption with aluminium hydroxide on the reactogenicity of pertussis vaccines. *Biologicals* 1999;**27**:111.

102. Scheifele, D. W., Halperin, S. A., et al., Assessment of injection site reactions to an acellular pertussis-based combination vaccine, including novel use of skin tests with vaccine antigens. *Vaccine* 2001;**19**:4720-6.

103. Eickhoff, T. C., Myers, M., Workshop summary. Aluminum in vaccines. *Vaccine* 2002;**20 Suppl 3**:S1-4.

104. Verdier, F., Burnett, R., et al., Aluminium assay and evaluation of the local reaction at several time points after intramuscular administration of aluminium containing vaccines in the Cynomolgus monkey. *Vaccine* 2005;**23**:1359-67.

105. Holt, L. B., *Developments in diphtheria prophylaxis*. London: Wm. Heinemann Ltd;1950.

106. Gupta, R. K., Chang, A.C., In vivo distribution of radioactivity in mice after injection of biodegradable polymer microspheres containing 14C-labelled tetanus toxoid. *Vaccine* 1996;**14**:1412-16.

107. Iyer, S., HogenEsch, H., et al., Relationship between the degree of antigen adsorption to aluminum hydroxide adjuvant in interstitial fluid and antibody production. *Vaccine* 2003;**21**:1219-23.

108. Mannhalter, J. W., Neychev, H. O., et al., Modulation of the human immune response by the non-toxic and non-pyrogenic adjuvant aluminium hydroxide: effect on antigen uptake and antigen presentation. *Clin Exp Immunol* 1985;**61**:143-51.

109. Morefield, G. L., Sokolovska, A., et al., Role of aluminium-containing adjuvants in antigen internalisation by dendritic cells in vitro. *Vaccine* 2005;**23**:1588-95.

110. White, R. G., Coons, A. H., et al., Studies on antibody production. III. Th alum granuloma. *J Exp Med* 1955 **102**:73-82.

111. Goto, N., Kato, H., et al., Local tissue irritating effects and adjuvant activities of calcium phosphate and aluminium hydroxide with different physical properties. *Vaccine* 1997;**15**:1364-71

112. Hornung, V., Bauernfeind, F., Silica crystals and aluminium salts activate the NALP3 inflammasome through phagosomal destabilisation. *Nat Immunol* 2008;**9**:847-56.

113. Hem, S. L., Elimination of aluminum adjuvants. *Vaccine* 2002;**20 Suppl 3**:S40-3.

114. Bergfors, E., Trollfors, B., et al., Unexpectedly high incidence of persistent itching nodules and delayed hypersensitivity to aluminium in children after the use of adsorbed vaccines from a single manufacturer. *Vaccine* 2003;**22**:64-9.

115. Pittman, P. R., Aluminum-containing vaccine associated adverse events: role of route of administration and gender. *Vaccine* 2002;**20 Suppl 3**:S48-50.

116. Rennels, M. B., Deloria, M. A., et al., Lack of consistent relationship between quantity of aluminum in diphtheria-tetanus-acellular pertussis vaccines and rates of extensive swelling reactions. *Vaccine* 2002;**20 Suppl 3**:S44-7.

117. Thierry-Carstensen, B. and Stellfeld, M., Itching nodules and hypersensitivity to aluminium after the use of adsorbed vaccines from SSI. *Vaccine* 2004;**22**:1845.

118. Cvjetanovic, B., Umera, K., The present status of field and laboratory studies of typhoid and paratyphoid vaccines with special reference to studies sponsored by the World Health Organisation. *Bull World Health Organ* ;**32**:29-36.

119. Davenport, F. M., Hennessy, A. V., et al., Lack of adjuvant effect of $AlPO_4$ on purified influenza virus haemagglutinins in man. *J Immunol* 1968;**100**:1139-40.

120. Gupta, R., Aluminium compounds as vaccine adjuvants. *Adv Drug Deliv Rev* 1998;**32**:155-172.

121. Lindblad, E. B., Elhay, M. J., et al., Adjuvant modulation of immune responses to tuberculosis subunit vaccines. *Infect Immun* 1997;**65**:623-9.

122. Francis, M. J., Fry, C. M., et al., Immune response to uncoupled peptides of foot-and-mouth disease virus. *Immunology* 1987;**61**:1-6.

123. Francis, M. J., Fry, C. M., et al., Immunological priming with synthetic peptides of foot-and-mouth disease virus. *J Gen Virol* 1985;**66** (Pt 11):2347-54.

124. Sturgess, A. W., Rush, K., et al., *Haemophilus influenzae* type b conjugate vaccine stability: catalytic depolymerization of PRP in the presence of aluminum hydroxide. *Vaccine* 1999;**17**:1169-78.

125. Gupta, R. K., Rost, B. E., et al., Adjuvant properties of aluminum and calcium compounds. *Pharm Biotechnol* 1995;**6**:229-48.

126. Jiang, D., Premachandra, G. S., et al., Structure and adsorption properties of commercial calcium phosphate adjuvant. *Vaccine* 2004;**23**:693-8.

127. Edelman, R., Vaccine adjuvants. *Rev Infect Dis* 1980;**2**:370-83.

128. Schultze, V., D'Agosto, V., et al., Safety of MF59™ adjuvant. *Vaccine* 2008;**26**:3209-22.

129. http://www.ifpma.org/influenza/content/images/MF59.jpg

130. Valensi, J. P. M., Carlson, J. R., et al., Systemic cytokine profiles in BALB/c mice immunized with trivalent influenza vaccine containing MF59 oil emulsion and other advanced adjuvants. *J Immunol* 1994;**153**:4029-39.

131. Higgins, D. A., Carlon, J. R., et al., MF59 enhances the immunogenicity of influenza vaccine in both young and old mice. *Vaccine* 1996;**14**:478-84.

132. Singh, M., Carlson, J. R., et al., A comparison of biodegradable microparticles and MF59 as systemic adjuvants for recombinant gD from HSV-2. *Vaccine* 1998;**16**:1822-7.

133. Singh, M., Ugozzoli, M., et al., A preliminary evaluation of alternative adjuvants to alum using a range of established and new generation vaccine antigens. *Vaccine* 2006;**24**:1680-16.

134. O'Hagan, D. T., Singh, M., et al., Synergistic adjuvant activity of immunostimulatory DNA and oil/water emulsions for immunization with HIV p55 gag antigen. *Vaccine* 2002;**20**:3389-98.

135. Ott, G., Singh, M., et al., A cationic sub-micron emulsion (MF59/DOTAP) is an effective delivery system for DNA vaccines. *J Control Release* 2002;**79**:1-5.

136. Wack, A., Baudner, B., et al., Combination adjuvants for the induction of potent, long-lasting antibody and T cell responses to influenza vaccine. *Vaccine* 2008;**26**:552-61.

137. Dupuis, M., Murphy, T. J., Dendritic cells internalize vaccine adjuvant after intramuscular injection. *Cell Immunol* 1998;**186**:18-27.

138. Dupuis, M., McDonald, D. M., Distribution of adjuvant MF59 and antigen gD2 after intramuscular injection in mice. *Vaccine* 1999;**18**:434-9

139. Dupuis, M., Denis-Mize1, K., et al., Immunization with the adjuvant MF59 induces macrophage trafficking and apoptosis. *Eur J Immunol* 2001;**31**:2910-8.

140. Baldrick, P., Richardson, D., et al., Safety evaluation of monophosphoryl lipid A (MPL): an immunostimulatory adjuvant. *Regul Toxicol Pharmacol* 2002;**35**:398-413.

141. Baldridge, J. R., Crane, R. T., Monophosphoryl lipid A (MPL) formulations for the next generation of vaccines. *Methods* 1999;**19**:103-7.

142. De Becker, G., Moulin, V., et al., The adjuvant monophosphoryl lipid A increases the function of antigen-presenting cells. *Int Immunol* 2000;**12**:807-15.

143. Ismaili, J., Rennesson, J., et al., Monophosphoryl lipid A activates both human dendritic cells and T cells. *J Immunol* 2002;**168**:926-32.

144. Martin, M., Michalek, S. M., et al., Role of innate immune factors in the adjuvant activity of monophosphoryl lipid A. *Infect Immun* 2003;**71**:2498-507.

145. Persing, D. H., Coler, R. N., et al., Taking toll: lipid A mimetics as adjuvants and immunomodulators. *Trends Microbiol* 2002;**10**:S32-7.

146. Todd, C. W., Balusubramanian, M., et al., Development of adjuvant-active nonionic block copolymers. *Adv Drug Deliv Rev* 1998;**32**:199-223.

147. Kovacsovics-Bankowski, M., Clark, K., et al., Efficient major histocompatibility complex class I presentation of exogenous antigen upon phagocytosis by macrophages. *Proc Natl Acad Sci U S A* 1993;**90**:4942-6.

148. Cox, J. C., Sjolander, A., et al., ISCOMs and other saponin based adjuvants. *Adv Drug Deliv Rev* 1998;**32**:247-271.

149. Myschik, J., Lendemans, D. G., et al., On the preparation, microscopic investigation and application of ISCOMs. *Micron* 2006;**37**:724-34.

150. Sjolander, A., Cox, J. C., et al., ISCOMs: an adjuvant with multiple functions. *J Leukoc Biol* 1998;**64**:713-23.

151. Copland, M. J., Rades, T., et al., Hydration of lipid films with an aqueous solution of Quil A: a simple method for the preparation of immune-stimulating complexes. *Int J Pharm* 2000;**196**:135-9.

152. Kersten, G. F., Crommelin, D. J., Liposomes and ISCOMs. *Vaccine* 2003;**21**:915-20.

153. Kersten, G. F., Spiekstra, A., et al., On the structure of immune-stimulating saponin-lipid complexes (iscoms). *Biochim Biophys Acta* 1991;**1062**:165-71.

154. Kamstrup, S., San Martin, R., et al., Preparation and characterisation of quillaja saponin with less heterogeneity than Quil-A. *Vaccine* 2000;**18**:2244-9.

155. Sjolander, A., van't Land, B., et al., Iscoms containing purified Quillaja saponins upregulate both Th1-like and Th2-like immune responses. *Cell Immunol* 1997;**177**:69-76.

156. Levy, D., Gulik, A., et al., Phospholipid vesicle solubilization and reconstitution by detergents. Symmetrical analysis of the two processes using octaethylene glycol mono-n-dodecyl ether. *Biochemistry* 1990;**29**:9480-8.

157. Gluck, R., Adjuvant activity of immunopotentiating reconstituted influenza virosomes (IRIVs). *Vaccine* 1999;**17**:1782-7.

158. Cevc, G., Transfersomes, liposomes and other lipid suspensions on the skin: permeation enhancement, vesicle penetration, and transdermal drug delivery. *Crit Rev Ther Drug Carrier Syst* 1996;**13**:257-388.

159. Krishnan, L., Dicaire, C. J., et al., Archaeosome vaccine adjuvants induce strong humoral, cell-mediated, and memory responses: comparison to conventional liposomes and alum. *Infect Immun* 2000;**68**:54-63.

160. Brewer, J. M., Alexander, J., The adjuvant activity of non-ionic surfactant vesicles (niosomes) on the BALB/c humoral response to bovine serum albumin. *Immunology* 1992;**75**:570-5.

161. Brewer, J. M., Alexander, J., Studies on the adjuvant activity of non-ionic surfactant vesicles: adjuvant-driven IgG2a production independent of MHC control. *Vaccine* 1994;**12**:613-9.

162. Gupta, R. K., Varanelli, C. L., et al., Adjuvant properties of non-phospholipid liposomes (Novasomes) in experimental animals for human vaccine antigens. *Vaccine* 1996;**14**:219-25.

163. Mannino, R. J., Canki, M., et al., Targeting immune response induction with cochleate and liposome-based vaccines. *Adv Drug Deliv Rev* 1998;**32**:273-87.

164. Jones, T., Cyr, S., et al., Protollin: a novel adjuvant for intranasal vaccines. *Vaccine* 2004;**22**:3691-7.

165. Lowell, G. H., Smith, L. F., et al., Peptides bound to proteosomes via hydrophobic feet become highly immunogenic without adjuvants. *J Exp Med* 1988;**167**:658-63.

166. Ruegg, C. L., Jaffe, R. I., et al., Preparation of proteosome-based vaccines. Correlation of immunogenicity with physical characteristics. *J Immunol Methods* 1990;**135**:101-9.

167. Langer, R., Cleland, J. L., et al., New advances in microsphere-based single-dose vaccines. *Adv Drug Deliv Rev* 1997;**28**:97-119.

168. Tabata, Y., Gutta, S., et al., Controlled delivery systems for proteins using polyanhydride microspheres. *Pharm Res* 1993;**10**:487-96.

169. Morita, T., Horikiri, Y., et al., Preparation of gelatin microparticles by co-lyophilization with poly(ethylene glycol): characterization and application to entrapment into biodegradable microspheres. *Int J Pharm* 2001;**219**:127-37.

170. Preis, I. and Langer, R. S., A single-step immunization by sustained antigen release. *J Immunol Methods* 1979;**28**:193-7.

171. Tabata, Y., Ikada, Y., Macrophage phagocytosis of biodegradable microspheres composed of L-lactic acid/glycolic acid homo- and copolymers. *J Biomed Mater Res* 1988;**22**:837-58.

172. Men, Y., Thomasin, C., et al., A single administration of tetanus toxoid in biodegradable microspheres elicits T cell and antibody responses similar or superior to those obtained with aluminum hydroxide. *Vaccine* 1995;**13**:683-9.

173. Moore, A., McGuirk, P., et al., Immunization with a soluble recombinant HIV protein entrapped in biodegradable microparticles induces HIV-specific CD8+ cytotoxic T lymphocytes and CD4+ Th1 cells. *Vaccine* 1995;**13**:1741-9.

174. Nixon, D. F., Hioe, C., et al., Synthetic peptides entrapped in microparticles can elicit cytotoxic T cell activity. *Vaccine* 1996;**14**:1523-30.

175. Rock, K. L., Clark, K., Analysis of the role of MHC class II presentation in the stimulation of cytotoxic T lymphocytes by antigens targeted into the exogenous antigen-MHC class I presentation pathway. *J Immunol* 1996;***156***:3721-6.

176. Donnelly, J. J., Deck, R. R., et al., Immunogenicity of a *Haemophilus influenzae* polysaccharide-*Neisseria meningitidis* outer membrane protein complex conjugate vaccine. *J Immunol* 1990;**145**:3071-9.

177. Eldridge, J. H., Meulbroek, J. A., et al., Vaccine-containing biodegradable microspheres specifically enter the gut-associated lymphoid tissue following oral administration and induce a disseminated mucosal immune response. *Adv Exp Med Biol* 1989;**251**:191-202.

178. Eskola, J., Kayhty, H., et al., A randomized, prospective field trial of a conjugate vaccine in the protection of infants and young children against invasive Haemophilus influenzae type b disease. *N Engl J Med* 1990;**323**:1381-7.

179. Gabutti, G., Zepp, F., et al., Evaluation of the immunogenicity and reactogenicity of a DTPa-HBV-IPV Combination vaccine co-administered with a Hib conjugate vaccine either as a single injection of a hexavalent combination or as two separate injections at 3, 5 and 11 months of age. *Scand J Infect Dis* 2004;**36**:585-92.

180. Eskola, J., Kayhty, H., Early immunization with conjugate vaccines. *Vaccine* 1998;**16**:1433-8.

181. Cadoz, M., Potential and limitations of polysaccharide vaccines in infancy. *Vaccine* 1998;**16**:1391-5.

182. McCluskie, M. J., Davis, H. L., CpG DNA is a potent enhancer of systemic and mucosal immune responses against hepatitis B surface antigen with intranasal administration to mice. *J Immunol* 1998;**161**:4463-6.

183. McCluskie, M. J.,Weeratna, R. D., et al., CpG is an effective oral adjuvant to protein antigens in mice. *Vaccine* 2001;**19**:950-7.

184. Krieg, A. M., Yi, A-K, et al., CpG motifs in bacterial DNA trigger direct B cell activation. *Nature* 1995;**374**:456-9.

185. Yi, A. K., Klinman, D. M., Rapid immune activation by CpG motifs in bacterial DNA. Systemic induction of IL-6 transcription through an antioxidant-sensitive pathway. *J Immunology* 1996; **157**:5394-402.

186. Klinman, D. M., Yi, A-K, et al., CpG motifs expressed by bacterial DNA rapidly induce lymphocytes to secrete IL-6, IL-12 and IFN-γ. *Proc Natl Acad Sci USA* 1996;**93**:2879.

187. Davis, H. L., Weeratna, R., et al., CpG DNA is a potent enhancer of specific immunity in mice immunized with recombinant hepatitis B surface antigen. *J Immunol* 1998;**160**:870-6.

188. Sparwasser, T., Koch, E. S., et al., Bacterial DNA and immunostimulatory CpG oligonucleotides trigger maturation and activation of murine dendritic cells. *Eur J Immunol* 1998;**28**:2045-54.

189. Halpern, M. D., Kurlander, R.J., et al., Bacterial DNA induces murine interferon-γ production by stimulation of interleukin-12 and tumor necrosis factor-α. *Cell Immunol* 1996;**167**:72.

190. http://www.landesbioscience.com/curie/images/chapters/Carpentier1color.gif

191. Roman, M., Martin-Orozco, E., et al., Immunostimulatory DNA sequences function as T helper-1-promoting adjuvants. *Nat Med* 1997;**3**:849-54.

192. Chu, R. S., Targoni, O. S., et al., CpG oligodeoxynucleotides act as adjuvants that switch on T helper 1 (Th1) immunity. *J Exp Med* 1997;**186**:1623-31.

193. Lipford, G. B., Bauer, M., et al., CpG-containing synthetic oligonucleotides promote B and cytotoxic T cell responses to protein antigen: a new class of vaccine adjuvants. *Eur J Immunol* 1997;**27**:2340-4.

194. Weiner, G., J., Liu, H. M., et al., Immunostimulatory oligodeoxynucleotides containing the CpG motif are effective as immune adjuvants in tumor antigen immunisation. *Proc Natl Acad Sci USA* 1997;**94**:10833-7.

195. Krieg, A. M., A to Z on CpG. *Trends Immunol* 2002;**23**:64-5.

196. Moyle, P. M., McGeary, R. P., et al., Mucosal immunisation: adjuvants and delivery systems. *Curr Drug Deliv* 2004;**1**:385-96.

197. Bauer, S., Kirchning, C. J., et al., Human TLR9 confers responsiveness to bacterial DNA via species-specific CpG motif recognition. *Proc Natl Acad Sci USA* 2001;**98**:9237-42.

198. Krieg, A. M., Wagner, H., Causing a commotion in the blood: immunotherapy progresses from bacteria to bacterial DNA. *Immunol Today* 2000;**21**:521-6.

199. Tran, T. T., Reich, C. F., et al., Specificity and immunochemical properties of ant-DNA antibodies induced in normal mice by immunisation with mammalian DNA with CpG oligonucleotide as adjuvant. *Clin Immunol* 2003;**109**:278-87.

200. Schlebusch, J., A briefing document on the use of the MeyerZall therapeautic system, based on Emzaloid™ technology, to increase the absorption of active ingredients, with special reference to MeyerZall Laboratories Tuberculosis Medicine Project. Briefing document as tribute to the colleagues at MeyerZall. 2002, George.

201. Grobler, A. F., Background to the Emzaloid™. [Confidential: Concept document]. 2004, North West University.

202. Colombo, P., Bettini, R., et al., Swellable matrices for controlled drug delivery: gel-layer behaviour, mechanisms and optimal performance. *Pharm Sci Technolo Today* 2000;**3**:198-204.

203. Hertzel, A. V., Bernlohr, D. A., The mammalian fatty acid-binding protein multigene family: molecular and genetic insights into function. *Trends in Endocrinol Metab* 2000;**11**:175- 80.

204. Drummond, D. C., Meyer, O., et al., Optimizing liposomes for delivery of chemotherapeutic agents to solid tumors. *Pharmacol Rev* 1999;**51**: 691- 743.

205. Bradley, D., Water insoluble drugs set for oral delivery. *Pharm Sci Technolo Today* 1999;**2**:427.

206. Kurzchalia, T. V., Parton, R. G., Membrane microdomains and caveolae. *Curr Opin Cell Biol* 1999;**11**:424-31.

207. Owen, D. J., Luzio, J. P., Structural insights into clathrin-mediated endocytosis. *Curr Opin Cell Biol* 2000;**12**: 467-74.

208. Falk, L. A., Ball, L. K., Current status and future trends in vaccine regulation--USA. *Vaccine* 2001;**19**:1567-72.

209. Sesardic, D., Regulatory considerations on new adjuvants and delivery systems. *Vaccine* 2006;**24 Suppl 2**:S2-86-7.

210. Sesardic, D., Dobbelaer, R., European union regulatory developments for new vaccine adjuvants and delivery systems. *Vaccine* 2004;**22**:2452-6.

211. Lindberg, A. A., Glycoprotein conjugate vaccines. *Vaccine* 1999;**17**:S28-36.

212. Ada, G., Carbohydrate-protein conjugate vaccines. *Clin Microbiol Infect* 2003;**9**:79-85.

213. Avery, O. T., Goebel, W. F., Chemo-immunological studies on conjugated carbohydrate proteins. II. Immunological specificity of synthetic sugar protein antigen. *J Exp Med* 1929;**50**:533-50.

214. Jones, C., Vaccines based on the cell surface carbohydrates of pathogenic bacteria. *Ann Bras Acad Sci* 2005;**77**:293-324.

215. Prymula, R., Chlibek, R., et al., Safety of the 11-valent pneumococcal vaccine conjugated to non-typeable *Haemophilus influenzae*-derived protein D in the first 2 years of life and immunogenicity of the co-administered hexavalent diphtheria, tetanus, acellular pertussis, hepatitis B, inactivated polio virus, *Haemophilus influenzae* type b and control hepatitis A vaccines. *Vaccine* 2008;**26**:4563-70.

216. Prymula, R., Kriz, P, et al., Effect of vaccination with pneumococcal capsular polysaccharide conjugated to *Haemophilus influenzae*-derived protein D on nasopharyngeal carriage of *Streptococcus pneumoniae* and *H. influenzae* in children under 2 years of age. Vaccine 2009 (in press);doi:10.1016/j.vaccine.2009.09.113.

217. Anderson, P. W., Pichichero M. E., et al., Vaccines consisting of eriodate-cleaved oligosaccharides from the capsule of *Haemophilus influenzae* type b coupled to a protein carrier: structural and temporal requirements for priming in human infants. *J Immunol* 1986;**137**:1181-6.

218. Ravenscroft, N., The application of NMR spectroscopy to track industrial preparation of polysaccharide and derived glycoconjugate vaccines. *Pharmeuropa 2000*, Special issue "Biologicals beyond 2000: Challenge for quality standards in an evolving field", pp 131-44.

219. Szu, S. C., Stone, A. L., et al., Vi capsular polysaccharide-protein conjugates for prevention of typhoid fever – preparation, characterisation, and immunogenicity in laboratory animals. *J Exp Med* 1987;**166**:1510-24.

220. Fattom, A., Vann, W. F., et al., Synthesis and physicochemical and immunological characterization of pneumococcal type 2F polysaccharide-diphtheria toxoid conjugates. *Infect Immunol* 1988;**56**:2292-8.

221. Fattom, A., Li, X., et al., Effect of conjugation methodology, carrier protein, and adjuvants on the immune response to *Staphylococcus aureus* capsular polysaccharides. *Vaccine* 1995;**13**:1288-93.

222. Shafer, D. E., Toll, B., et al., Activation of soluble polysaccharides with 1-cyano-4-dimethylaminopyridinium tetrafluoroborate (CDAP) for use in protein-polysaccharide conjugate vaccines and immunological reagents. II. Selective crosslinking of proteins for CDAP-activated polysaccharides. *Vaccine* 2000;**18**:1273-81.

223. Laferriere, C. A., Sood, R. K., et al., The synthesis of *Streptococcus pneumonia* polysaccharide-tetanus toxoid conjugates and the effects of chain length on immunogenicity. *Vaccine* 1997;**15**:179-86.

224. Laferriere, C. A., Sood, R. K., et al., *Streptococcus pneumonia* type 14 polysaccharide-conjugate vaccines: length stabilization of opsonophagocytic conformational polysaccharide epitopes. *Infect Immune* 1998;**66**:2441-6.

225. Ravenscroft, N., Feavers, I. M., Conjugate vaccines. In: Frosch, M., Maiden, M., Editors, *Handbook of meningococcal disease*, Weinheim, Wiley-VCH Verlag GmbH & Co, 2006, pp343-69.

226. Finn, A., Bacterial polysaccharide-protein conjugate vaccines. *Br Med Bull* 2004;**70**:1-14.

227. Crisel, R. M., Baker, R. S., et al., Capsular polymer of *Haemophilus influenzae* type b. I. Structural characterization of the capsular polymer of strain Eagan. *J Biol Chem* 1975;**250**:4926-30.

228. Wegner, J. D., Ward, J. I., *Haemophilus influenzae* vaccine. In *Vaccines*, Plotkin, S. A. and Orenstein, W. A., Editors. 4th edn, 2004, Elsevier Inc: Philadelphia. pp. 229-68.

229. Peltola, H., Rod, T. O., et al., Life threatening *Haemophilus influenzae* infections in Scandinavia: a five-country analysis of the incidence and the main clinical and bacteriologic characteristics. *Rev Infect Dis* 1990;**12**:708-15.

230. Claesson, B., Trollfors, B., et al., Incidence and prognosis of *Haemophilus influenzae* meningitis in children in a Swedish region. *Pediatr Infect Dis* 1984;**3**:35-9.

231. Salwen, K. M., Vikerfors, T., et al., Increased incidence of childhood bacterial meningitis: a 25-year study in a defined population in Sweden. *Scand J Infect Dis* 1987;**19**:1-11.

232. Trollfors, B., Claesson, B. A., et al., *Haemophilus influenzae* meningitis in Swden, 1981-1983. *Arch Dis Child* 1987;**62**:1220-3.

233. Valmari, P., Kataja, M., et al., Invasive *Haemophilus influenzae* and meningococcal infections in Finland: a climatic, epidemiologic and clinical approach. *Scand J Infect Dis*1987;**19**:19-27.

234. Peltola, H., Kayhty, H., et al., Prevention of *Haemophilus influenzae* type b bacteremic infection with the capsular polysaccharide vaccine. *N Engl J Med* 1984;**310**:1561-6.

235. Spanjaard, L., Bol, P., et al., The incidence of bacterial meningitis in the Netherlands – a comparison of three registration systems, 1977-1982. *J Infect* 1985;**11**:259-68.

236. Hanna, J. N., The epidemiology of invasive *Haemophilus influenzae* infections in children under 5 years of age in the Northern Territory: a three-year study. *Med J Aust* 1990;**152**:234-6.

237. Hammond, G. W., Rutherford, B. E., et al., *Haemophilus influenzae* meningitidis in Manitoba and the Keewatin District, NWT: potential for mass vaccination. *CMAJ* 1988;**139**:743-7.

238. Varaghese, P., *Haemophilus influenzae* infection in Canada, 1969-1985. *Can Dis Wkly Rep* 1986;**12**:37-43.

239. Hanna, J. N., Wild, B. E., Bacterial meningitis in children under five years of age in Western Australia. *Med J Aust* 1991;**155**:160-4.

240. Hansman, D., Hanna, J., et al., High prevalence of invasive *Haemophilus influenzae* disease in central Australia. *Lancet* 1986;**2**:927.

241. Takala, A., Eskola, J., et al., Spectrum of invasive *Haemophilus influenzae* type b disease in adults. *Arch Intern Med* 1990;**150**:2573-6.

242. Bijlmer, H. A., van Alphen, L., et al., The epidemiology of meningitis in children under 5 years of age in The Gambia, West Africa. *J Infect Dis* 1990;**161**:1210-15.

243. Wright, P. F., Approaches to prevent acute bacterial meningitis in developing countries. *Bull World Health Organ* 1998:67:479-86.

244. Bijlmer, H. A., Worldwide epidemiology and cost of *Haemophilus influenzae* meningitis: industrialized versus non-industralized countries. *Vaccine* 1991;**9 (suppl)**:S5-9.

245. Clements, D. A., Booy, R., et al., Comparison of the epidemiology and cost of *Haemophilus influenzae* type b disease in five western countries. *Pediatr Infect Dis J* 1993;**12**:362-7. [erratum appears in *Pediatr Infect Dis J* 1993;:570].**12**

246. Gomez, E., Peguero, M., et al., Population-based surveillance for bacterial meningitis in the Dominican Republic: implications for control by vaccination. *Epidemiol Infect* 2000;**125**:549-54.

247. Campagne, G., Schuchat, A., et al., Epidemiology of bacterial meningitis in Niamey, Niger, 1981-1996. *Bull World Health Organ* 1999;**77**:499-508.

248. Adegbola, R. A., Mulholland, E. K., et al., *Haemophilus influenzae* type b disease in the western region of The Gambia: background surveillance for a vaccine efficacy trial. *Ann Trop Paediatr* 1996;**16**;103-111.

249. Peltola, H., Burden of meningitis and other severe bacterial infections of children in Africa: implications for prevention. *Clin Infect Dis* 2001;**32**:64-75.

250. Lee, Y. S., Kumarasinghe, G., et al., Invasive *Haemophilus influenzae* type b infections in Singapore children: a hospital-based study. *J Pediatr Child Health* 2000;**36**:125-7.

251. Yonghong, Y., Zhigua, L., et al., Acute bacterial meningitis in children in Hefea, China, 1990-1992. *Chinese Medical J China* 1996;**109**:385-8.

252. Lau, Y. L., Low, L. C. K., et al., Invasive *Haemophilus influenzae* type b infections in children hospitalised in Hong Kong, 1986-1990. *Acta Paediatr* 1995;**84**:173-6.

253. Limcangco, M. R., Salole, E. G., et al., Epidemiology of *Haemophilus influenzae* type b meningitis in Manila, Philippines, 1994-1996. *Pediatr Infect Dis* J 2000;**19**:7-11.

254. Lupisan, S. P., Herva, E., et al., Incidence of invasive *Haemophilus influenzae* type b infections in Filipino children. *Pediatr Infect Dis J* 2000;**19**:1020-22.

255. Hsueh, P. R., Wu, J. J., et al., Invasive *Streptococcus pneumoniae* infection associated with rapidly fatal outcome in Taiwan. *J Formos Med Assoc* 1996;**95**:364-71.

256. Invasive Bacterial Infections Surveillance (IBIS) Group of the International Clinical Epidemiology Network. Are *Haemophilus influenzae* infections a significant problem in India? A prospective study and review. *Clin Infect Dis* 2002;**34**:949-57.

257. Nakano, T., Ihara, T., et al., Incidence of *Haemophilus influenzae* type b meningitis in Mie prefecture, *Japan. Pediatr Int* 2001;**43**:323-4.

258. Hougs, L., Juul, L., et al., The first dowse of a Haemophilus influenzae type b conjugate vaccine reactivates memory B cells: evidence for extensive clonal selection, intraclonal affinity maturation and multiple isotype switches to IgA2. *J Immunol* 1999;**162**:224-37. Erratum published in *J Immunol* 2001;**166**:2147.

259. Frasch C. E., Recent developments in *Neisseria meningitidis* group A conjugate vaccines. *Expert Opin Biol Ther* 2005;**5**:273-80.

260. Bergguist, C., Lagergard, T., et al., Antibody responses in serum and lung to intranasal immunisation with *Haemophilus influenzae* type b polysaccharide conjugated to cholera toxin B subunit and tetanus toxoid. *APMIS* 1998;**106**:800-6.

261. Mariotti, S., Teloni, R., et al., Immunogenicity of aniti-*Haemophilus influenzae* type b CRM_{197} conjugate following mucosal vaccination with oligodeoxynucleotide containing immunostimulatory sequences as adjuvant. *Vaccine* 2002;**20**:2229-39.

262. Ugozzoli, M., Mariani, M., Combinations of protein polysaccharide conjugate vaccines for intranasal immunisation. *J Infect Dis* 2002;**186**:1358-61.

263. Goldblatt, D., Pinto Vaz, A. J. P. M., et al., Antibody avidity as a surrogate marker of successful priming by *Haemophilus influenzae* type b conjugate vaccines following infant immunization. *J Infect Dis* 1998;**177**:1112-5.

264. Peltola, H., Kilpi, T., et al., Rapid disappearance of *Haemophilus influenzae* type b meningitis after routine childhood immunisation with conjugate vaccines. *Lancet* 1992;**340**:592-4.

265. Barbour, M. L., Mayon-White, R. T., et al., Th impact of conjugate vaccine on carriage of *Haemophilus influenzae* type b. *J Infect Dis* 1995;**171**:93-8.

266. Booy, R., Heath, P. T., et al., Vaccine failures after primary immunization with *Haemophilus influenzae* type b. *Lancet* 1997;**349**:1197-202. [Erratum in *Lancet* 1997;**349**:1630]

267. Jonsdotir, K. E., Steingrimsson, O., et al., Immunisation of infants in Iceland against *Haemophilus influenzae* type b. *Lancet* 1992;**340**:252-3.

268. Production and control of *Neisseria meningitidis* vaccines. In: *Vaccines*. Mizrahi, A., Editor, 1990, Wiley-Liss, New York, USA. pp. 123-45.

269. World Health Report. Geneva, Switzerland: World Health Organisation; 2000.

270. Vogel, U., Frosch, M., Mechanisms of Neisseria serum resistance. *Mol Microbiol* 1999;**32**:1133-9.

271. McNeil, G., Virji, M., et al., Interactions of *Neisseria meningitidis* with human monocytes. *Microbl Pathog* 1994;**16**:153-53.

272. Jones, C., NMR assays for carbohydrate-based vaccines. *J Pharm Biomed Anal* 2005;**38**:840-50.

273. Schwartz, B., Moore, P. S., et al., Global epidemiology of meningococcal disease.*Clin Microbiol Rev* 1989;**2 (Suppl)**:S118-24.

274. Wang, J. F., Caugant, D. A., et al., Clonal and antigenic analysis of serogroup A *Neisseria meningitidis* with particular reference to epidemiological features of epidemic meningitis in the People's Republic of China. *Infect Immune* 1992;**60**:5267-82.

275. Achtman, M., Global epidemiology of meningococcal diseases. In: *Meningococcal disease*. Cartwright, K. A., Editor, 1995, John Wiley and Sons, Chichester. pp. 159-75.

276. Rosenstein, N. E., Perkins, B. A., et al., The changing epidemiology of meningococcal disease in the United states, 1992-1996. *J Infect Dis* 1999;**180**:1894-901.

277. National Advisory Committee on Immunization (NACI) statement on recommended use of meningococcal vaccines. *Can Commun Dis Rep* 2001;**27**:ACS6 (http://www.phac-aspc.gc.ca/publicat/ccdr-rmtc/01vol27/27sup/acs6.html). Accessed 26 May 2009.

278. Baker, M., McNicholas, A., et al., Household crowding a major risk factor for epidemic meningococcal disease in Auckland children. *Pediatr Infect Dis J* 2000;**19**:983-90.

279. Diermayer, M., Hedberg, K., et al., Epidemic serogroup B meningococcal disease in Oregon: the evolving epidemiology of the ET-5 strain. *JAMA* 1999;**281**:1493-7.

280. Stuart, J. M., Cartwright, K. A., et al., An outbreak of meningococcal disease in Stonehouse: planning and execution of a large-scale survey. *Epidemiol Infect* 1987;**99**:579-89.

281. Centre for Disease Control and Prevention. Updat: Assessment of risk for meningococcal disease associated with the Hajj 2001. *Mortal Wkly Rep* 2001;**50**:221-2.

282. Guibourdenche, M., Hoiby E. A., et al., Epidemics of serogroup A *Neisseria meningitidis* of subgroup III in Africa, 1989-1994. *Epidemiol Infect* 1996;**116**:115-20.

283. Broome, C. V., Rugh, M. A., et al., Epidemic group C meningococcal meningitis in Upper Volta, 1979. *Bull World Health Organ* 1983;**61**:325-30.

284. Greenwood, B. M., Manson Lecture. Meningococcal meningitis in Africa. *Trans R Soc Trop Med Hyg* 1999;**93**:341-53.

285. Jodar, L., Feavers, I. M., et al., Development of vaccines against meningococcal disease. *Lancet* 2001;**359**:1499-508.

286. Yousuf, M., Nadeem, A., Meningococcal infection among pilgrims visiting Madinah Al-Munawarah despite prior A-C vaccination. *J Pak Med Assoc* 2000;**50**:184-6.

287. Taha, M. K., Achtman, M., et al., Serogroup W135 meningococcal disease in Hajj pilgrims. *Lancet* 2000;**356**:2159.

288. Wei, J., Zhang, W., et al., Changes of epidemic features of epidemic cerebrospinal meningitis after vaccination with purified meningococcal polysaccharide vaccine group A in Zhenghou. *J Chinese Preventive Med* 1993;**27**:160-1.

289. Sacchi, C. T., Pessoa, L. L., et al., Ongoing group B *Neisseria meningitidis* epidemic in Sao Paulo, Brazil, due to increased prevalence of a single clone of the ET-5 complex. *J Clin Micrbiol* 1992;**30**:1734-8.

290. Lystad, A., Aasen, S., The epidemiology of meningococcal disease in Norway 1975-91. *NIPH Am* 1991;**14**:57-65.

291. Peltola, H., Kataja, J. M., et al., Shift in the age-distribution of meningococcal disease as a predictor of an epidemic? *Lancet* 1982;**2**:595-7.

292. Poolman, J. T., Lind, I., et al., Meningococcal serotypes and serogroup B disease in north-west Europe. *Lancet* 1986;**2**:555-7.

293. Bovre, K., Holten, E., et al., *Neisseria meningitidis* infections in Northern Norway: an epidemic in 1974-1975 due mainly to group B organisms. *J Infect Dis* 1977;**135**:669-72.

294. De Maeyer, S., Seba, J. M., et al., Epidemiology of meningococcal meningitis in Belgium. *J Infect* 1981;**3**:63-70.

295. Mocca, L. F., del Real, G., et al., Serotypes and polyacrylamide gel electrophoresis types among disease-associated isolates of group B *Neisseria meningitidis* in Spain, 1976-1979. *J Infect Dis* 1983;**148**:249-53.

296. Jacobson, J. A., Chester, T. J., et al., An epidemic of disease due to serogroup B *Neisseria meningitidis* in Alabama: report on an investigation and community-wide prophylaxis with a solfonamide. *J Infect Dis* 1977;**136**:104-8.

297. Sierra, G. V., Campa, H. C., et al., Vaccine against group B *Neisseria meningitidis*: protection trial and mass vaccination results in Cuba. *NIPH Ann* 1991;**14**:195-207.

298. Cruz, C., Pavez, G., et al., Serotype-specific outbreak of group B meningococcal disease in Iquique, Chile. *Epidemiol Infect* 1990;**105**:119-26.

299. Costa, W., Sacchi, C. T., et al.,Meningococcal disease in Sao Paulo, Brazil. *NIPH Ann* 1991;**14**:216-6.

300. Ryder, C. S., Beatty, D. W., et al., Group B meningococcal infections in children during an epidemic in Cape Town, South Africa. *Ann Trop Paediatr* 1987;**7**:47-53.

301. Kirk, R., Two epidemics of cerebrospinal meningitis. *Sudan Notes and Records* 1950;**31**:43-53.

302. Finne, J., Bitter-Suermann, D., et al., An IgG monoclonal antibody to group B meningococci cross-reacts with developmentally regulated polysialic acid units of glycoproteins in neural and extraneural tissues. *J Immunol* 1987;**138**:4402-7.

303. Goldschneider, I., Gotschlich, E. C., et al., Human immunity to the meningococcus. I. The role of humoral antibodies. *J Exp Med* 1969;**129**:1307-26.

304. Pollard, A. J., Moxon, E. R., The meningococcus tamed? *Arch Dis Child* 2002;**87**:13-17.

305. Lepow, M. L., Beeler, J., et al., Reactogenicity and immunogenicity of a quadrivalent combined meningococcal polysaccharide vaccine in children. *J Infect Dis* 1986;**154**:1033-0.

306. Scheifele, D. W., Bjornson, G., et al., Local adverse effects of meningococcal vaccine. *CMAJ* 1994;**150**:14-5.

307. Prevention and control of meningococcal disease: recommendations of the Advisory Committee on Immunization Practices (ACIP). *Morb Mortal Wkly Rep* 2000;**49 (RR-7)**:1-10.

308. Rosenstein, N. E., Perkins, B. A., et al., Meningococcal diseas. *N Engl J Med* 2001;**344**:1378-88.

309. Lennon, D., Gellin, B., et al., Successful intervention in a group A meningococcal outbreak in Auckland, New Zealand. *Pediatr Infect Dis J* 1992;**11**:617-23.

310. Ramsay, M. E., Andrews, N., et al., Efficacy of meningococcal serogroup C conjugate vaccine in teenagers and toddlers in England. *Lancet* 2001;**357**:195-6.

311. Bilukha, O. O., Rosenstein, N., National Centre for Infectious Diseases, Centres for Disease Control and Prevention (CDC). Prevention and control of meningococcal disease. Recommendations of the Advisory Committee on Immunization Practices (ACIP). *MMWR Recomm Rep* 2005;**54**:1-21.

312. Rennels, M., King J. Jr., et al., Dosage escalation, safety and immunogenicity study of four dosages of a tetravalent meningococcal polysaccharide diphtheria toxoid conjugate vaccine in infants. *Pediatr Infect Dis J* 2004;**23**:429-35.

313. LaForce, F. M., Konde, K., Viviani, S., et al., The Meningitis Vaccine Project. *Vaccine* 2007;**25S**:A97-100.

314. Pletz, M. W., Maus, U., et al., Pneumococcal vaccines: mechanism of action, impact on epidemiology and adaptation of species. *Int J Antimicrob Agents* 2008;**32**:199-206.

315. 23-valent pneumococcal polysaccharide vaccine. WHO position paper. *Wkly Epidemiol Rec* 2008;**83**:373-84.

316. Trotter, C. L., McVernon, J., et al., Optimising the use of conjugate vaccines to prevent disease caused by Haemophilus influenzae type b, Neisseria meningitidis and Streptococcus pneumoniae. *Vaccine* 2008;**26**:4434-45.

317. Pneumococcal conjugate vaccine for childhood immunization. WHO position paper. *Wkly Epidemiol Rec* 2007;**82**:93-104.

318. Centre, K. J., Prevenar™ vaccination: Review of the global data, 2006. *Vaccine* 2007;**25**:3085-89.

319. Ravenscroft, N., Jones, C., Glycoconjugate vaccines. *Curr Opin Drug Discov Devel* 2000;**3**:222-31.

320. Baker, C. J., Paoletti, L. C., et al., Safety and immunogenicity of capsular polysaccharide-tetanus toxoid conjugate vaccines for group B streptococcal types Ia and Ib. *J Infect Dis* 1999;**179**:142-50.

321. Gravekamp, C., Kasper, S., et al., α C proteins as a carrier for type III capsular polysaccharide and as a protective protein in group B streptococcal vaccines. *Infect Immun* 1999;**67**:2491-6.

322. Baker, C. J., Paoletti, L. C., et al., Use of capsular polysaccharide-tetanus toxoid conjugate vaccine for type II group B streptococcus in healthy women. *J Infect Dis* 2000;**182**:1129-38.

323. Sru, S. C., Taylor, D. N., et al., Laboratory and preliminary clinical characterisation of Vi capsular polysaccharide-protein conjugate vaccines. *Infect Immun* 1994;**62**:4440-4.

324. Conlan, J. W., Cox, A. D., et al., Parenteral immunization with a glycoconjugate vaccine containing the O157 antigen of Escherichia coli O157:H7 elicits humoral immune response in mice, but fails to prevent colonization by the pathogen. *Can J Microbiol* 1999;**45**:279-86.

325. Pozsgay, V., Chu, C., et al, Protein conjugates of synthetic saccharides elicit higher levels of serum IgG lipopolysaccharide antibodies in mice than do those of the O-specific polysaccharide from *Shigella dysenteriae* type 1. *Proc Natl Acad Sci USA* 1999;**96**:5194-7.

326. Ashkenazi, S., Passwell, S. H., et al., Safety and immunogenicity of *Shigella sonnei* and *Shigella flexneri* 2a O-specific polysaccharide conjugates in children. *J Infect Dis* 1999;**179**:1565-8.

327. Gupta, R. K., Taylor, D. N., et al., Phase I evaluation of *Vibrio cholera* O1, serotype Inaba, polysaccharide-cholera toxin conjugates in adult volunteers. *Infect immune* 1998;**66**:3095-99.

DESCRIPTION OF PHYSICOCHEMICAL TECHNIQUES FOR THE CHARACTERISATION OF ADJUVANT AND VACCINE COMPONENTS

2.1 Analysis of Pheroid™ and raw materials by NMR spectroscopy and Coulter Counter

2.1.1 NMR spectroscopy

NMR spectroscopy is a technique that provides information about the electronic environment (composition) of a molecule and its structure. A sample dissolved in a suitable solvent and placed in a powerful magnetic field is irradiated with a short pulse of radiofrequency energy which disturbs the equilibrium balance of the ^{1}H and ^{13}C nuclei: some nuclei absorb the energy and are promoted to a higher energy level. When these nuclei fall back down to the lower energy level, the previously absorbed energy is released and quantified using a sophisticated radio receiver. In the 1D spectrum (Fig 2.1), the NMR signals are displayed as intensity against frequency (in parts per million or ppm)[1].

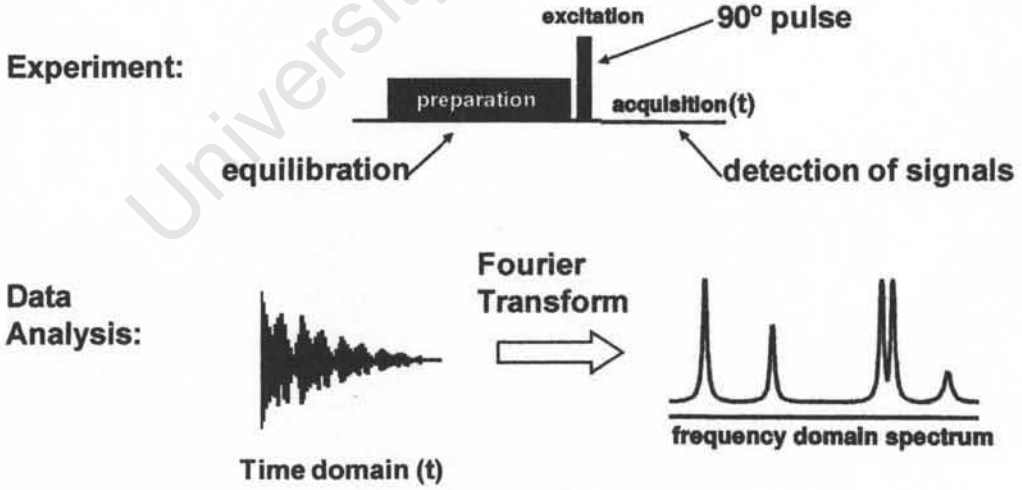

Fig 2.1: *The pulsed fourier transform NMR experiment*[2].

The samples used in this study were dissolved in d_6-DMSO (dipole moment = 3.96 D) or $CDCl_3$ (dipole moment = 1.01 D)[3]. Peaks for d_6-DMSO in ^{1}H- and ^{13}C-NMR spectra occur at 2.5 and 39.5 ppm respectively. $CDCl_3$ produces peaks in ^{1}H- and ^{13}C-NMR spectra at 7.26 and 77.0 ppm respectively. ^{1}H- and ^{13}C-NMR spectra obtained in both solvents were compared to ascertain which solvent gives the best spectra.

The spread of frequencies is caused by the different chemical (and hence magnetic) environments, therefore the signals are described as having a chemical shift (δ) from some standard frequency[4]. Tetramethylsilane $Si(CH_3)_4$ or TMS, was used as the reference sample and thus given a chemical shift of 0 ppm. Fig 2.2 shows the regions that ^{1}H-NMR spectra can typically be divided into. Tables of chemical shift data are available from published literature[5].

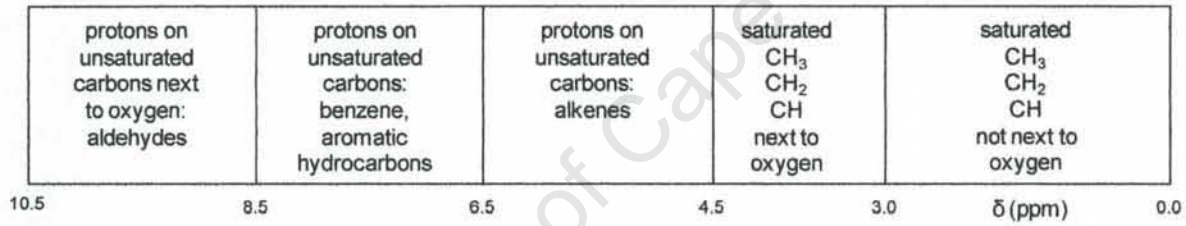

Fig 2.2: *Regions of ^{1}H-NMR spectra[6].*

All ^{13}C-NMR spectra can be divided into four major regions: saturated carbon atoms (0-50 ppm), saturated carbon atom next to oxygen (50-100 ppm), unsaturated carbon atoms (100-150 ppm) and unsaturated carbon atoms next to oxygen, i.e. C=O groups (150-200 ppm)[6].

2D correlation spectroscopy (COSY) can be used to provide useful structural information and consists of a plot of the 1D spectrum along the horizontal and vertical axes. Cross peaks obtained from the diagonal show scalar coupling between neighbouring protons[4]. In heteronuclear single quantum correlations (HSQC), the proton spectrum is correlated with the carbon spectrum. This permits assignments to be made and allows correlation between ^{13}C and the proton to which it is directly attached and confirms whether a proton signal and more importantly the integration is due to one or more proton. The long range ^{1}H-^{13}C COSY spectrum also known as heteronuclear multiple bond correlation (HMBC) allows connection between different spin systems. Thus, ^{13}C chemical shifts can be correlated with the

chemical shifts of protons separated from them by two ($^{1}H - C - {}^{13}C$) and three ($^{1}H - C - C - {}^{13}C$) bonds[4]. Technical details of the standard pulse sequences used in this study (COSY, HSQC, and HMBC) have been published and are provided in appendix A (pages 249-251)[7-9]. In the present study, emphasis is placed on the application of these pulse sequences to analyse the raw materials used to manufacture Pheroid™ and different Pheroid™ formulations.

2.1.2 Size analysis (Coulter Counter)

The Coulter Counter has been used to determine droplet size in oil-in-water emulsions[10-14]. Particles suspended in a weak electrolyte solution are drawn through a small aperture, separating two electrodes between which an electric current flows (Fig 2.3).

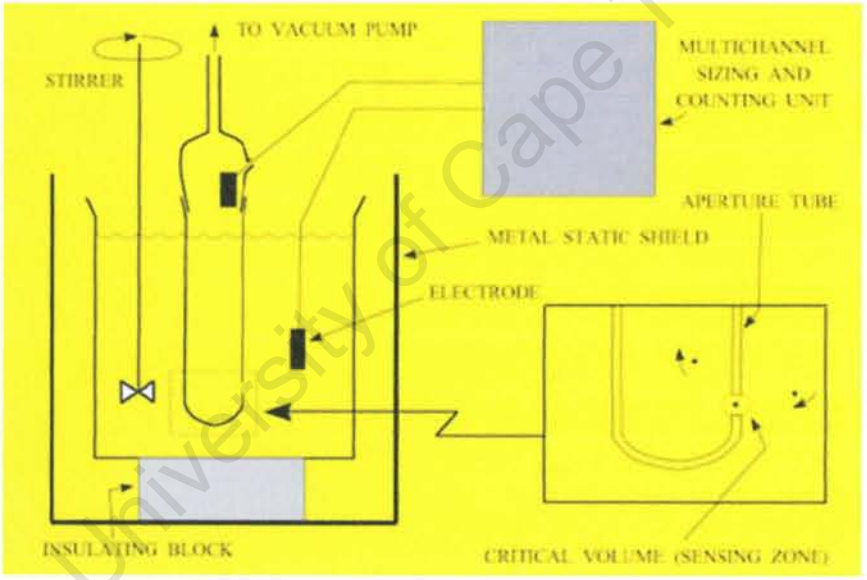

Figure 2.3: *Schematics of a Coulter Counter, used for analysis of particle size distributions in a suspension, with an analysis range of 0.4 – 1 200 µm*[15].

The voltage applied across the opening creates a "sensing zone". As a particle passes through the opening (or "sensing zone"), it displaces its own volume of electrolyte, briefly increasing the resistance across the aperture. This change can be measured as a current pulse that is digitally processed in real time. The Coulter principle states that the pulse is directly proportional to the three-dimensional volume of the particle that produced it. Analysing these pulses enables a size distribution to be acquired and displayed in volume (μm^3) and diameter (µm) (Fig 2.4).

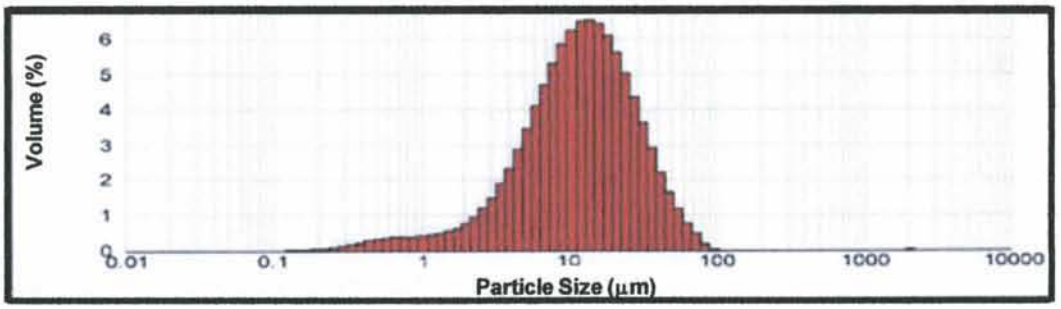

Figure 2.4: *A typical particle volume-size distribution obtained using a Coulter Counter*[16].

Furthermore, a metering device is used to draw a known volume of the particle suspension through the opening and a count of the number of pulses then yields the concentration of particles in the sample[17]. Consequently, particle number-size distribution curves are obtained which provide information on average particle sizes (Fig 2.5)[18].

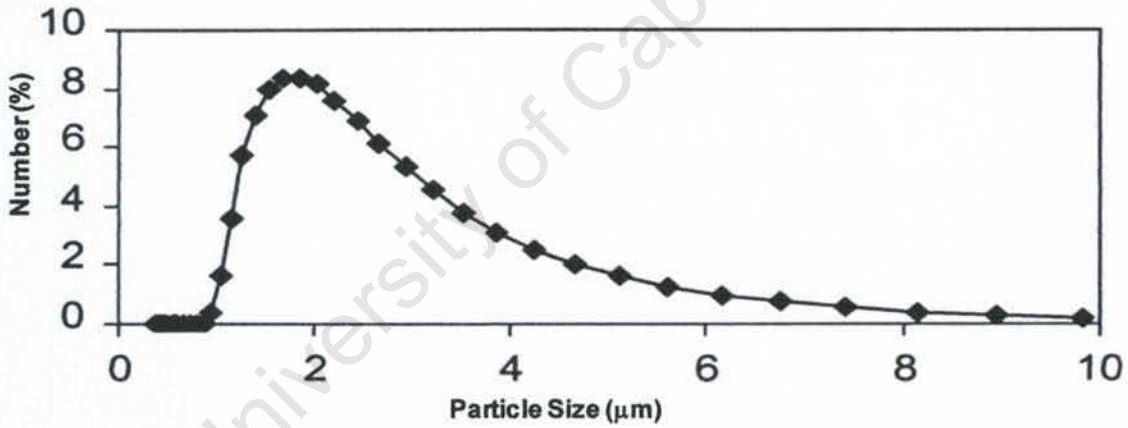

Figure 2.5: *A typical particle number-size distribution obtained using a Coulter Counter*[19].

Particle size is an important attribute of the adjuvant and was profiled by use of Coulter Counter analysis. Measurement using a Coulter Counter is fast and sizing rates of up to 10 000 particles per second are possible. Aperture size typically ranges from 15-2 000 µm. Each aperture can be used to measure particles within a series range of 2-60 % of its nominal diameter. Therefore, an overall particle size range of 0.4-1 200 µm is possible[20]. The ability of the technology to analyse particles is limited to those particles that can be suitably suspended in an electrolyte solution. The selection of the most suitable aperture size is dependent upon the particles to be measured. For example, a 30 µm aperture can measure particles from about 0.6-18 µm in diameter. A 140 µm aperture can measure particles from about 2.8-84 µm. If the particles to be measured cover a wider range than a

single aperture can measure, two or more apertures can be used and the test results overlapped to provide a complete particle size distribution[20].

2.2 Analysis of conjugate vaccines

It is customary to use quantitative methods (e.g. colorimetric assays) and biological assays including immunogenicity in animals for testing the quality control of different vaccine batches. However for Hib conjugate vaccines, immunogenicity in animals such as mice does not correlate well with protective immunity in children[21-23]. As such, consistency of different batches is assessed by determining the sugar-to-protein ratio, size distribution and integrity by free saccharide quantification[23]. For a conjugate vaccine to elicit an immune response in children, the oligo- or polysaccharide should remain attached to the carrier protein[24]. Degradation and depolymerisation of the saccharide chain reduces the immunogenicity of the vaccine. Thus, the integrity of a conjugate vaccine can be monitored by measuring the amount of free saccharide present[25-27]. Physicochemical assays such as ribose, phosphorus and high performance anion exchange chromatography with pulsed amperometric detection (HPAEC-PAD) can be used to quantify the capsular polysaccharide →5-D-ribitol-(1-1)-β—D-ribose-3-phosphate[28]. In addition, high performance size exclusion chromatography (HPSEC) can be used not only to monitor molecular size distributions for batch-to-batch consistency, but also to assess the stability of the vaccine over time by tracking changes in the molecular size distribution due to degradation[29].

2.2.1 Phosphorus determination

The ascorbic acid method is a technique most commonly used for phosphorus quantification in vaccines. All forms of phosphorus are converted to orthophosphate using a cocktail of perchloric and sulfuric acid. Orthophosphate reacts with molybdate to form phosphomolybdic acid which is reduced by ascorbic acid to form a blue-coloured complex[30].

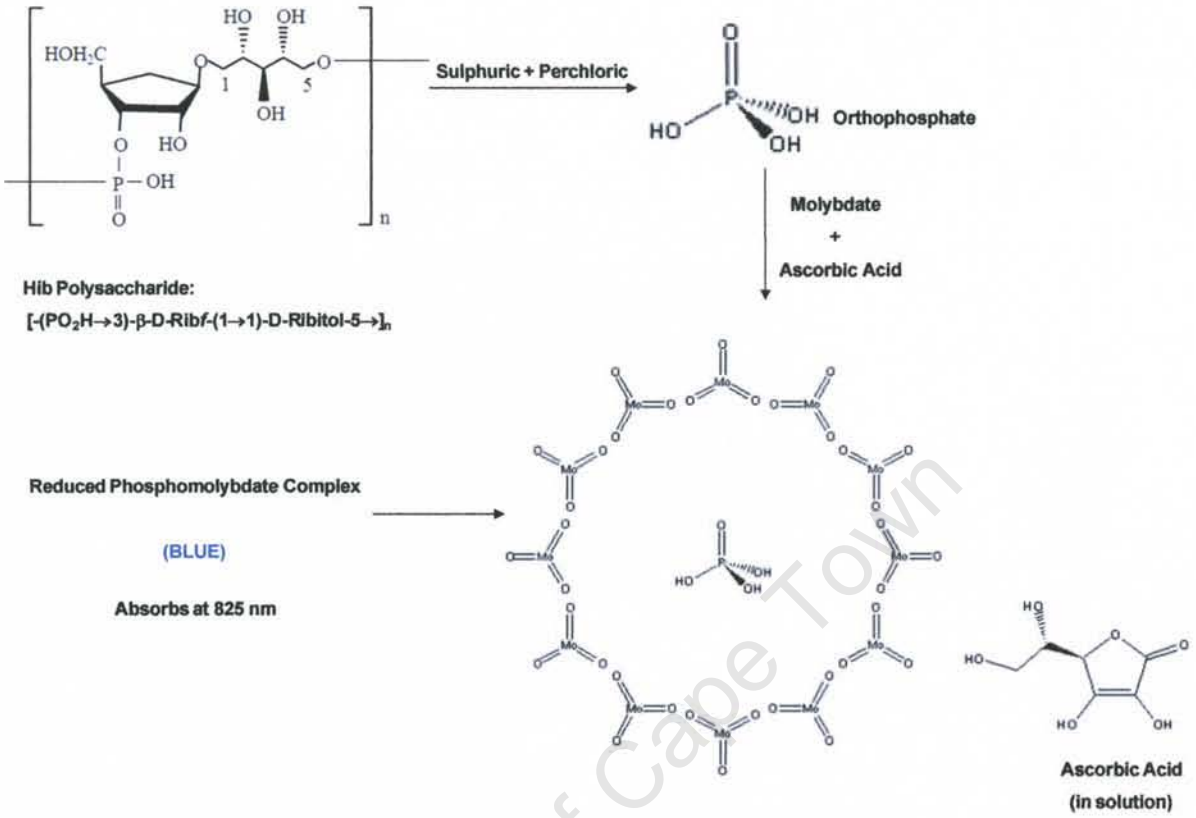

Fig 2.6: *The ascorbic acid method for the quantification of phosphorus in vaccines*[30].

The intensity of the colour is directly proportional to the concentration of phosphorus. A modification of Chen's method was used to determine phosphorus concentration in Hib and meningococcal A (Mn A-TT) conjugate vaccines. Details of the procedure followed to prepare reagents for the phosphate assay are provided in appendix B.

2.2.2 Orcinol method

Addition of a strong acid to a PRP-containing sample and subsequent heating at 100 °C hydrolyses the glycosidic and phosphodiester bonds in PRP to release the ribose moiety. Ribose in turn undergoes dehydration and the resulting furfural derivative forms coloured (blue-green) addition compounds in the presence of phenolic reagents[31, 32].

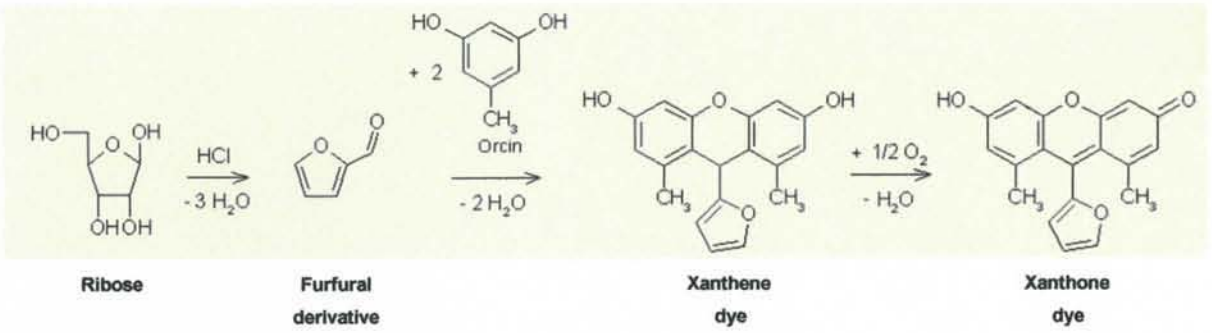

Figure 2.7: *The Orcinol Method for determination of ribose in vaccines*[33].

This colorimetric method can thus be used to determine the saccharide content in Hib conjugate vaccines. The procedure followed to prepare stock and working reagents required for the ribose assay are presented in appendix D.

2.2.3 High performance anion exchange chromatography (HPAEC)

In recent years HPAEC-PAD methods have been developed and applied to the analysis of glycoconjugate vaccines. It allows direct quantification of underivatised carbohydrates at potentially low picomole levels with minimal sample preparation and clean-up. HPAEC-PAD takes advantage of the fact that carbohydrates are weakly acidic at high pH. In a strong alkaline solution, the sugar hydroxyl groups are ionised oxyanions. The CarboPac series of columns (by Dionex) are packed with a strongly basic anion exchange pellicular resin for separation and analysis of mono-, oligo- and polysaccharides[34]. There are several factors that determine a molecule's affinity to the anion exchange column and thus provide a basis for the separation of molecules; these are effective charge, pKa values, steric effects, hydrophobic interactions and mass-to-charge ratios[35].

In general, the retention of a molecule on an anion exchange column is proportional to the amount of effective charges on the molecule. The affinity of carbohydrates to the CarboPac columns under alkaline elution conditions normally follows the order polysaccharides > oligosaccharides > monosaccharides, which is based on the number of oxyanions generated on these molecules in alkaline eluents[35, 36]. However, exceptions to this trend have been reported[36].

Another factor which influences the affinity of an anionic moiety to an anion exchange column is its pKa value. Binding affinity increases as the pKa value decreases [35, 37]. For

example, an acidic carbohydrate such as mannose-6-phosphate is retained much longer on the column than mannose itself, and neutral monosialyl, disialyl and trisialyl oligosaccharides are eluted in that order[38]. Similar trends were observed in earlier studies conducted using anion exchange chromatography, where the main acidic groups used in the chromatographic process were those of stronger acids (phospho-, sulfo- or sialyl derivatives) which are anionic under neutral or weakly acidic pHs[38]. HPAEC can also be used to separate carbohydrates based on subtle differences between the pKas of their OH-groups[39-41], an example is the separation of N-glycolyl-neuramic acid from N-acetyl-neuramic acid. Separation of galactose, mannose and glucose are possible by HPAEC despite similarities in their overall molecular size and the number of hydroxyl groups[39].

Since each of the hydroxyl groups on a monosaccharide has a slightly different pKa value, substitution of different hydroxyl groups by glycosylation would generate products with different affinities[36, 40]. The anomeric hydroxyl group has a much lower pKa value than the other hydroxyl groups and thus contributes significantly to the molecule's retention[41]. For example, the reduced retention of alditols as compared to the parent reducing sugars is based on acidity[38]. Since the anomeric hydroxyl group is the most acidic among all the OH-groups, replacing it with an ordinary OH-group (which is less acidic) would naturally result in less retention. Inositols are not well retained because of their lack of acidic anomeric hydroxyl group. Alkyl glycosides are not retained as much as the parent sugars for the same reason[38]. Similarly, the loss of hydroxyl groups, such as in rhamnose or fucose, reduces retention times. This also applies to the amino sugars, in which an OH group is replaced with amino or acetamido groups[38]. The pKa values of some alditols and saccharides are shown in Table 2.1.

Table 2.1: Dissociation constants of some alditols and saccharides in water at 25 °C[42]

Compound	pKa
D-Sorbitol	13.6
D-Dulcitol	13.43
D-Galactose	12.39
D-Arabinose	1 2.43
D-Glucose	12.28
D-Xylose	12.15
D-Mannose	12.15
D-Lyxose	12.11
D-Ribose	12.11
D-Fructose	12.03
Sucrose	12.62
Lactose	11.98
Maltose	11.94

Accessibility of the oxyanions on carbohydrates to the functional groups of the stationary phase (steric effects) is another important factor in determining the chromatographic behaviour of carbohydrates in HPAEC[35].

Carbohydrates show varying retention behaviour on the different pellicular anion exchange columns. The CarboPac PA-1 column is the most widely used for monomer analysis and quantification in oligo- and polysaccharides. It can withstand extreme conditions such as 1 M NaOH and 1 M HCl; therefore contaminants can easily be removed by washing with these solutions. One major limitation of the CarboPac PA-1 column is that the presence of organic solvents above 2 % can cause collapse of the column bed[35].

The properties of the CarboPac MA-1 column differ from the CarboPac PA-1 column in that the MA-1 column not only has much higher anion exchange capacity but is operated under a lower flow rate (0.4 ml/min). The high capacity and low flow rate of the MA-1 column make switching of ionic forms of the column (e.g. from OAc^- form to OH^- form) difficult, requiring a very long regeneration time. For that reason, application of the MA-1 column is mostly limited to analysis of reduced mono- or disaccharides, which can be eluted with NaOH; but is ideal for analysis of ribitol[34, 35].

A strong alkaline solution is required as the mobile phase for the ionisation of the hydroxyl groups of carbohydrates to oxyanions and for carbohydrate detection by the pulsed amperometric detector. The sodium hydroxide/sodium acetate (NaOAc) eluent system is the most widely used system for HPAEC-PAD. Under alkaline elution mode, dilute NaOH alone provides satisfactory separation of weakly bound monosaccharides. For the elution of polysaccharides or acidic saccharides, a stronger eluting agent such as nitrate or acetate is used[35].

2.2.4 Size exclusion chromatography (SEC)

Size exclusion chromatography (SEC) is a non-interactive mode of separation whereby the particles of the column packing have various pore sizes and pore networks, so that solute molecules are retained or excluded on the basis of their hydrodynamic molecular volume. As the sample passes through the column, the solute molecules are separated. Very large molecules cannot enter many of the pores and thus travel mostly around the exterior of the packing and elute at the bed void volume of the mobile phase. Very small molecules diffuse into all or many of the pores accessible to them. With a larger column volume at their disposal, small molecules exit the column last. Between these two extremes, intermediate-size molecules can penetrate some passages but not others and, consequently, their progress down the column is retarded and they exit at intermediate times[43]. Thus, solutes are eluted in order of decreasing molecular size from the stationary phase (Fig 2.8).

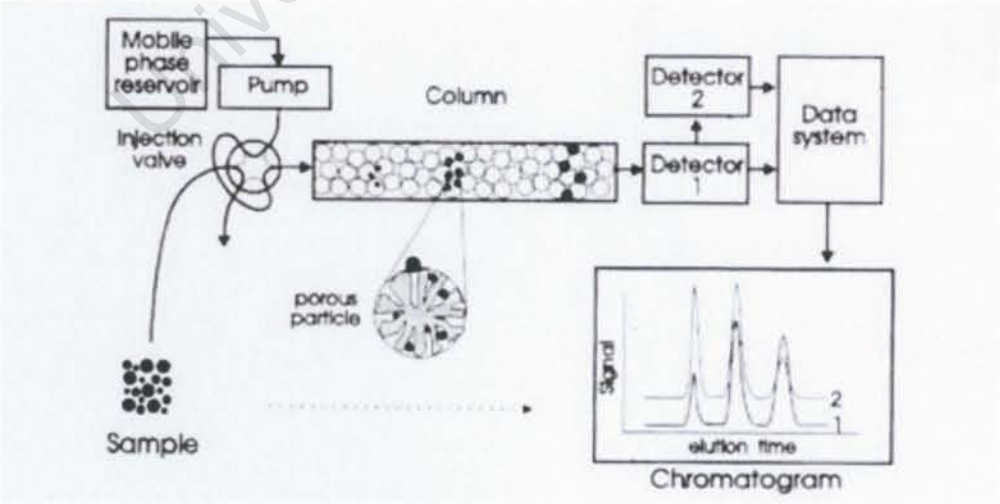

Figure 2.8: *SEC separates molecules on the basis of differences in hydrodynamic volume, or molecular sizes*[44].

The microparticulate sorbents (average particle diameter range between 5-13 μm) that are available for high performance SEC (HPSEC), usually in prepacked columns of length 25 or 30 cm, 4-8 mm I.D., are highly efficient and such columns have plate numbers of 10 000-50 000 per metre. Optimisation for fractionation of samples containing a wide distribution of molecular weight can be achieved by coupling columns containing stationary phases of the same type but differing in porosity (optimal length ranges between 50-100 cm)[45]. The type of column packing depends on the manufacturer[45]. Silica-based columns produced by Merck have a fractionation range of 10^3 - (>10^7). Agarose-based columns can be obtained from Pharmacia and have a fractionation range of $10^3 - 4 \times 10^7$. Columns obtained from Waters are methacrylate-based with a fractionation range of $<10^3 - 7 \times 10^6$. The Waters Ultrahydrogel column used in this study had a fractionation range of $10^2 - 7 \times 10^6$.

The pore volume in the stationary phase determines the maximum volume available for chromatographic separation. The relative pore volume of the modern sorbents for SEC is in the range 52-97 % of the column volume, the lower range being typical for silica-based materials and the larger values for polymeric sorbents[45]. The lower pore volume of silica-based stationary phases limits the number of peaks that can be resolved by the column, so that the resolution achieved is generally inferior to those of polymeric sorbents. Polymeric sorbents are also preferred over silica-based types for HPSEC because they are more stable at elevated temperatures and at high pH (conditions that may be necessary in SEC of polysaccharides of low solubility in water at room temperature).

The molecular size distribution of conjugate vaccines is a critical parameter that can be used to demonstrate batch-to-batch consistency and, over time provides an indication of the vaccine's stability[29, 46-48]. This feature of conjugate vaccines has been evaluated by gel filtration chromatography with soft gel such as Sepharose, fast protein liquid chromatography (FPLC) and recently by high performance size exclusion chromatography (HPSEC)[29, 47-49]. Exposure of the vaccine to degrading conditions such as elevated temperatures would result in hydrolysis of the saccharide moiety and a reduction in the size of the conjugate. As a result, the retention time of the conjugate would be expected to increase. Exposure of the vaccine to elevated temperatures can also cause slight unfolding and modification of the tertiary structure of the carrier protein and thereby change the retention time of the

conjugate. Thus, changes in the molecular size distribution of the vaccine indicate both instability of the protein and loss of the attached saccharide[29].

2.2.5 BCA protein assay

The BCA (bicinchoninic acid) assay involves the reduction of Cu^{2+} (blue) in an alkaline environment to Cu^{+}, which forms a chelate complex with peptides in the sample. This is commonly known as the biuret reaction. Peptides containing three or more amino acids residues form a chelate complex while single amino acids do not. In the next step of the reaction, the Cu^{+} ion is chelated by two molecules of BCA to form a purple coloured complex which exhibits linear absorbance at 562 nm with increasing protein concentration[50].

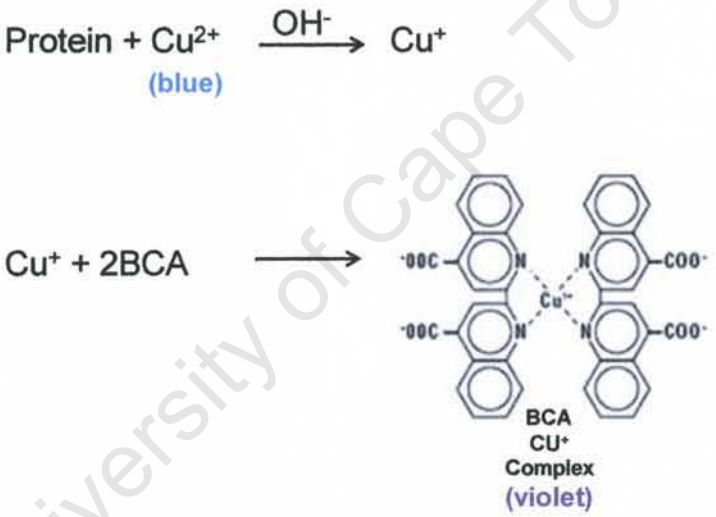

Figure 2.9: *Schematic representation of the BCA assay showing the reduction of copper by protein in an alkaline medium and the chelation of two BCA molecules by one cuprous ion*[51].

The BCA method was used (in chapter 5) to determine the presence of protein in ultrafiltered samples. The procedure followed to prepare stock and working solutions for the BCA assay are presented in appendix F.

2.3 References

1. Westler, W. M., The vector paradigm in modern NMR spectroscopy: I. Pulse sequences applied to isolated spin systems. Available at http://www.nmrfam.wisc.edu/~milo/notes/paradigm_I.pdf. Accessed 05 June 2009.

2. http://www.structbio.vanderbilt.edu/chazin/classnotes/.../Bioch-301.NMR.1.ppt. Accessed 9 June 2009.

3. http://chn.loyno.edu/chemistry/OrganicSolvents.htm. Accessed 24 June 2009.

4. Williams, D. H. and Fleming, I., *Spectroscopic methods in organic chemistry*. 1995, Berkshire: McGraw-Hill. pp. 63-169.

5. Gottlieb, H. E., Kotlyar, V., et al., NMR Chemical Shifts of Common Laboratory Solvents as Trace Impurities. *J Org Chem* 1997;**62**:7512-15.

6. Clayden, J., Greeves, N., et al., *Organic chemistry*. 2001, New York: Oxford University Press. pp. 47-79; 246.

7. Werner, M. H., BRUKER AVANCE user's guide, version 2.0. Available at www.cis.rit.edu/class/schp740/docu. Accessed 03 June 2009.

8. Mandal, P. K., Majumdar, A., A comprehensive discussion of HSQC and HMQC pulse sequences. *Concepts Magn Reson Part A* 2004;20A:1-23.

9. Shaka, A., Keeler, J., et al., Evaluation of a new broadband decoupling scheme: WALTZ-16. *J Magn Reson* 1983;53:313-40.

10. Ayannides, C. A., Ktistis, G., Stability estimation of emulsions of isopropyl myristate in mixtures of water and glycerol. *J Cosmet Sci* 2002;**53**:165-73.

11. Butler, B. D., Production of microbubbles for use as echo contrast agents. *J Clin Ultrasound* 1986;**14**:408-12.

12. Deitel, M., Friedman, K. L., et al., Emulsion stability in a total nutrient admixture for total parenteral nutrition. *J Am Coll Nutr* 1992;**11**:5-10.

13. Harnisch, S., Schuhmann, R., et al., Differences in the coalescence kinetics of fat emulsions in dependence on the amount of fat and age. *Pharmazie* 2002;**57**:54-8.

14. Iliano, L., Delanghe, M., et al., Effect of electrolytes in the presence of some trace elements on the stability of all-in-one emulsion mixtures for total parenteral nutrition. *J Clin Hosp Pharm* 1984;**9**:87-93.

15. www.pharmacybd.com/download/presentations/micrometrics.ppt. Accessed 03 June 2009.

16. http://www.pcisynthesis.com/news_articles/sept_2007/mastersizer_chart.gif. Accessed 03 June 2009.

17. Swanton, E. M., Curby, W. A., et al., Experiences with the Coulter counter in bacteriology. *Appl Microbiol* 1962;**10**:480-5.

18. Hess, B., Meinhardt, U., et al., Simultaneous measurements of calcium oxalate crystal nucleation and aggregation: impact of various modifiers. *Urol Res* 1995;**23**:231-8.

19. http://www.pnas.org/content/96/17/9469/F1.large.jpg. Accessed 03 June 2009.

20. http://www.beckmancoulter.com/coultercounter/homepage_tech_coulter_principle.jsp Accessed 03 June 2009.

21. Chu, C., Schneerson, R., et al., Further studies on the immunogenicity of Haemophilus influenzae type b and pneumococcal type 6A polysaccharide-protein conjugates. *Infect Immun* 1983;**40**:245-56.

22. Redhead, K., Sesardic, D., et al., Interaction of *Haemophilus influenzae* type b conjugate vaccines with diphtheria-tetanus-pertussis vaccine in control tests. *Vaccine* 1994;**12**:1460-66.

23. WHO Expert Committee on Biological Standardization. Forty-ninth report. *World Health Organ Tech Rep Ser* 2000;**897**:1-106.

24. Jones, C., Vaccines based on the cell surface carbohydrates of pathogenic bacteria. *An Acad Bras Cienc* 2005;**77**:293-324.

25. Cuervo, M. L., Perez, L. R., et al., Relationships among physico-chemical and biological tests for a synthetic Hib-TT conjugate vaccine. *Vaccine* 2007;***25***:194-200.

26. Peeters, C. C., Tenbergen-Meekes, A. M., et al., Immunogenicity of a *Streptococcus pneumoniae* type 4 polysaccharide-protein conjugate vaccine is decreased by admixture of high doses of free saccharide. *Vaccine* 1992;**10**:833-40.

27. Turula, V. E., Kim, J., et al., An integrity assay for a meningococcal type B conjugate vaccine. *Anal Biochem* 2004;**327**:261-70.

28. Mawas, F., Bolgiano, B., et al., Evaluation of the saccharide content and stability of the first WHO International Standard for *Haemophilus influenzae* b capsular polysaccharide. *Biologicals* 2007;**35**:235-45.

29. Parisi, L., von Hunolstein, C., Determination of the molecular size distribution of *Haemophilus influenzae* type b-tetanus toxoid conjugate vaccines by size-exclusion chromatography. *J Chromatogr A* 1999;**847**:209-11.

30. Chen, P. S., Toribara, T. Y., et al., Microdetermination of phosphorus. *Anal Chem* 1956;**28**:1756-58.

31. Ashwell, G., Colorimetric analysis of sugars. *Methods Enzymol* 1957;**3**:73-105.

32. Monsigny, M., Petit, C., et al., Colorimetric determination of neutral sugars by a resorcinol sulfuric acid micromethod. *Anal Biochem* 1988;**175**:525-30.

33. http://www.chemie.uniregensburg.de/Organische_Chemie/Didaktik/Keusch/p32_rib_rna-e.htm. Accessed 14 June 2009.

34. Dionex corporation, *Analysis of carbohydrates by high performance anion exchange chromatography with pulsed amperometric detection*. Dionex technical note 20. Sunnyvale, CA, LPN 032857. October 2004.

35. Zhang, Y., Lee, Y. C., High performance anion-exchange chromatography of carbohydrates on pellicular resin columns. In *Carbohydrate analysis by modern chromatography library*, Rassi, Z. E. I., Editor. 2002, Elsevier Science, pp. 207-50.

36. Lee, Y. C., The convenience of 2-keto-3-deoxyoctulosonic acid (KDO) analysis by HPAEC-PAD. *Anal Biochem* 1990;**189**:151-62.

37. Corradini, C., Canali, G., et al., Separation of alditols of interest in food products by high-performance anion-exchange chromatography with pulsed amperometric detection. *J Chrom A* 1997;**791**:343-49.

38. Lee, Y. C., Carbohydrate analyses with high-performance anion-exchange chromatography. *J Chrom* 1996;**720**:137-49.

39. Lee, Y. C., High performance anion-exchange chromatography for carbohydrate analysis. *Anal Biochem* 1990;**189**:151-62.

40. Paskach, T. J., Lieker, H.-P., et al., High-performance anion-exchange chromatography of sugars and sugar alcohols on quartenary ammonium resins under alkaline conditions. *Carbohydr Res* 1991;**215**:1-14.

41. Fransen, C. T. M., Van Laere, et. al., -D-Glcp-(1↔1)-β-D-Galp-containing oligosaccharides, novel products from lactose by the action of β-galactosidase. *Carbohydr Res* 1998;**314**:101-14.

42. Cataldi T. R. I., Margiotta, G., et al., Determination of sugars and alditols in food samples by HPAEC with integrated pulsed amperometric detection using alkaline eluents containing barium or strontium ions. *Food Chem* 1998;**62**:109-15.

43. Willard, H. H., Merritt, L. L. Jnr., et al., *Instrumental methods of analysis.* 1988, Belmont: Wadsworth Publishing Company. pp 614-55.

44. http://academic.sun.ac.za/polymer/gpectref.htm. Accessed 19 June 2009.

45. Churms, S. C., Recent progress in carbohydrate separation by high-performance liquid chromatography based on size exclusion. *J Chrom A* 1996;**720**;151-66.

46. Cuervo, M. L., Perez, L. R., et al., Relationships among physico-chemical and biological tests for a synthetic Hib-TT conjugate vaccine. *Vaccine* 2007;**25**:194-200.

47. WHO recommendations to assure the quality, safety and efficacy of group A meningococcal conjugate vaccines. Adopted by the 57th meeting of the WHO Expert Committee on Biological Standardization, 23-27 October 2006.

48. von Hunolstein, C., Parisi, L., et. al., A routine high-performance size-exlusion chromatography to determine molecular size distribution of *Haemophilus influenzae* type b conjugate vaccines. *Vaccine* 1999;**17**:118-25.

49. Plumb, J., E., Yost, S., E., Molecular size characterisation of *Haemophilus influenzae* type b polysaccharide-protein conjugate vaccines. *Vaccine* 1996;**14**:399-404.

50. Stoscheck, C. M., Quantitation of protein. *Meth Enzymol* 1990;**182**:50-69.

51. https:\\wiki.science.ru.nl/microbiology/lab/images/1/1c/BCA_reaction1.jpg

CHAPTER 3

CHARACTERISATION OF PHEROID™ AND RAW MATERIALS BY NMR SPECTROSCOPY AND COULTER COUNTER ANALYSIS

3.1 Introduction

Adjuvants can be used to enhance vaccine efficacy and to elicit specific immune responses to antigens[1]. Aluminium containing adjuvants have had the widest use in vaccines licensed for humans and thus the longest safety record[2]. In vaccines against diseases such as tuberculosis, which require cell-mediated immune responses for prevention and cure, aluminium adjuvants are inadequate[3]. Additional limitations include local reactions, production of IgE antibodies and ineffectiveness for some antigens[3]. Due to these limitations, there is an ongoing search for better adjuvants that would induce a broader immune response, permit lower amounts of antigen to be used and possibly require fewer immunisations[4]. A patented fatty acid-based formulation containing nitrous oxide results in a submicron emulsion (Pheroid™) which has shown potential for drug delivery and use as an adjuvant for viral vaccines[5-7]. Emulsions such as Pheroid™ are dispersions of at least two immiscible liquids stabilised by the presence of a surface active agent (surfactant) typically with both hydrophilic and hydrophobic moieties (See page 24 for a schematic representation of the materials used in Pheroid™)[8].

In view of the fact that full physicochemical characterisation and pre-clinical studies of Pheroid™ are required prior to clinical evaluation[9], the present study investigated the application of NMR spectroscopy to profile the raw materials used to prepare Pheroid™ and to study the composition of Pheroid™ formulations. This study also investigated whether NMR spectroscopy could be applied as a quick and easy method to monitor the consistency in production of Pheroid™ formulations. In addition, the Coulter Counter method, which had not been used in previous studies of Pheroid™, was investigated as an alternative method for evaluating the particle size distribution of Pheroid™.

3.2 Pheroid™ components

3.2.1 Oil phase

(a) Unsaturated fatty acids

A mixture of fatty acid ethyl esters of oleic, linoleic and linolenic acid is used in the formulation of Pheroid™. Some functions of the fatty acid component of Pheroid™ are maintenance of cell membrane integrity, energy homeostasis and modulation of the immune system through amongst others, the prostaglandins/leukotrins[7]. The numeric designation used for fatty acids comes from the number of carbon atoms, followed by the number of sites of unsaturation. The site of unsaturation is indicated by the symbol "D" and the number of the first carbon of the double bond (e.g. oleic acid is an 18-carbon fatty acid with one site of saturation between C9 and C10, and is designated $18:1^{D9}$)[10]. Chemical structures for the fatty acid ethyl esters are shown in Table 3.1.

Table 3.1: Numeric designation and structure of the fatty acid ethyl esters[10].

Symbol	Common Name	Structure
$18:1^{D9}$	Oleic acid ethyl ester	
$18:2^{D9, 12}$	Linoleic acid ethyl ester	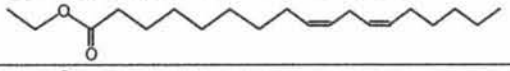
$18:3^{D9, 12, 15}$	Linolenic acid ethyl ester	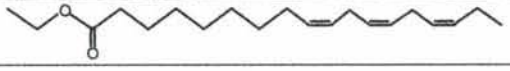

(b) Surfactants

Surface-active agents or surfactants are molecules distinguished by the presence of both a polar and a nonpolar region (Fig 3.1).

Fig 3.1: *Hydrophilic and hydrophobic regions on a surfactant*[11].

The molecule's hydrophobic section will dissolve in or be in contact with the oil phase, whereas hydrophilic portion can dissolve in or be attached to the aqueous phase of the emulsion. As a result of their structure, they are attracted to both the oil phase and the aqueous phase and will preferentially reside at the interface[12]. The nature of the hydrophilic group is used to classify surfactants into four categories: (a) non-ionic surfactant such as the polyoxyethylene (POE) derivatives; (b) cationic surfactants, the most important members being the quaternary nitrogen bases and amines, which can ionise to assume a positive charge; (c) anionic surfactants which bear a negative charge when dissolved in water and include the alkyl sulfates and the soaps; (d) amphoteric surfactants such as those containing both amino and carboxylic acid groups[13]. The surfactant used in Pheroid™ is the polyethylene castor oil derivative, a non-ionic surfactant.

Non-ionic surfactants differ from ionic surfactants in the absence of a charge on the molecule. The hydrophobic portion may include saturated and unsaturated fatty acids or fatty alcohols. The hydrophilic region may include polyoxyethylene, polyoxypropylene or polyol derivatives and the hydroxyl group. The balance between the hydrophilic and the hydrophobic properties of a surfactant is known as the hydrophile-lipophile balance (or HLB) and provides a practical and rational means for identifying combinations of emulsifiers and facilitates the formation of stable emulsions. Most non-ionic surfactants have HLB values in the range of 1-20. An HLB value of 1 indicates that the surfactant is

soluble in oil while an HLB value of 20 signifies that it is soluble in water. Surfactants with low HLB values are good stabilisers for water-in-oil emulsions, while those with high HLB values serve as good stabilisers for oil-in-water emulsions[13].

Commercially available polyethylene glycol (PEG) hydrogenated castor oil (also known as Cremophor® RH 40 and available from BASF, Germany) is the surfactant used in the production of Pheroid™. It is manufactured by reacting hydrogenated castor oil with ethylene oxide. The reaction yields a complex mixture with glycerol polyethylene glycol oxystearate (Fig 3.2 (a)) as the main constituent and ethoxylated glycerol (Fig 3.2 (b)), fatty acid esters of PEG (Fig 3.2 (c)) and polyethylene glycols[14].

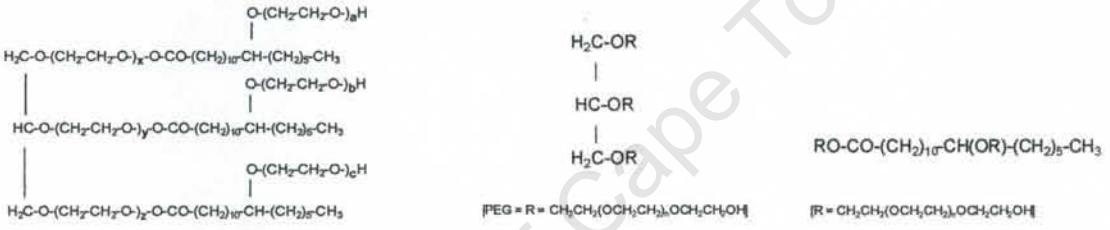

Fig 3.2: (a) Glycerol polyethylene glycol oxystearate (b) Ethoxylated glycerol. (c) Fatty acid esters of PEG

PEG hydrogenated castor oil has an HLB value in the range of 14-16 and approximately 75 % of the components of the mixture are hydrophobic. These comprise of the fatty acid esters of glycerol polyethylene glycol and fatty acid esters of polyethylene glycol. The hydrophilic section consists of polyethylene glycols and glycerol ethoxylates[15].

(c) Anti-oxidants

Many oils and fats used in emulsion formulation are obtained from plants or animals and can be susceptible to oxidation by atmospheric oxygen or by the action of micro-organisms. The resulting rancidity is manifested by the formation of degradation products of unpleasant odour and taste. Oxidation by micro-organisms is controlled by the use of antimicrobial preservatives and atmospheric oxidation by the use of anti-oxidants[16]. The term anti-oxidant refers to a substance that when present at low concentrations compared to those of an oxidisable substrate significantly delays or prevents oxidation of that substrate. Butylated hydroxyanisole (BHA) is a widely used antioxidant for the protection of fixed oils and fats at concentrations of up to 0.02 % and butylated hydroxytoluene (BHT) is recommended as an alternative to dl-α-tocopherol at

a concentration of 10 ppm. Other anti-oxidants include propyl, octyl and dodecyl esters of gallic acid, recommended for use at concentrations of 0.001 % for fixed oils and fats and up to 0.1 % for essential oils[16]. In Pheroid™, dl-α-tocopherol is the anti-oxidant used to protect against atmospheric oxidation.

3.2.2 Aqueous phase of Pheroid™ components

(a) Nitrous oxide saturated water

Nitrous oxide (N_2O), also called laughing gas, is a colourless gas with a sweet odour and taste[17]. Formal charge considerations suggested that the most important resonance structure is $[N^-=N^+=O] \leftrightarrow [N\equiv N^+-O^-]$. Despite the large difference in electronegativity between nitrogen and oxygen, the molecule is only slightly polar. The low polarity of the gas makes it both fat and water soluble[18]. At 20 °C and 2 atm, one litre of the gas dissolves in 1.5 litres of water[19]. Prior to the formulation of Pheroid™, water is gassed with N_2O gas for four days because studies performed using confocal laser scanning microscopy (CLSM) showed that the presence of N_2O is necessary for the formation of clearly defined, ordered and stable droplets[8]. However, the precise mechanism by which this role is provided is still under investigation. After formulation, Pheroid™ is stored in the fridge at 2-8 °C and usually discarded after 6 months.

3.3 General properties of emulsions and Pheroid™

NMR spectroscopy can potentially be used to study the chemical structures of the fatty acid based component of Pheroid™. ^{1}H- and ^{13}C-NMR have been used to determine the fatty acid composition in mixtures e.g. plant extracts[20-22]. Stoffel and co-workers have presented the ^{13}C-NMR data for the fatty acids palmitic, stearic, oleic, linoleic, α-linolenic and arachidonic acid[23]. Miyake and co-workers reported the use of ^{1}H- and ^{13}C-NMR for the quantification of specific fatty acids in vegetable oils[22]. In a more recent study, Knothe and associates have outlined a method by which information on the amounts of individual fatty acids can be obtained using ^{1}H-NMR spectroscopy in an oil or fat sample or in the form of derivatives such as methyl esters[21].

Emulsions such as Pheroid™ do not form spontaneously but rather require an input of energy and are therefore thermodynamically unstable[24]. Processes that can destabilise emulsions include flocculation, coalescence and creaming (Fig 3.3). Fig 3.3 (a)

represents the metastable state before the onset of instability. The droplets can be polydisperse and in real systems are animated by thermal events in the continuous phase (Brownian motion)[25].

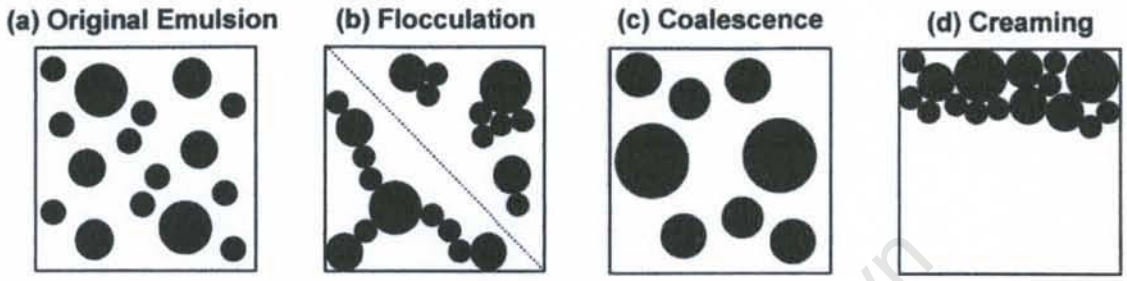

Fig 3.3: *Major instability processes that emulsions undergo[24].*

Flocculation occurs when there is a net attractive force between droplets which is large enough to overcome thermal agitation and cause persistent aggregation (Fig 3.3 (b)). This is distinct from being close together because of a chance encounter due to Brownian motion. Whilst the droplets are held together they are not in intimate contact and are usually separated by a layer of surfactant. When the surfactant fails, their contents flow together and bigger droplets are formed. This process is called coalescence and the coalescing emulsion is characterised by a wide size distribution of the droplets, but no clusters are present (Fig 3.3 (c))[25].

Creaming occurs when there is a difference between the density of the dispersed and continuous phases. Under the influence of gravity, separation occurs with the most dense phase collecting at the bottom and the less dense phase at the top (Fig 3.3 (d))[25]. Flocculation usually leads to enhanced creaming because flocs rise faster than individual drops due to their larger effective radius. Flocculation is enhanced by polydispersity since the differential creaming speeds of small and large drops cause them to come into close proximity (and hence possibly aggregate) more often than would occur in a monodispersed system[26]. These processes must be minimised to enhance the stability of an emulsion. For example creaming in a dilute emulsion can be inhibited by reducing the average drop size, reducing the density difference of the phases or by increasing the viscosity of the continuous phase[26]. Another technique by which emulsions are stabilised is by the addition of surface-active material (or surfactant)

which protects the newly formed drops from re-coalescence. An emulsifier is a surfactant which facilitates emulsion formation and aids in stabilisation through a combination of surface activity and possible structure formation at the interface[26].

Zeta potential measurements provide information on the stability of an emulsion. Zeta potential is defined as the difference in potential between the surface of the tightly bound layer of ions on the particle surface and the electroneutral region of the solution. When the zeta potential is high (25 mV or more, absolute value) the repulsive forces exceed the attractive van der Waal's forces (or London forces). The particles are dispersed and the system is deflocculated. When the zeta potential is low (less than 25 mV, absolute value), the attractive forces exceed the repulsive forces. The particles come together, leading to flocculation. Particle charge is an important attribute of the adjuvant and has been profiled using zeta potential measurements. The stability of Pheroid™ is related to the zeta potential of the system. Its value reflects the stability of the emulsion in a chosen environment[27]. Previous studies in which zeta potential measurements of Pheroid™ samples containing varying amounts of fatty acid were taken demonstrated that all Pheroid™ particles were negatively charged and that this property enabled the formation of a stable emulsion by providing steric repulsion between droplets to prevent flocculation and creaming of the droplets[5, 8].

The average size and the distribution of sizes are very important properties of an emulsion since they determine the safety of the preparation in the case of intravenous preparations or the release properties of the active ingredient in topical formulations[27-31]. Turbidity measurements obtained for any given Pheroid™ formulation provide a reflection of the number and size of particles and can be used routinely to monitor formulations. The turbidity measurements of activated Pheroid™ samples at different concentrations of surfactant or different fatty acid concentrations recorded over 2-4 weeks revealed that the size and number of Pheroid™ particles per volume can be tailor-made by changing the composition of the Pheroid™ formulation[8]. The present study investigated the Coulter Counter method as an alternative for analysis of particle size distributions in Pheroid™ formulations.

3.4 NMR analysis of Pheroid™ components

Pheroid™ raw materials were provided by the North West University (Potchefstroom) and consisted of a mixture of fatty acid methyl esters, vegetable oil containing ricinoleic acid-PEG and dl-α-tocopherol. The composition and identity of these raw materials were investigated by NMR spectroscopy.

2 drops of each was thoroughly mixed with 500 µl of d_6-DMSO and subjected to analysis by ^{1}H- and ^{13}C-NMR spectroscopy. With the exception of dl-α-tocopherol, the above procedure was repeated in 500 µl of $CDCl_3$ in order to determine which solvent gave the best spectra. d_6-DMSO is hygroscopic and so all spectra obtained using this solvent showed a water peak at 3.33 ppm[32]. A description of the samples analysed is displayed in Table 3.2.

Table 3.2: Sample description

Sample Name	Description
Fatty acid ethyl esters	Mixture of oleic, linoleic and linolenic fatty acid ethyl esters
Vegetable oil	PEG hydrogenated castor oil
dl-α-tocopherol	Surfactant

NMR spectra were acquired in d_6-DMSO and $CDCl_3$ and recorded at 300 K. ^{1}H-NMR spectra were obtained at 400 MHz using a Varian Unity 400 instrument and a probe temperature of 300K. The relative intensities of signals were determined by electronic integration. ^{13}C and 2-D NMR spectra were obtained using a Varian Mercury 300 instrument. The HSQC experiment was optimized for J = 140 Hz. The HMBC experiment was optimized for J = 8 Hz. Spectra were processed using standard Mestrec software.

3.4.1 Oleic, linoleic and linolenic fatty acid ethyl esters

High resolution NMR spectroscopy has been used for the determination of fatty acid composition[21, 22, 33, 34]. In the present study, the sample consisted of a mixture of oleic ($18{:}1^{D9}$), linoleic ($18{:}2^{D9, 12}$) and linolenic ($18{:}3^{D9, 12, 15}$) fatty acid ethyl esters. Although these fatty acid ethyl esters have the same chain length, they contain different numbers of double bonds. ^{1}H- and ^{13}C-NMR spectra were recorded in $CDCl_3$ and d_6-DMSO. The 2D experiments performed were COSY, HSQC and HMBC (details provided in section 3.4 and in Appendix A). However, only data from the ^{1}H, ^{13}C and COSY experiments will

be presented and discussed. The ^{1}H-NMR spectra obtained in $CDCl_3$ and d_6-DMSO are presented in Fig 3.4 and some characteristic proton assignments are indicated. Assignments were made by inspection and consultation of literature and confirmed by 2D (COSY, HSQC and HMBC (details provided in section 3.4 and in Appendix A, pages 252-253).

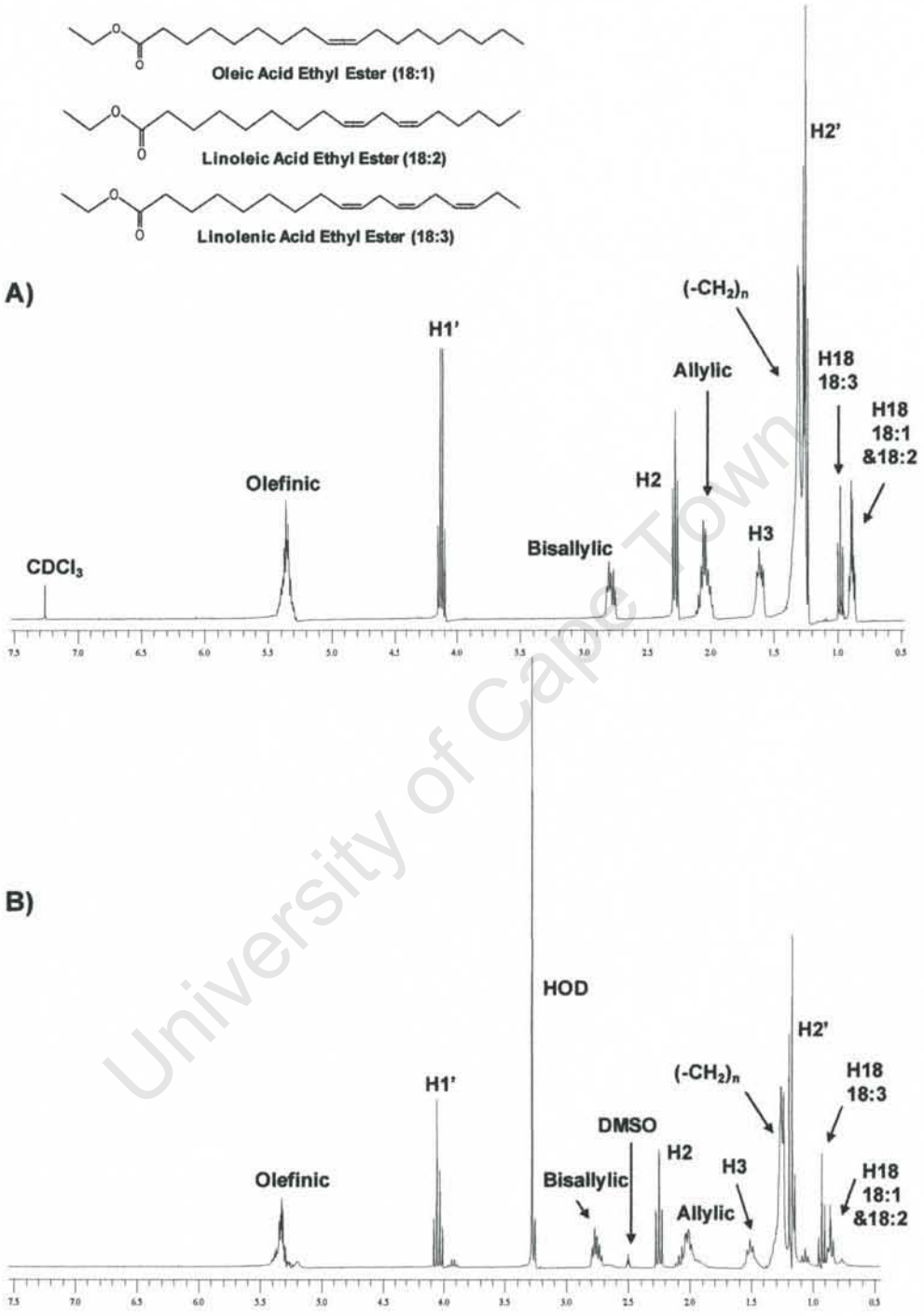

Fig 3.4: *^{1}H-NMR spectra (400 MHz) for a mixture of oleic, linoleic and linolenic fatty acid ethyl esters in $CDCl_3$ and d_6-DMSO. Some characteristic proton assignments are indicated*

The ^{1}H-NMR spectra obtained in $CDCl_3$ and d_6-DMSO had similar peak resolution. The carbon atoms in the fatty acid were numbered from C1 (carbonyl carbon) to C18 (terminal carbon) while those of the ester were numbered C1' and C2' and the ^{13}C spectrum was well dispersed (Table 3.4). Protons were labelled H and have numbers corresponding to that of the carbon atom to which they are attached.

The 2D ^{1}H,^{1}H COSY spectrum recorded in $CDCl_3$ and d_6-DMSO for the fatty acid ethyl esters were similar and so only the 2D spectrum obtained in $CDCl_3$ is displayed in Fig 3.5. The 1D spectrum appears on the diagonal of the COSY spectrum.

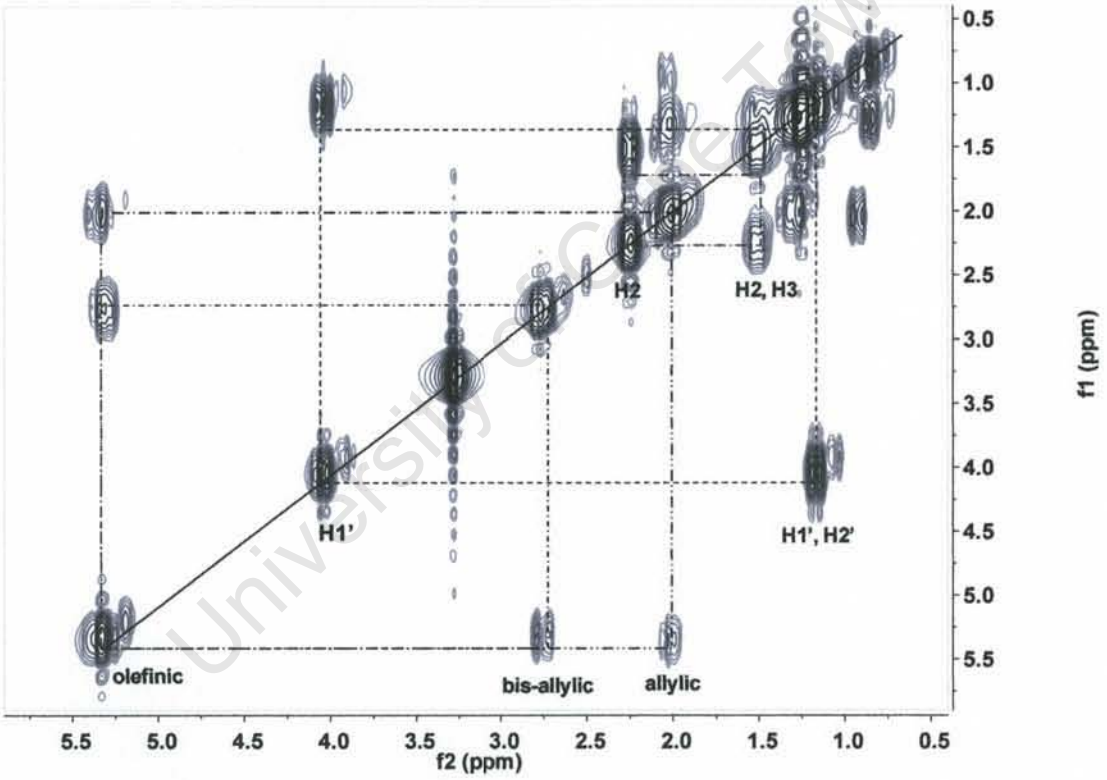

Fig 3.5: *COSY spectrum (300 MHz) for a mixture of oleic, linoleic and linolenic fatty acid ethyl esters in $CDCl_3$ recorded at 300 K. Some crosspeaks are labelled*

Crosspeaks in the COSY spectrum show scalar coupling between neighbouring hydrogens. Major cross peaks between allylic (2.02-2.07 ppm,), bis-allylic (2.77-2.80 ppm) and olefinic (5.33-5.37 ppm) protons were identified. The quartet at 4.13 ppm (from H1') is coupled to the triplet at 1.25 ppm (from H2'). Crosspeaks can also be

observed for H2 (2.28 ppm) which is coupled to H3 (1.60 ppm). The effect of the electronegative oxygen atom of the carbonyl group resulted in a downfield shift of the signal from H2 compared to H3[35]. The functional group assignments and integrations for oleic, linoleic and linolenic fatty acid ethyl esters in $CDCl_3$ and d_6-DMSO are displayed in Table 3.3. HSQC data (presented in Appendix A, page 252-253) confirmed the proton assignments and methylene pairs. Initially, it was thought that the mixture contained only ethyl esters of oleic, linoleic and linolenic fatty acids. However, it was later discovered that saturated fatty acids of varying chain lengths were also present. Therefore the calculation of relative amounts of each fatty acid, based on peak integration, could not be determined.

Table 3.3: ^{1}H-NMR functional group assignments and integration for oleic, linoleic and linolenic fatty acid ethyl esters

ppm	18:1	18:2	18:3	Integration ($CDCl_3$)	Integration (d_6-DMSO)
0.89 (t)	H18 $-CH_3$	H18 $-CH_3$	-	6.72	3.8
0.98 (t)	-	-	H18 $-CH_3$	3	3
1.25 (t)	H2' ($-CH_3$)	H2' ($-CH_3$)	H2' ($-CH_3$)	24.20	12.5
1.28-1.31 (m)	$(-CH_2)_n$	$(-CH_2)_n$	$(-CH_2)_n$	33.72	33.3
1.60 (m)	H3 ($-CH_2$)	H3 ($-CH_2$)	H3 ($-CH_2$)	5.81	6.4
2.02-2.07 (m)	H8, H11 $(-CH_2)_2$	H8, H14 $(-CH_2)_2$	H8, H17 $(-CH_2)_2$	11.35	10.5
2.28 (t)	H2 ($-CH_2$)	H2 ($-CH_2$)	H2 ($-CH_2$)	6.25	5.1
2.77-2.80 (m)	-	H11 ($-CH_2$)	H11, H14 $(-CH_2)_2$	6.10	5.5
4.13 (q)	H1' ($-CH_2$)	H1' ($-CH_2$)	H1' ($-CH_2$)	6.78	4.5
5.33-5.37 (m)	H9, H10 $(=CH)_2$	H9, H10, H12, H13 $(=CH)_4$	H9, H10, H12, H13, H15, H16 $(=CH)_6$	11.90	9.4

According to Knothe and co-workers, the ^{1}H-NMR signals that may be used for the quantification of unsaturated fatty acids are those from the olefinic protons (5.33-5.37 ppm), protons attached to the bis-allylic carbons (2.77-2.80 ppm), protons attached to the allylic carbons (2.02-2.07 ppm) and the terminal methyl group protons[21]. The terminal methyl group protons of linolenic acid resonated downfield (0.98 ppm) compared to those of oleic and linoleic acid (0.89 ppm), due to the proximity of the C15-C16 double bond. Its signal is therefore unique and was assigned a relative integral of 3. A comparison of the relative ratios of $-CH_3$ (0.89 ppm), $-CH_2$ (1.60 ppm)

and –CH (5.33-5.37 ppm) in each solvent (Table 3.3) was used to determine whether the integration was internally consistent and therefore reliable; the expected ratios being 1:1:2 respectively. Integration values obtained in $CDCl_3$ gave the expected ratio of 1:1:2 and therefore were internally consistent while those obtained in d_6-DMSO (1:2:2 respectively) differed from the expected values and so were inconsistent. This was because better peak resolution in $CDCl_3$ enabled them to be integrated accurately. The signal from H2' in $CDCl_3$ (1.25 ppm) overlapped slightly with the methylene protons (1.28-1.31 ppm) and therefore had a higher integration value (24.2) than expected (10.2).

The ^{1}H- and ^{13}C chemical shifts for the mixture of oleic, linoleic and linolenic fatty acid ethyl esters in $CDCl_3$ are provided in Table 3.4 and are in agreement with those in the literature[23].

Table 3.4: ^{1}H and ^{13}C-NMR data for a mixture of oleic, linoleic and linolenic fatty acid ethyl esters in $CDCl_3$

Atom	Proton and Carbon Chemical Shifts (ppm)		
	18:1	18:2	18:3
H-1	-	-	-
C-1	173.9	173.9	173.9
H-2	2.28	2.28	2.28
C-2	34.43	34.43	34.43
H-3	1.60	1.60	1.60
C-3	25.02	25.02	25.02
H-4	1.28-1.31	1.28-1.31	1.28-1.31
C-4	29.15-31.95[a]	29.15-31.95[a]	29.15-31.95[a]
H-5	1.28-1.31	1.28-1.31	1.28-1.31
C-5	29.15-31.95[a]	29.15-31.95[a]	29.15-31.95[a]
H-6	1.28-1.31	1.28-1.31	1.28-1.31
C-6	29.15-31.95[a]	29.15-31.95[a]	29.15-31.95[a]
H-7	1.28-1.31	1.28-1.31	1.28-1.31
C-7	29.15-31.95[a]	29.15-31.95[a]	29.15-31.95[a]
H-8	2.02-2.07	2.02-2.07	2.02-2.07
C-8	27.24	27.24	27.24
H-9	5.33-5.37	5.33-5.37	5.33-5.37
C-9	127.2-132.0[b]	127.2-132.0[b]	127.2-132.0[b]
H-10	5.33-5.37	5.33-5.37	5.33-5.37
C-10	127.2-132.0[b]	127.2-132.0[b]	127.2-132.0[b]
H-11	2.02-2.07	2.77-2.80	2.77-2.80
C-11	27.24	25.68	25.68
H-12	1.28-1.31	5.33-5.37	5.33-5.37
C-12	29.15-31.95[a]	127.2-132.0[b]	127.2-132.0[b]
H-13	1.28-1.31	5.33-5.37	5.33-5.37
C-13	29.15-31.95[a]	127.2-132.0[b]	127.2-132.0[b]
H-14	1.28-1.31	2.02-2.07	2.77-2.80
C-14	29.15-31.95[a]	27.24	25.68
H-15	1.28-1.31	1.28-1.31	5.33-5.37
C-15	29.15-31.95[a]	29.15-31.95[a]	127.2-132.0[b]
H-16	1.28-1.31	1.28-1.31	5.33-5.37
C-16	29.15-31.95[a]	29.15-31.95[a]	127.2-132.0[b]
H-17	1.28-1.31	1.28-1.31	2.02-2.07
C-17	22.71	22.60	20.59
H-18	0.89	0.89	0.98
C-18	14.11-14.29[c]	14.11-14.29[c]	14.11-14.29[c]
H-1'	4.13	4.13	4.13
C-1'	60.16	60.16	60.16
H-2'	1.25	1.25	1.25
C-2'	14.11-14.29[c]	14.11-14.29[c]	14.11-14.29[c]

[a]Resonances are: 29.15, 29.19, 29.38, 29.55, 29.63, 29.73, 29.81, 31.57, 31.95 ppm; [b]Resonances are: 127.18, 127.79, 127.97, 128.10, 128.34, 129.80, 130.09, 130.25, 130.31, 132.00 ppm; [c]Resonances are: 14.11, 14.29 ppm

The ^{13}C assignments were compared with those of Stoffel and associates who chemically synthesised oleic and linoleic acids with ^{13}C in positions 1, 3, 8, and 14[23].

Enriching particular carbon atoms with 88–99 % ^{13}C allowed the accurate assignment of the chemical shifts of the carbon atoms and also increased sensitivity[23]. The ^{13}C label of C14 in linoleic acid showed that the unequivocal chemical shift of this C atom was 27.0 ppm. The same was observed for oleic acid ^{13}C-enriched in C8 and C11. Their conclusion therefore was that carbon atoms in juxtapositions pointing to the carboxy and methyl ends of cis-olefinic bonds are characterised by this resonance. In the present study, the chemical shift of these allylic protons, as confirmed by HSQC and HMBC was 26.5 ppm, which is close to the value reported by Stoffel and co-workers[23]. It has been observed however that the chemical shift for C17 of α-linolenic acid occurs at higher field[23]. Our result of 19.94 ppm for this C atom is therefore in agreement with reported literature and confirmed by HSQC correlation between ^{1}H at 1.3-2.0 ppm and ^{13}C at 20.6-22.7 ppm. The chemical shift for the bisallylic groups is in the range 25.02-25.12 ppm and is very close to that reported in the literature of 25.5 ppm[23]. Other characteristic resonances include that of the carbonyl function at 172.7 ppm and the α- and β-carbon atoms at 33.5 and 24.4 ppm respectively and are in agreement with those measured by Stoffel and co-workers[23].

NMR spectroscopy has been successfully applied to study the composition of a mixture of oleic, linoleic and linolenic fatty acid ethyl esters dissolved in $CDCl_3$ or d_6-DMSO. Signals due to unsaturated carbons (at 5.33-5.37 ppm and 127-132 ppm in the ^{1}H and ^{13}C spectra respectively) and ethyl ester (H1'/H2' at 4.13/1.25 ppm and 60.2/14.1 ppm in the ^{1}H and ^{13}C spectra respectively) confirmed the presence of the above unsaturated fatty acid ethyl esters. The relative ratios of $-CH_3$, $-CH_2$ and –CH signals in each solvent were compared in order to establish consistency. Compared to d_6-DMSO, the integration values obtained in $CDCl_3$ were more internally consistent and thus more reliable.

3.4.2 PEG hydrogenated castor oil

In this study, the compounds present in commercially available PEG hydrogenated castor oil was analysed in both $CDCl_3$ and d_6-DMSO by ^1H- and ^{13}C-NMR. The assignment of all proton and carbon atoms was achieved using COSY, HSQC and HMBC spectra. Data from the ^1H, ^{13}C and COSY experiments are presented and discussed. The ^1H-NMR spectra obtained in $CDCl_3$ and d_6-DMSO are displayed in Fig 3.6 and some characteristic signals are labelled. Assignments were made by inspection and consultation of literature and confirmed by 2D. However, the presence of a mixture of components in the sample complicated the analysis.

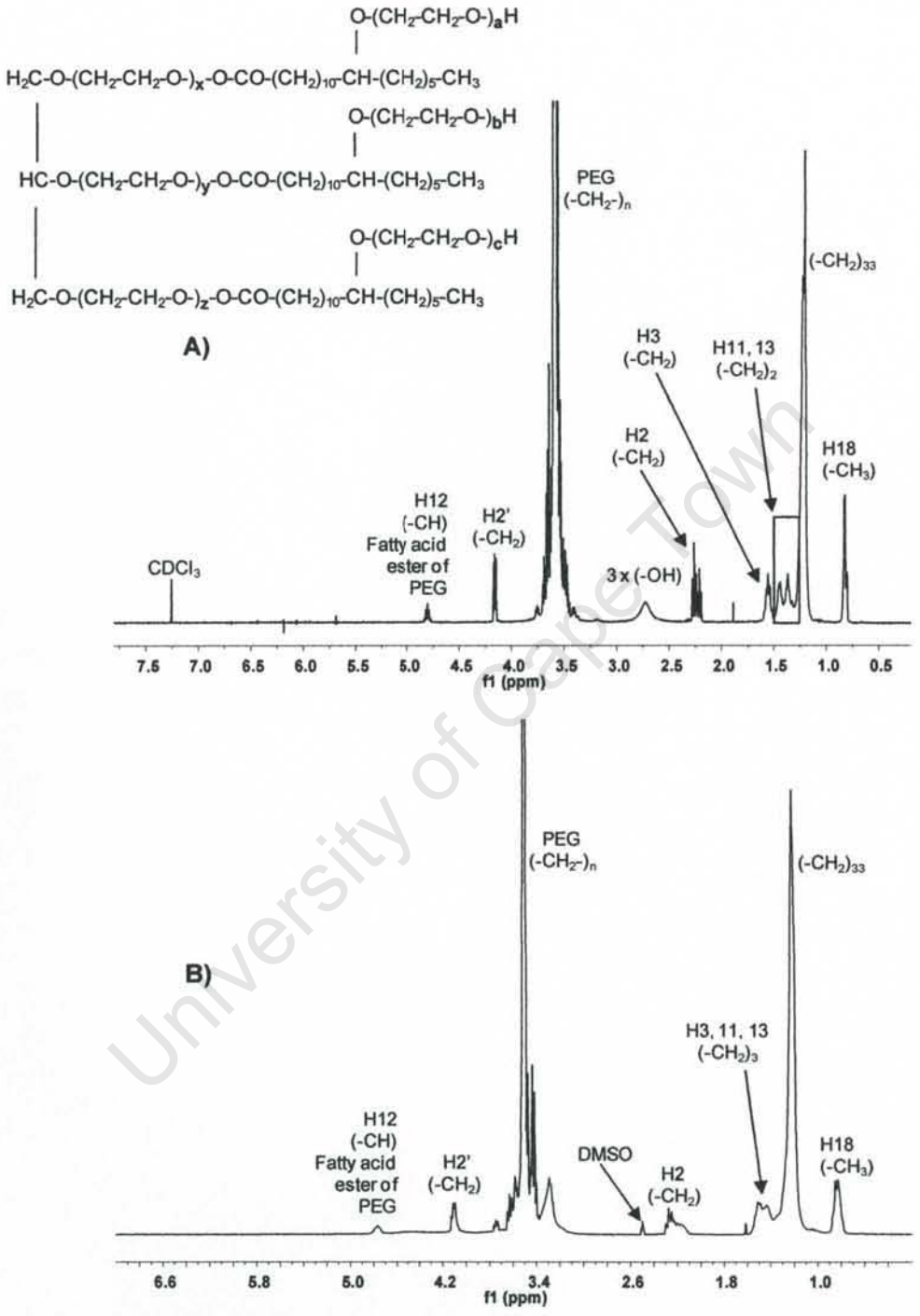

Fig 3.6: *^{1}H-NMR spectra (400 MHz) for PEG hydrogenated castor oil in $CDCl_3$ (A) and d_6-DMSO (B) recorded at 300 K. Some characteristic proton assignments are indicated*

Numbering of the carbon atoms in the fatty acid started at the carbonyl carbon (C1) and ended at the terminal carbon (C18). Again, protons were labelled H and have numbers corresponding to that of the carbon atom to which they are attached. Carbon atoms in the glycerol backbone were labelled C1', C2' and C3'. Better peak resolution was obtained in $CDCl_3$.

The 2D $^1H,^1H$ COSY spectrum in $CDCl_3$ and d_6-DMSO for PEG hydrogenated castor oil were similar and so only the 2D spectrum obtained in $CDCl_3$ is displayed in Fig 3.7.

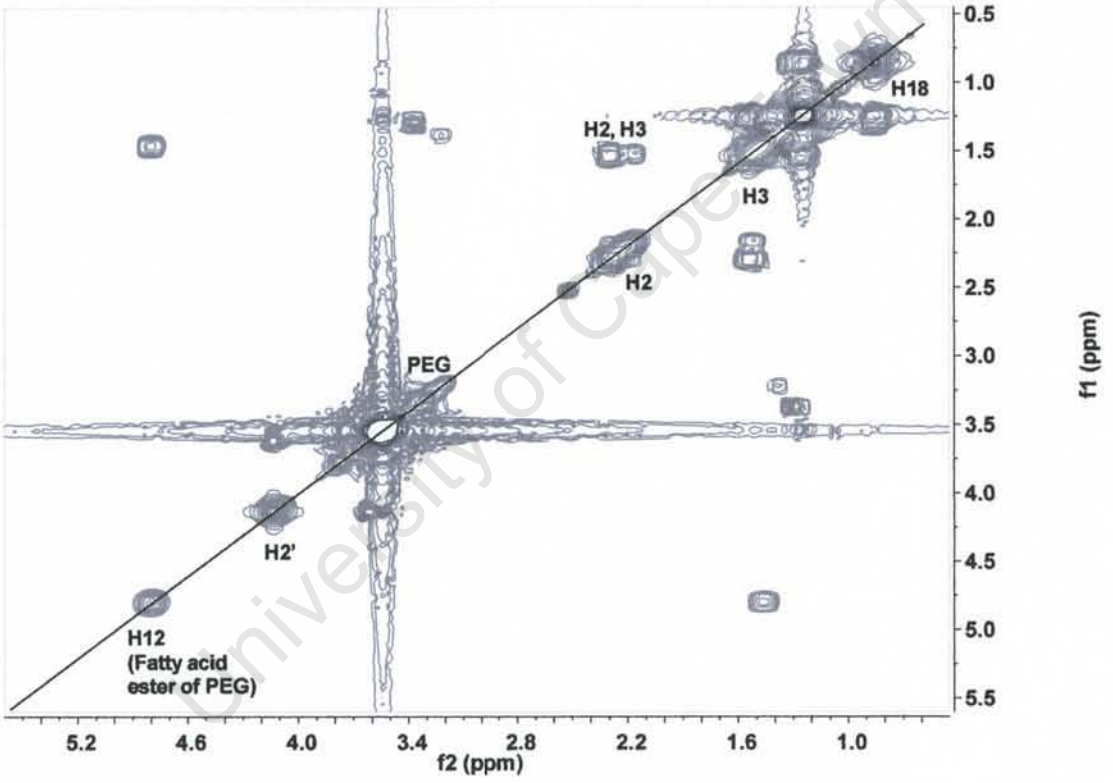

Fig 3.7: *COSY spectrum (300 MHz) for PEG hydrogenated castor oil in $CDCl_3$ recorded at 300 K. Some crosspeaks are labelled*

The spectrum is dominated by resonances from the polyethylene glycol (PEG) moiety. However, crosspeaks between H18 protons and the methylene protons were detected. Cross peaks were also identified for proton coupling between H2 and H3. The large PEG signal overlapped with signals for H12 (of glycerol polyethylene glycol oxystearate). The PEG methylene groups resonated at 3.41-3.76 ppm.

The ^{1}H-NMR functional group assignments, as confirmed by HSQC (data presented in Appendix A page 254), and integration values for PEG hydrogenated castor oil in $CDCl_3$ and d_6-DMSO respectively are provided in Table 3.5.

Table 3.5: ^{1}H-NMR functional group assignments and integration for glycerol polyethylene glycol oxystearate

δ (ppm)	Glycerol polyethylene glycol oxystearate	Expected integration	Integration in $CDCl_3$	Integration in d_6-DMSO
0.82 (t)	H18 (3 x $-CH_3$)	9	9	9
1.20-1.22(bs)	H4-10 and H14-17 [3 x $(-CH_2)_{11}$]	66	65.38	69.78
1.37-1.44 (m)	H11, H13 (3 x $(-CH_2)_2$)	12	16.34	12.36
1. 56 (m)	H3 (3 x $(-CH_2)$	6	6.75	
2.26 (t)	H2 (3 x $(-CH_2)$	6	6.82	5.42
2.73 (bs)	PEG (3 x OH)	3	5.64	-
3.41-3.76 (m)	$[-CH_2-CH_2-O]_n$, H1', H3' (2 x $-CH_2$)	-	211	216
4.16 (d)	H2' (-CH)	1	3.72	1.81
4.80 (m)	H12 (-CH) of the fatty acid ester of PEG	1	1.37	0.51

The terminal methyl group ($-CH_3$) in each fatty acid of the triacyl glyceride molecule was assigned an integration value of three and so their combined integration value was expected to be 9. The ^{1}H-NMR spectrum exhibited signals at δ 0.82 (t, 9H, terminal $-C\underline{H}_3$), 1.20-1.22 (bs, 66H, methylene protons [3 x $(-C\underline{H}_2)_{11}$], 1.37-1.44 (m, 12H, $-CH_2C\underline{H}_2CH(OR)$), 1.56 (m, 6H, $-C\underline{H}_2-CH_2-C=O$), 2.26 (t, 6H, $-C\underline{H}_2-C=O$), 2.73 (bs, 3H, $-CH_2-CH_2O\underline{H}$ (PEG), 3.41-3.76 (m, 3H, ($-CH_2CH_2C\underline{H}(OR)$) signal overlaps with that of $[-C\underline{H}_2-C\underline{H}_2O]_n$ (PEG) and $-C\underline{H}_2CHC\underline{H}_2-$ (glycerol CH_2), 4.16 (m, 1H, $-CH_2C\underline{H}CH_2$ (glycerol CH), 4.80 (m, 1H, ($-CH_2CH_2C\underline{H}(OR)$ (the fatty acid ester of polyethylene glycol). The signal at 4.80 ppm originates from H12 of the fatty acid ester of polyethylene glycol because it was coupled to H11 and H13 in the COSY spectrum and has an integration value of approximately 1. The H12 proton of glycerol polyethylene glycol oxystearate would have an expected integration value of 3. Variations between the expected and experimental integration values for glycerol polyethylene glycol oxystearate is probably due to the fact that the sample was a complex mixture and contained small amounts of ethoxylated glycerol, fatty acid esters of polyethylene glycol and polyethylene glycols. In $CDCl_3$, not only was better peak resolution obtained but the integration values were also more internally consistent compared to those obtained in d_6-DMSO. As such, spectra

obtained in $CDCl_3$ were used for proton and carbon assignments and as the basis for any conclusions drawn.

The signal from the PEG hydroxyl protons, though not detected in d_6-DMSO, was detected in $CDCl_3$. The expected integration was 3 since there were 3 attached PEG groups for every triglyceride molecule. The higher integration value obtained (5.64) could indicate the presence of free PEG in the sample. Other possible components include ethoxylated glycerol and fatty acid esters of polyethylene glycol (derived from the reaction of hydrogenated ricinoleic acid in the castor oil sample with ethylene oxide) (Fig 3.2 (b) and (c))[14, 36]. As a result, it will not be possible to use the integral of the PEG moiety to determine the number of subunits present in the polymer.

The ^{1}H- and ^{13}C chemical shifts for PEG hydrogenated castor oil in $CDCl_3$ are provided in Table 3.6. These assignments were confirmed using HSQC and HMBC spectra (data presented in Appendix A pages 253-255).

Table 3.6:

Atom	^{1}H and ^{13}C Chemical Shifts (ppm)	Literature value (ppm)	Reference
C-1	173.65, 173.78	172.23-173.23	37, 38
H-2	2.26	2.23-2.36	39
C-2	34.12, 34.67	33.3-34.9	37, 41, 42
H-3	1.56	1.52-1.57	39
C-3	24.85, 25.18	24.3-25.3	37, 38, 40, 41
H-4	1.20-1.22	1.22-1.42	39
C-4	29.12-29.67[b]	28.2-30.7	37, 41
H-5	1.20-1.22	1.22-1.42	39
C-5	29.12-29.67[b]	28.2-30.7	37, 41
H-6	1.20-1.22	1.22-1.42	39
C-6	29.12-29.67[b]	28.2-30.7	37, 41
H-7	1.20-1.22	1.22-1.42	39
C-7	29.12-29.67[b]	28.2-30.7	37, 41
H-8	1.20-1.22	1.22-1.42	39
C-8	29.12-29.67[b]	28.2-30.7	37, 41
H-9	1.20-1.22	1.22-1.42	39
C-9	29.12-29.67[b]	28.2-30.7	37, 41
H-10	1.20-1.22	1.22-1.42	39
C-10	29.12-29.67[b]	28.2-30.7	37, 41
H-11	1.37-1.44	-	-
C-11	29.12-29.67[b]	27.0-29.6	37
H-12	3.41-3.76	3.55	42
C-12	70.25-73.98[c]	60-75	38
H-13	1.37-1.44		
C-13	29.12-29.67[b]	27.0-29.6	37
H-14	1.20-1.22	1.22-1.42	39
C-14	25.12-25.58[a]	27.24-29.71	37
H-15	1.20-1.22	1.22-1.42	39
C-15	25.12-25.58[a]	29.39-29.24	37
H-16	1.20-1.22	1.22-1.42	39
C-16	31.81	31.57-31.98	37
H-17	1.20-1.22	1.22-1.42	39
C-17	22.56	22.62-22.74	37
H-18	0.82	0.83-0.93	39
C-18	14.04	13.4-14.6	41
H-1'	4.16	4.10-4.32	39
C-1'	61.53, 63.29	62.1	38
H-2'	4.80	5.20-5.26	39
C-2'	69.16, 69.70	68.9	37
H-3'	4.16	4.10-4.32	39
C-3'	61.53, 63.29	62.1	38
PEG: H-	3.41-3.76	3.54-3.70	43
C-	70.25-73.98[c]		

[a] Resonances are: 25.12, 25.21, 25.26, 25.58 ppm; [b]Resonances are: 29.12, 29.21, 29.36, 29.45, 29.53, 29.61, 29.67 ppm; [c]Resonances are: 70.25,70.53, 70.73; 70.79, 71.25, 72.65, 73.98 ppm;

Characteristic ^{13}C-NMR signals for triacyl glycerols occur at 61.2 ppm (for the α-glycerol carbon atoms at positions 1' and 3') and 68.9 ppm (for the β-glycerol carbon atom at position 2')[38]. As shown in Table 3.5, two values were obtained for each of these carbon atoms because their chemical environment in glycerol polyethylene glycol oxystearate (Fig 3.2 (a)) differs slightly from ethoxylated glycerol (Fig 3.2 (b)).

In summary, detailed 1D (^{1}H and ^{13}C) and 2D NMR experiments (^{1}H,^{1}H correlation, COSY and ^{1}H,^{13}C correlation, HSQC) were conducted on a sample of PEG hydrogenated castor oil (^{13}C, HSQC and HMBC spectra presented in Appendix A pages 253-255). The results indicated the presence of glycerol polyethylene glycol oxystearate. Fatty acid esters of PEG, ethoxylated glycerol and free PEG were also present in the sample. Analysis of the NMR data was complicated by the presence of a mixture of components in the sample, as well as by the very large signal from the PEG moiety.

3.4.3 dl-α-Tocopherol (Vitamin E)

Tocopherols are widely used in the pharmaceutical and food industries due to their antioxidative properties. Vitamin E consists of four tocopherol homologues, namely α-, β-, γ- and δ-tocopherol which possess different bioavailabilities (Fig 3.8)[43]. α-tocopherol has the highest biological activity. The tocopherol molecule has three chiral centres (positions 2, 4' and 8') and dl- α-tocopherol, the anti-oxidant used in Pheroid™, is chemically synthesised and contains a mixture of the d and l isomers of α-tocopherol (mixture of eight stereoisomers)[44].

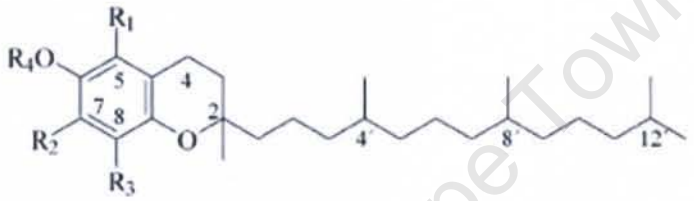

	R_1	R_2	R_3	R_4
δ–tocopherol	-H	-H	$-CH_3$	-H
γ–tocopherol	-H	$-CH_3$	$-CH_3$	-H
β–tocopherol	$-CH_3$	-H	$-CH_3$	-H
α–tocopherol	$-CH_3$	$-CH_3$	$-CH_3$	-H

Fig 3.8: *Chemical structure of the tocopherol homologues[43].*

A sample of dl-α-tocopherol dissolved in d_6-DMSO was analysed by ^{1}H- and ^{13}C-NMR spectroscopy. $CDCl_3$ was not used for this experiment because the residual solvent peak at 7.3 ppm would have interfered with the analysis. Assignments were made by inspection and consultation of literature and confirmed by 2D (COSY, HSQC and HMBC). Data from the ^{1}H, ^{13}C and COSY experiments are presented and discussed. The ^{1}H-NMR spectrum obtained in d_6-DMSO is presented in Fig 3.9 and some characteristic signals are labelled.

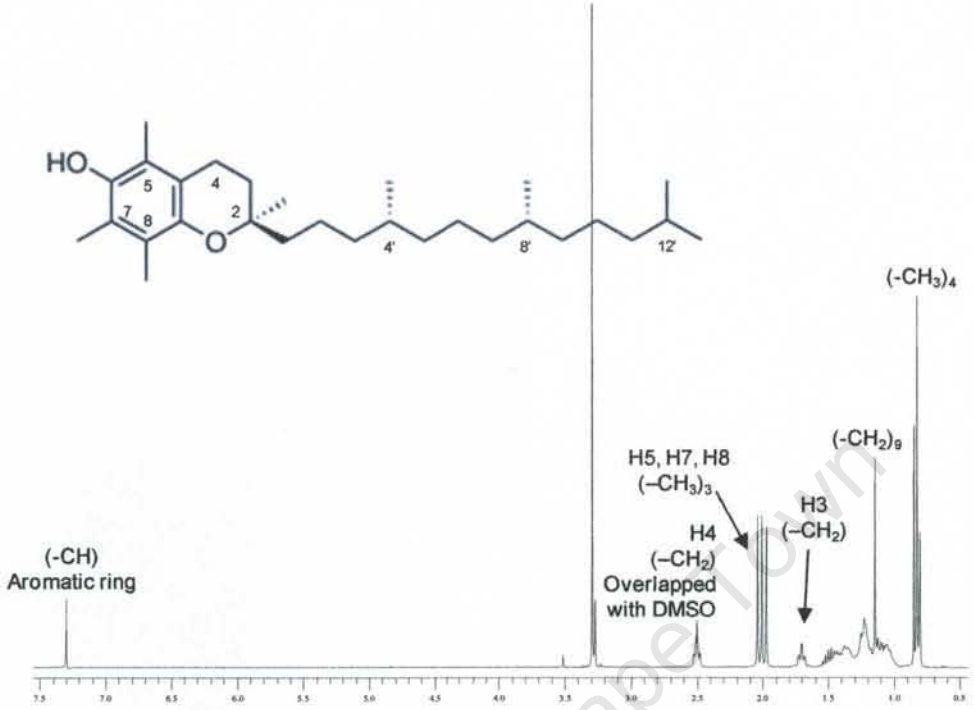

Fig 3.9: *^{1}H-NMR spectrum (400 MHz) for dl-α-tocopherol in d_6-DMSO recorded at 300 K. Some characteristic proton assignments are labelled*

The carbon atoms were numbered as shown in Fig 3.9. Carbon atoms in the aromatic ring were numbered 2-8 and those in the phytyl chain 1' to 12'. The protons have numbers corresponding to that of the carbon atom to which they are attached. The ^{1}H-NMR spectrum of dl-α-tocopherol (Fig 3.9) can be divided into three sections, an aromatic region at ~7.3 ppm, a region at ~2.0 ppm corresponding to the protons of the methyl groups bound to the aromatic ring, and a high-field region between 0.8 and 1.6 ppm showing the signals of protons in the saturated phytyl side chain[44]. Two important additional peaks are visible at ~2.5 and 1.7 ppm representing protons at positions 4 and 3 respectively.

The 2D ^{1}H,^{1}H COSY spectrum for dl-α-tocopherol in d_6-DMSO is shown in Figs 3.10 and some proton assignments are labelled.

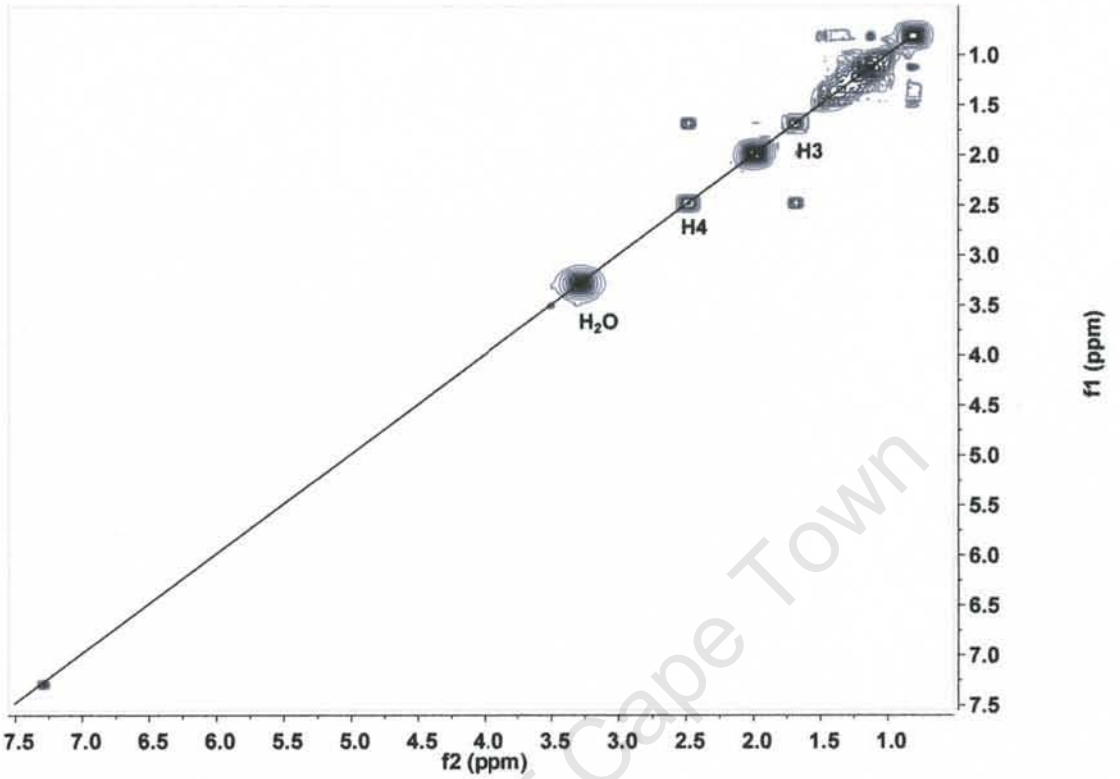

Fig 3.10: *COSY spectrum (300 MHz) for dl-α-tocopherol in d_6–DMSO recorded at 300 K. Some crosspeaks are labelled*

Crosspeaks in the COSY spectrum identify scalar coupling between neighbouring hydrogens. Major cross peaks were detected between H3 and H4 and in the phytyl chains between 0.8 and 1.6 ppm (upon expansion of the spectrum). In this region there is coupling between the methyl, methylene and methine protons, confirming their ^{1}H-NMR assignments. The four methyl groups of the phytyl chain (4', 8', 12') show cross-peaks to the methine protons. The cross peaks among the methylene protons in the phytyl side chain are also visible.

The ^{1}H-NMR functional group assignments for dl-α-tocopherol are presented in Table 3.7.

Table 3.7: ^{1}H-NMR functional group assignments and integration for dl-α-tocopherol

^{1}H Chemical Shift (ppm)	dl-α Tocopherol	Integration	Expected integration
0.85 (d)	$(-CH_3)_4$	12.00	12
1.0-1.8 (m)	H2 (CH_3); H1', H2', H3', H5', H6', H7', H9', H10', H11' (9 x ($-CH_2$); 4', 8', 12', (3 x (-CH)	24.09	24
1.70 (t)	H3 ($-CH_2$)	2.02	2
1.2 (s)	(CH_3)	-	3
1.97-2.04 (3 x s)	H5, H7, H8 (3 x $-CH_3$)	9	9
2.50 (t)	H4 ($-CH_2$)	2.77	2
7.30 (s)	H5/H7 (-CH)	1.02	1

Each methyl group in the aromatic ring was assigned an integration value of three (combined value of nine). The following peaks were identified: δ 0.85 (d, 12H, two methyl groups at the end of the phytyl chain [(H12' (2 x $-CH_3$)] and an additional two methyl groups within the chain [4'-, 8' (2 x $-CH_3$)], 1.0-1.8 [24H, overlapping signals due to the methyl group at position 2, the methylene protons on the phytyl chain and the methine protons (4', 8', 12')], 1.20 (s, 3H, methyl group at position 2), 1.70 (t, 2H, protons attached to C-3), 1.97-2.04 (3x s, 9H, methyl groups attached to the aromatic ring), 2.50 (t, 2H, protons attached to C-4), 7.3 (s, -CH on aromatic ring).

In dl-α-tocopherol, no proton is present on the aromatic ring and therefore the signal at 7.3 ppm indicated the presence of either β-tocopherol (one proton at position 7) or γ-tocopherol (one proton at position 5) and not δ-tocopherol because as shown in Table 3.6, the integration value at 7.3 ppm was 1. The HMBC spectrum (presented in Appendix A pages 257-259) showed coupling of the proton to C5 and C8 (consistent with a proton at position 7). No additional long-range coupling with C4 was observed, therefore it was concluded that the vitamin E sample contained dl-α-tocopherol and a small amount of β-tocopherol.

The ^{1}H- and ^{13}C chemical shifts for dl-α-tocopherol as confirmed by HSQC and HMBC are presented in Table 3.8 and are in agreement with those in the literature[44, 45]. Peaks in the ^{13}C spectrum were well dispersed (Table 3.8).

Table 3.8: ^{1}H- and ^{13}C-NMR data for dl-α-tocopherol in DMSO

Atom	^{1}H and ^{13}C Chemical Shifts (ppm)
H-2	1.20
C-2	73.7
H-3	1.70
C-3	31.2
H-4	2.50
C-4	19.5
H-5	2.00
C-5	116.6-122.4[a]
H-6	7.3
C-6	144.4
H-7	2.00
C-7	116.6-122.4[a]
H-8	2.00
C-8	116.6-122.4[a]
H-1'	1.0-1.8
C-1'	36.5-36.9[b]
H-2'	1.0-1.8
C-2'	36.5-36.9[b]
H-3'	1.0-1.8
C-3'	36.5-36.9[b]
H-4'	0.80
C-4'	31.8-32.0
H-5'	1.0-1.8
C-5'	36.5-36.9[b]
H-6'	1.0-1.8
C-6'	36.5-36.9[b]
H-7'	1.0-1.8
C-7'	36.5-36.9[b]
H-8'	0.80
C-8'	31.8-32.0
H-9'	1.0-1.8
C-9'	36.5-36.9[b]
H-10'	1.0-1.8
C-10'	36.5-36.9[b]
H-11'	1.0-1.8
C-11'	36.5-36.9[b]
H-12'	0.80
C-12'	27.3

[a]Resonances are: 11.56, 120.14, 120.78, 122.42 ppm; [b]Resonances are: 36.52, 36.62, 36.81, 36.87 ppm

3.5 NMR analysis of different lots of Pheroid™ formulations

Four Pheroid™ lots (labelled A, B, C and D) were provided by North West University (Potchefstroom) and analysed by NMR spectroscopy to determine whether the individual components of Pheroid™ can be identified and quantified and whether differences between batches can be detected.

10 ml of each Pheroid™ preparation was freeze-dried following which two drops of the resulting oil was placed in an NMR tube and 500 µl of d_6-DMSO added. The samples were subjected to analysis by ^{1}H- and ^{13}C-NMR spectroscopy. For comparative purposes, the above study was repeated using $CDCl_3$ as solution (500 µl). The differences between Pheroid™ formulations are summarised in Table 3.9.

Table 3.9: Description of the Pheroid™ formulations

Sample	Lot number	Description
Pheroid™ A	NWU-B21062005	Prepared with starting material from lot NWU-A21062005
Pheroid™ B	NWU-B14112005	Prepared with starting material from lot NWU-A14112005
Pheroid™ C	NWU-B08022006	Prepared with starting material from lot NWU-A08022006 (formulated with dl-α-tocopherol)
Pheroid™ D	NWU-C08022006	Prepared in parallel with Pheroid™ C and with starting material from lot NWU-A08022006 (formulated without dl-α-tocopherol)

NMR spectra were acquired in d_6-DMSO and $CDCl_3$ as described in section 3.4. The ^{1}H spectra obtained of Pheroid™ samples A and B (prepared from lots NWU-A21062005 and NWU-A14112005 respectively) in $CDCl_3$ are displayed in Fig 3.11.

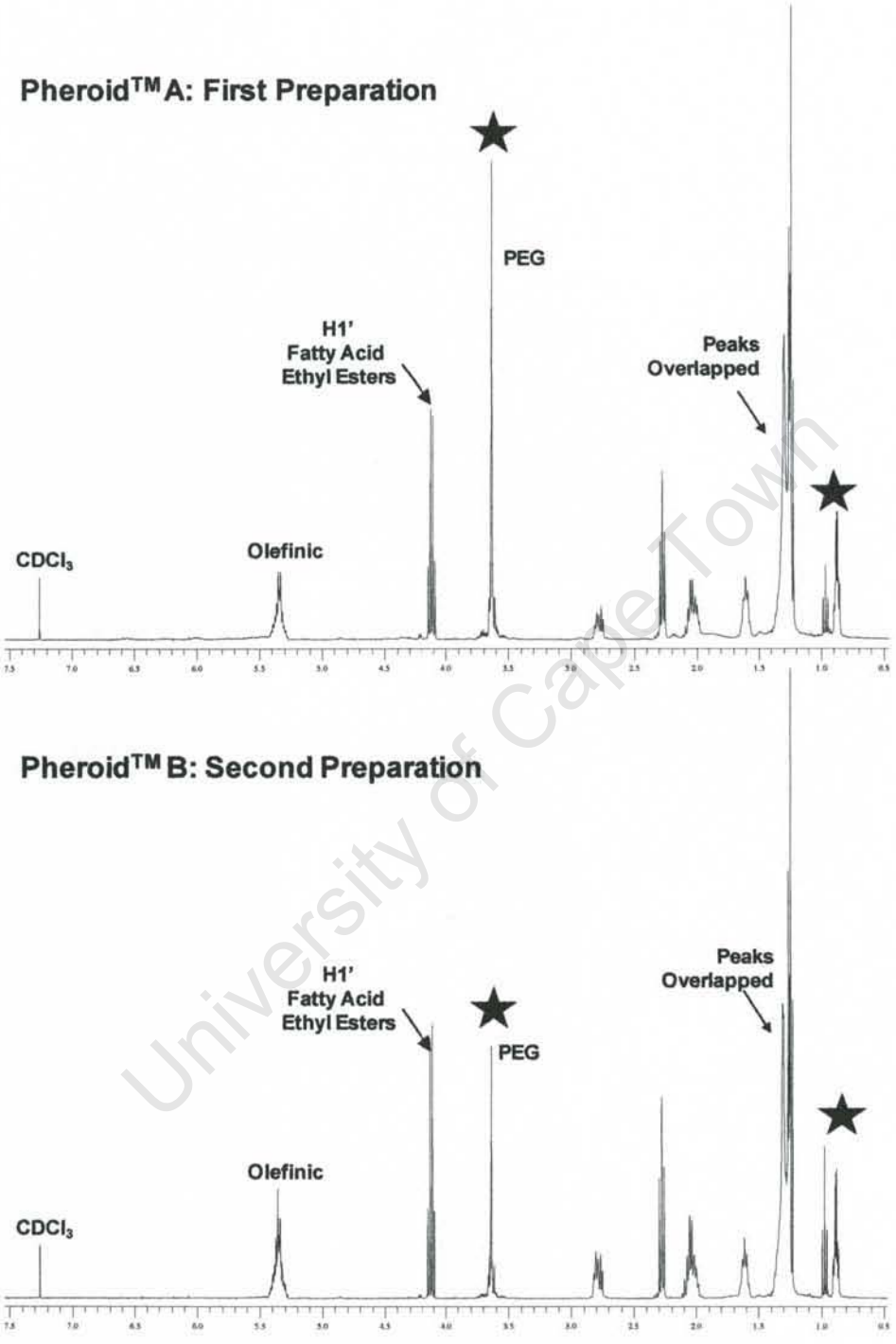

Fig 3.11: *^{1}H-NMR spectra (400 MHz) for Pheroid™ samples A and B in $CDCl_3$ recorded at 300 K. Some characteristic proton assignments are labelled and the stars highlight differences between the two spectra*

The peak height for the terminal methyl proton of linolenic acid (sample A) was markedly lower than the combined signal from oleic and linoleic acid whereas in sample B, the signal due to terminal methyl protons of linolenic acid was higher than the other two fatty acids (Fig 3.11). The intensity of the PEG signal in sample A was higher than that of H1' while in sample B the signal due to H1' was slightly higher than that of PEG. The fact that both spectra were similar suggested that samples A and B contained the same ingredients but different amounts. The ^{1}H-NMR spectra obtained in d_6-DMSO are presented in Figs 3.12.

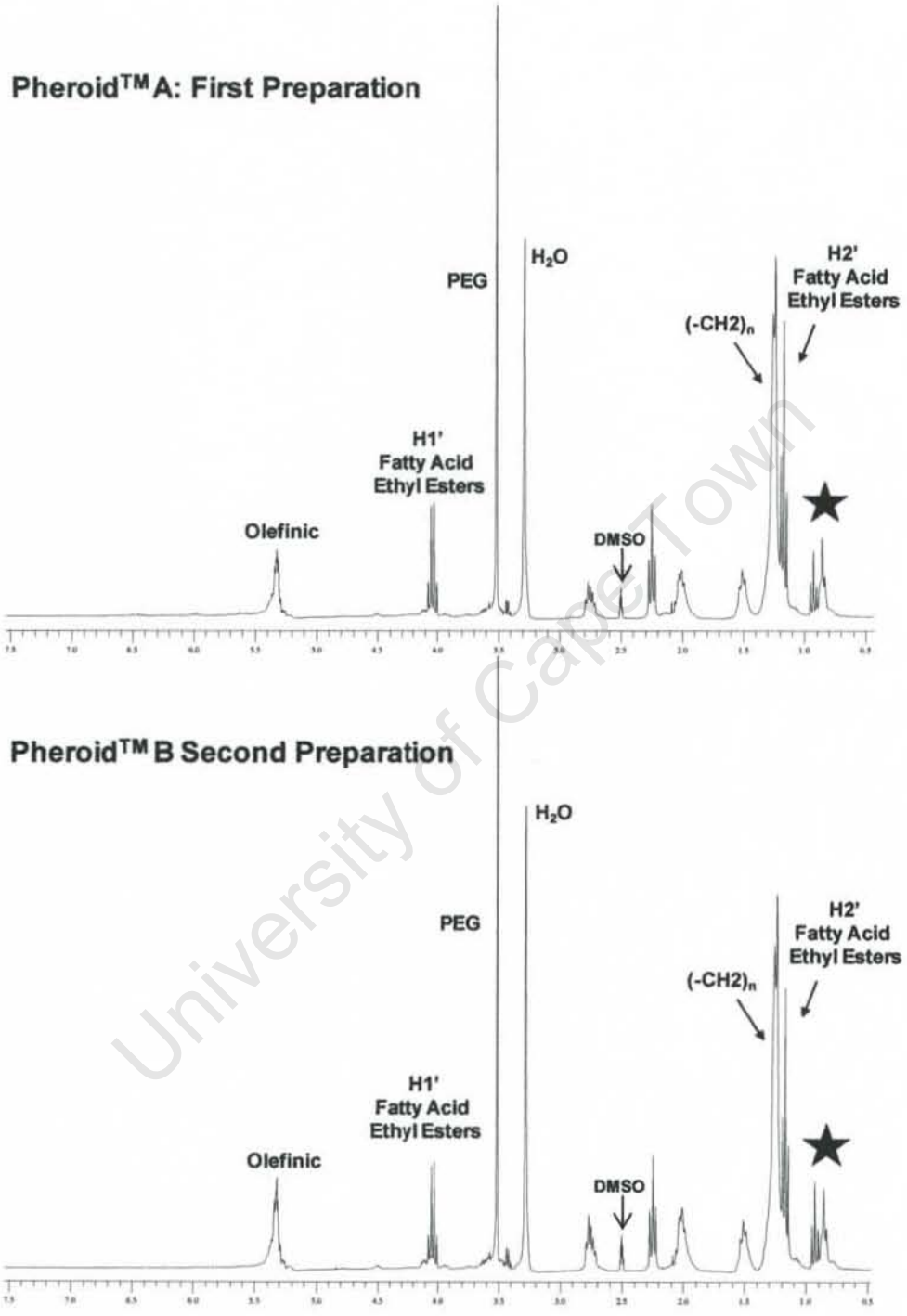

Fig 3.12: *^{1}H-NMR spectra (400 MHz) for Pheroid™ samples A and B in d_6-DMSO recorded at 300 K. Some characteristic signals are labelled and the stars highlight differences between the two spectra*

In d_6-DMSO the peak height for the terminal methyl group of linolenic acid (in sample A) was slightly lower than the other two fatty acids suggesting its presence in lower concentrations compared to oleic and linoleic acids (Fig 3.12). In sample B however, the opposite was observed. The peak height for the terminal methyl group of linolenic acid was now higher than the other two fatty acids suggesting its presence in higher concentrations compared to oleic and linoleic acids. Whereas the signals from H2' and $(-CH_2)_n$ overlapped in $CDCl_3$, better peak resolution was obtained in d_6-DMSO. The spectra obtained of samples A and B in d_6-DMSO contained the same peaks but with slightly different intensities supporting the observation that the Pheroid™ samples contained the same ingredients but in different amounts. This observation was supported by the ^{13}C spectra which were also similar for all the Pheroid™ formulations analysed (Fig 3.13).

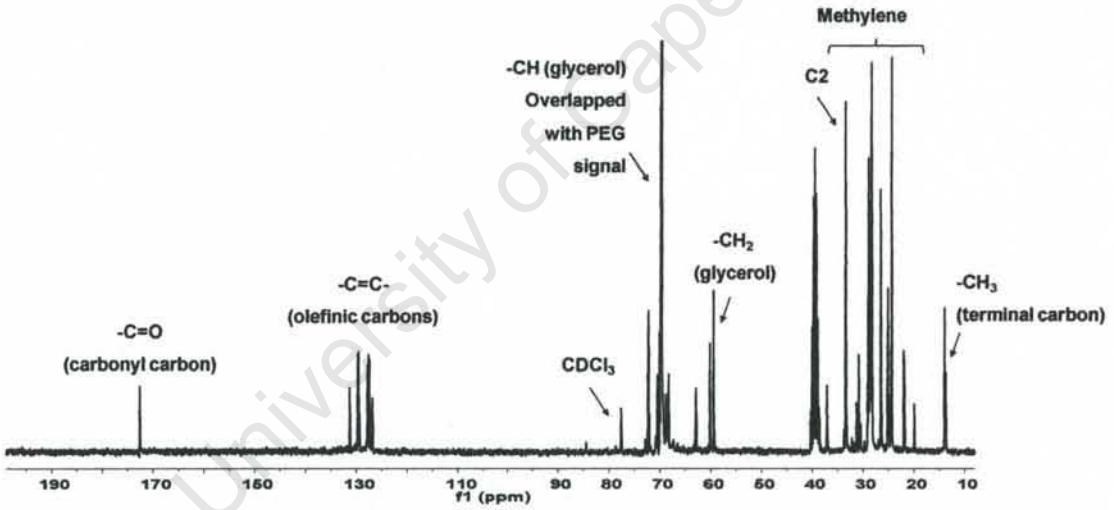

Fig 3.13: *Typical ^{13}C-NMR spectrum obtained for Pheroid™ formulations in $CDCl_3$. Spectrum shows a carbonyl signal (174 ppm), signals for the unsaturated carbon atoms (127-132 ppm), the PEG signal (70-74 ppm) and signals for glycerol (68.9 and 62.1 ppm).*

The function group assignments and integration values for Pheroid™ samples A and B in $CDCl_3$ and d_6-DMSO are presented in Table 3.10.

Table 3.10: ^{1}H chemical shifts and integration of Pheroid™ Samples A and B in $CDCl_3$ and d_6-DMSO

Pheroid™ Sample A						
ppm	18:1	18:2	18:3	Glycerol polyethylene glycol oxystearate	Integration in $CDCl_3$	Integration in d_6-DMSO
0.87 (t)	H18 ($-CH_3$)	H18 ($-CH_3$)	-	H18 ($-CH_3$)	9.05	3.61
0.97 (t)	-	-	H18 ($-CH_3$)	-	3	3
1.22-1.34 (bs)	H2' ($-CH_3$), ($-CH_2$)$_n$,	H2' ($-CH_3$), ($-CH_2$)$_n$,	H2' ($-CH_3$), ($-CH_2$)$_n$,	($-CH_2$)$_n$	82.63	41.71
1.61 (t)	H3 ($-CH_2$)	H3 ($-CH_2$)	H3 ($-CH_2$)	-	11.27	5.01
2.03 (m)	H8, C11 ($-CH_2$)$_2$	H8, H14 ($-CH_2$)$_2$	H8, H17 ($-CH_2$)$_2$	-	12.78	5.84
2.27 (t)	H2 ($-CH_2$)	H2 ($-CH_2$)	H2 ($-CH_2$)	-	9.37	3.83
2.76 (m)	-	H11 ($-CH_2$)	H11, H14 ($-CH_2$)$_2$	-	4.60	3.14
3.61-3.65 (bs)	-	-	-	[$-CH_2-CH_2-O$]$_n$, H9-H12 (CH)$_2$, H2' ($-CH_2$)$_3$	18.85	16.05
4.0 (q)	H1' ($-CH_2$)	H1' ($-CH_2$)	H1' ($-CH_2$)	-	7.21	3.78
4.1 (t)	-	-	-	H1' ($-CH_2$)	0.39	0.44
5.3 (m)	H9, H10 (=CH)$_2$	H9, H10, H12, H13 (=CH)$_4$	H9, H10, H12, H13, H15, H16 (=CH)$_6$	-	8.75	6.07
Pheroid™ Sample B						
0.89 (t)	H18 $-CH_3$	H18 $-CH_3$	-	H18 ($-CH_3$)	6.78	4.66
0.97 (t)	-	-	H18 $-CH_3$	-	3	3
1.1.23-1.31 (bs)	H2' ($-CH_3$), ($-CH_2$)$_n$,	H2' ($-CH_3$), ($-CH_2$)$_n$,	H2' ($-CH_3$), ($-CH_2$)$_n$,	-	57.15	47.03
1.61 (t)	H3 ($-CH_2$)	H3 ($-CH_2$)	H3 ($-CH_2$)	-	6.42	5.54
2.05 (m)	H8, H11 ($-CH_2$)$_2$	H8, H14 ($-CH_2$)$_2$	H8, H17 ($-CH_2$)$_2$	-	10.48	7.74
2.28 (t)	H2 ($-CH_2$)	H2 ($-CH_2$)	H2 ($-CH_2$)	-	6.43	4.38
2.79 (m)	-	H11 ($-CH_2$)	H11, H14 ($-CH_2$)$_2$	-	5.64	4.72
3.61-3.65 (bs)	-	-	-	[$-CH_2-CH_2-O$]$_n$, H9-H12 (CH)$_2$, H2' ($-CH_2$)$_3$	7.70	18.51
4.11 (q)	H1' ($-CH_2$)	H1' ($-CH_2$)	H1' ($-CH_2$)		6.17	3.80
4.20 (t)	-	-	-	H1' (-CH2)	0.17	0.48
5.36 (m)	H9, H10 (=CH)$_2$	H9, H10, H12, H13 (=CH)$_4$	H9, H10, H12, H13, H15, H16 (=CH)$_6$	-	11.08	7.87

CHAPTER 3

This investigation has established that ^{1}H-NMR spectroscopy can be used as a qualitative method to confirm the identity of Pheroid™ components and that the same ingredients were used to formulate Pheroid™ samples A and B. The spectra obtained for samples A and B were similar, with small differences in the intensities of the signals indicating slight differences in the relative amounts of these components. Of the two solvents used to dissolve Pheroid™, d_6-DMSO gave better peak resolution than $CDCl_3$. Immunogenicity studies will be required to determine what effects, if any, these differences have on the adjuvant activity of the emulsion.

^{1}H-NMR spectroscopy was then applied to study two Pheroid™ samples C and D which were prepared in parallel from the same starting materials; however, sample C contained dl-α-tocopherol whereas D did not. The anti-oxidant properties of dl-α-tocopherol help to stabilise the Pheroid™ emulsion. The spectra obtained in $CDCl_3$ are displayed in Figs 3.14. There was a problem with sample D. The concentration of dissolved sample D was very low compared to sample C and so the intensity of the signals obtained especially at 0.89, 2.0, 2.76 and 5.3 ppm (indicated by the stars) were also very low.

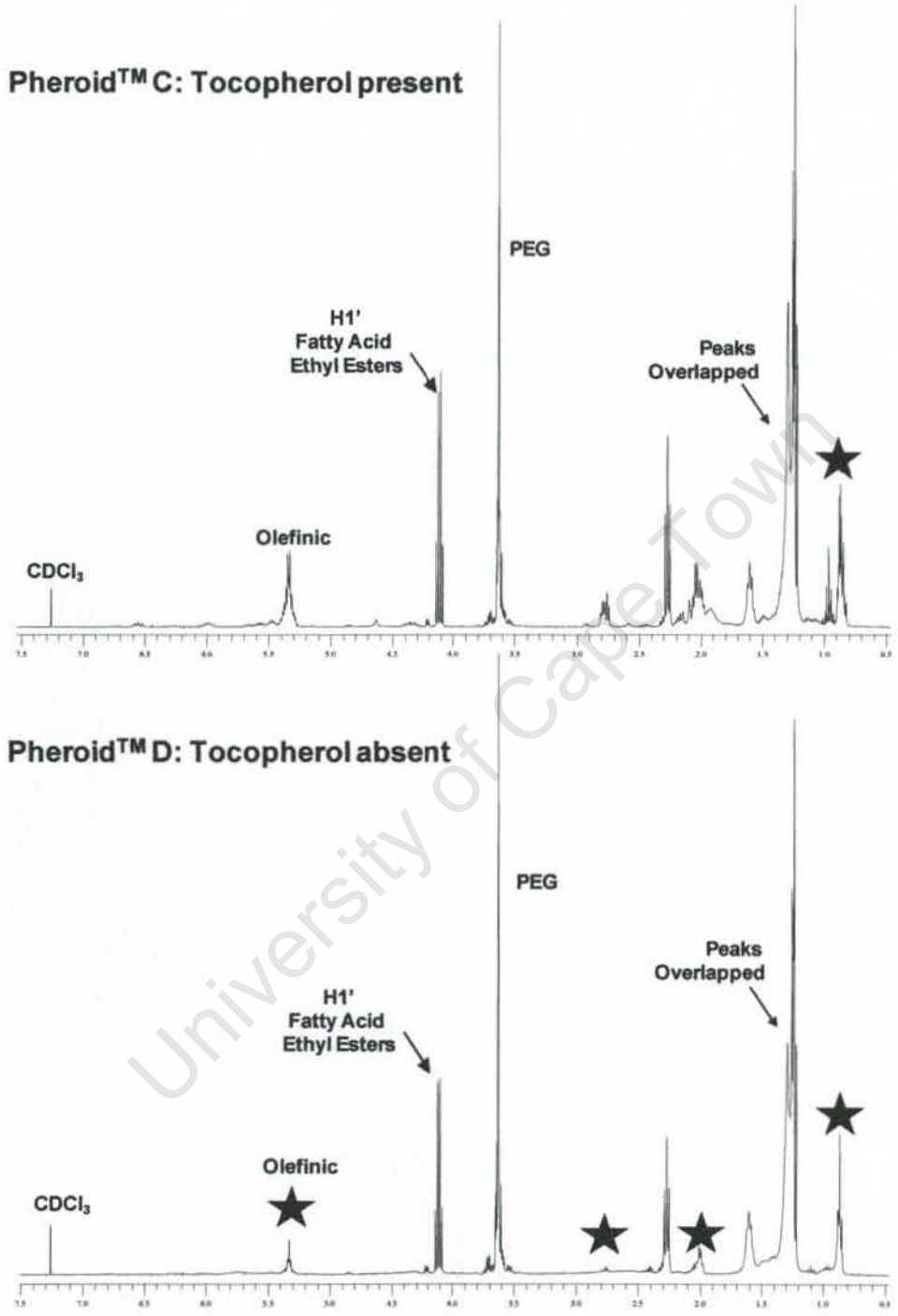

Fig 3.14: *^{1}H-NMR spectra (400 MHz) for Pheroid™ samples C and D in $CDCl_3$ recorded at 300 K. Some characteristic signals are labelled and the stars highlight differences between the two spectra*

The spectra obtained in d_6-DMSO are displayed in Figs 3.15. The ^{1}H-NMR spectra of both Pheroid™ formulations in d_6-DMSO were similar. The terminal methyl group signal for linolenic acid was consistently lower in intensity than that of oleic and linoleic acids. One significant difference is that in sample C, the peak height of the signal due to protons on H2' (1.17 ppm) is greater than that of the methylene protons (1.23 ppm). In sample D however, the reverse is true. So again there is evidence that even though samples C and D were prepared in parallel using the same ingredients, the fatty acid components were present in slightly different amounts.

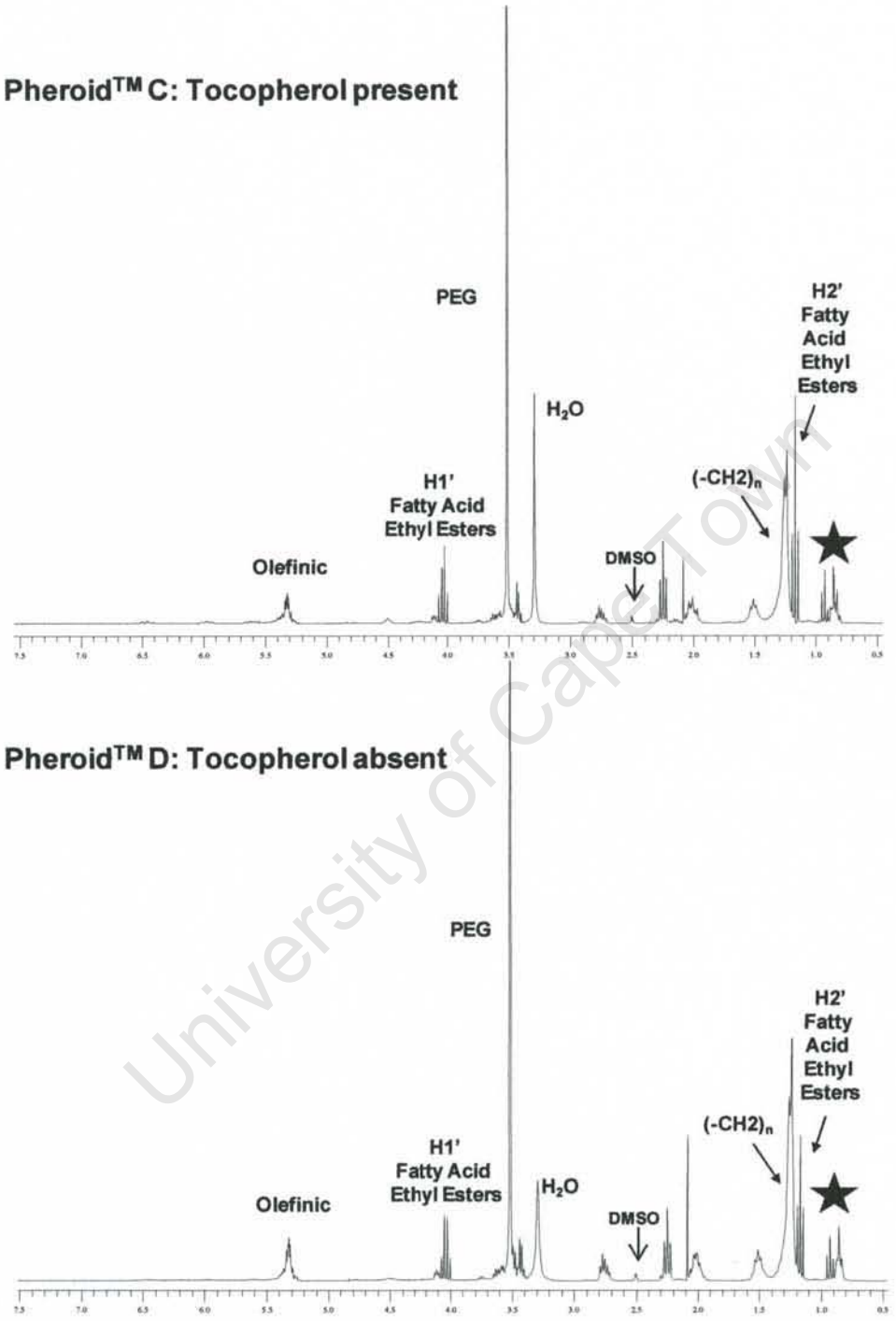

Fig 3.15: *^{1}H-NMR spectra (400 MHz) for Pheroid™ samples C and D in d_6-DMSO recorded at 300 K. Some characteristic signals are labelled and the stars highlight differences between the two spectra*

Table 3.11 shows the functional group assignments and integration values for Pheroid™ samples C and D in $CDCl_3$ and d_6-DMSO.

Table 3.11: Proton chemical shifts and integration for Pheroid™ Samples C and D in $CDCl_3$ and d_6-DMSO

Pheroid™ Sample C						
Ppm	**18:1**	**18:2**	**18:3**	**Glycerol polyethylene glycol oxystearate**	**Integration in $CDCl_3$**	**Integration in d_6-DMSO**
0.85 (t)	H18 -CH_3	H18 -CH_3	-	H18 (-CH_3)	7.49	3.31
0.93 (t)	-	-	H18 -CH_3	-	3	3
1.15-1.36 (bs)	H2' (-CH_3), (-CH_2)$_n$,	H2' (-CH_3), (-CH_2)$_n$,	H2' (-CH_3), (-CH2)$_n$,	(-CH_2)$_n$	51.00	33.39
1.60 (t)	H3 (-CH_2)	H3 (-CH_2)	H3 (-CH_2)	-	5.81	4.81
2.05 (m)	H8, H11 (-CH_2)$_2$	H8, H14 (-CH_2)$_2$	H8, H17 (-CH_2)$_2$	-	8.92	4.58
2.27 (t)	H2 (-CH_2)	H2 (-CH_2)	H2 (-CH_2)	-	5.80	3.21
2.76-2.79 (m)	-	H11 (-CH_2)	H11, H14 (-CH_2)$_2$	-	2.73	2.36
3.59-3.69	-	-	-	[-CH_2-CH_2-O]$_n$, H9-H12 (CH)$_2$, H2' (-CH_2)$_3$	15.56	41.6
4.10 (q)	C1' (-CH_2)	C1' (-CH_2)	C1' (-CH_2)	-	5.20	2.93
4.19 (t)	-	-	-	H1' (-CH_2)	0.418	0.50
5.32-5.39 (m)	H9, H10 (=CH)$_2$	H9, H10, H12, H13 (=CH)$_4$	H9, H10, H12, H13, H15, H16 (=CH)$_6$	-	6.52	4.89
Pheroid™ Sample D						
0.87 (t)	H18 -CH_3	H18 -CH_3	-	H18 (-CH_3)	6.24	5.08
0.93 (t)	-	-	H18 -CH_3	-	-	3
1.15-1.29 (bs)	H2' (-CH_3), (-CH_2)$_n$,	H2' (-CH_3), (-CH_2)$_n$,	H2' (-CH_3), (-CH_2)$_n$,	(-CH_2)$_n$	47.36	57.78
1.60 (t)	H3 (-CH_2)	H3 (-CH_2)	H3 (-CH_2)	-	8.84	8.64
2.00 (m)	H8, H11 (-CH_2)$_2$	H8, H14 (-CH_2)$_2$	H8, H17 (-CH_2)$_2$	-	3.43	7.98
2.27 (t)	H2 (-CH_2)	H2 (-CH_2)	H2 (-CH_2)	-	6.00	7.00
2.75 (m)	-	H11 (-CH_2)	H11, H14 (-CH_2)$_2$	-	1.33	4.30
3.51-3.74	-	-	-	[-CH_2-CH_2-O]$_n$, H9-H12 (CH)$_2$, H2' (-CH_2)$_3$	21.45	76.22
4.11 (q)	H1' (-CH_2)	H1' (-CH_2)	H1' (-CH_2)	-	6.08	5.14
4.19 (t)	-	-	-	H1' (-CH_2)	0.59	1.62
5.335 (m)	H9, H10 (=CH)$_2$	H9, H10, H12, H13 (=CH)$_4$	H9, H10, H12, H13, H15, H16 (=CH)$_6$	-	2.30	8.84

The ^{1}H-NMR spectrum of Pheroid™ contained characteristic signals due to the fatty acid ethyl esters at 1.2 ppm (H2'), 4.0 ppm (H1') and 5.3 ppm (olefinic protons). The presence of PEG hydrogenated castor oil was ascertained from the PEG signal at 3.6 ppm. A characteristic peak for dl-α-tocopherol would be the 3 singlets at 2.0 ppm for the methyl groups in the aromatic ring of α-tocopherol. However, they would overlap with the signal for the allylic protons in the fatty acid ethyl esters. Alternatively, a peak at 1.7 ppm (in d_6-DMSO) should have been observed for the H3 protons of dl-α-tocopherol, but is not. The fact that only approximately 0.3 % dl-α- tocopherol is added to Pheroid™ formulations means its concentration is probably below the limit of detection by NMR.

The region between 0.8-1.0 ppm contained signals from the fatty acid ethyl esters and PEG hydrogenated castor oil, therefore it was not possible to use these signals to determine the ratio of linolenic acid to the other fatty acids in the Pheroid™ formulations. Also, the PEG signal at 3.6 ppm overlaps with signals from H12 of glycerol polyethylene glycol oxystearate and so these signals could not be used to determine the ratio of the fatty acid ethyl esters to PEG hydrogenated castor oil. Another consequence of overlapping signals was that the integration values in Tables 3.8 and 3.9 could not be used to determine quantitative differences in the amounts of each component present in the Pheroid™ preparation. Thus, ^{1}H-NMR spectroscopy was limited because overlapping peaks hindered quantitative determination of each component. In addition, it was not sensitive enough to detect dl-α-tocopherol in the formulation. However, ^{1}H-NMR analysis of Pheroid™ formulations provided a structural fingerprint of the formulations and although the method was not quantitative for the individual components, it indicated the relative proportions of the major components present. Therefore, similarities in the ^{1}H- and ^{13}C-NMR spectra of different production lots of Pheroid™ can be used to confirm manufacturing consistency. While reliable integration values were obtained for the fatty acid ethyl esters in $CDCl_3$, d_6-DMSO gave better peak resolution for the Pheroid™ preparations.

The results obtained from the present study demonstrated that NMR spectroscopy (in d_6-DMSO) can be used as a qualitative method to monitor batch-to-batch consistency of Pheroid™ formulations. However, it permitted the analysis of composition alone and the procedure used was invasive as it resulted in the destruction of the Pheroid™ emulsion. Progress in the field of NMR spectroscopy now provides a non-invasive method of

characterising colloidal systems[46]. With respect to emulsions, pulsed field gradient (PFG) NMR now offers a variety of unique insights into both molecular orientation and transport kinetics within the various phases. Moreover, it provides a non-invasive means of measuring the droplet size distribution of emulsions. This is achieved via its ability to quantify molecular self diffusion using pulsed field gradients technique[46]. Therefore, an area worth investigating in future studies is the characterisation of the particle size distribution of Pheroid™ emulsions by pulsed field gradient NMR methods in order to determine whether the particle size distribution is altered by the entrapment of vaccines or drugs.

3.6 Coulter Counter analysis of Pheroid™

^{1}H- and ^{13}C-NMR analysis of Pheroid™ yields information on its composition, but provides no information on its particle size distribution which is considered to be important for antigen uptake, delivery and activity of the adjuvant[6]. Confocal laser scanning microscopy studies established that the presence of nitrous oxide (N_2O) in Pheroid™ facilitated particle formation and provided some indication of the range of particle size in the formulation[8]. Data from turbidity studies showed that the concentration of the different components in a Pheroid™ formulation affected the size of droplets[8]. The stability of the emulsion is kinetically driven, therefore in a stable emulsion there is no discernible change in the number, size distribution and spatial arrangement of droplets within the experimental timescale which can vary from a few seconds to years[26]. Coulter Counter analysis is one method by which the stability of the emulsion can be assessed. The Coulter Counter yields particle size distribution as average particle volume-size and number-size distributions and was investigated as a possible complimentary method to turbidimetry or confocal laser scanning microscopy.

3.6.1 Experimental

Pheroid™ samples A and B, prepared from lots NWU-A21062005 and NWU-A14112005 respectively, were subjected to analysis by Coulter Counter to investigate the effect of Pheroid™ concentration and activation on particle size distribution. A Coulter Counter (Malvern Instruments Ltd., Worcestershire, UK) fitted with a 140 µm orifice (2.8-90 µm particle size range) was used to measure the particle size distribution in Pheroid™ samples, resulting in particle volume-size and particle number-size distributions. 20 ml of 0.001, 0.01 and 0.1 % concentrations of Pheroid™ samples A and B were prepared in 50 ml beakers using either milli-Q water (control) or nitrous oxide saturated water (activated samples). The samples were incubated in an oven set at 37 °C after which Coulter Counter measurements of particle volume-size and particle number-size distributions were taken (in triplicate). The mean particle size and standard error were calculated for each sample. P-values were not calculated because the sample size was too small.

3.6.2 Particle size distribution in Pheroid™/milli-Q water

Investigation of the average size distribution of Pheroid™ particles was initially measured in milli-Q water in order to establish a baseline. Three different concentrations were selected in order to determine the effect of concentration on the average size distribution and the performance of the instrument at the different concentrations (especially at low concentration). The analysis was performed three times at each concentration (represented by the pink, blue and green peaks).

The particle volume-size distribution curves obtained for *Pheroid™ A in milli-Q water* is displayed in Fig 3.16.

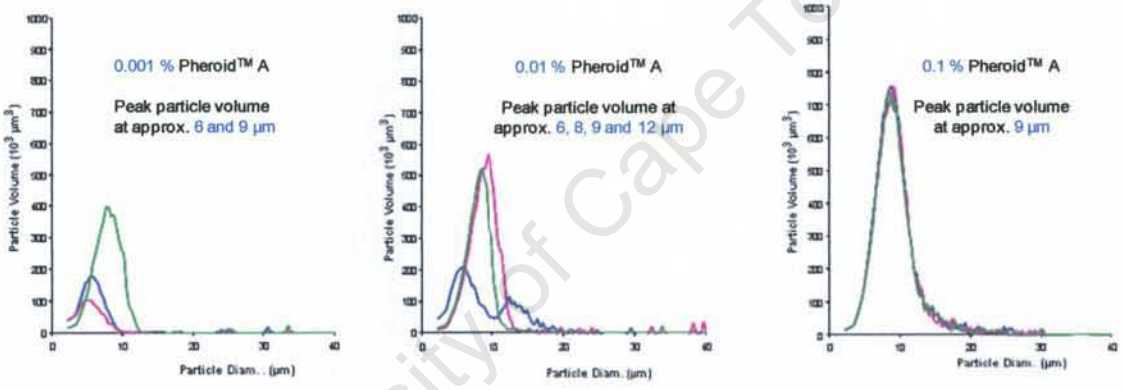

Fig 3.16: *Particle volume-size distribution curves for Pheroid™ A obtained at concentrations of 0.001, 0.01, 0.1 % in milli-Q water (inactive samples). Each sample was analysed three times and each colour represents a single run.*

As the concentration of Pheroid™ was increased, it was expected that the total particle volume would also increase. This was indeed the case as Fig 3.16 shows that particle volume increased with increasing Pheroid™ concentration from approximately 400 (x 10^3 µm^3) in the 0.001 % sample to 600 (x 10^3 µm^3) in the 0.01 % sample and finally to nearly 800 (x 10^3 µm^3) in the 0.1 % sample but greater variability was observed at 0.001 and 0.01 % Pheroid™ concentration. At low concentrations (0.001 and 0.01 %), the average size distribution of particles was in the range 6-12 µm. At the higher concentration of 0.1 %, the particle volume-size distribution showed a single peak at 9 µm.

The particle volume-size distribution curves obtained for *Pheroid™ B in milli-Q water* is presented in Fig 3.17.

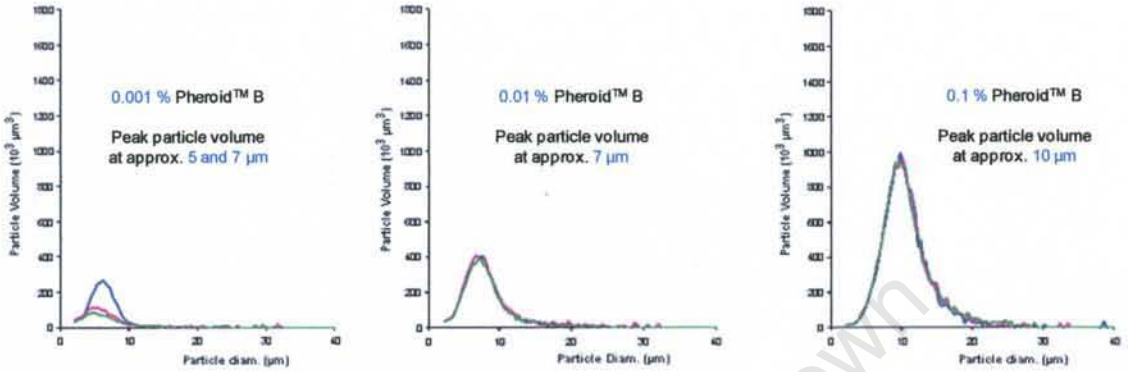

Fig 3.17: *Particle volume-size distribution curves for Pheroid™ B obtained at concentrations of 0.001, 0.01, 0.1 % in milli-Q water (inactive samples). Each sample was analysed three times and each colour represents a single run.*

As with Pheroid™ A, particle volume increased with increasing Pheroid™ B concentration from approximately 300 (x 10^3 µm^3) in the 0.001 % sample to about 400 (x 10^3 µm^3) in the 0.01 % sample and finally to nearly 1 000 (x 10^3 µm^3) in the 0.1 % sample (Fig 3.17) and again the data obtained at 0.001 % Pheroid™ concentration showed greater variability. The range of particle sizes obtained in the inactive Pheroid™ B samples was 5-10 µm which was similar to that of the Pheroid™ A preparation. At low concentration (0.001 and 0.01 %) the main difference between the particle size distributions in sample A (Fig 3.16) compared to B (Fig 3.17) was that sample A showed less uniformity in the size of particles present and had a wider distribution of particle sizes. This observation was supported by the number-size distribution curves obtained for the control (Fig 3.20, blue peaks). The difference in particle size distributions of Pheroid™ formulations prior to the addition of N_2O has been noted in previous studies and addition of N_2O resulted in an increase in the mean particle size, presumably due to the inclusion of N_2O[8]. In summary, a similar range of droplet sizes (5-12 µm) was obtained in both preparations in the absence of N_2O. However, at low Pheroid™ concentration (0.001 and 0.01 %), the volume-size distribution curves showed poor reproducibility.

3.6.3 Particle size distribution in Pheroid™/N_2O saturated water

A key prerequisite for Pheroid™ formation and activation is saturation with nitrous oxide (N_2O)[8]. It has been suggested that addition of N_2O stabilises the emulsion by imparting the required size distribution of droplets and zeta potential[47]. N_2O would also cause flocs to disaggregate to individual droplets. This would be manifested by a decrease in total particle volume while the total particle number would increase. The particle volume-size distribution curves obtained for *Pheroid™ A in N_2O* saturated water is shown in Fig 3.18.

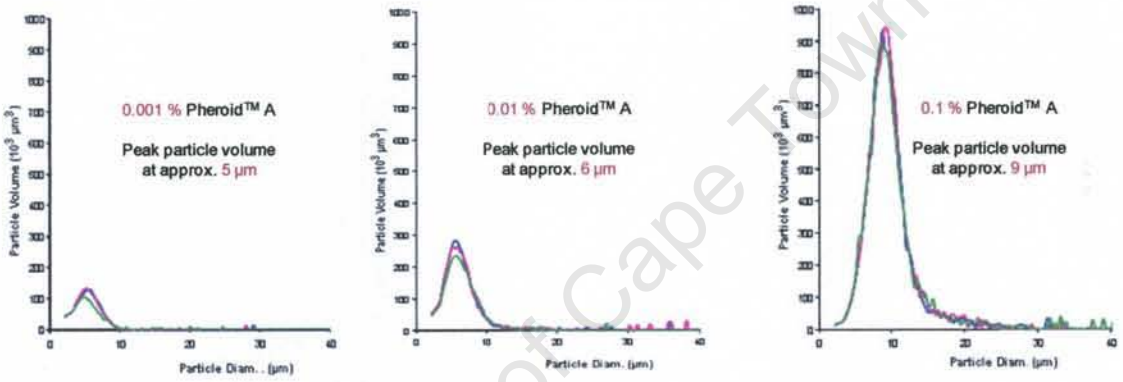

Fig 3.18: *Particle volume-size distribution curves for Pheroid™ A obtained at concentrations of 0.001, 0.01, 0.1 % in N_2O saturated water (active samples). Each sample was analysed three times and each colour represents a single run.*

Again, increasing concentration resulted in an increase in total particle volume (150 x 10^3 µm^3 at 0.001 %, 300 (x 10^3 µm^3) at 0.01 % and nearly 950 (x 10^3 µm^3) at 0.1 %). The range of particle sizes obtained for the activated Pheroid™ A samples was 5-9 µm. It was expected that the presence of N_2O would stabilise the emulsion by causing a decrease in total particle volume (by decreasing aggregation or flocculation) and an increase in the total particle number.

The results presented in Fig 3.18 and 3.18 were compared in Fig 3.19 and showed a decrease in the total size volume at 0.001 and 0.01 % Pheroid™ concentration but not when the concentration was 0.1 %. In general, better reproducibility of the particle volume-size distribution curves was obtained for the activated samples. Dilution of sample A with N_2O saturated water to a final concentration of 0.1 % yielded no observable effect as the volume-size distribution curves for the control and activated

samples were similar. Incubation of the samples at 37 °C could contribute to the loss of N_2O in activated samples and in the absence of a method to confirm N_2O saturation in activated samples, it is uncertain whether the N_2O levels in the activated samples were indeed different from the control.

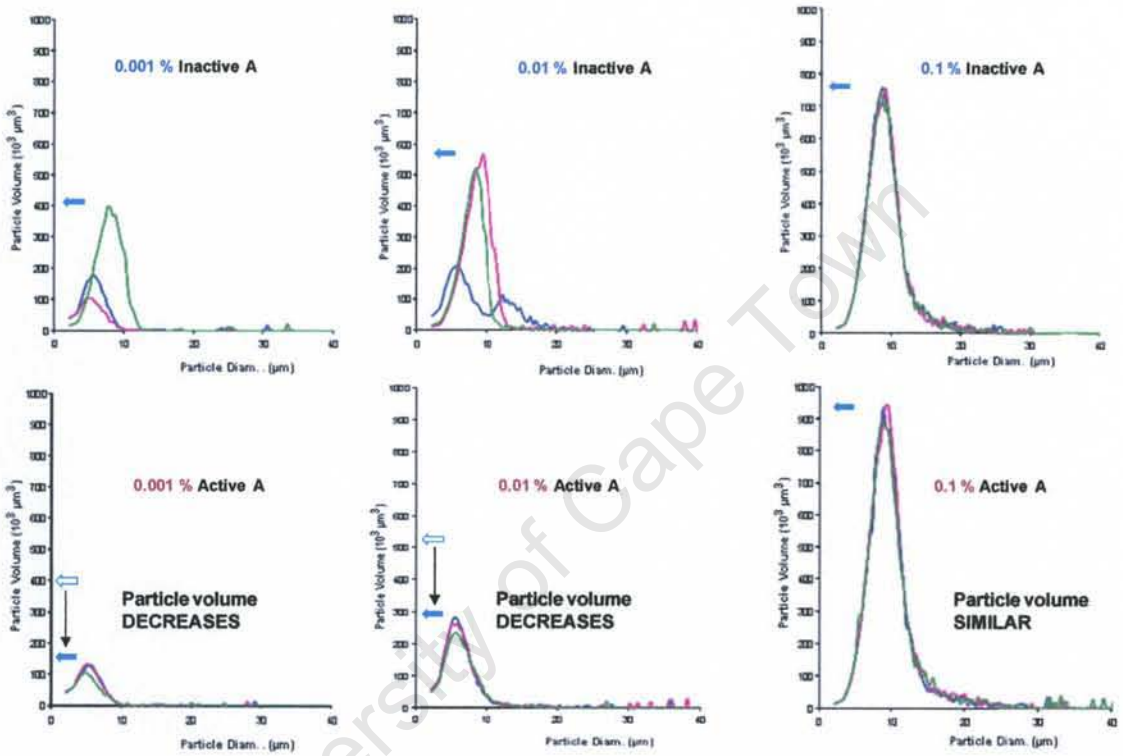

Fig 3.19: *Particle volume-size distribution curves for Pheroid™ A in milli-Q water (top panel) and N_2O saturated water (bottom panel) at concentrations of 0.001, 0.01, 0.1 %. Arrows indicate the peak particle volume.*

A summary of the results obtained for sample A are presented in Table 3.12. Generally activation with N_2O resulted in a decrease in the mean particle size.

Table 3.12: Mean size of *Pheroid™ A* particles before and after activation with N_2O saturated water

	Pheroid™ A (CTRL)	Pheroid™ A (Activated)
Pheroid™ A	Ave size±SE (µm)	Ave size±SE (µm)
0.001 %	6.07±1.72	5.46±0.01
0.01 %	7.89±1.87	5.83±0.01
0.10 %	9.12±0.01	9.09±0.01

The effect of N_2O on the Pheroid™ formulation has been investigated in earlier studies using confocal laser scanning microscopy (CLSM) and an increase in the size of the particles was observed upon addition of N_2O. Based on that observation, it was suggested that the nitrous oxide may form part of the structure of the Pheroid™ particles. However, it is still unknown how N_2O interacts with the other components in the formulation. The Coulter counter data obtained for sample A contradicted those obtained using CLSM. The analysis by Coulter Counter was complicated by the fact that there is currently no method developed to measure the degree of N_2O saturation prior to analysis. It would be worthwhile investigating the application of techniques such as infrared spectroscopy and gas chromatography with electron capture detector for determining the presence of nitrous oxide in activated samples.

The number-size distribution for *Pheroid™ A* is shown in Fig 3.20. Each sample was analysed in triplicate and the results for the control samples are shown in blue while the activated samples are in pink. Uniform number-size distribution curves were obtained for all activated samples. The control samples yielded number-size distribution curves with poor reproducibility at 0.001 and 0.01 % Pheroid™ concentration. However, at 0.1 % Pheroid™ concentration, the control samples showed a uniform number-size distribution similar to that of the activated samples.

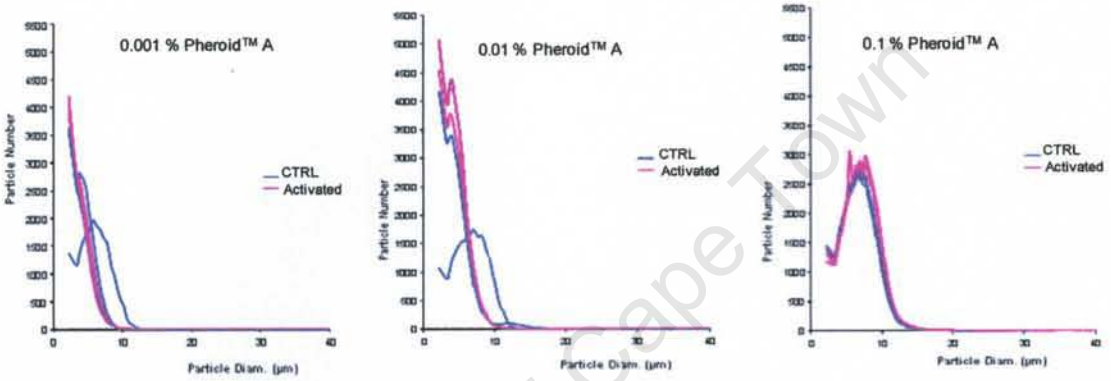

Fig 3.20: *Particle number-size distribution curves obtained for Pheroid™ A at concentrations of 0.001, 0.01, 0.1 %. The control samples are shown in blue while the activated samples are in pink.*

The particle volume-size distribution curves obtained for *Pheroid™ B* in N_2O saturated water is shown in Fig 3.21. Once again, an increase in total particle volume occurred when the concentration of the emulsion was increased (300 x 10^3 μm^3 at 0.001 %, 400 x 10^3 μm^3 at 0.01 % and nearly 1800 x 10^3 μm^3 at 0.1 %). The range of particle sizes obtained in the activated Pheroid™ B samples was 6-14 µm.

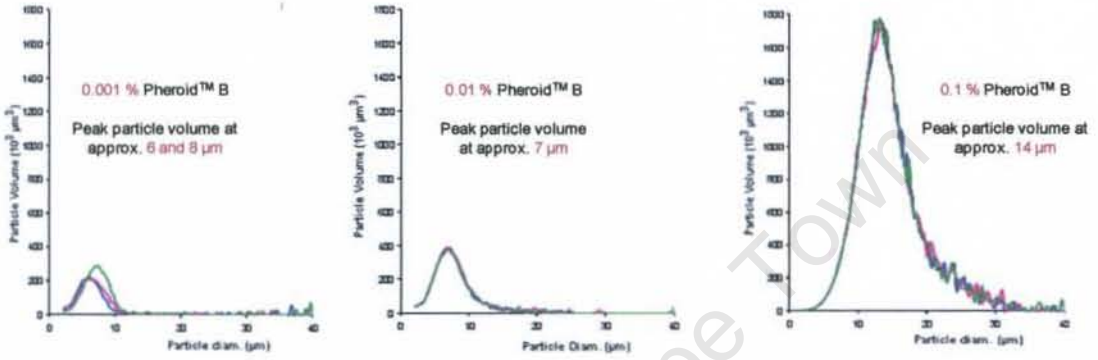

Fig 3.21: *Particle volume-size distribution curves for Pheroid™ B obtained at concentrations of 0.001, 0.01, 0.1 % in N_2O saturated water (active samples).*

The distribution curves obtained here were compared with the control sample in Fig 3.17 to determine whether addition of N_2O resulted in disaggregating of the emulsion droplets and consequently a decrease in particle volume or not (Fig 3.22).

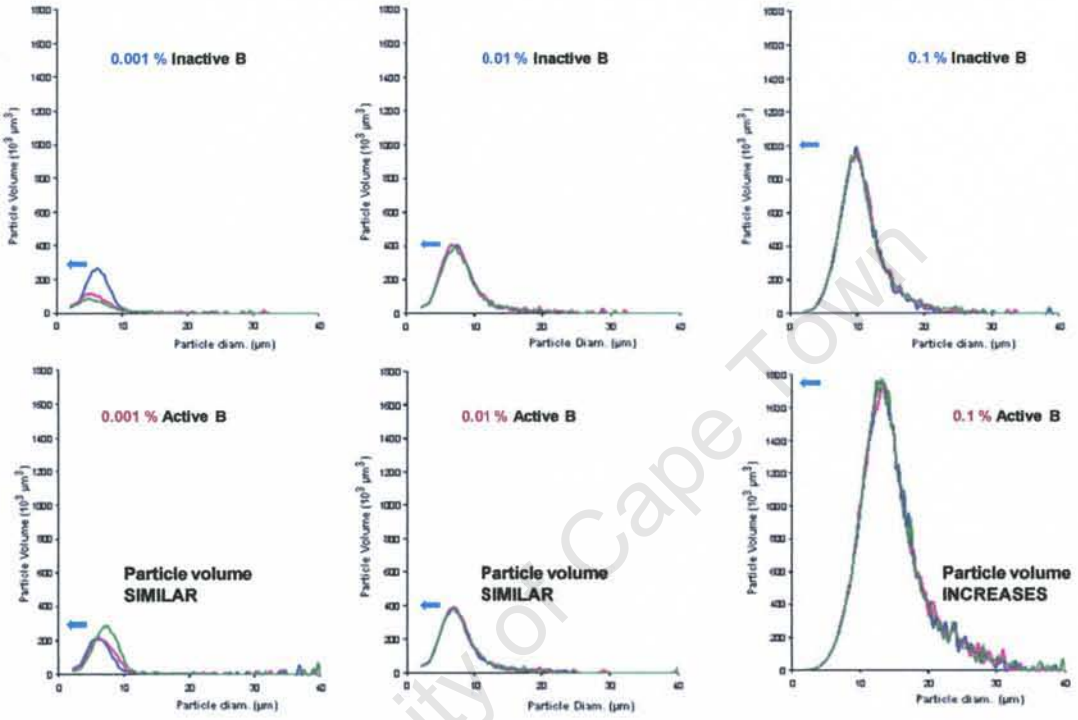

Fig 3.22: Particle volume-size distribution curves for Pheroid™ B in milli-Q water (top panel) and N_2O saturated water (bottom panel) at concentrations of 0.001, 0.01, 0.1 %. Arrows indicate the peak particle volume

Unlike sample A, sample B showed an increase in the mean particle size following activation. The trend observed here is similar to that observed with CLSM, however, further investigation is required to ascertain the saturation level of N_2O in the formulation and whether the differences observed between samples A and B were the result of differences in the level of N_2O saturation and/or the composition of the two formulations.

Table 3.13: Particle size of *Pheroid™ B* before and after activation with N_2O saturated water

	Pheroid™ B (CTRL)	Pheroid™ B (Activated)
Pheroid™ B	Ave size±SE (µm)	Ave size±SE (µm)
0.001 %	5.59±0.84	7.04±1.05
0.01 %	7.29±0.01	6.92±0.01
0.10 %	9.84±0.01	13.5±0.01

The number-size distribution for *Pheroid™ B* at concentrations of 0.001, 0.01 and 0.1 % is shown in Fig 3.23. Results for the control samples are shown in pink while the activated samples are in blue. Each sample was analysed in triplicate.

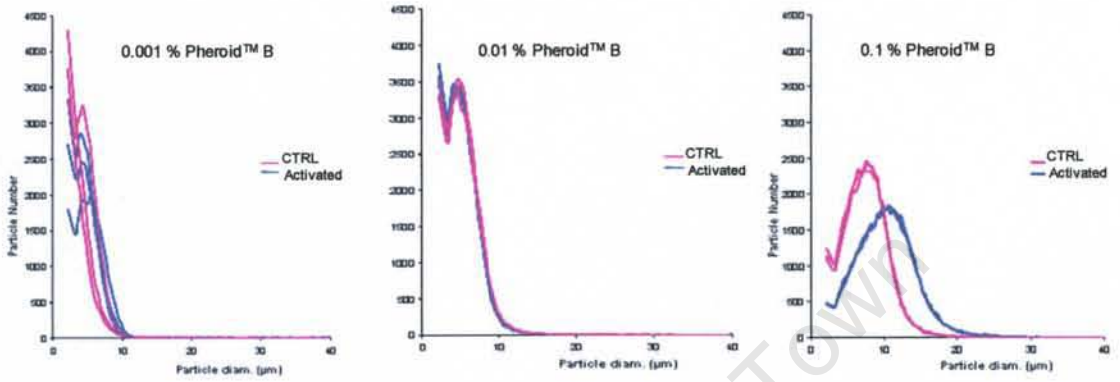

Fig 3.23: *Particle number-size distribution obtained for Pheroid™ B at concentrations of 0.001, 0.01, 0.1 %. The control samples are shown in pink while the activated samples are in blue.*

At 0.001 and 0.01 % the number-size distribution curves for the control were similar to those of the activated sample. Dilution of Pheroid™ with N_2O saturated water in previous samples had resulted in little or no effect in the volume-size and number-size distributions, thus it was surprising that at 0.1 % Pheroid™ B concentration, a distinct shift in the number-size distribution was observed after addition of the N_2O saturated water. Both the decrease in particle number and accompanying increase in the average particle size point not to a more stable emulsion but rather to a less stable one in which flocculation may have occurred.

In summary, conflicting data was obtained for the effect of N_2O on the particle *volume-size distribution* curves of Pheroid™ formulations. At low concentrations (0.001 and 0.1 %), addition of N_2O saturated water resulted in a decrease in the peak particle volume for sample A, while no change was observed for sample B. When the concentration of Pheroid™ was increased to 0.1 %, addition of N_2O saturated water yielded no change in the peak particle volume of sample A, while that of sample B increased.

Inconsistencies were also observed in the *number-size distribution* curves, especially at 0.1 % Pheroid™ concentration. In sample A, activation yielded no change in the distribution of the curve while in sample B, activation caused a decrease in the total particle number and an accompanying increase in the particle size, indicating a less stable emulsion. Interpretation of the data was complicated by the fact that no method has been developed to measure the saturation level of N_2O in activated samples especially after incubation at 37 °C. In addition, it has been reported that dilution may distort the dispersion characteristics of the emulsion such as rheological properties, particle size and surface chemistry[20, 48, 49], thus it would be preferable to analyse Pheroid™ in its original concentrated form and since the Coulter Counter method requires sample dilution, it is not recommended for the characterisation of Pheroid™ in future studies. Acoustic and electroacoustic spectroscopy are two new ultrasound-based techniques which offer a unique opportunity to characterise concentrated dispersion, emulsions and microemulsions in their natural state without dilution because ultrasound can propagate through samples that not transparent to light[48, 49]. The interaction of an ultrasound pulse with dispersed particles causes it to attenuate. An acoustic spectrometer measures this attenuation for a set of frequencies and calculates the corresponding particle size. An ultrasound pulse also disturbs the particle double layer. Consequently, the particles generate an electric current, referred to as the colloid vibration current. An electroacoustic spectrometer measures this current and calculates the zeta potential. It has been reported that the combination of acoustic and electroacoustic spectroscopy provides a reliable and complete characterisation of concentrated dispersed systems[50]. These techniques maybe better suited to characterise Pheroid™ formulations and therefore worth investigating in future studies.

3.7 Conclusion

NMR spectroscopy has been successfully employed to confirm the identity of the starting materials used in formulating Pheroid™. The high polarity of d_6-DMSO resulted in slight changes in chemical shifts compared to those obtained in $CDCl_3$. The mixture of fatty acid ethyl esters contained oleic, linoleic and linolenic fatty acid ethyl esters. The PEG hydrogenated castor oil sample contained a complex mixture of compounds including, glycerol polyethylene glycol oxystearate, ethoxylated glycerol, fatty acid esters of polyethylene glycol and polyethylene glycols. $CDCl_3$ was found to be a better solvent than DMSO for NMR analysis of the fatty acid-based components, because it gave well resolved peaks and internally consistent integration values for the different functional groups.

However, for the Pheroid™ samples, better peak resolution was obtained in d_6-DMSO. The ^{1}H- and ^{13}C-NMR spectra obtained for all Pheroid™ samples were comparable and showed the presence of the major components. Characteristic signals due to the fatty acid ethyl esters occurred at 1.2 ppm (H2'), 4.0 ppm (H1') and 5.3 ppm (olefinic protons). The presence of PEG hydrogenated castor oil was ascertained from the PEG signal at 3.6 ppm. A minor component, dl-α-tocopherol (± 0.3 %), was probably below the limit of detection. Overlapping signals prevented the use of this technique to quantitatively determine the ratio of the individual components in the different Pheroid™ preparations. In addition, the process was invasive because lyophilisation of Pheroid™ prior to analysis by NMR resulted in the destruction of the emulsion. Nevertheless, NMR spectroscopy provides a structural fingerprint of Pheroid™ formulations and indicates the relative proportions of the major components. For future studies, low resolution pulsed field gradient NMR spectroscopy would be recommended in addition to classical NMR spectroscopy because it permits the structural elucidation of complex multicomponent mixtures while preserving their structure. The collection of measurement capability available via low resolution pulsed field gradient NMR spectroscopy (droplet sizing, spatially resolved concentration and droplet size mapping) coupled with rheological measurements, has tremendous potential to explore the link between microstructure (droplet size) distribution and emulsion rheology or stability.

Previous studies conducted using turbidimetry demonstrated that the droplet size of Pheroid™ can be altered by varying the concentration of the different components. The

effect of N_2O on the Pheroid™ formulation, investigated using confocal laser scanning microscopy, showed an increase in the size of the particles following addition of N_2O. In this study, evaluation of the particle size distribution of Pheroid™ was performed using a Coulter Counter. In both Pheroid™ preparations analysed, the total particle volume increased with increasing Pheroid™ concentration. The range of particle sizes obtained in Pheroid™ A samples prepared in milli-Q water and N_2O saturated water was 6-12 and 5-9 µm respectively. Similarly, the range of particle sizes obtained in Pheroid™ B samples prepared in milli-Q water and N_2O saturated water was 5-10 and 6-14 µm respectively. The similarity between the volume-size distribution curves of control and activated samples raised the question of whether the water was indeed saturated with N_2O and highlighted the need to develop other methods such as gas chromatography with electron capture detector which can be used to test the saturation levels of N_2O in activated samples[51].

Sample dilution is a major drawback of the Coulter Counter method because it can distort the dispersion characteristics of the emulsion such as its rheological properties, particle size and surface chemistry. This may be one reason why the effect of dilution with N_2O saturated water gave conflicting results in the two Pheroid™ formulations studied. For example dilution of Pheroid™ with N_2O saturated water to a concentration of 0.1 % caused no change in the peak particle volume of sample A relative to the control, while that of sample B increased. Also, the number-size distribution curves at 0.1 % Pheroid™ concentration showed no difference between the control and activated sample A, while in sample B, activation cased a decrease in the total particle number and an accompanying increase in the particle size, indicating a less stable emulsion. Due to the above discrepancies, it was concluded that the Coulter Counter method is not ideal for studying Pheroid™ formulations.

Alternative techniques which permit the analysis of concentrated emulsion without dilution, such as acoustic and electroacoustic spectroscopy will be worth investigating for future studies. The acoustic spectrometer generates sound pulses that pass through a sample system and are then measured by a receiver which detects the sound energy losses (attenuation) and the sound speed. The attenuation data is used to calculate particle size distributions. Electroacoustic spectroscopy deals with the interaction of both electric (colloid vibration current) and acoustic (attenuation and sound speed data)

fields. The colloid vibration current is used to calculate zeta potential taking into account the particle size calculated from the acoustic measurement as well as particle interaction. Therefore, both acoustic and electroacoustic spectroscopy can potentially be used to characterise the particle size, zeta potential and other properties of Pheroid™ and would be worth investigating in future studies.

Studies on Pheroid™ have investigated the effect of processing parameters such as emulsification rate and temperature of the aqueous phase, number of days the aqueous phase was gassed and the concentration of the surfactant on the particle size distribution and zeta potential of the resulting emulsion[8]. At present, no studies have been conducted to investigate the relationship between the physicochemical properties of Pheroid™ and its adjuvanticity because until recently, focus has been primarily on the use of Pheroid™ as a drug delivery system[52, 53]. It would be worthwhile investigating the link between selected physicochemical properties of Pheroid™ (such as particle size, charge and viscosity) and its adjuvanticity. For example, apoptosis (an active form of cell death) has been recognised as an important trigger and regulator of the immune response[54]. The apoptotic and necrotic responses induced by surfactants in vaccine adjuvants have therefore been suggested to play important roles in the immunological effects elicited by surfactant-containing adjuvants. Pheroid™-induced apoptosis and necrosis, investigated in cell viability studies using MTT (3-(4,5-dimethylthiazol-2-yl)-2,5-diphenyltetrazolium bromide) reduction and LDH (Lactate Dehydrogenase) release assays, will provide much needed insight into the mode of action of Pheroid™ as an adjuvant.

3.8 References

1. Cox, J. C. and Coulter, A. R., Adjuvants-a classification and review of their modes of action. *Vaccine* 1997;**15**:248-56.

2. Hunter, R. L., Overview of vaccine adjuvants: present and future. *Vaccine* 2002;**20 Suppl 3**:S7-12.

3. Gupta, R. K., Rost, B. E., et al., Adjuvant properties of aluminum and calcium compounds. *Pharm Biotechnol* 1995;**6**:229-48.

4. Gupta, R. K. and Siber, G. R., Adjuvants for human vaccines–current status, problems and future prospects. *Vaccine* 1995;**13**:1263-76.

5. Grobler, A., Composition in the form of a microemulsion containing free fatty acids and/or free fatty acid derivatives. International patent WO/2007/096833/A3. 30 August 2007.

6. Saunders, J. C. J., Davis, H. J., et al., A novel skin penetration enhancer: evaluation by membrane diffusion and confocal microscopy. *J Pharm Pharmceut Sci* 1999;**2**:99-107.

7. Grobler, A. F., Background to the Emzaloid™. [Confidential: Concept document]. 2004, North West University.

8. Uys, C. E., Preparation and characterisation of Pheroid™ vesicles. Thesis, 2006, North West University, Potchefstroom. pp. 46-96.

9. Sesardic, D. and Dobbelaer, R., European union regulatory developments for new vaccine adjuvants and delivery systems. *Vaccine* 2004;**22**:2452-6.

10. http://themedicalbiochemistrypage.org/lipids.html. Accessed 24 June 2009.

11. Friberg, S. E., Quencer, L. G., et al., Theory of emulsions, *In Pharmaceutical dosage forms: dispersion systems vol. 1.* 2nd ed, Lieberman, H. A., Rieger, M. M., Banker, G. S., Editors. 1996, Marcel Dekker: New York. pp. 53-90.

12. Marti-Mestres, G., Neilloud, F., Main surfactants used in the pharmaceutical field, In *Pharmaceutical emulsions and suspensions*, Neilloud, F., Marti-Mestres, G., Editors. 2000, Marcel Dekker: New York. pp. 1-18.

13. Rieger, M. M., Surfactants, In *Pharmaceutical dosage forms: dispersion systems vol. 1.* 2nd ed, Lieberman, H. A., Rieger, M. M., Banker, G. S., Editors. 1996, Marcel Dekker: New York. pp. 211-86.

14. Cremophor® RH 40 technical information. Available at http://www.samkwang-chem.com/incCmd/download.php?db=js_product_1&no=21&tp=1. Accessed 03 August 2009.

15. Yu, C. D., Polyoxyethylene castor oil derivatives, In *Handbook of pharmaceutical excipients.* 4th ed. Rowe, R. C., Sheskey, P. J., Weller, P. J., Editors. 2003, Pharmaceutical Press: London. pp. 474-8.

16. Billany, M. R., Emulsions, In *Pharmaceutics*: The science of dosage form design, Aulton, M. E., Editor. 1996, Churchill Livingstone: Hong Kong. pp. 282-99.

17. Laguerre, M., Lecomte, J., et al., Evaluation of the ability of antioxidants to counteract lipid oxidation: existing methods, new trends and challenges. *Prog Lipid Res* 2007;**46**:244-82.

18. http://antione.frostburg.edu/chem/senese/101/inorganic/faq/laughing-gas.shtml. Accessed 24 June 2009.

19. The Merck index. 13th ed. 2001, p. 1818.

20. Hu, F., Furihata, K., et al., Nondestructive observation of bovine milk by NMR spectroscopy: analysis of existing States of compounds and detection of new compounds. *J Agric Food Chem* 2004;**52**:4969-74.

21. Knothe, G. and Kenar, J. A., Determination of the fatty acid profile by 1H-NMR spectroscopy. *Eur J Lipid Sci Technol* 2004;**106**:88-96.

22. Miyake, Y., Yokomizo, K., et al., Determination of unsaturated fatty acid composition by high-resolution nuclear magnetic resonance spectroscopy. *JAOCS* 1998;**75**:1091-4.

23. Stoffel, W., Zierenberg, O., et al., 13 C-nuclear magnetic resonance spectroscopic studies on saturated, mono-, di- and polyunsaturated fatty acids, phospho- and sphingolipids. *Hoppe Seylers Z Physiol Chem* 1972;**353**:1962-9.

24. Egger, H., McGrath, K. M., Aging of oil-in-water emulsions: the role of the oil. *J Colloid Interface Sci* 2006;**299**:890-99.

25. Robins, M. M. and Hibberd, D. J., Emulsion Flocculation and Creaming, In *Modern aspects of emulsion science*, Binks, B. P., Editor. 1999, RSC publishing: Cambridge. pp. 115-43.

26. Binks, B. P., Emulsions-recent advances in understanding, In *Modern aspects of emulsion science*, Binks, B. P., Editor. 1999, Royal Society of Chemistry Publishing: Cambridge. pp. 1-55.

27. Roland, I., Piel, G., et al., Systematic characterization of oil-in-water emulsions for formulation design. *Int J Pharm* 2003;**263**:85-94.

28. Chanana, G. D. and Sheth, B. B., Particle size reduction of emulsions by formulation design-II: effect of oil and surfactant concentration. *PDA J Pharm Sci Technol* 1995;**49**:71-6.

29. Friedman, D. I., Schwarz, J. S., et al., Submicron emulsion vehicle for enhanced transdermal delivery of steroidal and nonsteroidal antiinflammatory drugs. *J Pharm Sci* 1995;**84**:324-9.

30. Liedtke, S., Wissing, S., et al., Influence of high pressure homogenisation equipment on nanodispersions characteristics. *Int J Pharm* 2000;**196**:183-5.

31. Opawale, F. O. and Burgess, D. J., Influence of Interfacial Properties of Lipophilic Surfactants on Water-in-Oil Emulsion Stability. *J Colloid Interface Sci* 1998;**197**:142-50.

32. Gottlieb, H. E., Kotlyar, V., et al., NMR Chemical Shifts of Common Laboratory Solvents as Trace Impurities. *J Org Chem* 1997;**62**:7512-15.

33. Sacco, A., Brescia, M. A., et al., Characterisation of Italian olive oils based on analytical and nuclear magnetic resonance determinations. *JAOCS* 2000;**77**:619-25.

34. Zverev, L. V., Prudnikov, S. M., et al., Determination of the main fatty acids in sunflower-seed oil by a nuclear magnetic relaxation technique. *J Anal Chem* 2001;**56**:1029-31.

35. Williams, D. H. and Fleming, I., Spectroscopic methods in organic chemistry. 1995, Berkshire: McGraw-Hill. pp. 63-169.

36. Fruijtier-Pölloth, C., Safety assessment of polyethylene glycols (PEGs) and their derivatives as used in cosmetic products. *Toxicology* 2005;**214**:1-38.

37. Lie Ken Jie, M. S. F., Lam, C. C., ^{13}C-NMR studies of polyunsaturated triacylglycerols of type AAA and mixed triacylglycerols containing saturated, acetylenic and ethylenic acyl groups. *Chem Phys Lipids*1995;**78**:1-13.

38. Spitzer, V., Screening analysis of unknown seed oils. *Fett/Lipid* 1999;**101**:S2-19.

39. Guillén, M. D., Ruiz, A., ^{1}H nuclear magnetic resonance as a fast tool for determining the composition of acyl chains in acylglycerol mixtures. *Eur J Lipid Sci Technol* 2003;**105**:502-7.

40. Lie Ken Jie, M. S. F., Mustafa, J., High-resolution nuclear magnetic resonance spectroscopy – applications to fatty acids and triacylglycerols. *Lipids* 1997;**32**:1019-34.

41. Gao, L., Sedman, J., García-González, D. L., et al., ^{13}C NMR as a primary method for determining saturates, cis- and trans-monounsaturates and polyunsaturates in fats and oils for nutritional labelling purposes. *Eur J Lipid Sci Technol* 2009; **111**:612-22.

42. Borsotti, G., Guglielmetti, G., et al., Synthesis of phosphotydlcholines containing ricinoleic acid. *Tetrahedron* 2001;**57**:10219-27.

43. Yang, H., Moris, J. J., et al., Polyethylene glycol-polyamidoamine dendritic micelle as solubility enhancer and the effect of the length of the polyethylene glycol arms on the solubility of pyrene in water. *J Colloid Interface Sci* 2004;**273**:148-154.

44. Krucker, M., Lienau, A., et al., Hyphenation of capillary HPLC to microcoil ^{1}H NMR spectroscopy for the determination of tocopherol homologues. *Anal Chem* 2004;**76**:2623-8.

45. Lienau, A., Glaser, T., et al., Qualitative and quantitative analysis of tocopherols in toothpastes and gingival tissue employing HPLC NMR and HPLC MS coupling. *Anal Chem* 2002;**74**:5192-8.

46. Johns, M. L., NMR studies of emulsions. *Curr Opin Colloid Interfaces Sci* 2009;**14**:178-83.

47. Grobler, A., Kotze, A., Lipid and nitrous oxide combination as adjuvant for the enhancement of the efficacy of vaccines. International patent WO 2006079989/A3. 3 August 2006.

48. Dukhin, A. S., Goetz, P. J., et al., Acoustic and electroacoustic spectroscopy. *Colloids Surf A Physicochem Eng Asp* 2000;**173**:127-58.

49. Dukhin, A. S., New developments in acoustic and electroacoustic spectroscopy for characterising concentrated dispersions. *Colloids Surf A Physicochem Eng Asp* 2001;**192**:267-306.

50. Dukhin, A. S., Goetz, P. J., Characterisation of aggregation phenomena by means of acoustic and electroacoustic spectroscopy. *Colloids Surf A Physicochem Eng Asp* 1998;**144**:49-58.

51. Elkins, J. W., Determination of dissolved nitrous oxide in aquatic systems by gas chromatography using electron-capture detection and multiple phase equilibrium. *Am Chem Soc* 1980;**52**:263-7.

52. Gerber, M., Breytenbach, J. C., et al., Transdermal penetration of zalcitabine, lamivudine and synthesised N-acyl lamivudine esters. *Int J Pharm* 2008;**351**:186-93.

53. Ojewole, E., Mackraj, I., et al., Exploring the use of novel drug delivery systems for antiretroviral drugs. *Eur J Pharm Biopharm* 2008;**70**:697-710.

54. Yang, Y-W., Wei, A-C., et al., The immunogenicity-enhancing effect of emulsion vaccine adjuvants is independent of the dispersion type and antigen release rate – a visit of the role of hydrophile-lipophile balance (HBL) value. *Vaccine* 2005;**23**:2665-75.

CHAPTER 4

INVESTIGATION OF AN INTEGRITY ASSAY FOR ANALYSING MONOVALENT CONJUGATE VACCINES

4.1 Introduction

The introduction of *Haemophilus influenzae* type b (Hib) conjugate vaccines into routine childhood immunization programmes has greatly reduced the incidence of invasive Hib infections in young children and infants. Chemical conjugation of the active ingredient polyribosylribitolphosphate (PRP) to a carrier protein such as diphtheria toxoid (PRP-D), a diphtheria toxoid-like protein (PRP-CRM_{197}), tetanus toxoid (PRP-T) or meningococcal outer membrane protein (PRP-OMP), converts the normally T-cell independent PRP antigen into a T-cell dependent immunogen[1, 2]. Thus, conjugate vaccines induce an antibody immune response in infants under two years of age who are the major group at risk of meningitis infection[3].

The disease has largely disappeared from Western Europe, Canada, the United States, Australia and New Zealand, where Hib conjugate vaccines have been in use since the 1990s. The effectiveness of Hib conjugate vaccines has also been demonstrated in developing countries such as Chile, Uruguay and the Gambia[1]. The vaccine is usually administered in infancy as repeated doses together with diphtheria/tetanus/pertussis (DTP) and other vaccines of the national childhood immunization program[1]. Children in South Africa currently receive vaccines against DTP, Hepatitis B (HBV) and Hib at 6, 10 and 14 weeks[4]. Combining these vaccines into one pentavalent vaccine would be advantageous because it would spare patients the discomfort of multiple injections, result in reduced clinic visits, use of syringes and needles and decrease the requirement for cold storage of vaccines[1, 5].

A local vaccine manufacturing company is in the process of developing a tetravalent DTP-HBV vaccine as well as a liquid pentavalent DTP-HBV-Hib vaccine. The DTP, HBV and Hib vaccines can be obtained as bulk products and formulated together as required. As new formulations, these combined vaccines will have to be tested again after formulation for lack of interference and for safety and immune responses. Traditionally, biological tests including immunogenicity in animals have played a major role in the quality control of vaccine batches[6]. However, the Hib vaccine is a semi-synthetic carbohydrate-protein conjugate for which immunogenicity in animals does not correlate

well with protective immunity in children and therefore various *in vitro* physicochemical procedures are used as an indicator of the vaccine's *in vivo* specificity and immunogenicity[7-10]. In this study, the Hib vaccine contains the purified PRP attached to tetanus toxoid. PRP must remain conjugated to the carrier protein in order to be immunogenic in infants. In vaccines formulated with aluminium-containing adjuvants, factors such as temperature and interactions with the adjuvant may result in hydrolysis of the phosphodiester bond between PRP monomers and the generation of free PRP fragments[11]. Investigating the stability and integrity of Hib conjugate vaccines requires determination of the total saccharide and unbound or free saccharide which is expressed as the percentage of free saccharide present[11]. In formulated vaccines, total and free saccharide analysis requires a high degree of selectivity (since the saccharide must be isolated from all other vaccine components), a high degree of sensitivity (because vaccine dose concentrations are usually low and the detection of even smaller amounts of free saccharide is necessary) and accuracy that provides the true concentration[12].

The primary objective of this study was to develop a free saccharide assay for evaluating the structural integrity of the Hib conjugate in combination vaccines. The challenge was that the Hib conjugates available to this study either contained thiomersal or sucrose, both of which interfere with the phosphate or ribose colorimetric assays used to quantify Hib. Therefore, model compounds such as human serum albumin (HSA), meningococcal A capsular polysaccharide (PsA) and the corresponding conjugate vaccine (Mn A-TT) were used to investigate methods of free saccharide separation by solid phase extraction (SPE), acid precipitation using deoxycholate (DOC/HCl) and ultrafiltration (UF). The phosphate or high performance anion exchange chromatography (HPAEC) methods were used to determine the amount of saccharide present and descriptive statistics such as mean and standard error (SE) are reported. P-values are not reported due to the small sample size. Validation of the free saccharide assay was not possible because no vaccine intermediates were available. Thus, a thermal study was performed.

4.2 Analytical methods to detect polysaccharide concentration

The free saccharide assay is a key indicator of the stability of the conjugate vaccine [10]. Free saccharide is separated from conjugate and quantified using a method sensitive enough to detect low levels of free saccharide and specific enough to determine the dosage of Hib in combination vaccines[13]. Saccharide content was measured with a

colorimetric assay for phosphorus or by monomer determination using high performance anion exchange chromatography (HPAEC) coupled to pulsed amperometric detection (PAD). Methods for the separation of free from bound saccharide depend on the nature of the conjugate (polysaccharide- or oligosaccharide-based), matrix and adjuvant[13, 14]. Solid phase extraction, gel filtration, ultrafiltration, ultracentrifugation, hydrophobic chromatography, acid precipitation and precipitation with carrier protein-specific antibodies are all methods that have been used to separate free from bound saccharide[10, 11, 15-19]. In the present study, solid phase extraction (SPE), selective precipitation and ultrafiltration were investigated as methods to effect separation of free saccharide from conjugate.

4.2.1 Phosphate assay

The amount of PRP in Hib vaccines can be quantified by determining the phosphorus content[10]. Like PRP, the repeating unit of Mn A polysaccharide (PsA) contains phosphate (Fig 4.1) and so was used for the development of this assay. Mn A polysaccharide standard (PsA) and conjugates were obtained from the Meningitis Vaccine Project (MVP)[20].

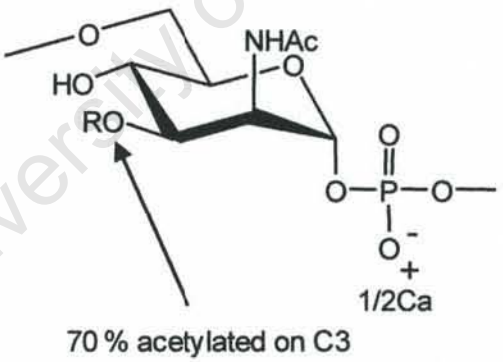

Fig 4.1: *Repeating unit N-acetyl mannosamine-6-phosphate*[21].

A survey of the literature on analysis of sugar phosphates revealed a large variety of experimental methods regarding the temperature and heating time for release of orthophosphate[22-24]. In order to determine the length of the heating period required, a sample of Mn A polysaccharide standard (PsA) was heated at a chosen temperature of 250 °C for several hours and analysed by use of the phosphate assay (details in appendix B).

No further release of phosphorus occurred after 60 min (as indicated by the arrow in Fig 4.2). Therefore, heating at 250 °C for 60 min was considered to be sufficient for the release of organic phosphate.

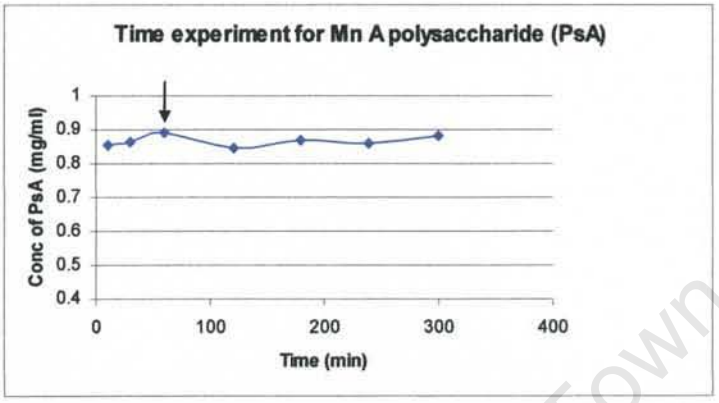

Fig 4.2: *Effect of heating time on release of phosphorus in PsA.*

Time optimisation experiments conducted from 10-60 min using Mn A-TT conjugate lots 1-3 (Fig 4.3) confirmed that 60 min was more than adequate for complete release of phosphate. Fig 4.3 shows that similar amounts of saccharide were released over the three time periods tested, however because data from Fig 4.2 showed the amount of saccharide released to increase until 60 min, an incubation time of 60 min was adopted.

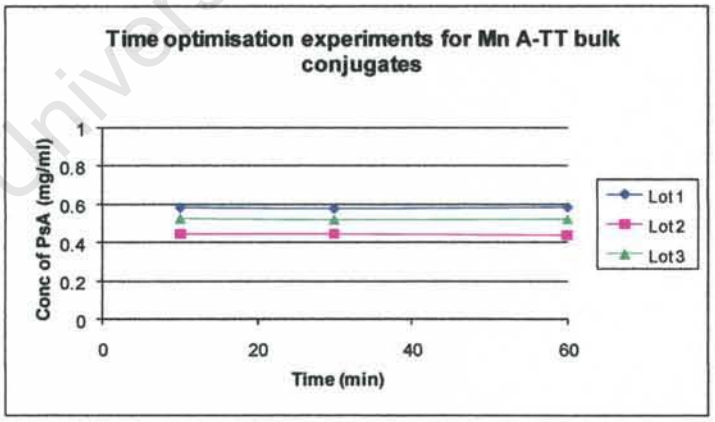

Fig 4.3: *Effect of heating time on release of phosphorus in Mn A-TT conjugate lots 1-3.*

The phosphate assay was subsequently applied to determine the total saccharide content of Mn A-TT conjugate development lots 1-3 and the results obtained are displayed in Table 4.1.

Table 4.1: Total saccharide content of Mn A-TT conjugate lots 1-3 as determined by the phosphate assay*

Test conjugate	Total Saccharide (µg/ml) (Mean±SE)#	n-value
Lot 1	607±8	6
Lot 2	454±7	4
Lot 3	525±8	4

*Data presented in appendix B

#SE = Standard error and describes the uncertainty of how the sample mean represents the population mean

The amount of total saccharide in each vaccine lot, as determined using the phosphate assay, was in agreement with the values sent by the supplier which were determined using a validated phosphorus assay (Table 4.1). This protocol can therefore be used to determine total saccharide content in Mn A–TT samples. However, a disadvantage of the assay was the large standard errors obtained.

4.2.2 High performance anion exchange chromatography with pulsed amperometric detection (HPAEC-PAD)

In the current study, stock solutions of three different development lots of Mn A conjugate (Lots 4-6) were diluted using milli-Q water to a final concentration of 100 µg/ml. 450 µl Mn A samples (in duplicate) to which 150 µl of 8 M TFA (Saarchem) (final TFA concentration: 2 M) had been added were hydrolysed at 100 °C in closed screw-cap tubes. The samples were allowed to cool to room temperature and then neutralised with 600 µl of 2 M NaOH (Sigma). Samples were filtered through 0.22 µl nylon filters (National Scientific) and directly analysed by HPAEC-PAD on a CarboPac PA-1 column as follows: 0 to 200 mM NaOAc (Merck) in 100 mM NaOH over 12 min, 200 to 300 mM NaOAc over the next 13 min, then to the original 100 mM NaOH after 28 min and 7 min of equilibration. The NaOH concentration is maintained throughout the run as NaOAc and has no buffering capacity.

Carbohydrate analysis of Mn A samples was performed on a Dionex BioLC ion chromatograph system equipped with an AS50 autosampler (Rheodyne rotary injection valve with a 25 µl PEEK sample loop), an ED50 electrochemical detector, LC30 oven and GS50 pump. The detector cell incorporated a gold working electrode and a pH Ag/AgCl reference electrode. Chromatographic data were recorded on a personal computer equipped with Chromeleon software.

The mannosamine-6-phosphate (M6P) peak eluted at approximately 18 min. The chromatograms obtained under the elution conditions used show a split peak because the anomeric proton can be oriented in either alpha or beta positions (Fig 4.4). The total peak area was used to determine the M6P content. The PsA standard (1, 5, 10, 25, 50 and 100 µg/ml), hydrolysed as outlined above, was used to obtain a standard curve of peak area versus PsA concentration. The total saccharide content of lots 4-6 as determined by HPAEC-PAD was 94.3, 96.4 and 98.5 µg/ml respectively.

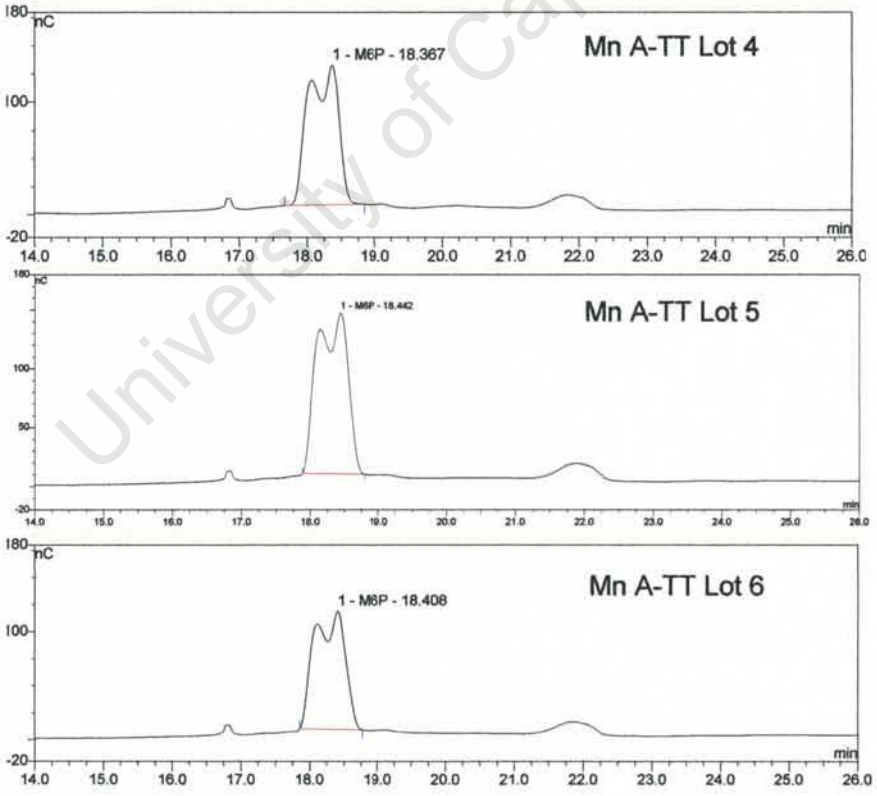

Fig 4.4: *HPAEC-PAD chromatograms for Mn A lots 4-6 showing the M6P peak eluting near 18 min.*

4.3 Methods of separation

In developing the free saccharide assay, it is important that unconjugated and free saccharide be separated from the conjugate in a selective and reproducible manner[11]. The following section investigates three of these techniques namely solid phase extraction, selective precipitation and ultrafiltration. The lack of an appropriate Hib conjugate was a major limitation in the present study. As a result, the selective precipitation and ultrafiltration methods were further evaluated and the data obtained presented in chapter 5.

4.3.1 Solid phase extraction (SPE)

Reversed phase SPE cartridges have been applied to the separation of conjugated saccharide from unconjugated saccharide in vaccine samples[17]. The stationary phase consists of alkyl or aryl-bonded silicas of various chain lengths to which the carrier protein binds via van der Waals interactions. The SPE device is considered to be efficient if it retains at least 90 % of the conjugated saccharide and allows 90 % or more of the unconjugated saccharide to pass through as effluent[17].

For quantitative analysis, the amount of sample passed through the SPE device should not exceed its breakthrough volume, i. e. the point at which the sample volume exceeds the retention capacity of the sorbent. The breakthrough volume for a given sample can be determined by plotting a breakthrough curve, in which a sample of fixed concentration and at a constant velocity enters the SPE device and the effluent analysed. The retentate is quantitatively retained during the initial phase by the sorbent until the moment in which the sample volume exceeds the retention capacity of the sorbent. The point on the curve at which some of the retentate is detected at the outlet of the SPE device is the breakthrough volume[17].

In the current study, the SPE device was selected to retain the conjugated saccharide while the unconjugated or free saccharide passed through as effluent. To determine the breakthrough volume of the C18 cartridge used in this study, it was pre-conditioned by washing sequentially with 1 column volume of methanol (Kimix), three column volumes of milli-Q water and 1 column volume of 0.9 % NaCl (Saarchem). As a water miscible organic solvent, methanol wets the surface of the sorbent and penetrates bonded alkyl phases, allowing water to wet the silica surface efficiently[25].

A solution of HSA was passed through the C18 cartridge to determine the breakthrough volume. 3 ml of 0.1 mg/ml solutions of HSA were prepared in 0.1 M, 0.5 M and 1 M NaCl to determine whether the amount of protein retained is affected by the concentration of salt. The samples were passed through C18 cartridges under gravity and 0.5 ml aliquots were collected and their OD_{280} nm readings taken. The capacity of the sorbent was defined as the maximum amount of carrier protein retained by 200 mg of C18. The breakthrough curves are displayed in Fig 4.5.

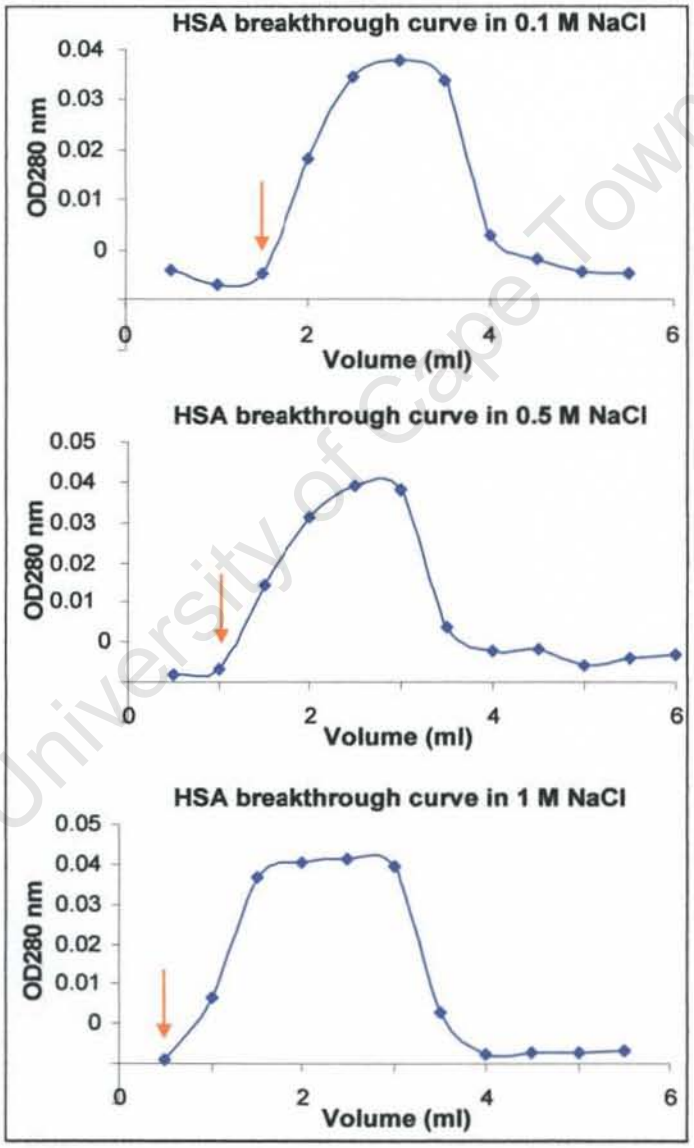

Fig 4.5: *SPE using HSA in different concentrations of NaCl. Arrows indicate breakthrough volume.*

Of the 0.3 mg of HSA loaded onto the cartridge, SPE in 0.1, 0.5 and 1 M NaCl resulted in the adsorption of only 0.210 (70 %), 0.152 (51 %) and 0.111 mg (37 %) of HSA respectively by 200 mg of sorbent. Under the conditions used, protein binding did not improve with increasing NaCl concentration. It appeared that the lower the salt concentration, the more protein was adsorbed, however when the above experiment was performed using milli-Q water in place of NaCl, protein was detected in the first aliquot collected (data not presented).

This investigation demonstrated that SPE on reversed phased cartridges is not applicable to toxoid-based vaccines because only a maximum of 70 % was retained by the sorbent. However, it can be applied to oligosaccharide-based Hib conjugates manufactured using CRM_{197} as the carrier protein, with 90 % retention being reported[17]. For reversed phased SPE procedures on bonded silicas, optimum retention occurs if the analyte is not charged[25]. Proteins are typically retained after they have been denatured for example after acid treatment, which was not the case for the HSA samples. Lowering the pH could improve protein retention but would not be applicable to Hib-TT samples because it could induce PRP hydrolysis. The binding capacity of the cartridge was very low under the conditions used and so this method was not investigated further.

4.3.2 Acid precipitation and ultrafiltration

Acid precipitation with deoxycholic (DOC) sodium salt/HCl and ultrafiltration (UF) are two published methods for the separation of unbound saccharide from conjugate and were investigated in this study.

DOC/HCl precipitation has been used for the separation of free saccharide in conjugate vaccines[14, 16, 17]. Deoxcholate binds to the protein component of the conjugate which is then precipitated by HCl resulting in co-precipitation of the conjugate leaving the free saccharide in the supernatant. The advantage of this method is that it is fast, simple and suitable for use on an analytical scale and does not result in dilution of the sample. The disadvantages are that it may also precipitate charged polysaccharides or the acid used to precipitate the DOC may cause hydrolysis of the saccharide during the analysis. To precipitate conjugate, 100 µl of 1 % DOC solution (Sigma) at pH 6.8 was added to 1 ml of sample and incubated in the fridge for 30 min. 50 µl of 1M HCl was added to the mixture which was then centrifuged at 10 000 rpm for 15 min. The supernatant was transferred to an Eppendorf tube and evaporated to dryness on the speed-vac system

consisting of a centrifuge, refrigerated vapour trap and vacuum pump. The sides of the Eppendorf tubes were washed once with 200 µl saline and spin-evaporated to dryness again. This served to concentrate the samples and thus improved the sensitivity of the assay. The pellet was reconstituted in saline for analysis by use of the phosphate or HPAEC-PAD methods (as described in sections 4.2.1 and 4.2.2 respectively).

Ultrafiltration is another simple and effective method of separation[11, 13]. The membrane used in this study had a 100 kDa molecular weight cutoff (Millipore). TT has a molecular weight of 150 kDa and so the protein and the saccharide to which it is attached should be retained on the membrane, whereas any saccharide chains smaller than 100 kDa would pass through the membrane. The Mn A-TT vaccine manufacturing process includes diafiltration using a 100 kDa membrane for conjugate purification supporting the choice of this molecular weight cutoff. A filter preconditioned by washing twice with 500 µl milli-Q water and once with 500 µl saline, was used to separate free from bound saccharide. 500 µl of sample was placed into a pre-washed filter and spun at 10 000 rpm for 10 min or until the membrane was almost dry. This process was repeated once more and then the membrane was washed with 500 µl saline. Filtrate from the sample and washing were pooled (± 1.5 ml) in an Eppendorf tube and evaporated to dryness on the speed-vac system. The sides of the Eppendorf tubes were washed once with 200 µl saline and spin-evaporated to dryness again in order to have concentrated samples and thus improve sensitivity. The pellet was reconstituted in saline for analysis by use of the phosphate or HPAEC-PAD methods (detailed protocols for these assays are provided in sections 4.2.1 and 4.2.2 respectively).

Total and free saccharide analysis

Mn A-TT Conjugate lots 1-3

Total saccharide in 50 µg/ml samples of Mn A conjugate development lots 1-3 formulated in Tris buffer was determined using the phosphate and HPAEC-PAD methods as described in sections 4.2.1 and 4.2.2 respectively. Free saccharide was separated from bound in these samples using the DOC/HCl method described above and the amount of free saccharide quantified using the phosphate and HPAEC-PAD methods. The HPAEC-PAD chromatograms for Mn A conjugate-TT lots 1-3 are displayed in Fig 4.6 and the results for the % free saccharide determinations presented in Table 4.2.

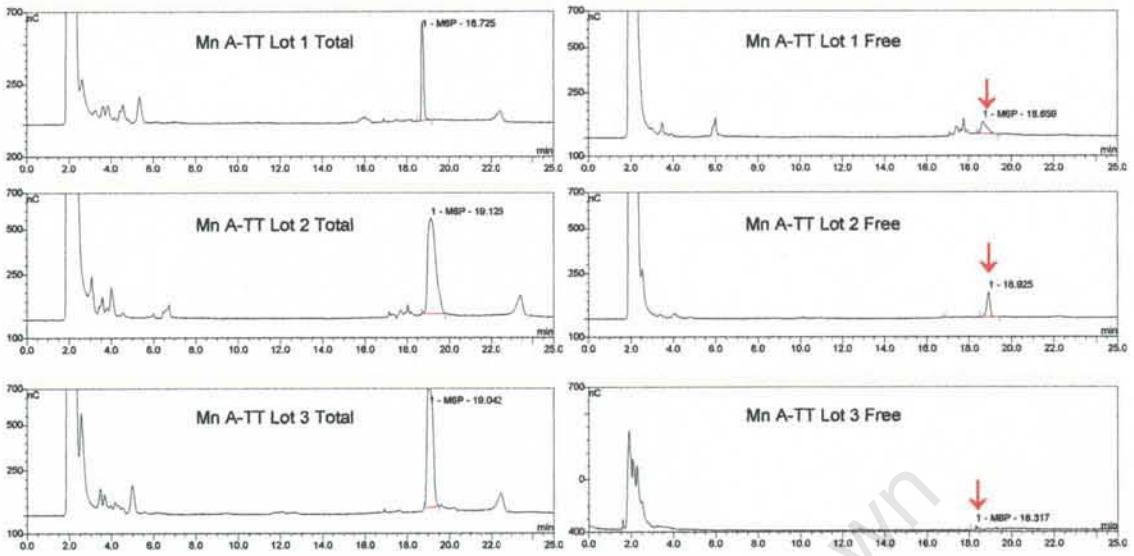

Fig 4.6: *HPAEC-PAD chromatograms of total (left panel) and free (right panel) saccharide for Mn A-TT conjugate lots 1-3. The arrow indicates the M6P peak.*

The left and right panels show chromatograms for total and free saccharide analysis respectively. The single M6P peak eluted at approximately 18-19 min without interference from other components and indicates that under the conditions used, M6P can be used for the quantification of Mn A-TT conjugates. The amount of free saccharide was expected to vary between the three lots which were manufactured at different times (in order of their lot number). This was confirmed by the free saccharide determinations displayed in Table 4.2 in which the % free saccharide followed the trend lot 1 > lot 2 > lot 3.

Table 4.2: % free saccharide results obtained using phosphate assay and HPAEC-PAD for Mn A-TT conjugate lots 1-3*

Test conjugate	Phosphate assay (Mean ± SE)	HPAEC-PAD (Mean ± SE)
Mn A lot 1	11±1.1	26±0.8
Mn A lot 2	13±1.2	10±0.6
Mn A lot 3	7±0.1	1.0±0.4

*Data presented in appendix B (including limit of detection and limit of quantification).

Ideally the detection method used should be able to detect levels of free saccharide as low as 2 % of the total saccharide present[13]. The results varied depending on which method was used (phosphate assay vs. HPAEC-PAD). From the phosphate assay it

would appear that lots 1 and 2 had similar amounts of free saccharide while lot 3 had the least amount of free saccharide. The HPAEC-PAD method confirmed that lot 3 had the lowest concentration of free saccharide as expected. However, it also showed that lot 1 had twice as much free saccharide as lot 2. The results obtained using the HPAEC-PAD method appears to be more reliable than the phosphate assay. The phosphate assay is less sensitive than the HPAEC-PAD method and the low OD values obtained introduced a high margin of error (the phosphate assay yielded slightly higher standard error values compared to the HPAEC-PAD method).

Mn A-TT Conjugate lots 4-6

The free saccharide analysis methods were tested on more recently manufactured lots of Mn A-TT conjugate. Total saccharide in 100 µg/ml samples of Mn A-TT conjugate lots 4-6 was determined using the phosphate and HPAEC-PAD methods as described in sections 4.2.1 and 4.2.2 respectively. Free saccharide was separated from bound in these samples using both the DOC/HCl and UF methods described above and the amount of free saccharide quantified using the phosphate and HPAEC-PAD methods. The HPAEC-PAD chromatograms of total and free saccharide obtained for lots 4-6 were very similar and so only chromatograms for lot 4 are displayed in Fig 4.7. The total saccharide peak (A) corresponded to 94.3 µg/ml saccharide. Free saccharide analysis using DOC/HCl (B) and UF (C) yielded 6.5 and 9.9 % free saccharide respectively.

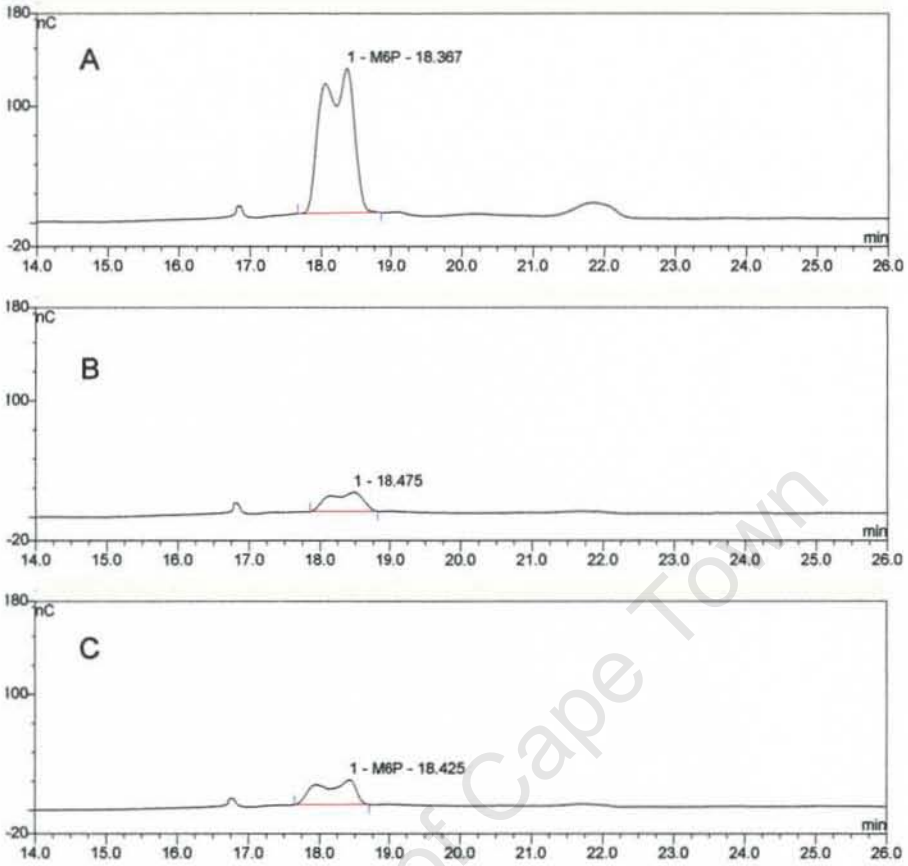

Fig 4.7: *HPAEC-PAD chromatograms of total (A) and free saccharide using DOC/HCl (B) and UF (C) for Mn A-TT conjugate lot 4.*

Table 4.3 summarises the percentage of free saccharide obtained in Mn A-TT conjugate lots 4-6 by use of the different methods.

Table 4.3: % free saccharide results obtained using phosphate assay and HPAEC-PAD for Mn A-TT conjugate lots 4-6*

		Phosphate assay (Mean±SE)		HPAEC-PAD (Mean±SE)	
Test conjugate	**Total (µg/ml)**	**DOC**	**UF**	**DOC**	**UF**
Mn A Lot 4	94±1.1	4.8±0.9	11±1.1	6.5±0.8	9.9±1.3
Mn A Lot 5	96±2.2	4.9±1.3	14±1.5	6.3±0.2	8.8±0.1
Mn A Lot 6	99±0.5	35±0.6	12±0.5	6.1±0.1	9.7±0.1

*Data presented in appendix.

When the phosphate assay was used for saccharide quantification, the DOC/HCl method yielded lower free saccharide compared to the UF method for all of the conjugates analysed (Table 4.3). This could be caused by entrapment of some of the free saccharide by the deoxycholate and co-precipitation during the acid treatment. Moreover, since neither a washing step nor a reprecipitation step is included, it is likely that not all unconjugated/free saccharide was recovered in the supernatant. By comparison, when free saccharide was separated using UF, the ultrafiltration membrane was washed to ensure removal of all unconjugated/free saccharide. These factors could account for the lower free saccharide results obtained using DOC/HCl compared to UF.

The amount of free saccharide by UF obtained by the phosphate assay was slightly higher than those obtained from saccharide determination by HPAEC-PAD, whereas the DOC/HCl results were somewhat lower. The phosphate assay involves dilution of the samples prior to analysis resulting in relatively low OD values with a higher margin of error.

Published studies in which conjugate vaccines have been analysed for their free saccharide content report the use of a single method of free saccharide separation. For example, Lei and co-workers used the DOC/HCl method for analysis of the free saccharide content of meningococcal conjugate vaccines and a non-adjuvanted Hib-TT vaccine[16, 17]. The UF method (30 kDa membrane) alone has also been applied for free saccharide separation in both Hib-TT and Men C-TT conjugates[26, 27]. The difference between the present study and other published studies on free saccharide separation was that both methods were applied. The results suggest that the DOC/HCl method may result in the underestimation of the amount of free saccharide present. However, passage of conjugated saccharide through the ultrafiltration membrane would result in erroneously elevated free saccharide values. In the absence of appropriate vaccine intermediates, further investigation of both methods was conducted and is presented in chapter 5.

In summary, Mn A quantification for total and free saccharide was determined by use of two techniques: phosphorus assay and HPAEC-PAD. Both the DOC/HCl and UF methods were investigated for the separation of free from bound saccharide. These free saccharide methods were developed on Mn A-TT test lots 1-3 and applied to lots 4-6. The low sensitivity of the phosphate assay can be circumvented by use of the HPAEC-

PAD method, which also appeared to give more reliable results. In general, the DOC/HCl method gave lower free saccharide values than the UF method; this was attributed to possible saccharide entrapment during the DOC/HCl precipitation step. In the absence of appropriate vaccine intermediates, spiking experiments could not be performed to confirm this postulate. Higher free saccharide recovery was obtained using the UF method, which included a washing step. The two separation methods for free saccharide determination were applied to Mn A-TT samples subjected to a thermal stability study.

4.4 Accelerated thermal stability study

A thermal stability study is used to evaluate the stability of conjugate vaccines stored under adverse conditions such as elevated temperatures or cycles of freeze-thawing[26, 27]. The structural stability, hydrodynamic size and molecular integrity can be monitored using a combination of physicochemical methods[12, 13, 27, 28]. Mn A-TT conjugate lot 4 was subjected to a thermal accelerated stability study and the free saccharide generated monitored using the methods developed in section 4.3. This served to evaluate both the stability of the vaccine and the performance of the free saccharide assay.

Total and free saccharide assay

100 µg/ml samples of Mn A-TT conjugate lot 4 were incubated at 25 and 40 °C for a period of 3 and 5 weeks and thereafter evaluated for their free saccharide content. Free saccharide was separated from conjugate by DOC/HCl and UF (100 kDa membrane) and detected using the phosphate and HPAEC-PAD methods. To improve sensitivity of the HPAEC-PAD method, the sample loop was increased from 25-80 µl. The chromatograms for DOC/HCl and UF were similar and so only those for DOC/HCl are presented here. The HPAEC-PAD chromatograms for total (A) and free saccharide using DOC/HCl at 0 (B) and 5 (C) weeks for the conjugate stored at 25 °C are presented in Fig 4.8. The major peak at 18-19 min is the M6P peak and the % free saccharide at 0 and 5 weeks corresponds to 15 and 16 % respectively.

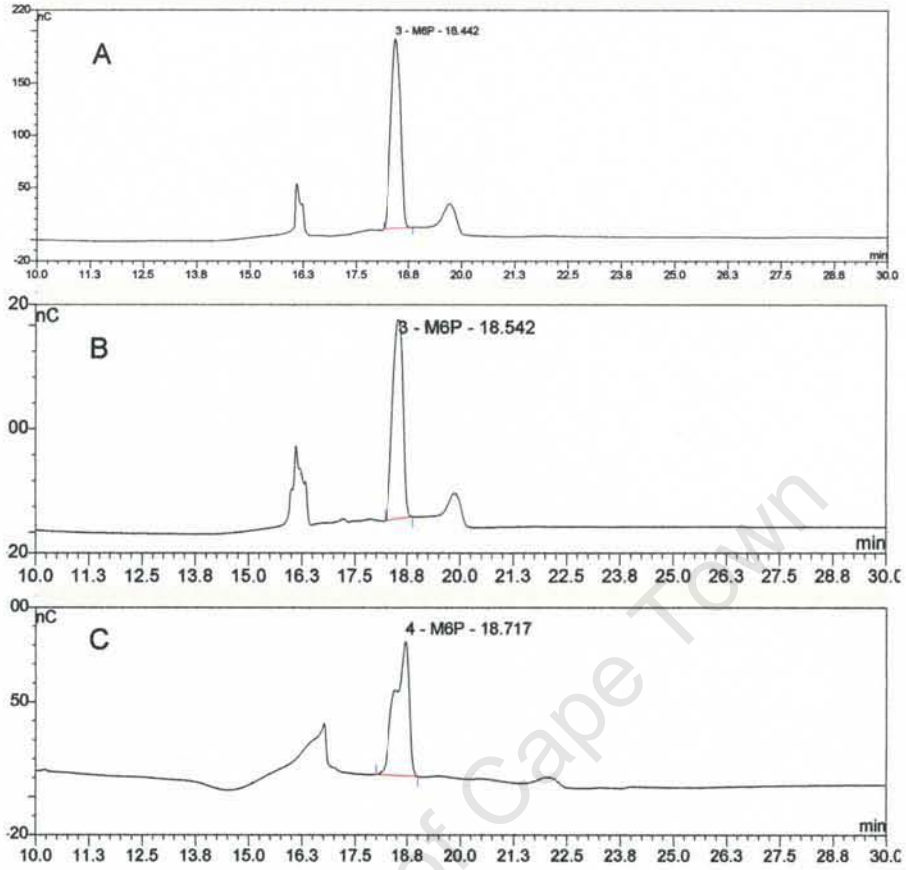

Fig 4.8: *HPAEC-PAD chromatograms at 25 °C for total (A) and free saccharide using DOC/HCl at 0 (B) and 5 (C) weeks respectively.*

The HPAEC-PAD chromatograms for total (A) and free saccharide using DOC/HCl at 0 (B) and 5 (C) weeks for the conjugate stored at 40 °C are presented in Fig 4.9. The M6P peak eluted at approximately 18 min and the % free saccharide at 0 and 5 weeks corresponds to 15 and 45 % respectively.

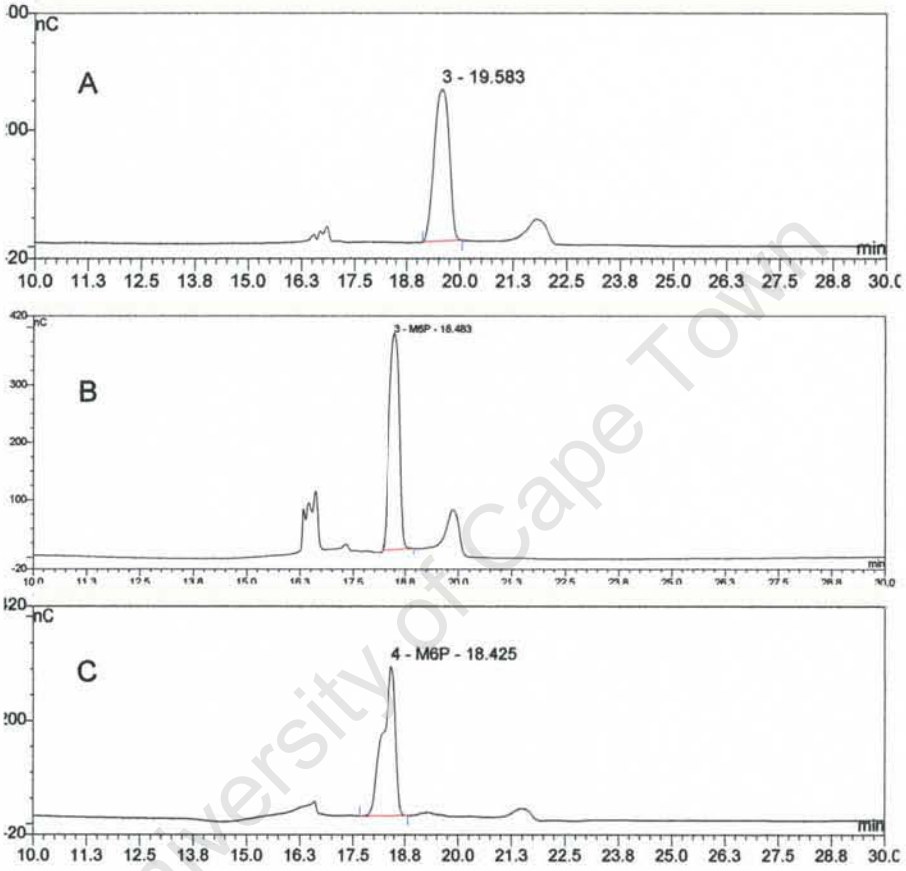

Fig 4.9: *HPAEC-PAD chromatograms at 40 °C for total (A) and free saccharide using DOC/HCl at 0 (B) and 5 (C) weeks respectively.*

A summary of the results obtained by use of the different methods are shown in Table 4.4.

Table 4.4: % free saccharide results obtained using the phosphate assay and HPAEC-PAD for Mn A-TT conjugate lot 4 stored at 25 and 40 °C for 0-5 weeks

	% free saccharide determined by phosphorus assay (Mean±SE)				**% free saccharide determined by HPAEC-PAD (Mean±SE)**			
	DOC		**UF**		**DOC**		**UF**	
Week	25 °C	40 °C	25 °C	40 °C	25 °C	40 °C	25 °C	40 °C
0	8±0.8	8±0.8	26±3	26±3	15±0.4	15±0.4	14±0.4	14±0.4
3	14±0.5	64±2	25±2	110±0.5	12±0.1	33±0.7	9±0.7	42±0.4
5	33±2	70±1	28±0.8	116±2	16±0.2	45±0.8	31±1.2	86±0.5

The % free saccharide determined using the phosphorus assay showed large variation for the same conjugate sample depending on the method of separation used. The DOC/HCl results for the conjugate stored at 25 °C showed a 4-fold increase over the 5 week period (from 8 % to 33 %), whereas the samples analysed by UF had a much higher initial % free saccharide (26 %), which barely changed over the 5 week period. However, for analysis of the conjugate stored at 40 °C, both methods of separation showed a increase in % free saccharide after storage for 3 and 5 weeks.

Analysis by HPAEC-PAD gave good agreement for the free saccharide determined for the initial sample by use of DOC/HCl and UF. The DOC/HCl results for the conjugate stored at 25 °C showed little change over the 5 week period (15 % to 16 %) suggesting that the conjugate is relatively stable at this temperature. There was a problem with the samples analysed by UF as the analysis showed a decrease at 3 weeks (14 % to 9 %) followed by a sharp increase in free saccharide at 5 weeks (31 %). However, for analysis of the conjugate stored at 40 °C, both methods of separation showed a large increase in % free saccharide after storage for 3 and 5 weeks (45 % using DOC/HCl and 86 % using UF).

The % free saccharide as detected by HPAEC-PAD is in broad agreement with results obtained using the phosphate assay and indicates that vaccine samples are stable at 25 °C for five weeks. At 40 °C hydrolysis results in a 50 % increase in free saccharide after 3 weeks which reaches nearly 90 % after 5 weeks. The fact that the free

saccharide assay could detect increasing amounts of free saccharide generated during the stability study confirms that it has the potential to evaluate the stability of conjugate vaccines.

Low OD values were a major limitation of the phosphate assay. In addition, the DOC/HCl method may result in entrapment of some of the free saccharide by the deoxycholate and co-precipitation during the acid treatment. Washing of the UF membrane may have resulted in better recovery of free saccharide compared to the DOC/HCl method. Furthermore, saccharide quantification using the HPAEC-PAD method appeared to be more reliable than the phosphate assay and has the advantage of being more sensitive and specific for M6P.

In order to corroborate the findings on the stability of the Mn A-TT conjugate, the samples were analysed by size exclusion chromatography (SEC) and the results compared with those obtained with the free saccharide assay.

Molecular size distribution

High performance size exclusion chromatography (HPSEC) has been used for determining the molecular size distribution of conjugate vaccines and provides a complementary method for monitoring the stability of these vaccines. HPSEC-UV was applied to investigate variations in the molecular size distribution of Mn A-TT conjugate lot 4 stored at 4, 25 and 40 °C for 5 weeks. HPSEC-UV was performed using a Waters Ultrahydrogel 2000 column (Waters, USA) (300 mm x 7.8 mm, 12 µm particle size) serially equipped with a Waters Ultrahydrogel guard column (40 mm x 6 mm). The fractionation range of the column was 8 000-40 000 kDa and a void and total volume of 11.0 and 23.2 min respectively. Elution was performed at 1 ml min^{-1} with 0.1 M sodium phosphate, 0.1 M NaCl, pH 7 and absorbance at 280 nm. The chromatograms obtained are shown in Figs 4.10-12.

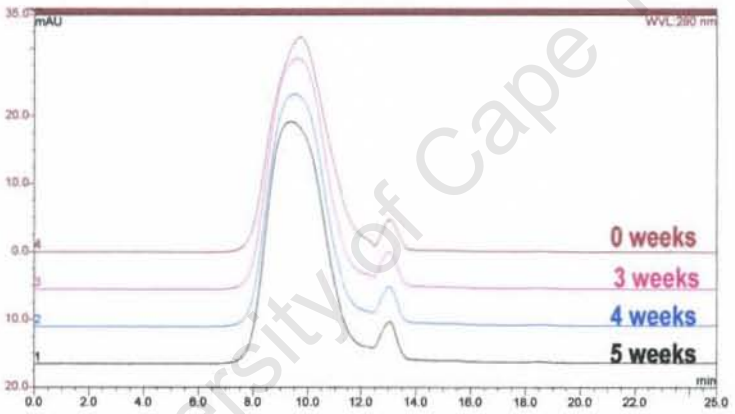

Fig 4.10: *HPSEC-UV traces at 0-5 weeks of Mn A-TT bulk conjugate lot 4 at 25 °C obtained using the Waters Ultrahydrogel 2000 column eluted with 0.1 M sodium phosphate, 0.1 M NaCl, pH 7 (flow rate 1ml min^{-1}).*

The HPSEC-UV method separates molecules based on their hydrodynamic size differences. Fig 4.10 contains the chromatograms for Mn A-TT stored at 25 °C. The HPSEC-UV profile for the control sample (0 weeks) showed a large peak at approximately 9 min (for conjugate) and a smaller peak at approximately 13 min (assigned to unconjugated TT). The chromatograms of the conjugates stored at 25 °C for 3, 4 and 5 weeks showed a similar molecular size distribution, which indicated that the conjugate i.e. both TT and the attached Mn A saccharide, is stable at this temperature. These results agree with the free saccharide assay determined by

DOC/HCl separation and HPAEC-PAD analysis which showed that the conjugate is stable at 25 °C for 5 weeks.

Fig 4.11 contains the chromatograms for Mn A-TT stored at 40 °C. After 3 weeks at 40 °C the major peak at approximately 9 min (for conjugate) has been replaced by a small broad peak and there was an increase in the peak due to unconjugated TT. This suggests that the protein-conjugate had degraded during the storage conditions and most of it had denatured and precipitated although some was present as unconjugated TT. These findings support the results of the free saccharide assay which showed greater degradation of the conjugate stored at 40 °C compared to the sample kept at 25 °C.

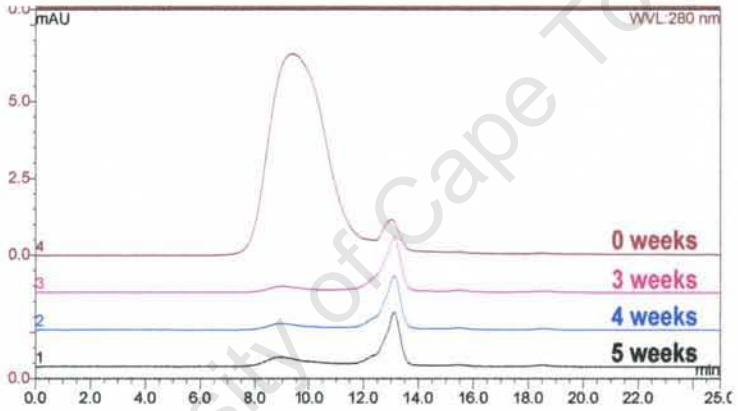

Fig 4.11: *HPSEC-UV traces at 0-5 weeks of Mn A-TT bulk conjugate lot 4 at 40 °C acquired using the Waters Ultrahydrogel 2000 column eluted with 0.1 M sodium phosphate, 0.1 M NaCl, pH 7 (flow rate 1ml min^{-1}).*

Results obtained from the accelerated thermal stability study are summarised in Fig 4.12. At 4 and 25 °C, Mn A-TT was stable, however increasing the temperature to 40 °C resulted in possible loss of the saccharide and denaturation and precipitation of the conjugated protein with an increase in the peak due to unconjugated TT. Therefore, changes in the molecular size distribution of the conjugate can be monitored by HPSEC-UV. However, unlike the free saccharide/HPAEC-PAD method, the HPSEC-UV method is qualitative and relatively insensitive. More comprehensive results may be obtained by using HPSEC with both UV and refractive index (RI) detectors as the latter can detect free saccharide generated.

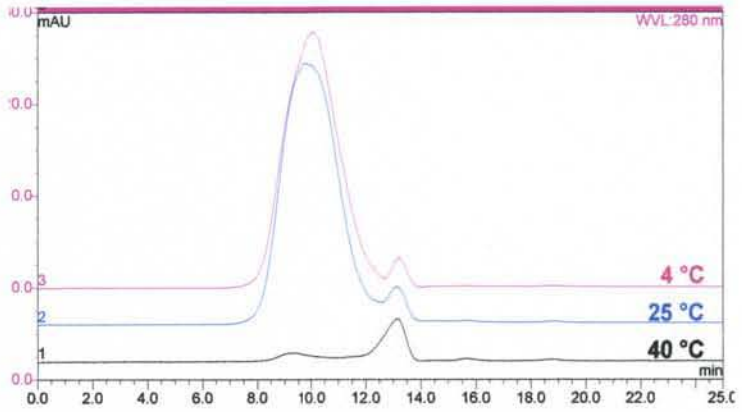

Fig 4.12: *HPSEC-UV traces of Mn A-TT bulk conjugate lot 4 after 5 weeks at 4, 25 and 40 °C. The conjugate was eluted on the Waters Ultrahydrogel 2000 column with 0.1 M sodium phosphate, 0.1 M NaCl, pH 7 (flow rate 1ml min^{-1}).*

An investigation of the thermal stability of meningococcal groups A, C, Y and W135 polysaccharides following storage at 37 and 50 °C and analysis by HPSEC has been reported by Hunolstein and co-workers[29]. Following exposure to thermal stresses, the antigenicity of the polysaccharides was determined by reaction with group specific antisera. Mn A showed a change in elution profile, consistent with degradation, after incubation at 37 °C for only 3 days and no reaction with the group specific antiserum was observed. Thus, degradation of the Mn A polysaccharide led to a loss of its antigenicity. Meningococcal groups C, Y and W135 were stable after storage at 37 and 50 °C for 30 days as no change in the elution curves of these polysaccharides was observed. In addition, they always reacted with their specific antiserum which indicated that they had not lost their antigenicity. Results from the accelerated stability study presented in this thesis (free saccharide determination and HPSEC) agreed with previous studies which showed Mn A conjugates to be stable at 4 °C but subject to degradation following incubation at 37 °C or higher[17, 29].

A recent study conducted by Lee et al. in mice investigated the effect of free saccharide on the immunogenicity of Mn A-TT admixed with up to 400 % of free PsA[30]. The presence of free saccharide had no effect on the immunogenicity of the vaccine and these researchers concluded that the vaccine contained **sufficient** conjugated PsA to induce functional antibody production in mice. Immunogenicity data obtained from real-time stability studies or accelerated stability studies provide a better indication of the

effect of free saccharide generation (due to hydrolysis) on the immunogenicity of the vaccine.

It has been demonstrated that antibodies induced by meningococcal polysaccharide-protein conjugate vaccines protect against meningococcal disease in humans[31, 32]. Binding of the antigen to the target cell occurs via meningococcal-specific protein or carbohydrate moieties. The C1q subunit of complement component C1 binds to the Fc portion of the surface-bound immunoglobulin. This activates the classical pathway of complement that ultimately leads to lysis of the target cell (Fig 4.13)[33, 34]. In order for vaccines to be accepted for licensure, ≥ 90 % of immunised subjects must have at least a four-fold increase in serum bactericidal antibody (SBA) titre[35].

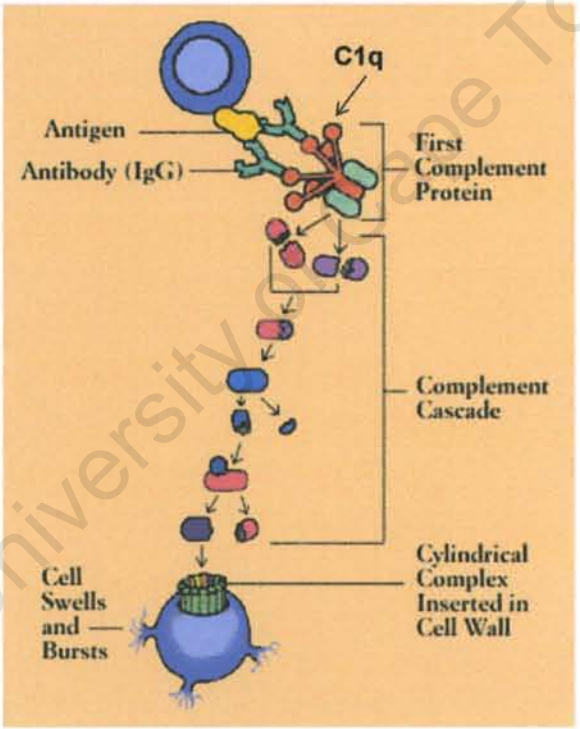

Fig 4.13: *The classical pathway of complement activation, complement proteins bind to the Fc region of IgG and IgM antibody molecules that have interacted with the antigen. A cascade of events leads to formation of a membrane attack complex alongside the complement protein. The attack complex is simply a hollow tube that is pushed into the membrane creating a hole through which water enters. Water will swell the organism until it bursts*[33].

The accelerated thermal stability study has demonstrated that the free saccharide assay can be utilised to monitor the long term stability of conjugate vaccines. HPAEC-PAD was the preferred method for saccharide quantification because it is more sensitive and specific than the phosphate assay. It is possible to underestimate the amount of free saccharide using the DOC/HCl method and further investigation should be conducted to determine whether this is due to entrapment of some of the free saccharide by the DOC and co-precipitation during the acid treatment. Further investigation into the UF method is required to ensure that conjugated saccharide does not pass through the UF membrane and yield erroneously high free saccharide values. It is recommended that both UF and DOC/HCl should be used for comparative purposes when performing the free saccharide assay. Little change in the molecular size distribution was observed when the conjugate was stored at 4 or 25 °C for 5 weeks. However, dramatic changes were observed after 3 weeks at 40 °C due to saccharide hydrolysis and denaturation and precipitation of conjugated TT together with an increase in the amount of unconjugated TT present. These changes in the conjugate at 40 °C supported the free saccharide assay results determined by HPAEC-PAD and use of DOC/HCl and UF.

4.5 Conclusion

The stability of Hib conjugate vaccines is critical for its effectiveness, and therefore the saccharide hydrolysis must be monitored using physicochemical methods. As no suitable unformulated Hib conjugate vaccine was available, PsA and the corresponding Mn A-TT conjugate vaccine (obtained from the Meningitis Vaccine Project) was used to investigate integrity assays for analysing monovalent conjugate vaccines.

The saccharide content of conjugate vaccines was measured with a colorimetric assay for phosphorus as well as by HPAEC-PAD of the monomer after acid hydrolysis. In all vaccine lots tested using the phosphate assay, the total saccharide determined agreed well with results from the manufacturer, thus confirming that this assay can be used for saccharide quantification. The HPAEC-PAD method was also investigated for saccharide analysis in conjugate vaccines. Conjugate samples were analysed after acid hydrolysis on a CarboPac PA-1 column using pulsed amperometric detection. The HPAEC-PAD chromatograms confirmed that the column and analysis conditions were suitable to determine the saccharide content in these vaccines.

The stability and integrity of conjugate vaccines requires determination of the total saccharide and quantification of the unbound or free saccharide present. The published methods of free saccharide separation by DOC/HCl and UF followed by detection using the phosphate and HPAEC-PAD methods were investigated. The DOC/HCl assay is used as a release test by the manufacturer, while the UF method (100 kDa membrane) is applied to purify the conjugate during the manufacturing process. The DOC/HCl method gave low free saccharide recovery and further investigation to determine whether this is due to entrapment of some of the free saccharide by the deoxycholate and co-precipitation during the acid treatment was conducted using the Hib conjugate (and is presented in chapter 5). Higher free saccharide values were obtained using the UF method and further investigation of whether the ultrafiltration membrane is allowing conjugate through is conducted in chapter 5. Unlike the phosphate assay, the HPAEC-PAD method permitted quantification of free saccharide at low levels and afforded higher specificity and sensitivity for free saccharide analysis in these conjugate vaccines. For comparative purposes, it is recommended that both the DOC/HCl and UF methods be used for separation of free saccharide and HPAEC-PAD for saccharide detection.

Validation of the free saccharide assay was not possible because no appropriate vaccine intermediates were available. However, proof of concept was established by conducting an accelerated stability study in which Mn A-TT conjugate samples were stored at 25 and 40 °C for 5 weeks. Quantification of the amount of free saccharide in these samples by the phosphate and HPAEC-PAD methods after separation using the DOC/HCl and UF methods showed a substantial increase in free saccharide following storage at 40 °C. It was concluded from this investigation that free saccharide detection by HPAEC-PAD gave more reliable results because the HPAEC-PAD method is specific for M6P quantification and has a higher sensitivity than the phosphate assay. Statistical analysis was limited to descriptive statistics. However, the availability of adequate quantities of vaccine samples in the near future will make it possible to increase the sample size and number of experiments in order to perform inferential statistics.

As part of the accelerated stability study, changes in the molecular size distribution of the conjugate induced by exposure to elevated temperatures was monitored by HPSEC-UV on a Waters Ultrahydrogel 2000A column. Conjugated TT remained stable at 25 °C, however when kept at 40 °C, the chromatographic profile changed dramatically after 3 weeks. The peak at approximately 9 min for the conjugate disappeared and the

second peak at approximately 13 min for unconjugated TT increased in height. However, this method was limited in that it provided no quantitative indication of the effect of elevated temperatures on the amount of free saccharide generated. Nevertheless, the HPSEC-UV method was sensitive enough to monitor the molecular size distribution of conjugated TT. More comprehensive results could be obtained with the use of a refractive index detector which may provide information on the free saccharide generated and thus be used to corroborate the results of the free saccharide assay. The Mn A conjugate vaccine confers protection by inducing a humoral antibody response. The induced antibody protects via complement mediated bactericidal killing and induction of serum bactericidal antibody (SBA) is a good surrogate for efficacy. The applicability of the above methods to the analysis of Hib in monovalent and combination vaccines was subsequently investigated and is described in Chapter 5.

4.6 References

1. Global Programme for Vaccines and Immunization (GPV). The WHO position paper on *Haemophilus influenzae* type b conjugate vaccines. *Wkly Epidemiol Rec* 1998;**73**:64-8.

2. Sturgess, A. W., Rush, K., et al., *Haemophilus influenzae* type b conjugate vaccine stability: catalytic depolymerization of PRP in the presence of aluminum hydroxide. *Vaccine* 1999;**17**:1169-78.

3. Eskola, J., Kayhty, H., Early immunization with conjugate vaccines. *Vaccine* 1998;**16**:1433-8.

4. http://www.doh.gov.za/programmes/index.html. Accessed 26 March 2008.

5. Weniger, B. G., Chen, R. T., et al., Addressing the challenges to immunization practice with an economic algorithm for vaccine selection. *Vaccine* 1998;**16**:1885-97.

6. Sesardic, D., Requirements for valid alternative assays for testing of biological therapeutic agents. *Dev Biol Stand* 1996;**86**:311-8.

7. Chu, C., Schneerson, R., et al., Further studies on the immunogenicity of *Haemophilus influenzae* type b and pneumococcal type 6A polysaccharide-protein conjugates. *Infect Immun* 1983;**40**:245-56.

8. Metz, B., Hendriksen, C. F., et al., Reduction of animal use in human vaccine quality control: opportunities and problems. *Vaccine* 2002;**20**:2411-30.

9. Redhead, K., Sesardic, D., et al., Interaction of *Haemophilus influenzae* type b conjugate vaccines with diphtheria-tetanus-pertussis vaccine in control tests. *Vaccine* 1994;**12**:1460-66.

10. WHO Expert Committee on Biological Standardization. Forty-ninth report. *World Health Organ Tech Rep Ser* 2000;**897**:i-vi, 1-106.

11. Belfast, M., Lu, R., et al., A practical approach to optimization and validation of a HPLC assay for analysis of polyribosyl-ribitol phosphate in complex combination vaccines. *J Chromatogr B Analyt Technol Biomed Life Sci* 2006;**832**:208-15.

12. Turula, V. E., Kim, J., et al., An integrity assay for a meningococcal type B conjugate vaccine. *Anal Biochem* 2004;**327**:261-70.

13. Bardotti, A., Ravenscroft, N., et al., Quantitative determination of saccharide in *Haemophilus influenzae* type b glycoconjugate vaccines, alone and in combination with DPT, by use of high-performance anion-exchange chromatography with pulsed amperometric detection. *Vaccine* 2000;**18**:1982-93.

14. Guo, Y. Y., Anderson, R., et al., A simple and rapid method for measuring unconjugated capsular polysaccharide (PRP) of *Haemophilus influenzae* type b in PRP-tetanus toxoid conjugate vaccine. *Biologicals* 1998;**26**:33-8.

15. Hsieh, C., L., Characterisation of saccharide-CRM197 conjugate vaccines. *Dev Biol (Basel)* 2000;**103**:93-104.

16. Lei, Q. P., Lamb, D. H., et al., Quantitation of low level unconjugated polysaccharide in tetanus toxoid-conjugate vaccine by HPAEC/PAD following rapid separation by deoxycholate/HCl. *J Pharm Biomed Anal* 2000;**21**:1087-91.

17. Lei, Q. P., Shannon, R.K., et al., Quantification of free polysaccharide in meningococcal polysaccharide-diphtheria toxoid conjugate vaccines, In *Physico-Chemical procedures for the characterization of vaccines*, Brown, F., Corbel, M., et al., Editors. 2000, Karger. Basel. pp. 259-64.

18. Bardotti, A., Ricci, S., et al., Separation of unconjugated polysaccharide by solid phase extraction. International patent WO/2005/090985. 29 September 2005.

19. Suker, J., Feavers, I., M., et. al., Control and lot release of meningococcal group C conjugate vaccines. *Expert Rev Vaccines* 2004;**3**:533-40.

20. MVP is a partnership between WHO and PATH with the goal of eliminating epidemic meningitis (group A) from sub-Saharan Africa through the development, testing, licensure and widespread use of conjugate meningococcal vaccines (www.meningvax.org).

21. Ricci, S., Bardotti, A., et. al., Development of a new method for the quantitative analysis of the extracellular polysaccharide of *Neisseria meningitidis* serogroup A by use of high-performance anion-exchange chromatography with pulsed-amperometric detection. *Vaccine* 2001;**19**:1989-97.

22. Chen, P. S., Toribara, T. Y., et al., Microdetermination of phosphorus. *Anal Chem* 1956;**28**:1756-58.

23. Ames B. N., Assay of inorganic phosphate, total phosphate and phosphatises. *Methods Enzymol* 1966;**8**:115-8.

24. Mawas, F., Bolgiano, B., et al., Evaluation of the saccharide content and stability of the first WHO international standard for *Haemophilus influenzae* capsular polysaccharide. *Biologicals* 2007;**35**:235-45.

25. www.sigmaaldrich.com/Graphics/Supelco/objects/4600/4538.pdf. Accessed 04 April 2008.

26. Cuervo, M. L., Perez, L. R., et al., Relationships among physico-chemical and biological tests for a synthetic Hib-TT conjugate vaccine. *Vaccine* 2007;**25**:194-200.

27. Ho, M. M., Mawas, F., et al., Physico-chemical and immunological examination of the thermal stability of tetanus toxoid conjugate vaccines. *Vaccine* 2002;**20**:3509-22.

28. WHO recommendations to assure the quality, safety and efficacy of group A meningococcal conjugate vaccines. Adopted by the 57th meeting of the WHO Expert Committee on Biological Standardization, 23-27 October 2006.

29. von Hunolstein, C., Parisi, L., et al. Simple and rapid technique for monitoring the quality of meningococcal polysaccharides by high performance size-exclusion chromatography. *J Biochem Biophys Methods* 2003;**56**:291-6.

30. Lee, C-H., Kuo, W-C., et al., Preparation and characterization of an immunogenic meningococcal group A conjugate vaccine for use in Africa. *Vaccine* 2009;**27**:726-32.

31. De Moraes, J. C., Perkins, B. A., et al., Protective efficacy of a serogroup B meningococcal vaccine in Sao Paulo Brazil. *Lancet* 1992;**340**:1074-8.

32. Keyserling, H., Papa, T., et al., Safety, immunogenicity and immune memory of a novel meningococcal (groups A, C, Y and W-135) polysaccharide diphtheria toxoid conjugate vaccine (MCV-4) in healthy adolescents. *Arch Pediat Adolesc Med* 2005;**159**:907-13.

33. http://z.about.com/d/thyroid/1/0/c/07.gif. Accessed 15 October 2009.

34. Frasch, C. E., Borrow, R., et al., Bactericidal antibody is the immunologic surrogate of protection against meningococcal disease. *Vaccine* 2009;**27**:B112-6.

35. WHO requirements for meningococcal polysaccharide vaccine. *World Health Organ Tech Rep Ser* 1976;**594**:50-75.

CHAPTER 5

PHYSICOCHEMICAL ANALYSIS OF *HAEMOPHILUS INFLUENZAE* TYPE B IN MONO- AND PENTAVALENT VACCINES FORMULATED WITH ADJUVANT

5.1 Introduction

Vaccination is recognised worldwide as a cost-effective medical intervention to save lives and has the potential for disease control, elimination and eradication[1]. In recent years, the number of injections required to fully immunise a child has been increasing as national immunisation programmes endeavour to cover more vaccine preventable diseases. Combination vaccines can induce immunity to several diseases simultaneously and thus reduce the number of injections and required medical visits. They are convenient, ensure improved compliance, better disease control and help reduce the overall costs of vaccination programmes[2].

Multidisease combination vaccines are developed by mixing several antigens into a single formulation. The DTP (triple vaccine against Diphtheria, Tetanus and Pertussis) combination vaccine has been available for over 50 years and is a required paediatric vaccine in most countries worldwide. It is typically given 3-4 times in the first 2 years of life with a subsequent booster (in developing countries). The D and T components are obtained from toxins of *Corynebacterium diphtheriae* and *Clostridium tetani* respectively which are purified and chemically inactivated into toxoids. The P component was originally developed as an inactivated whole-cell pertussis (wP) vaccine for combination into DTwP which has been the world's most widely used combination vaccine. Reactogenicity attributed to the wP component led to the development of a better tolerated acellular pertussis (aP) vaccine. There are 7 different aP vaccines (which have been developed into DTaP vaccines) that consist of mixtures of 2-5 proteins purified from *Bordetella pertussis*[3]. These vaccines have been evaluated in protective efficacy studies, in which they showed better tolerability than DTwP but somewhat lower rates of efficacy[4]. DTwP and DTaP vaccines have formed a platform for the development of newer combination vaccines, with added components such as hepatitis B (HBV), inactivated polio vaccine (IPV) and *Haemophilus influenzae* type b (Hib).

HBV vaccine is produced in several systems including recombinant yeast cells in which expression of the surface antigen gene results in the formation of 22-nm hepatitis B surface antigen (HBsAg) particles. The vaccine is administered in a 3-dose series to individuals of all ages; it can be administered 3 times in the first year of life in paediatric combination vaccines[3]. Some countries have replaced the oral polio vaccine (OPV) by the inactivated polio vaccine (IPV) to avoid the small risk of OPV associated paralytic poliomyelitis[5]. IPV is a combination of the 3 serotypes of poliovirus, each of which is purified and inactivated prior to mixing. The capsular polysaccharide of Hib is not immunogenic in children less than 2 years of age. Therefore the polysaccharide is conjugated to a carrier protein (typically D or T toxoids; a diphtheria toxoid-like protein, CRM_{197}; or meningococcal outer membrane protein, OMP). Immunisation of infants with one of these conjugate vaccines has shown to be protective against Hib meningitis because they induce a T-cell dependent response, rather than the T-cell independent response of polysaccharide vaccines[6-8].

South African children currently receive vaccines against Diphtheria, Tetanus, Pertussis (administered as DTP), Hepatitis B (HBV) and *Haemophilus Influenzae* type b (Hib) at 6, 10 and 14 weeks[9]. The Hib vaccine is the most expensive of those administered. When the national immunisation programme was extended to include Hib conjugate vaccine in 1999, the national budget for immunisation doubled. To lower the cost of immunisation, a local vaccine manufacturer is in the process of developing a tetravalent DTP-HBV as well as a liquid pentavalent DTP-HBV-Hib vaccine. This DTP-HBV-Hib vaccine will be introduced into the childhood immunization programme in South Africa, and possibly Southern Africa. The Hib vaccine is a semi-synthetic carbohydrate-protein conjugate, which is usually formulated as a lyophilized product due to the relative instability of the PRP saccharide moiety in aqueous solution[10-12]. The disadvantage of lyophilized vaccines is the increased logistical requirements and the number of clinical manipulations required prior to obtaining a preparation suitable for administration. This problem can be avoided by development of a single vial liquid pentavalent DTP-HBV-Hib vaccine.

The challenge is to achieve chemical stability and compatibility of the Hib antigenic component in the presence of the other antigens and adjuvant. Aluminium hydroxide has been found to catalyse the hydrolysis of PRP when added to Hib conjugate vaccines and although this problem can be circumvented by using aluminium phosphate, there is

a need for alternative adjuvants. One such candidate is Pheroid™. This is an experimental fatty acid-based adjuvant which has shown potential for use as an adjuvant for viral vaccines. Pre-clinical studies of this promising adjuvant are required prior to clinical evaluation[13].

The stability of the Hib conjugate is essential to maintain its immunogenicity and therefore saccharide hydrolysis must be monitored in the conjugate vaccine alone and when in combination with other antigens. Biological assays alone cannot be used in the quality control of individual vaccine batches because they do not correlate well with Hib immunogenicity in humans[14, 15]. As a result, physicochemical techniques are used to measure the concentration, stability and purity of these conjugate vaccines[16].

The saccharide content of Hib conjugate vaccines can be measured with a colorimetric assay for phosphorus and ribose (orcinol method). One disadvantage of using these colorimetric assays for saccharide determination in vaccines is that they are not sensitive enough to detect free saccharide in a single vial of the final product[17]. Also, the presence of other immunogens, adjuvants, sugar stabilisers and associated buffers in combination vaccines results in interferences that make it difficult to monitor the stability of Hib in the mixture[18]. An alternative method uses HPAEC-PAD which allows measurement of the total PRP content in complex samples including commercial vaccine products[17, 19-22]. Minimal sample preparation is required and PAD only detects molecules in the mixture that are ionisable at high pH (11-13). PRP in the vaccine is depolymerised by acid-hydrolysis to ribitol[17, 19] or by base-hydrolysis to its subunit ribitol-ribose-phosphate[18, 20, 21] and quantified by HPAEC-PAD[21]. The method is applicable to conjugate vaccines formulated with aluminium-containing adjuvants and for quantifying unconjugated PRP after separation from the conjugate[17, 22]. However, matrix effects can make the analysis more complicated and cause interference with detection of the analyte.

The objective of this study is to apply the total and free saccharide methods (developed in chapter 4) to investigate the concentration of the Hib component in the monovalent and pentavalent formulation produced by a local vaccine manufacturer. To accomplish this, three methods were investigated for the quantification of saccharide in the locally manufactured Hib vaccine lots, namely the phosphate and ribose assays and HPAEC-PAD. The advantage of these colorimetric assays is that they are quick and easy to use

and are relatively inexpensive. The phosphate assay was used for the analysis of samples that did not contain aluminium phosphate adjuvant while the ribose assay was applied to quantify PRP in samples formulated with aluminium phosphate adjuvant. Poor sensitivity is a major drawback of these colorimetric assays and therefore HPAEC-PAD, which is a relatively more expensive method but provides higher sensitivity and specificity, was investigated especially for the analysis of formulated vaccine samples which contain low PRP concentrations. The DOC/HCl and UF methods were investigated for separation of free saccharide from bound. Also presented in this chapter are two different methods for the pre-treatment of adjuvanted vaccines prior to analysis. As in chapter 4, a thermal stability study was conducted to evaluate both the stability of the vaccines and the performance of the free saccharide assay. The presence of high concentrations of sucrose in vaccine samples interfered with free saccharide determination by HPAEC-PAD, thus the free saccharide assay was used to analyse sucrose-free vaccines and fucose was investigated as an alternative internal standard to sorbitol. The present study focused on developing methods for the analysis of Hib mono- and pentavalent vaccines, therefore a complete validation of the methods used will be performed in future studies and was not a primary objective of this thesis. However, some key parameters necessary for methods validation were established.

5.2 Materials

All Hib conjugates, capsular polysaccharide (PRP), tetravalent DTP-HBV and pentavalent DTP-HBV-Hib vaccines used in this study were provided by a local vaccine manufacturer. The PRP standard was obtained from the National Institute for Biological Standards and Control (Hertfordshire, UK) as part of a WHO study[23]. Pheroid™ was obtained already prepared as an emulsion from the North West University (Potchefstroom).

All vaccine samples in the present study were analysed in duplicate or triplicate. Microsoft Excel was subsequently used to obtain descriptive statistics which included the mean, standard error (SE) and confidence level. P-values were not calculated because the sample size was too small. The sample size will be increased in future studies to enable a more comprehensive statistical analysis to be performed which include calculation of p-values.

5.3 Methods to be investigated

5.3.1 Phosphate assay

The phosphate assay was applied initially to two commercially available Hib conjugates, Hib-TT-**A** and Hib-TT-**B**, but interference with the assay occurred due to the presence of sucrose and thiomersal (a preservative) respectively (results not presented). The assay was subsequently applied to a sample of Hib conjugate formulated with Tris buffer (Hib-TT-**C**) which contained neither thiomersal nor sucrose. Hib-TT-**C** with a stock concentration of 1.30 mg/ml (as determined by the manufacturer using the ribose assay) was diluted to target concentrations of 20 and 100 µg/ml prior to analysis using the phosphorus assay described in section 4.2.1. The standard curve used for phosphorus quantification is shown in appendix C and good linearity was obtained ($R^2 > 0.99$). The limit of detection for the phosphate assay was 0.65 µg/ml. The weight ratio PRP/P = 346/31 was used to convert phosphorus concentration to PRP concentration.

The phosphate assay confirmed total saccharide content of the samples to be 20.6 and 107 µg/ml respectively. The phosphate assay has been shown to be a valuable research assay for quantifying the amount of saccharide present in vaccines. However, its use is limited to vaccines that have not been formulated in phosphate buffer or that do not contain aluminium phosphate adjuvant. For such vaccines, the ribose assay was developed and applied to determine free saccharide content. This assay will be discussed in the following section.

5.3.2 Ribose assay (Orcinol method)

Polysaccharide vaccines can also be analysed by measuring the ribose content[16]. A 100 µg/ml standard solution of D-ribose was prepared and used to construct a standard curve (2, 4, 10, 50 and 100 µg/ml). Details of the procedure followed to prepare reagents for the ribose assay are provided in appendix D. 500 µl sample, blank and standards were added to separate test tubes followed by 1 ml $FeCl_3.6H_2O$ working solution then 100 µl 4 % orcinol solution (in duplicate). The tubes were heated in an oven set at 100 °C for 20 min. Ribose (liberated from acid hydrolysis of PRP in the sample) reacts with orcinol reagent in a concentrated hydrochloric acid-ferric chloride solution to produce a green colouration[24, 25]. After cooling, absorbance measurements were obtained using a Beckman Coulter DU 530 single cell module, Life Science UV/VIS spectrophotometer set at 580 and 670 nm. The difference (670-580 nm) was plotted against the standard concentrations and the amount of ribose in the samples

determined. The ribose standard curve is presented in appendix D and it showed good linearity ($R^2 > 0.99$).

Hib-TT-**C** with a stock concentration of 0.9 mg/ml (as determined by the manufacturer using the ribose assay) was diluted to a target concentration of 100 µg/ml. Analysis of this sample using the ribose assay gave 40 µg/ml ribose content. Conversion to PRP based on weight ratio PRP/ribose gave a concentration of 92 µg/ml. The ribose assay is therefore a useful method that can replace the phosphate assay for analysing conjugate samples if prepared in phosphate buffer.

5.3.3 HPAEC-PAD

In the present study, saccharides were hydrolysed in HCl to yield ribitol which was then analysed on a CarboPac MA-1 column. The CarboPac MA-1 column with its high anion exchange capacity is ideal for the analysis of sugar alcohols such as ribitol. A typical protocol for the HPAEC-PAD method is as follows: 1 ml Hib samples (in duplicate) were treated with 50 µl of 6 M HCl (Aldrich) (final HCl concentration: 0.3 M). The samples were heated at 100 °C for 2 hours in a closed screw-cap test tube. The hydrolysates were allowed to cool to room temperature and then neutralised with 400 µl of 1 M NaOH (Sigma). Samples were passed first through a 0.22 µm nylon filter (National Scientific) to remove particulates then through a SPE reverse phase C18 column (Isolute) to remove proteins. Detection of PRP (as ribitol) was permitted using HPAEC-PAD on a CarboPac MA1 column (250 mm × 4 mm) coupled with a CarboPac MA1 guard column. Isocratic elution with 580 mM NaOH at a flow rate of 0.4 ml/min achieved separation of the ribitol peak from sorbitol (Fluka) which was added as an internal standard. In final fill samples, isocratic elution was at 470 mM NaOH.

Carbohydrate analysis of Hib samples was performed on a Dionex BioLC ion chromatograph system equipped with an AS50 autosampler (Rheodyne rotary injection valve with a 25 µl PEEK sample loop; for the thermal stability study, the sample loop was increased to 80 µl in order to improve sensitivity), an ED50 electrochemical detector, LC30 oven and GS50 pump. The detector cell incorporated a gold working electrode and a Ag/AgCl reference electrode. Chromatographic data were recorded on a personal computer equipped with Chromeleon software. Three different Hib vaccine formulations were investigated; Hib-TT-**A** (conjugate formulated with sucrose), Hib-TT-**B** (conjugate formulated with thiomersal) and Hib-TT-**C** (unformulated conjugate).

5.3.3.1 Determining the limit of detection

The limit of detection was determined using a stock solution of Hib-TT-**B** at a concentration of 0.405 mg/ml of the polysaccharide (based on concentration provided by the supplier). Progressively more dilute samples of Hib-TT-**B** (0.18, 0.5, 1.0, 2.5, and 5 µg/ml) were prepared and analysed in order to establish the limit of detection. Following acid hydrolysis, neutralisation and filtering, the samples were chromatographed on a CarboPac MA1 column with isocratic elution (580 mM NaOH) and pulsed amperometric detection as described in section 5.3.3. Some of the HPAEC-PAD chromatograms are displayed in Fig 5.1.

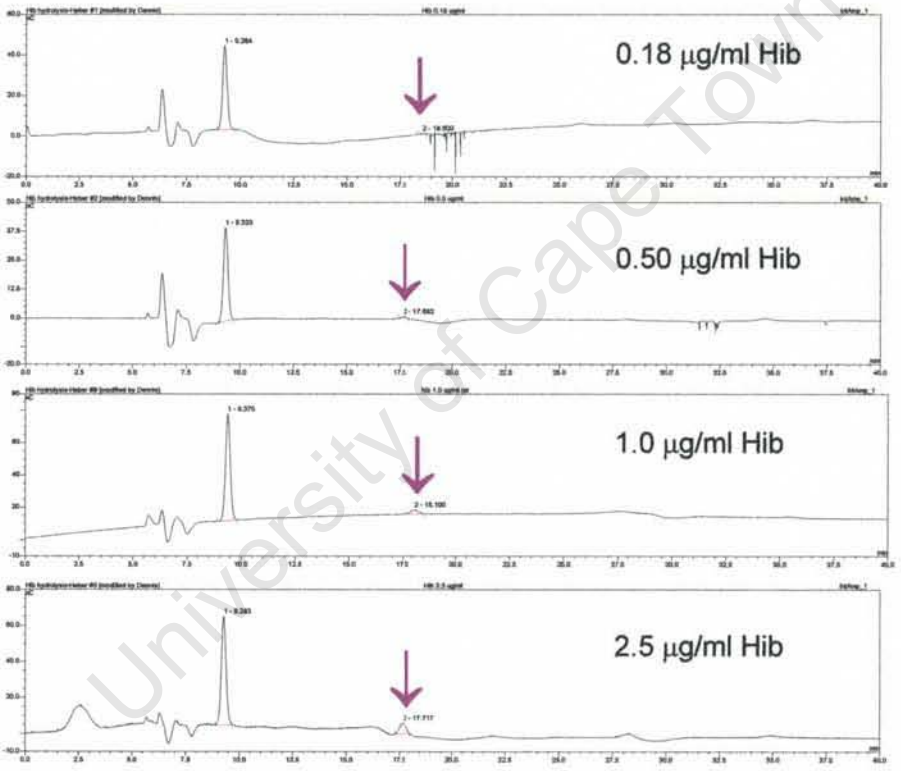

Fig 5.1: *HPAEC-PAD chromatograms for 0.18-2.5 µg/ml of Hib-TT-**B** used to establish the limit of detection. Arrows indicate the ribitol peak.*

The ribitol peak eluted at approximately 18 min under the conditions used without interference from thiomersal and the detection limit was approximately 1 µg/ml.

5.3.3.2 Investigating the use of sorbitol as an internal standard

An internal standard is a substance that is added at a constant concentration to all standards and samples. Since the internal standard is always present at a constant amount, it can be used to account for factors such as concentration changes during sample preparation and clean-up and changes in the performance and sensitivity of the chromatographic system[26]. Sorbitol was investigated as a potential internal standard because it has a similar structure to ribitol. It was expected to be stable and measurable under the conditions used because it elutes at a different retention time to ribitol.

Stock solutions of Hib-TT-**A**, Hib-TT-**B** and Hib-TT-**C** were diluted to a final concentration of 20 µg/ml (based on concentration provided by the supplier) and analysed by HPAEC-PAD as outlined in section 5.3.3. All samples were spiked with 2.32 µg of the internal standard sorbitol after the hydrolysis and neutralisation steps. Total peak area was used to determine ribitol and sorbitol content. The PRP standard (1, 5, 10, 25, 50 and 100 µg/ml) was used to obtain a standard curve of peak area versus PRP content. A calibration curve of peak area versus sorbitol content was generated using the sorbitol standard (1, 5, 10, 25, 50 and 100 µg/ml). The HPAEC-PAD chromatograms obtained for the Hib conjugates following acid hydrolysis are presented in Fig 5.2.

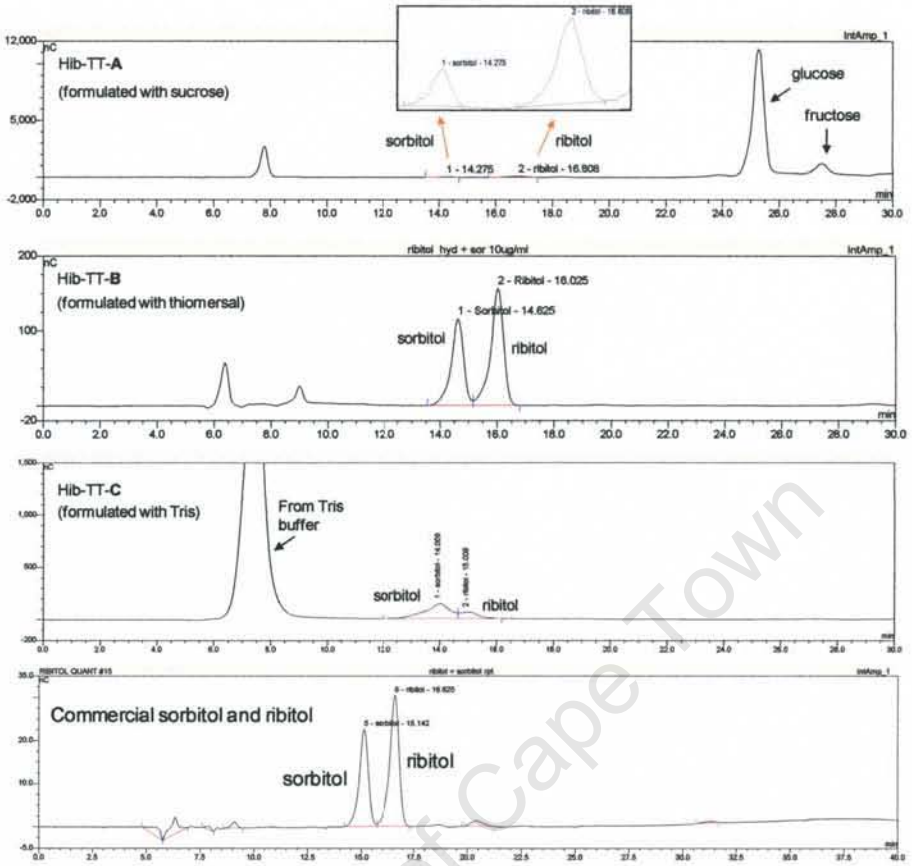

Fig 5.2: *HPAEC-PAD chromatograms for Hib-TT-**A**, Hib-TT-**B**, Hib-TT-**C** and commercial sorbitol and ribitol respectively.*

Analysis of Hib-TT-**A** was complicated by the presence of a large amount of sucrose (85 000 µg sucrose: 20 µg Hib) which was detected as glucose and fructose after hydrolysis. However, the peaks for sorbitol and ribitol could be resolved and integrated when the chromatogram was expanded. For Hib-TT-**B**, there was no interference from thiomersal although its presence had been a problem for the colorimetric assays. Peaks for sorbitol and ribitol eluted close to each other in the Hib-TT-**C** chromatogram but they could be integrated separately and the large peak at 7 min is due to the Tris buffer (Fig 5.2). In all conjugate samples, the sorbitol peak eluted at approximately 14 min while the ribitol peak eluted at approximately 16 min. Sorbitol can therefore be used as an internal standard because it will not interfere with ribitol quantification.

In summary, the PRP content of three different Hib vaccines (Hib-TT-**A**, Hib-TT-**B** and Hib-TT-**C**) was successfully determined after hydrolysis in HCl and quantification of

ribitol using HPAEC-PAD. This method was found to be sensitive (detection limit was 1 µg/ml) and specific because ribitol could be separated and quantified without interference from sucrose (which is used as a stabiliser), thiomersal (which serves as a preservative) and Tris buffer. Sorbitol, which has a similar chemical structure to ribitol, was found to be a suitable internal standard. It had a different retention time to ribitol under the elution conditions used and could be integrated and quantified separately.

PRP depolymerisation has been achieved in some studies by base hydrolysis in NaOH to yield the PRP single repeating unit (as a mixture of ribitol-ribose-3-phosphate or ribitol-ribose-2-phosphate)[17, 18, 21, 27]. Other studies relied on trifluoroacetic acid (TFA) to hydrolyse PRP followed by ribitol quantification[17, 19]. The PRP hydrolysis protocol used in this study varied from previous ones in that HCl was used instead of TFA. Generally, a single human dose (0.5 ml) contains 10 µg of PRP conjugated to a carrier protein. Physicochemical methods used to measure the amount of saccharide present should be sensitive enough to detect as low as 2 % of the total saccharide present in the final product[17]. The above HPAEC-PAD method could detect down to 5 % of the total saccharide of the Hib vaccines investigated; the applicability of this method is probably vaccine and formulation specific.

5.4 Methods of separation

The structural integrity of conjugate vaccines was determined by analysing the final formulation for the evolution of free saccharide. This section describes the total and free saccharide analysis of the monovalent Hib conjugates Hib-TT-**A** and Hib-TT-**C**. The separation of free saccharide from conjugate using selective precipitation by DOC/HCl and ultrafiltration as described in section 4.3.2 was applied. Saccharide quantification was performed using HPAEC-PAD.

5.4.1 Hib-TT-A

Hib-TT-**A** samples were diluted to a target concentration of 20 µg/ml (based on the concentration provided by the supplier). Separation of free from bound saccharide was achieved using the DOC/HCl and UF methods described in section 4.3.2. In order to confirm the separation efficiency of both methods, some samples were spiked separately with 25 and 50 % of an activated PRP intermediate (PRP-ADH). Samples were treated as described in section 5.3.3 and 3.3 µg of sorbitol was added to each sample prior to filtration. The HPAEC-PAD chromatograms for DOC/HCl and UF samples were very similar and so only chromatograms for UF are displayed in Fig 5.3.

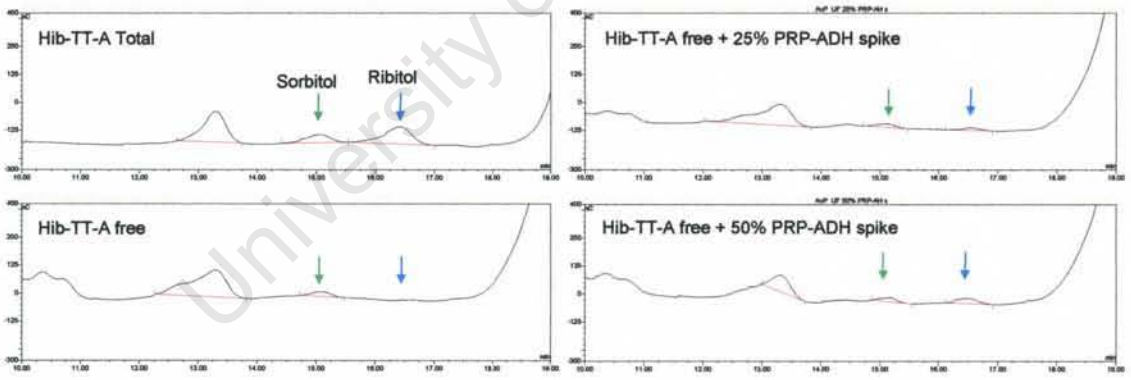

Fig 5.3: *HPAEC-PAD chromatograms of total and free saccharide (left panel) with 25 and 50 % PRP-ADH spikes (right panel) for Hib-TT-**A**. Sorbitol and ribitol peaks are indicated by the green and blue arrows respectively.*

The sorbitol (internal standard) and ribitol peaks elute at 15 and 16 min respectively, before the large peaks derived from sucrose; use of the internal standard sorbitol permitted correction of the ribitol amounts. Quantitative results are provided in Table 5.1.

Table 5.1: % free saccharide results obtained using HPAEC-PAD for Hib-TT-**A** analysis with spike recovery

Test conjugate	PRP Conc.±SE (µg/ml)*		% Free		% recovery	
Total	15±0.6	-	-	-	-	-
	DOC	**UF**	**DOC**	**UF**	**DOC**	**UF**
Free	1.6±0.4	0.9±0.2	11	6	-	-
Free + 25 % spike	6.7±0.3	5.7±0.1	45	38	102	96
Free + 50 % spike	11±0.2	10±0.1	73	67	94	91

*Data in appendix E

The total saccharide concentration in the vaccine was determined as 15 µg/ml; this is lower than the expected value of 20 µg/ml determined from the concentration provided by the supplier. The free saccharide content determined using the DOC/HCl and UF methods was 1.6±0.4 and 0.9±0.2 µg/ml respectively. If 5 % of the total saccharide was free saccharide, its concentration would be near the limit of detection of the instrument (i.e. ≈ 1 µg/ml) and therefore a larger margin of error would be expected. That would explain the difference in the free saccharide value between the DOC/HCl (11 %) and UF (6 %) samples. Vaccines demonstrating adequate immunogenicity in clinical studies currently contain amounts of unbound polysaccharide ranging from less than 10 % to up to 40 % of the total saccharide, depending on the vaccine saccharide, coupling chemistry, protein carrier and formulation[16]. Prior to licensing, the vaccine must therefore be evaluated for immunogenicity in the target age group[16].

Two spiked samples were used to test the separation efficiency of the DOC/HCl and UF methods; 20 µg/ml Hib-TT-**A** spiked with 5 µg of PRP-ADH (25 % spike) and 20 µg/ml Hib-TT-**A** spiked with 10 µg of PRP-ADH (50 % spike). Using the DOC/HCl method, the results showed > 90 % recovery for both the 25 % spiked sample (i.e. (6.7 – 1.60)/5 x 100 = 102 %) and 50 % spike sample (i.e. (11 – 1.60)/10 x 100 = 94 %). PRP recovery when the UF method was used, was also > 90 %. For both the 25 % spiked sample (i.e. (5.7 – 0.9)/5 x 100 = 96 %) and 50 % spike sample (i.e. (10 – 0.9)/10 x 100 = 91 %). These results indicate that the HPAEC-PAD method is capable of measuring varying levels of free saccharide, however because the amount of free saccharide was close to the limit of detection (1 µg/ml), the experiment was repeated using Hib TT-**C** which had a higher free saccharide content compared to Hib TT-**A**.

5.4.2 Hib-TT-C

Hib-TT-**C** with a stock concentration of 1.30 mg/ml (as determined by the manufacturer using the ribose assay) was diluted to 50 µg/ml and 500 µl aliquots were used to conduct the total and free saccharide assay. Separation of free from bound saccharide was performed using UF alone. The separation efficiency was tested using samples spiked separately with 50 and 100 % of an activated PRP intermediate (PRP-ADH). Samples were hydrolysed as described in section 5.3.3 and 16 µg of sorbitol was added to each sample prior to filtration. The HPAEC-PAD chromatograms for Hib-TT-**C** (total, free and free with 50 and 100 % spike samples respectively) are shown in Fig 5.4.

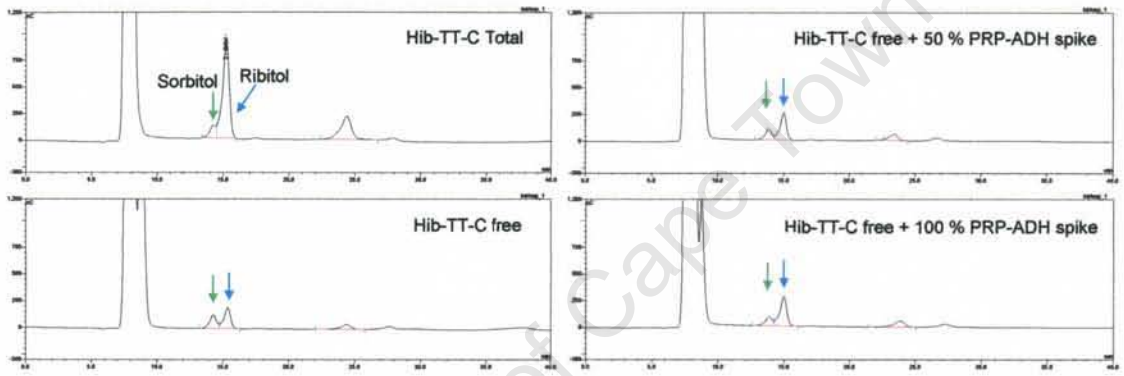

Fig 5.4: *HPAEC-PAD chromatograms of total and free saccharide (left panel) with 50 and 100 % PRP-ADH spikes (right panel) for Hib-TT-**C**. Sorbitol and ribitol peaks are indicated by the green and blue arrows respectively.*

Peaks for sorbitol and ribitol eluted close together at nearly 15 min but could be integrated separately when the chromatogram was resized. The internal standard sorbitol was used to correct for any ribitol lost during the sample preparation and analysis steps. A summary of the results is presented in Table 5.2.

Table 5.2: % free saccharide results obtained using HPAEC-PAD for Hib-TT-**C** with spike recovery

Conjugate	PRP Conc.±SE (µg/ml)*	% free	% recovery
Total	49±1.0	-	-
Free (UF)	13±1.5	27	-
Free (UF) + 50 % spike	38±1.0	78	100
Free (UF) + 100 % spike	62±0.7	126	98

*Data in appendix E

The concentration of total and free saccharide was found to be 49 and 13 µg/ml respectively; this corresponded to 27 % of the total saccharide. Separation of PRP and Hib-TT-**C** was tested with two mixed PRP-ADH/Hib-TT-**C** samples; 50 µg/ml Hib-TT-**C** spiked with 25 µg PRP-ADH (50 % spike) and 50 µg/ml Hib-TT-**C** spiked with 50 µg PRP-ADH (100 % spike). The former showed 100 % recovery (i.e. (38 – 13)/25 x 100) while the latter gave 98 % recovery (i.e. (62 – 13)/50 x 100).

This investigation has demonstrated again that free saccharide can be efficiently separated by UF (with > 90 % recovery) and analysed quantitatively by HPAEC-PAD. This free saccharide assay would therefore be appropriate for analysing the integrity and stability of conjugate vaccines during development.

5.4.3 Analysis of Hib in combination vaccines

Analysis of Hib saccharide in combination vaccines is complicated by interference from the other vaccine antigens and components such as preservatives, adjuvants, buffers, salts and stabilisers. The challenges are vaccine specific. For example, in one study, evaluation of Hib saccharide using the ribose assay in a combination vaccine containing DTP was not be possible due to interference from the DTP component[17]. Even vaccines evaluated by base hydrolysis and quantification of the Hib subunit using HPAEC-PAD can be hampered by interference from DTP[17]. Thus, the present study was undertaken to investigate a method based on HCl hydrolysis followed by the chromatographic separation and quantification of ribitol with an internal standard, sorbitol, on a CarboPac MA-1 column.

Tetravalent (DTP-HBV) and pentavalent (DTP-HBV-Hib-TT-**B**) liquid non-adjuvanted vaccines were supplied by a local vaccine manufacturer. Hib-TT-**B** contained thiomersal but no sucrose excipient (see Fig 5.2). 100 µl of the tetravalent (DTP-HBV) vaccine was diluted to 1 ml using milliQ water. 10 µg/ml samples of the pentavalent vaccine were

prepared for analysis. Samples were hydrolysed and treated as described in section 5.3.3. Pentavalent samples were spiked with 2.64 µg of sorbitol solution before filtration and the amount of saccharide quantified by HPAEC-PAD as previously described in section 5.3.3. The HPAEC-PAD chromatograms are shown in Fig 5.5.

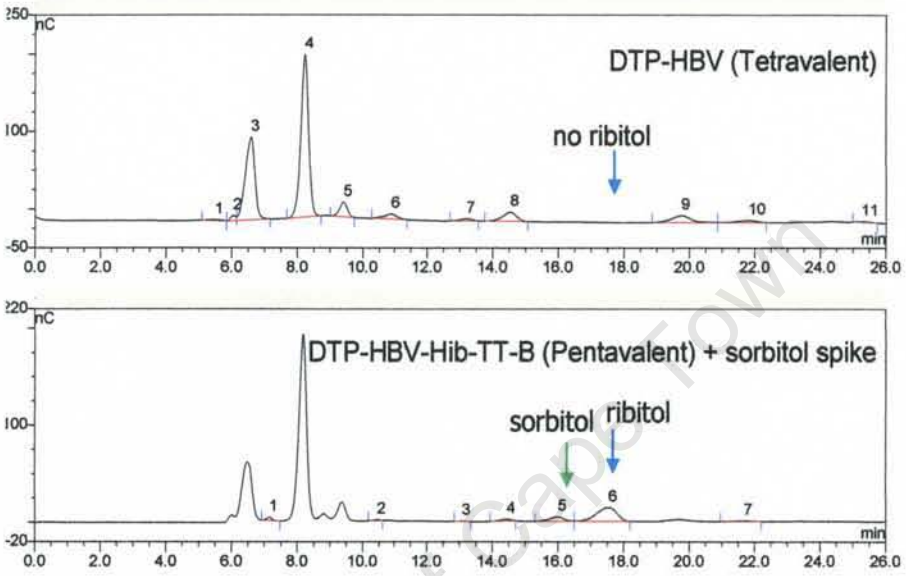

Fig 5.5: *HPAEC-PAD chromatograms for tetra- and pentavalent combination vaccines. The green arrow indicates sorbitol and the blue arrow ribitol.*

The chromatogram of the hydrolysed tetravalent DTP-HBV vaccine shows that under the conditions used, no peaks eluted at the retention times of either ribitol or sorbitol (Fig 5.5), therefore this method could be applied to the analysis of the DTP-HBV-Hib vaccine without interference from the DTP-HBV components. The internal standard sorbitol eluted near 16 min and ribitol near 17.5 min so the method was selective for these analytes. The different retention times permitted integration of the sorbitol and ribitol peaks and thus determination of the corrected ribitol concentration.

The free saccharide assay was then applied to the pentavalent vaccine to evaluate its potency (total saccharide content) and integrity (% free saccharide). This study was performed using Hib-TT-**A**, formulated with sucrose. 500 µl samples of the pentavalent DTP-HBV-Hib-TT-**A** vaccine (20 µg/ml Hib; based on the concentration provided by the

supplier) were prepared for total and free saccharide analysis. Separation of free from bound saccharide was achieved by DOC/HCl and UF (detailed procedure provided in section 4.3.2). The recovery of the free saccharide assay was tested by spiking some samples with 25 and 50 % of a PRP intermediate (PRP-ADH). Samples were treated as described in section 5.3.3 and 3.3 µg of sorbitol was added to each sample after hydrolysis. The HPAEC-PAD chromatograms for DOC/HCl and UF samples were very similar and so only chromatograms for UF are displayed in Fig 5.6.

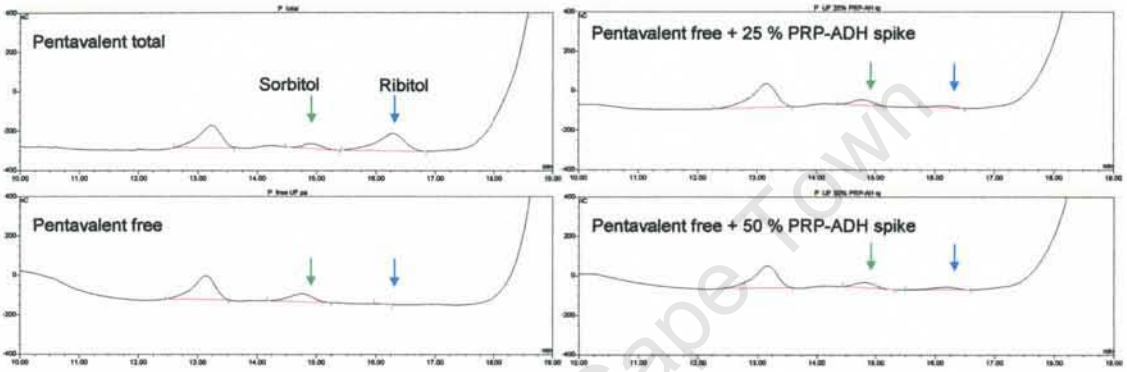

Fig 5.6: *HPAEC-PAD chromatograms of total and free saccharide (left panel) with 25 and 50 % PRP-ADH spikes (right panel) for the pentavalent DTP-HBV-Hib vaccine. Sorbitol and ribitol peaks are indicated by the green and blue arrows respectively.*

The internal standard sorbitol eluted first at approximately 14.7 min and the ribitol near 16 min, after which the chromatogram was dominated by large peaks derived from sucrose. The results obtained are presented in Table 5.3.

Table 5.3: Total and free saccharide results obtained using HPAEC-PAD for DTP-HBV-Hib-TT-A with spike recovery

Test conjugate	PRP Conc±SE (µg/ml)*		% Free		% recovery	
Total	13±0.8	-	-	-	-	-
	DOC	**UF**	**DOC**	**UF**	**DOC**	**UF**
Free	2.0±0.5	1.8±0.3	15	14	-	-
Free + 25 % spike	6.2±0.3	6.1±0.2	48	47	84	86
Free + 50 % spike	11±0.3	11±0.2	85	85	90	92

*Data in appendix E

The concentration of total saccharide was found to be 13 µg/ml; this is lower than the expected value of 20 µg/ml determined from the concentration provided by the supplier. The concentration of free saccharide determined using the DOC/HCl method was 2.0±0.7 µg/ml which corresponded to 15 % of the total saccharide present. Similar results were obtained when UF was used for free saccharide separation (i.e. 1.8 µg/ml and 14 %). The pentavalent vaccine contains less than 20 % free saccharide, but will need to be assessed for its immunogenicity in the target age group before licensure[16].

The recovery of the free saccharide assay was tested with two spike samples; pentavalent + 5 µg of PRP-ADH (25 % spike) and pentavalent + 10 µg of PRP-ADH (50 % spike). When the DOC/HCl method was used, the free saccharide value increased to 48 and 85 % for the 25 and 50 % spike samples respectively. Similar values were obtained using UF which saw an increase to 47 and 85 % for the 25 and 50 % spike samples respectively. PRP recovery in the above samples was ≥ 84 % which was lower than that obtained for the monovalent vaccine and is an indication that the presence of other antigens affects free saccharide recovery. In the pentavalent vaccine, there may be an increased possibility of entrapment of free saccharide as the protein antigens are precipitated with DOC/HCl. The interaction of free saccharide with other antigens present in the formulation is also a possibility. The tetravalent components may interfere with the UF separation because some of the pores in the UF membrane became blocked and therefore longer spin times were required.

5.5 Analysis of Hib in adjuvanted vaccines

Formulations of conjugate vaccines vary, but many are adsorbed onto or dispersed into adjuvants, which serve as excellent vehicles for delivery. Aluminium-based adjuvants have been extensively used in vaccine formulations for this purpose. The WHO

recommends that antigen adsorption should be demonstrated to be within the range of values found for vaccine lots shown to be clinically effective[16]. Adjuvants and buffer systems are formulated to ensure conjugate structural integrity for the specified shelf life of the vaccine. Analysis of the final formulation for the evolution of free saccharide provides a good way to determine structural wholeness or integrity[28]. To accomplish this however requires elution of the antigen if adsorbed to the adjuvant. A survey of the literature revealed different strategies for desorption of the antigen from aluminium-containing adjuvants. For example, dissolution of aluminium-containing adjuvants to release adsorbed antigens has been reported[26, 27, 29]. In addition, anions such as phosphate have been effective in causing elution of antigens from aluminium-containing adjuvants. In the case of ALH adjuvant, elution is caused by adsorption of phosphate anion by the adjuvant which lowers its isoelectric point (IP). High phosphate concentrations cause the surface charge of ALH to change from positive to negative. Consequently, electrostatic repulsive forces between the negatively charged adjuvant and the negatively charged antigen resulted in elution. Adsorption of additional phosphate anions by ALP adjuvant also reduces its IP and increases its negative surface charge thus resulting in increased electrostatic repulsion with a negatively charged antigen[30].

Following confirmation that PRP was adsorbed to ALH adjuvant, the current study investigated the dissolution of adjuvant in NaOH and sodium citrate[27] and the displacement of bound antigen by the phosphate anion when pH and ionic strength are increased[29, 30]. Antigen elution in the presence of Pheroid™ was also investigated. In these experiments saccharide quantification was made by use of the ribose assay.

5.5.1 Adsorption study

Adsorption refers to interactions at surfaces without formation of covalent bonds. In the context of vaccine production, adsorption refers to the attraction between antigens dissolved in the medium and the adjuvant. The zero charge point of aluminium hydroxide (ALH) has been reported as 11.4 and for aluminium phosphate (ALP) as 5.0[29]. At neutral pH, electrostatic attraction would result in the efficient binding of PRP to ALH whereas electrostatic repulsion would lead to poor binding of PRP to ALP. As a result, adsorption studies were performed using only ALH.

Adjuvanted Hib vaccines (mono- and pentavalent) available to this study were obtained already formulated by the manufacturer. Therefore, a series of experiments to determine how long it takes the antigen to adsorb at different pH, concentration or salt concentration have already been performed by the manufacturer. However, to show that TT and PRP are adsorbed to the ALH adjuvant, 1 mg/ml solutions of each were prepared separately and stirred gently overnight in 1 mg/ml ALH. MilliQ water was used as diluent. Samples were then centrifuged at 10 000 rpm for 10 min and $OD_{280\ nm}$ readings of the supernatant was determined followed by the colorimetric assay for ribose. The results confirmed that both TT and PRP were adsorbed to the adjuvant (data not shown). In subsequent studies incubation of PRP with the adjuvant was performed overnight.

These results are in agreement with studies that have shown that TT adsorbs to ALH[31]. Interaction between the adjuvant and antigen is electrostatic regardless of whether the antigen is a polysaccharide or protein. Ligand exchange and hydrophobic interactions (especially with proteins) occur over time making it increasingly difficult for full recovery of antigen. The following three sections investigate various conditions that would favour adjuvant dissolution or desorption of the attached antigen prior to quantification of PRP.

5.5.2 Methods investigated for the separation of adjuvant from conjugate vaccines

5.5.2.1 Adjuvant dissolution with sodium hydroxide and sodium citrate

In the current study, two conditions published in the literature for adjuvant dissolution were investigated[27, 29]. The effect of a 10 % sodium citrate solution on the dissolution of ALH was tested at pH 10 by dissolving 0.1 g sodium citrate in 1 ml aluminium hydroxide (1 mg/ml)[27]. The mixture was incubated overnight at 40 °C. Under these conditions, the adjuvant did not dissolve. Increasing the amount of citrate to 15 then 20 % did not dissolve the adjuvant either.

The solubility of aluminium phosphate (ALP) adjuvant (0.6 mg/ml) was tested using NaOH solutions of varying concentrations (40-600 mM)[29]. A 10 M stock solution of NaOH was prepared by diluting 2.8 ml conc. NaOH to a final volume of 5 ml with milliQ water. This solution was further diluted to 2 M and used to prepare 500 µl samples of ALP containing 40, 80, 120, and 200 mM NaOH. The more concentrated 10 M NaOH stock solution was used to prepare 500 µl samples of ALP containing 500 and 600 mM NaOH. After preparation, all samples were vortexed to aid dissolution. ALP dissolved

only when NaOH concentration was ≥ 500 mM. This method would not be suitable for routine analysis of Hib because the harsh alkaline conditions would induce hydrolysis of the PRP, resulting in an erroneously high free saccharide concentration.

5.5.2.2 Antigen recovery with addition of phosphate anion

In order to determine if the adsorption of PRP to aluminium adjuvants and Pheroid™ is due to electrostatic interactions which are interrupted by increasing phosphate concentration, a modification of the method developed by Jendrek and co-wokers was applied first to samples of PRP mixed with the adjuvants and then to both non-adjuvanted and adjuvanted Hib conjugates[32]. The free saccharide assay was subsequently used to analyse a Hib conjugate formulated with aluminium-containing adjuvants.

A 200 mM phosphate buffer at pH 7.5 was prepared by dissolving 3.57 g of anhydrous monosodium phosphate (Lasechem) and 7.71 g of trisodium phosphate dodecahydrate (Lasechem) in 250 ml milli-Q water (**Buffer 1**). Stock solutions of PRP and ALH adjuvant with concentrations of 7.92 mg/ml and 30 mg/ml respectively were used. Two separate mixtures containing 40 and 100 µg/ml PRP in 1 mg/ml ALH adjuvant were prepared. The mixtures were stirred gently overnight to aid adsorption of PRP onto the adjuvant. 0.5 ml of each mixture was diluted to 20 and 50 µg/ml respectively using the phosphate buffer and a 0.9 % saline solution to obtain 1 ml samples containing 10, 20, 30, 40, 50 and 100 mM phosphorus (n = 2). The control sample was diluted with *saline* alone and contained no phosphorus. These samples were vortexed, incubated at room temperature for 1 hour and then centrifuged at 10 000 rpm for 10 min to precipitate the adjuvant, leaving the desorbed PRP in the supernatant. The supernatant was then analysed for its ribose content as described in section 5.3.2. A conversion factor of 2.31 was used to convert ribose to PRP. The results obtained are shown in Fig 5.7.

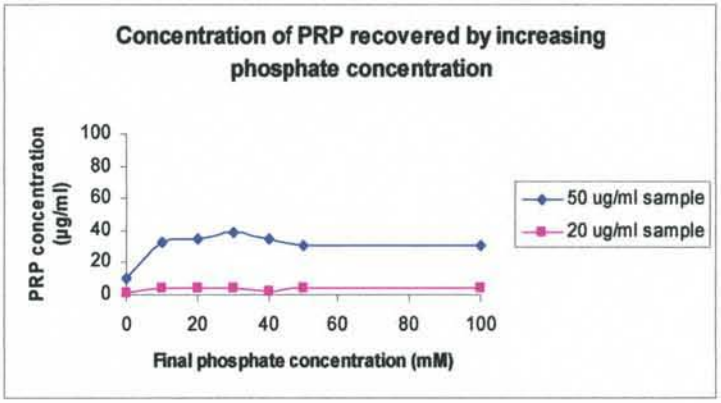

Fig 5.7: *PRP recovery from ALH at two different concentrations.*

PRP is a highly charged polyanion which is expected to bind to ALH by electrostatic interactions. At low PRP concentration (20 µg/ml), all the PRP was adsorbed to ALH and virtually no desorption of PRP occurred with addition of the phosphate anion (Fig 5.7). This may be because of the low concentration of PRP. As a result, PRP binds to some but not all of the sites on ALH so that the phosphate anion can bind to the remaining sites without having to displace PRP[33]. The OD values obtained at 20 µg/ml PRP were low and therefore only the graph obtained at 50 µg/ml was used for further interpretation of the data.

In section 5.5.1, 1 mg/ml PRP was completely adsorbed by 1 mg/ml ALH when water was used as the diluent. However it has been reported by Jendrek and co-workers that an increase in ionic strength reduces electrostatic forces[32]. This might explain why the control sample (prepared in saline and not water and therefore possessing a higher ionic strength) contained 10 % unadsorbed PRP. At 50 µg/ml PRP, the maximum percentage of PRP recovered was 70 % and this occurred at 30 mM phosphate anion concentration. Thereafter, increasing phosphate concentration did not result in further release of PRP (Fig 5.7). The fact that the presence of phosphate led to the desorption of at least 60 % of bound PRP suggests that the binding of PRP to ALH is primarily electrostatic in nature.

In conclusion, addition of phosphate anion at neutral pH caused 60 % of the adsorbed PRP to be released into the supernatant. The ultimate objective would be to obtain greater than 90 % recovery of the adsorbed PRP from ALH. Other factors that affect the amount of adsorbed antigen and the strength of adsorption include pH and the type of

buffer (ionic strength or type of ions). In an attempt to improve PRP recovery, the effect of increasing adjuvant pH (from 6.5 to 7.0) on release of the adsorbed antigen was investigated.

5.5.2.3 Effect of modifying pH from 6.5 to 7.0 on PRP recovery with addition of phosphate anion

The pH of the ALH and ALP adjuvant stock solutions was adjusted from 6.5 to 7.0. Two separate mixtures containing 200 µg/ml PRP in 1 mg/ml ALH and 0.6 mg/ml ALP were prepared and allowed to stir gently overnight. 0.5 ml of each was diluted using the phosphate buffer and the 0.9 % saline solution to obtain 1 ml samples containing 100 µg/ml PRP in 50 and 100 mM phosphate buffer (**Buffer 1**). The control sample was diluted with *saline* alone and contained no phosphorus. Samples were vortexed, incubated at room temperature for 1 hour and then centrifuged at 4 000 rpm for 20 min. Supernatants were transferred to fresh eppendorf tubes and the pellets resuspended in 0.5 ml saline (control) and 0.5 ml 50 and 100 mM phosphate buffer (**Buffer 1**) then centrifuged at 10 000 rpm for 10 min. This wash step was included to maximise recovery of PRP. Supernatant and washings were pooled (± 1 ml) and the saccharide content quantified using the ribose assay (described in section 5.3.2). The percentage of PRP recovered in each sample is presented in Fig 5.8.

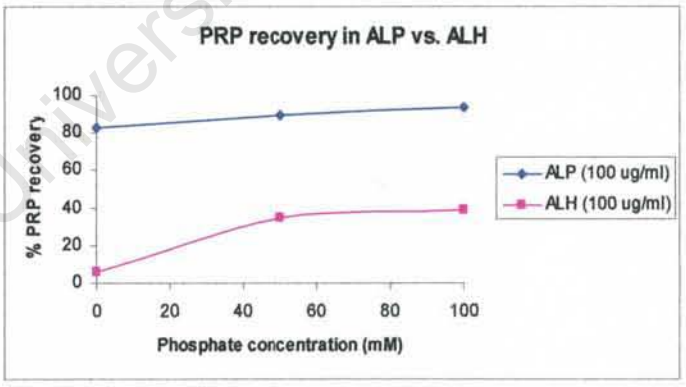

Fig 5.8: *PRP recovery from both ALH and ALP by increasing phosphate ion concentration (pH 7.0).*

Although PRP was poorly adsorbed to ALP (zero phosphate concentration showed 80 % recovery), at 100 mM phosphate concentration an increased electrostatic repulsion between the adjuvant and PRP yielded over 90 % PRP recovery. At pH 7 the ALH

adjuvant is positively charged, addition of the negatively charged PRP resulted in immediate binding. 100 mM phosphate concentration was not sufficient to desorb all adsorbed antigen from ALH as only 40 % PRP was recovered. Compared to Fig 5.7, it is evident from Fig 5.8 that adjusting the pH and including a wash step was not effective in improving PRP recovery from ALH.

In adsorption experiments conducted with purified diphtheria toxoid or tetanus toxoid as used in vaccines, Matheis and co-workers demonstrated complete adsorption of these toxoids onto ALH[31]. In the case of ALP, only partial adsorption was observed. Desorption of the antigens (diphtheria toxoid or tetanus toxoid) was easier from ALP adsorbed vaccines in comparison to ALH adsorbed vaccines. Although these investigators used negatively charged proteins[31], the present study has confirmed that when the antigen is a negatively charged saccharide (in this instance PRP), it is more readily eluted from ALP than ALH.

5.5.2.4 Using Pheroid™ as adjuvant

Pheroid™ is a patented fatty-acid based formulation which has shown potential for use as an adjuvant. Zeta potential studies revealed that Pheroid™ forms a micro-emulsion with negatively charged particles[34]. Previous studies on emulsions have demonstrated that electrolytes such as NaCl can be used to decrease the elastic behaviour of the interfacial film, resulting in interfacial film breakdown and the release of entrapped antigens[35]. Thus, the present study was undertaken to investigate PRP recovery after overnight incubation with Pheroid™ and diluted using a 1x PBS buffer prepared by dissolving 8 g NaCl, 0.2 g KCl, 1.44 g Na2HPO4 and 0.24 g KH2PO4 in a litre of MilliQ water and adjusting the pH to 7.4 (**Buffer 2**).

In previous studies conducted using Pheroid™ as adjuvant, the vaccines were formulated with either 1.85 or 100 % Pheroid™ (v/v) therefore these two concentrations were used[34]. 200 µg/ml PRP in 1.85 and 100 % Pheroid™ were stirred gently overnight. Both samples were then diluted to 100 µg/ml PRP with **Buffer 2**. Centrifugation of the mixture at 13 400 rpm allowed separation of a relatively thin layer of oil on top of the aqueous phase. The centrifugation step was repeated for PRP in 100 % Pheroid™ in order to recover as much of the aqueous layer as possible. The amount of PRP present in this aqueous phase was analysed using the ribose assay (as outlined in section 5.3.2). The results obtained are displayed in Table 5.4. 100 % recovery was obtained at 1.85 % Pheroid™ concentration. Under the conditions used, only 75 % recovery was possible at 100 % Pheroid™ concentration probably because complete separation of the oil and aqueous phase was not achieved.

Table 5.4: PRP recovery from samples containing Pheroid™

Sample	Ribose Conc (µg/ml)	PRP Conc (µg/ml)	% Recovery
PRP in 1.85 % Pheroid	43.8	102	102
PRP in 100 % Pheroid	31.1	72	72

From the above results it is evident that **Buffer 2** is a suitable elution buffer which can inhibit PRP adsorption to aluminium phosphate adjuvant and Pheroid™. Initial experiments also revealed that following centrifugation of the adjuvant, the free saccharide assay with ribose quantification can be used to determine the amount of free saccharide in the vaccine.

5.5.2.5 Pre-treatment of Hib-TT-D adsorbed to aluminium-containing adjuvants

Hib-TT-**D** conjugate was provided by the manufacturer with a stock concentration of 0.9 mg/ml and high free saccharide content. The effect of **Buffer 2** on desorption of Hib-TT-**D** from ALP (**Hib-TT-D/ALP**) adjuvant was investigated. The pH of ALP was adjusted from 6.5 to 7.0 before sample preparation. A sample containing 200 µg/ml Hib-TT-**D** and 0.6 mg/ml ALP in **Buffer 2** was stirred gently overnight. 0.5 ml aliquots were diluted with **Buffer 1** to yield 1 ml samples containing 100 µg/ml Hib-TT-**D** in 50 and 100 mM additional phosphorus (duplicate). The control sample was diluted with 0.5 ml *saline* and contained no phosphate ions Samples were vortexed, incubated at room temperature for 1 hour and then centrifuged at 4 000 rpm for 20 min. Supernatants were transferred to fresh eppendorf tubes and the pellets resuspended in 0.5 ml saline (control) and 0.5 ml 50 and 100 mM phosphate buffer then centrifuged at 10 000 rpm for 10 min. Samples were evaluated for their PRP content using the ribose assay (see section 5.3.2 for detailed procedure).

Similar amounts of PRP were recovered from the control and from samples to which 50 and 100 mM additional phosphate had been added (95±1.3, 95±1.4 and 97±1.0 % respectively). The results from this study suggest that in the presence of **Buffer 2** alone, the antigen is unadsorbed and the amount of PRP recovered was >90%. Addition of phosphate buffer (10 mM) has been used to extract the Hib conjugate in vaccines formulated with aluminium phosphate adjuvant[17]. In that study the conjugate consisted of PRP oligosaccharides attached to a non-toxic variant of the diphtheria toxin (Cross-Reacting Material, CRM_{197}). Thus, the addition of phosphate anions was successful in extracting the conjugate into the supernatant in ALP-adjuvanted Hib-CRM and Hib-TT vaccines.

5.5.2.6 Determination of free saccharide in Hib-TT-D formulated with aluminium-containing adjuvants

Hib-TT-**D** conjugate provided by the manufacturer with a stock concentration of 0.9 mg/ml and high free saccharide content was used to prepare two sets of samples. The first set consisted of separate mixtures of 100 µg/ml Hib-TT-**D** and 1 mg/ml ALH in **Buffer 2** (**Hib-TT-D/ALH**) and 100 µg/ml Hib-TT-**D** and 0.6 mg/ml ALP in **Buffer 2** (**Hib-TT-D/ALP**). The second batch was prepared in the same way but saline was used instead of **Buffer 2**. The mixtures were stirred gently overnight to aid adsorption of the conjugate onto the aluminium-containing adjuvants. 0.5 ml aliquots were diluted with

Buffer 1 to yield 1 ml samples containing 100 µg/ml Hib-TT-**D** in 50 and 100 mM additional phosphate. The control samples were diluted with 0.5 ml saline. Samples were vortexed, incubated at room temperature for 1 hour and then centrifuged at 4 000 rpm for 20 min. Supernatants were transferred to fresh Eppendorf tubes and the pellets resuspended in 0.5 ml saline (control) and 0.5 ml 50 and 100 mM phosphate buffer then centrifuged at 10 000 rpm for 10 min. The supernatants were pooled and ultrafiltered as described in section 4.3.2 then analysed using the ribose assay (see section 5.3.2 for detailed procedure). Fig 5.9 shows the results obtained.

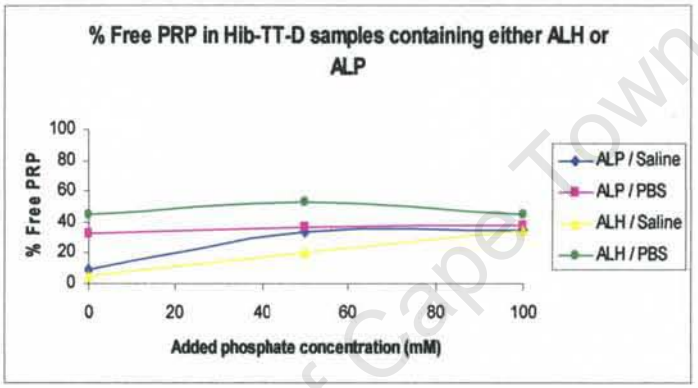

Fig 5.9: *Free saccharide determination of Hib-TT-**D** vaccine adsorbed to ALH and ALP.*

The adsorption of phosphate anions has been found to lower the isoelectric point of ALH[30]. Hence addition of PBS (**Buffer 2**) would increase the electrostatic repulsion between the adjuvant and PRP and UF would separate free PRP into the filtrate. The amount of free saccharide recovered from samples prepared in **Buffer 2** was expected to be higher than those prepared in saline and this was indeed the case as shown in Fig 5.9. When Hib-TT-**D** was prepared with ALH (**Hib-TT-D/ALH**) in saline, the amount of free saccharide increased with increasing phosphate anion concentration until a maximum of 35 % indicating that the conjugate and some free saccharide is still adsorbed to the adjuvant. However, when **Buffer 2** was used in place of saline, a maximum of 53 % free saccharide was obtained. Further evidence that **Buffer 2** alone is sufficient for conjugate desorption can be seen in the fact that addition of extra phosphate did not improve free saccharide recovery because at 0 and 100 mM phosphate concentration, the amount of free saccharide remained the same.

In the case of ALP which is negatively charged at neutral pH, PBS (**Buffer 2**) would increase the repulsive forces between the adjuvant and conjugate (**Hib-TT-D/ALP**)[30]. Previous experiments in saline (see Fig 5.8) had shown successful recovery of PRP from the adjuvant, therefore no dramatic variation in free saccharide was expected when saline and PBS was compared. This was indeed the case as shown in Fig 5.9. In saline, free saccharide concentration increased with increasing phosphate to reach a maximum of 35 %. In **Buffer 2**, addition of extra phosphate caused the amount of free saccharide to increase slightly to 38 %.

This investigation has demonstrated that **Buffer 2** alone can be used for elution of free saccharide without addition of extra phosphate. However, the amount of free saccharide recovered from ALH and ALP varied (53 and 38 % respectively). Therefore, to determine the correct concentration of free saccharide, this experiment was repeated using the DOC/HCl and UF methods of free saccharide separation and the more sensitive HPAEC-PAD method for saccharide quantification.

5.5.3 Comparison of DOC/HCl and UF methods for the separation of free saccharide in Hib-TT-D formulated with aluminium-containing adjuvants

The total and free saccharide assay was now applied to Hib-TT-**D**, **Hib-TT-D/ALH** and **Hib-TT-D/ALP**. The pH of both ALH and ALP was adjusted to 7.0 by dropwise addition of 0.1 M NaOH. 100 µg/ml samples of **Hib-TT-D/ALH** and **Hib-TT-D/ALP** were prepared in **Buffer 2** and allowed to stir gently overnight. 100 µg/ml samples of Hib-TT-**D** served as the control. Separation of free from bound saccharide was achieved by the DOC/HCl and UF (100 kDa membrane) methods. Samples were hydrolysed as described in section 5.3.3 and 16.4 µg of sorbitol was added to each sample prior to filtration. Total and free saccharide quantification was conducted using the HPAEC-PAD method. The results obtained are presented in Fig 5.10.

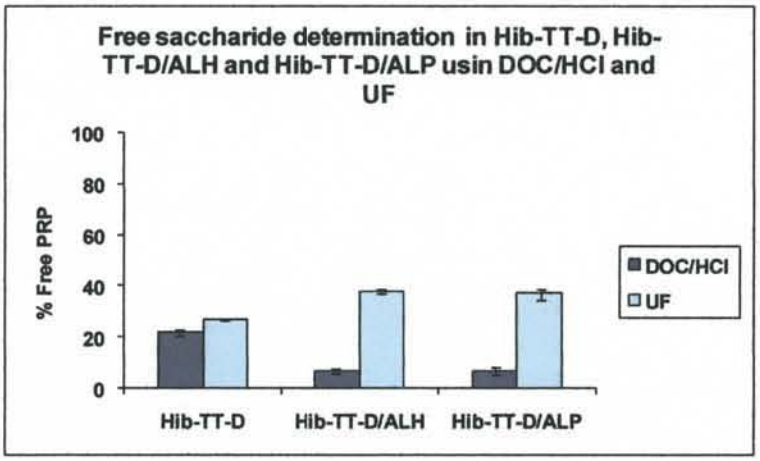

Fig 5.10: *% free saccharide determination for Hib conjugate alone (Hib-TT-**D**), conjugate formulated in ALH (**Hib-TT-D/ALH**) and conjugate formulated in ALP (**Hib-TT-D/ ALP**). The error bars represent the standard error.*

In the conjugate sample formulated without adjuvant, the DOC/HCl and UF methods indicated the presence of 22±1.8 and 27±0.4 % free saccharide respectively. It may be that the wash step included in the UF method resulted in better recovery of free saccharide or perhaps the 100 kDa membrane was permitting some conjugate to pass through. Additional experiments were later conducted (and presented in section 5.7) to determine firstly whether the 100 kDa membrane was permitting some conjugate to pass through and secondly what effect if any the type of buffer had on PRP recovery when the DOC/HCl method was used.

When the DOC/HCl method was used, free saccharide was lower in **Hib-TT-D/ALH** (7±1.4 %) compared to the control (22±1.8 %). Therefore, compared to the unadjuvanted control, the DOC/HCl method may underestimate the amount of free saccharide present. The decrease in free saccharide did not correspond to the free saccharide results obtained using UF (38±1.4 %) and was therefore attributed to the method of free saccharide separation since the selection of a buffer and the ionic strength of the vaccine formulation can affect both the amount of antigen that is adsorbed as well as the strength of the adsorption force[32].

In **Hib-TT-D/ALP**, the DOC/HCl and UF methods yielded 7±2.2 and 37±2.8 % free saccharide respectively. A decrease in the amount of free saccharide was also observed compared to **Hib-TT-D** alone when the DOC/HCl method was used for free

saccharide separation. Therefore, it may be worth investigating what effect different buffers would have on PRP recovery when the DOC/HCl method is used.

Differences in the free saccharide data obtained using the DOC/HCl and UF methods were investigated and are presented in section 5.7. In the following section however, analysis of Hib-TT-D was performed using the free saccharide assay with spike recovery.

5.5.4 Total and free saccharide analysis (with spike recovery) of Hib-TT-D formulated with aluminium-containing adjuvants

The pH of both ALH and ALP was adjusted to 7.0 by dropwise addition of 0.1 M NaOH. The 0.9 mg/ml stock solution of Hib-TT-**D** was used to prepare 100 µg/ml samples of **Hib-TT-D/ALH** and **Hib-TT-D/ALP** in PBS (**Buffer 2**) and allowed to stir gently overnight. 100 µg/ml samples of Hib-TT-**D** served as the control. 500 µl aliquots were subsequently diluted to 1 ml and a final concentration 50 µg/ml with **Buffer 2** (for samples containing adjuvant) or saline (for the Hib conjugate alone). Samples containing adjuvant were centrifuged at 4 000 rpm for 20 min prior to determination of free saccharide. Supernatants were collected in fresh Eppendorf tubes and the pellets washed by resuspending in 250 µl of **Buffer 2** and centrifuged at 10 000 rpm for 10 min. Supernatants were pooled and ultrafiltered as described in section 4.3.2. Some samples were spiked separately with 50 % (i.e. 25 µg) and 100 % (i.e. 50 µg) of an activated PRP intermediate (PRP-ADH) for two reasons. Firstly, to establish proof of concept by confirming the separation efficiency of UF in samples formulated with aluminium-containing adjuvants. Secondly, to establish that the HPAEC-PAD method can accurately detect an increase in the amount of free saccharide and therefore be used to analyse the stability of conjugate vaccines formulated with aluminium-containing adjuvants. Samples were hydrolysed as described in section 5.3.3 and 16.4 µg of sorbitol was added to each sample after hydrolysis. Total and free saccharide quantification was performed using the HPAEC-PAD method. A summary of the results is presented in Fig 5.11.

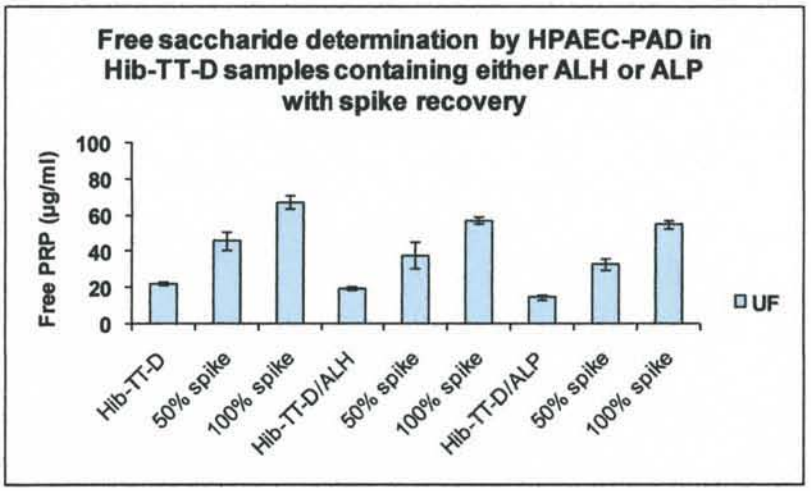

Fig 5.11: *HPAEC-PAD quantification of free saccharide with 50 and 100 % PRP-ADH spikes for Hib conjugate alone (Hib-TT-**D**), conjugate formulated in ALH (**Hib-TT-D/ALH**) and conjugate formulated in ALP (**Hib-TT-D/ALP**). Error bars represent the standard error.*

The concentration of total and free saccharide in the conjugate sample formulated without adjuvant (Hib-TT-**D**) was 56±0.4 and 22±1.8 µg/ml respectively. The results showed 96 and 92 % recovery in the low (50 %) and high (100 %) concentration spike samples respectively. Analysis of **Hib-TT-D/ALH** yielded total and free saccharide concentrations of 43±1.4 and 20±1.4 µg/ml respectively. This time only 72 and 74 % of the spiked PRP was recovered from the low and high concentration spike samples respectively. Total and free saccharide content in **Hib-TT-D/ALP** samples was 40±5.7 and 14±2.2 µg/ml respectively. 76 and 82 % of spiked PRP was recovered from the low and high concentration spike samples respectively.

Free saccharide determination of aluminium-adjuvanted Hib vaccines has been reported for Hib-CRM[17] and Hib-OMPC[27], however not for Hib-TT conjugates. No published studies have described the use of UF for the analysis of free saccharide in Hib-TT vaccines formulated with ALH or ALP. This investigation specifically examined the separation of free saccharide in a Hib-TT conjugate vaccine formulated with ALH and ALP adjuvants. PBS was used for desorption and extraction of the antigen from ALH and ALP respectively prior to separation and saccharide quantification was performed using HPAEC-PAD.

In summary, the amount of free saccharide determined in this study was in the range 35-47 %. For **Hib-TT-D**, **Hib-TT-D/ALH** and **Hib-TT-D/ALP** samples, a corresponding increase in percentage free saccharide accompanied both the 50 and 100 % spike samples. PRP recovery was > 90 % in the conjugate samples formulated without adjuvant but < 90 % when ALH and ALP were used. This method shows potential for use in monitoring the stability of Hib-TT in the presence of aluminium-containing adjuvants during routine vaccine manufacturing. Therefore, this method was tested by performing a thermal stability study on Hib-TT in a pentavalent formulation containing adjuvant.

5.6 Accelerated thermal stability study

A key criterion for determining the quality and stability of conjugate vaccines is the measurement of free saccharide. This can be a challenge in combination vaccine formulations due to the presence of different components which may cause interference with detection of ribitol. In addition, the use of aluminium-containing adjuvants with combination vaccines necessitates the development of sample preparation methods to desorb the antigen of interest from the adjuvant prior to analysis. Previous experiments have established that using a high ionic strength phosphate buffer like PBS (**Buffer 2**), even at physiological pH of 7.4 could result in the phosphate anion electrostatically competing or exchanging ions with the aluminium hydroxide and aluminium phosphate adjuvant complexes in Hib vaccines thus releasing free saccharide. Preliminary experiments indicated that **Buffer 2** was also a suitable elution buffer in samples formulated with Pheroid™.

Analysis of Hib in the pentavalent vaccine (DTP-HBV-Hib-TT-**A**) formulated with adjuvant was investigated. Four combination vaccines were prepared: **Penta** (control vaccine formulated without adjuvant), **Penta/ALH**, **Penta/ALP** and **Penta/Pheroid™** (containing 1.85 % Pheroid™) were the pentavalent vaccine formulated with ALH, ALP and Pheroid™ respectively. The vaccines were supplied by a local vaccine manufacturer. Hib-TT-**A** contained sucrose excipient. The Hib component was 40 µg/ml (concentration provided by the manufacturer). The thermal stability of these vaccine formulations was monitored at 4, 25 and 40 °C for a period of 0, 2 and 5 weeks. All samples were stored at 4 °C until testing. For analysis, 500 µl aliquots were diluted to 20 µg/ml with 500 µl of **Buffer 2** (based on concentration provided by the manufacturer). Samples containing adjuvant were centrifuged at 4 000 rpm for 20 min prior to

determination of free saccharide. Supernatants were collected in fresh Eppendorf tubes and the pellets washed by resuspending in 250 µl **Buffer 2** and centrifuging at 10 000 rpm for 10 min. Supernatants were pooled and ultrafiltered to obtain the free saccharide (as described in section 4.3.2). Following hydrolysis (see section 5.3.3 for detailed procedure), 16.4 µg of sorbitol was added to each sample prior to filtration and analysis. Saccharide quantification was performed using HPAEC-PAD. Total peak areas were used to determine ribitol and sorbitol content. The ribitol concentration was corrected using the internal standard sorbitol.

The HPAEC-PAD chromatograms for **Penta** obtained at 25 °C showing total (A) and free at 2 (B) and 5 (C) weeks respectively are presented in the left panel of Fig 5.12. The right panel contains chromatograms obtained at 40 °C for total (D) and free at 2 (E) and 5 (F) weeks respectively.

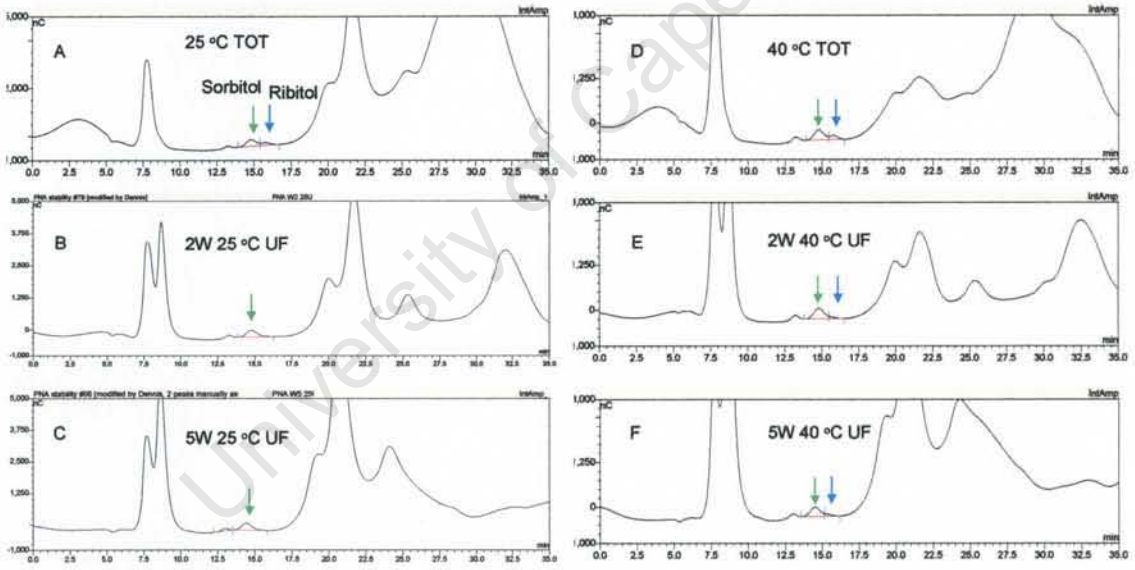

Fig 5.12: *HPAEC-PAD chromatograms for* ***Penta*** *showing total and free saccharide after 2 and 5 weeks at 25 °C (A-C) and 40 °C (D-F). Sorbitol and ribitol peaks are indicated by the green and blue arrows respectively.*

Hib analysis of the combination vaccine was complicated by the presence of a large amount of sucrose (added to the vaccine as a stabiliser) which was detected as glucose and fructose after approximately 17 min. A large peak for the Tris buffer was detected at approximately 8-9 min. Isocratic elution with NaOH yielded partial separation of the

sorbitol and ribitol peaks which eluted between 14-16 min. The chromatograms were resized and the peaks for sorbitol and ribitol estimated. It is evident from Fig 5.12 that the vaccine was stable for 5 weeks at 25 °C because no ribitol was detected (only sorbitol was detected at approximately 15 min). Ribitol was detected in all samples stored at 40 °C for 2-5 weeks. Deterioration of the column during analysis led to poor resolution of the sorbitol and ribitol peaks. Amino acid residues that are not retained on the SPE cartridge used for sample clean up or on the guard column will irreversibly bind to the resins on the column thus reducing the separation efficiency of the column over time. The use of an AminoTrap column in future studies may help to eliminate this problem[36]. The presence of interfering matrix components such as sucrose also complicated the analysis. Partial overlap of peaks for sorbitol and ribitol meant that the peak areas were estimated, thus increasing the margin of error.

The HPAEC-PAD chromatograms for **Penta/ALH** obtained at 25 °C showing total (A) and free at 2 (B) and 5 (C) weeks respectively are presented in the left panel of Fig 5.13. The right panel contains chromatograms obtained at 40 °C for total (D) and free at 2 (E) and 5 (F) weeks respectively.

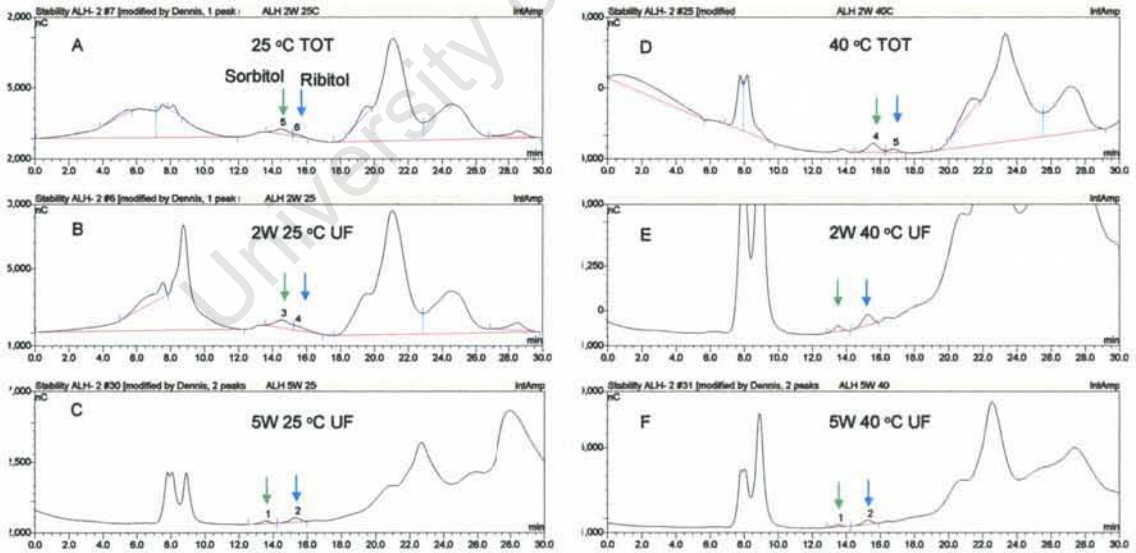

Fig 5.13: *HPAEC-PAD chromatograms for* ***Penta/ALH*** *showing total and free saccharide after 2 and 5 weeks at 25 °C (A-C) and 40 °C (D-F). Sorbitol and ribitol peaks are indicated by the green and blue arrows respectively.*

Peaks for sorbitol and ribitol were detected between 14-16 min. Free saccharide was detected in all **Penta/ALH** samples analysed. At both 25 and 40 °C, the amount of free saccharide generated increased over time. The amount of free saccharide also increased with increasing temperature (25 °C < 40 °C). The peaks for sorbitol and ribitol were very small in comparison to that of the other vaccine components such as Tris (near 9 min), glucose and fructose (after 17 min) and hence analysis of the chromatograms was complex. In addition, peak overlap caused difficulties in accurately integrating the peak areas for sorbitol and ribitol.

The HPAEC-PAD chromatograms for **Penta/ALP** obtained at 25 °C showing total (A) and free at 2 (B) and 5 (C) weeks respectively are illustrated in the left panel of Fig 5.14. The right panel contains chromatograms obtained at 40 °C for total (D) and free at 2 (E) and 5 (F) weeks respectively.

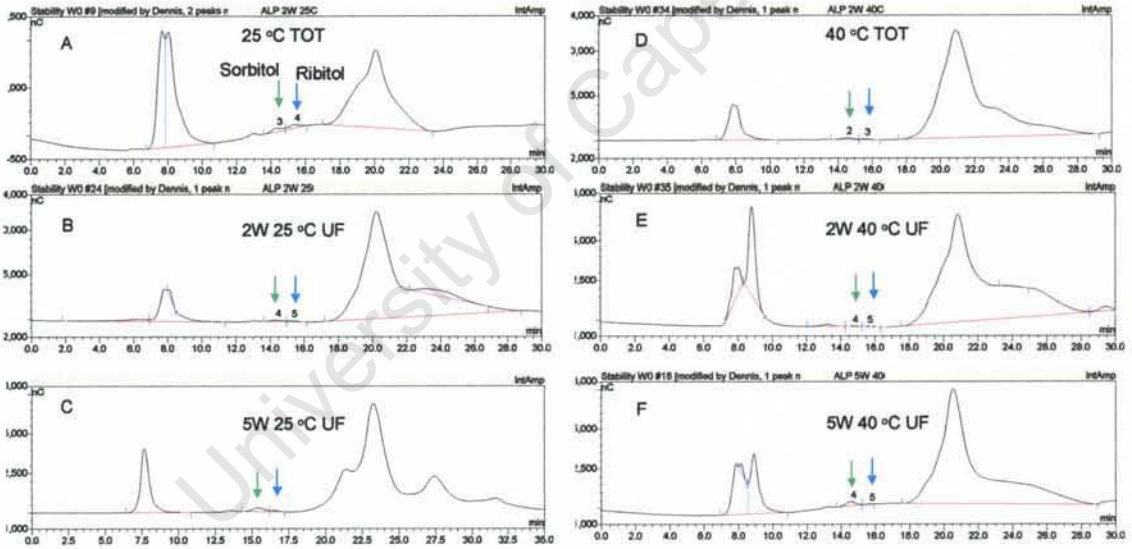

Fig 5.14: *HPAEC-PAD chromatograms for* ***Penta/ALP*** *showing total and free saccharide after 2 and 5 weeks at 25 °C (A-C) and 40 °C (D-F). Sorbitol and ribitol peaks are indicated by the green and blue arrows respectively.*

Peaks for sorbitol and ribitol eluted between 14-16 min. As with **Penta/ALH**, **Penta/ALP** samples contained some ribitol after 2-5 weeks of storage at 25 and 40 °C but the sorbitol and ribitol peak areas could not be accurately integrated due to peak overlap.

The HPAEC-PAD chromatograms for **Penta/Pheroid™** obtained at 25 °C showing total (A) and free at 2 (B) and 5 (C) weeks respectively are illustrated in the left panel of Fig 5.15. The right panel contains chromatograms obtained at 40 °C for total (D) and free at 2 (E) and 5 (F) weeks respectively.

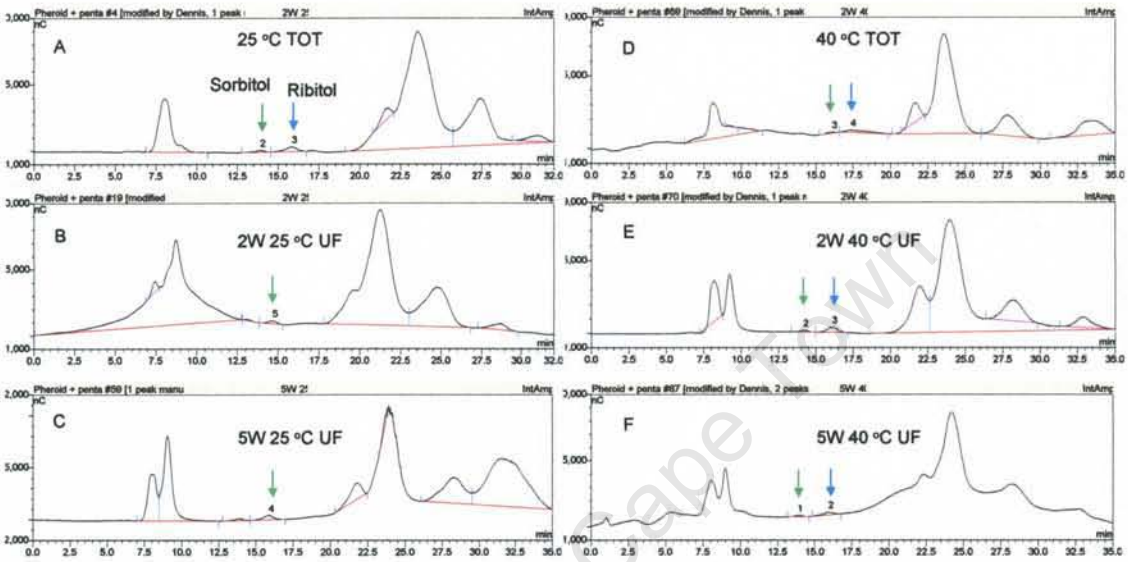

Fig 5.15: *HPAEC-PAD chromatograms for* ***Penta/Pheroid™*** *showing total and free saccharide after 2 and 5 weeks at 25 °C (A-C) and 40 °C (D-F). Sorbitol and ribitol peaks are indicated by the green and blue arrows respectively.*

In **Penta/Pheroid™** formulations, peaks for sorbitol and ribitol were detected between 14-16 min. Again, the chromatograms were dominated by peaks derived from sucrose. The amount of ribitol detected generally increased with increasing temperature. The vaccine appeared to be stable when stored at 25 °C because no ribitol was detected over the 5 week period. However, ribitol was detected in samples stored at 40 °C for 2-5 weeks. Therefore, it is likely that free saccharide was present at 25 °C but poor free saccharide extraction from the adjuvant by PBS, especially at low concentrations resulted in it not being detected. Hence, future studies will investigate alternative methods for release of free saccharide from Pheroid™ in Pheroid™-adjuvanted vaccines.

A summary of the quantitative results obtained are presented in Table 5.5.

Table 5.5: % free saccharide (± standard error) obtained for the pentavalent DTP-HBV-Hib-**A** vaccine formulations stored at 4, 25 and 40 °C for 0-5 weeks.

Penta			
Week	4 °C	25 °C	40 °C
0	ND*	ND	ND
2	ND	ND	77±1.4
5	ND	ND	82±1.1
Pent/ALH			
Week	4 °C	25 °C	40 °C
0	35±1.4	35±1.4	35±1.4
2	42±1.3	49±2.1	75±1.8
5	50±2.0	58±2.2	95±1.8
Penta/ALP			
Week	4 °C	25 °C	40 °C
0	ND	ND	ND
2	ND	35±1.5	98±1.9
5	ND	52±1.0	99±1.5
Penta/Pheroid™			
Week	4 °C	25 °C	40 °C
0	ND	ND	ND
2	ND	ND	90±1.6
5	ND	ND	99±2.0

*ND = not detected

The control non-adjuvanted **Penta** sample contained no detectable free saccharide in the filtrate at the start of the investigation, indicating a stable formulation. Similar results were obtained for **Penta/ALP** and **Penta/Pheroid™**. **Penta/ALH** had the highest initial free saccharide value (35 %). Because 4 °C represented the normal storage temperature of the vaccine, it was expected to remain stable at this temperature with very low levels of free saccharide[14]. This was indeed the case for all samples analysed, with the exception of **Penta/ALH**.

The Hib conjugate has been reported by Cuervo and co-workers to retain its stability at 25 and 37 °C for 5 weeks and therefore a large increase in % free saccharide was not expected[14]. Their study used a monovalent Hib-TT conjugate formulated without sucrose. The present study investigated the stability of Hib-TT in a pentavalent vaccine formulated with sucrose excipient. The results indicated that in the absence of adjuvant, the vaccine was stable at 25 °C because no free saccharide was detected. At 40 °C, the elevated temperature and presence of other antigens were expected to affect the

stability of Hib. However, the Hib conjugate was expected to be more stable than Mn A-TT because PsA is more susceptible to decomposition from exposure to suboptimum temperatures due to the lability of the phosphodiester bond[37]. This was not the case. At 40 °C the % free saccharide in the **Penta** control increased by 77 % and 82 % after 2 and 5 weeks respectively (while the Mn A-TT conjugate had shown an increase from 14 % to 86 % after storage for 5 weeks at 40 °C). Consequently, the large increases in % free saccharide were attributed to interference from the large amount of sucrose present in the formulation, which made accurate integration of the sorbitol and ribitol peaks difficult (standard error values were > 1 and were generally higher than in all previous experiments).

The **Penta/ALH** formulation had the highest initial free saccharide value of 35 %. At all temperatures, the % free saccharide increased over time. Only in **Penta/ALH** samples did the percentage of free saccharide reach 50 % at 4 °C providing evidence that the adjuvant catalyses depolymerisation of PRP. Similar large increases in % free saccharide was observed at 25 (58 %) and 40 °C (95 %). Evidence of catalytic depolymerisation of PRP in the presence of ALH has been reported[21, 26, 38]. The mechanism of this reaction is thought to be that the multivalent aluminium cation acts as a Lewis acid catalyst, coordinating to the phosphorus atom in the PRP chain and making it more electrophilic. The nucleophilic OH group on C2 of ribose donates its lone pair of electrons to the phosphorus, causing cleavage of the phosphorus-oxygen bond in the chain and the production of 2,3-cyclophosphate[21].

No free saccharide was detected in **Penta/ALP** samples stored at 4 °C for 5 weeks. The amount of free saccharide increased to 52 % after storage for 5 weeks at 25 °C. The vaccine was least stable at 40 °C. After only 2 weeks at 40 °C, the amount of free saccharide was 98 % of its original value and after 5 weeks had reached 99 %. Thus, exposure of the vaccine to temperatures above 4 °C facilitated its degradation. The % free saccharide detected after storage at 40 °C for 5 weeks was greater for **Penta/ALP** than for **Penta/ALH** and was attributed not to the fact that the **Penta/ALP** was a less stable formulation but possibly due to better recovery of free saccharide in **Penta/ALP** samples.

The current study also included a pentavalent vaccine formulated with Pheroid™ (**Penta/Pheroid™**). Under the conditions used, at 4 and 25 °C no free saccharide was detected over the 5 week period. This may be either because Pheroid™ had a stabilising effect on the vaccine or because of poor extraction of free saccharide from the adjuvant prior to separation. At 40 °C however, the % free saccharide detected was 90 % and 99 % after 2 and 5 weeks respectively. Therefore, it is unlikely that no degradation occurred at 25 °C. A more probable explanation is that use of PBS resulted in poor free saccharide extraction from the adjuvant. Column degradation over time added to the problem and led to peak integration errors resulting from the partial overlap of peaks for sorbitol and ribitol. A different strategy for free saccharide extraction in Pheroid™-adjuvanted vaccines will be investigated in future studies.

Most combination vaccines are formulated with aluminium-containing adjuvants. It is vital that such vaccines remain stable to maintain their immunogenicity. The WHO recommends that each batch of conjugate should be tested for free, unconjugated saccharide in order to ensure that the amount present is within previously set limits based on lots shown to be clinically safe and efficacious[16]. In the present study, the control vaccine (i.e. **Penta**) which contained no adjuvant was stable at 4 and 25 °C for 5 weeks. The **Penta/ALP** formulation was stable at 4 °C for 5 weeks. The amount of free saccharide reached 35 % after exposure to 25 °C for 2 weeks. In the control pentavalent vaccine and aluminium phosphate-adjuvanted vaccine, the finding that the free saccharide assay could detect increasing amounts of free saccharide generated showed the potential of this method for these formulations. Rapid degradation of **Penta/ALH** was observed after storage for 5 weeks at 4 °C (50 %). This observation agrees with published reports that ALH catalyses the depolymerisation of PRP and is a major hindrance to the Hib conjugate vaccine's stability. Use of **Buffer 2** was not very effective in extracting low concentrations of free saccharide in the Penta/Pheroid™ formulation. Therefore, future studies will investigate alternative methods of free saccharide extraction from Pheroid™-adjuvanted vaccines. Based on this study therefore, ALP would be preferable to ALH for use in the pentavalent liquid vaccine because it can potentiate the immune response without hindering vaccine stability. Hence, the vaccine will have a longer shelf-life.

Accelerated degradation of Hib conjugate vaccines has been used to check whether the applied experimental technique and conditions were suitable to determine any variations

in the short-term stability of the vaccine at elevated temperatures[42, 43]. That was the primary objective of the present study and as demonstrated in Table 5.5 this objective was accomplished because increases in free saccharide which correlated with a decrease in vaccine integrity could be monitored using the free saccharide assay developed in this study.

The effect of degradation on the biological activity of the vaccine can be monitored using animal immunogenicity assays. With Hib vaccines in particular, immunogenicity studies in animals do not correlate well with protective immunity in the target population. However, such studies are necessary because physicochemical methods alone cannot be assumed to predict the biological activity of Hib conjugate vaccines without extensive validation against immunological data. In a study by Bolgiano and co-workers, two Hib-CRM_{197} vaccines (one contained no adjuvant and the other was formulated with aluminium phosphate adjuvant) were subjected to adverse storage conditions and used to establish correlates between physicochemical characteristics and immunogenicity[44]. Vaccines were stored at 4 (control), 37 and 55 °C and oligosaccharide depolymerisation was significantly higher in samples stored at 55 °C compared to the control. Following subcutaneous injection of the samples into CBA mice and New Zealand White rabbits, the amount of IgG raised against CRM_{197} was significantly lower for samples incubated at 37 or 55 °C compared with the control due to conformational changes in the protein induced at elevated temperatures. Moreover, there was a parallel reduction in the amount of IgG raised against PRP by the vaccines stored at 55 °C and this was consistent with the observed depolymerisation of the oligosaccharide chains. Importantly, carrier protein conformational changes resulting from storage under adverse conditions did not affect the immunogenicity to PRP in laboratory animals unless associated with loss of bound saccharide presumably because the carrier protein retains continuous T-helper cell epitopes which are unaffected by conformational changes. The TT conjugates used in this thesis would be expected to have higher thermal stability than the above CRM_{197} conjugate because previously published stability studies have demonstrated that the former retained their immunogenicity following incubation at elevated temperatures[22].

Hib vaccines can have a shelf-life of up to 3 years[44]. The stability of the conjugate vaccine during this period is also dependent on whether the formulation is in the lyophilised or aqueous state. When compared with liquid formulations, lyophilised

formulations of conjugate vaccines have been shown to be resistant to storage at elevated temperatures or to freeze-thawing[22]. The stability of lyophilised final fill vaccines has been reported to extend past their licensed expiry dates by up to 6 years, with no variations in the endotoxin content, total saccharide and percentage free saccharide content[44].

5.7 Investigating methods by which the free saccharide assay may be improved

5.7.1 Vaccine formulation without sucrose

The presence of sucrose in the pentavalent formulations used for the thermal stability study greatly interfered with the accurate determination of ribitol in these samples. To investigate whether this problem was vaccine specific, the free saccharide assay was determined for two aluminium phosphate-adjuvanted pentavalent formulations **PentaL/ALP** and **PentaH/ALP, formulated without sucrose**. **PentaL/ALP** was formulated with Hib-TT-**E** while **PentaH/ALP** contained Hib-TT-**F**. The vaccines were supplied by a local vaccine manufacturer. The % free saccharide for Hib-TT-**E** and Hib-TT-**F** prior to formulation was determined as 0 % (low % free saccharide) and 16.5 % (high % free saccharide) respectively by the manufacturer using the DOC/HCl method. The Hib component was 40 µg/ml (concentration provided by the manufacturer). Samples containing adjuvant were pre-treated with **Buffer 2** at pH 7 prior to separation of free saccharide. Free saccharide separation was performed using the UF method described in section 4.3.2. Following hydrolysis (detailed procedure in section 5.3.3), a fixed amount of the internal standard sorbitol (4.4 µg) was added to each sample prior to filtration. Saccharide quantification was performed using HPAEC-PAD. Ribitol amounts were calculated from peak areas and then corrected using the internal standard sorbitol. The HPAEC-PAD chromatograms for total (A) and free saccharide for **PentaL/ALP** (B) and **PentaH/ALP** (C) are displayed in Fig 5.16.

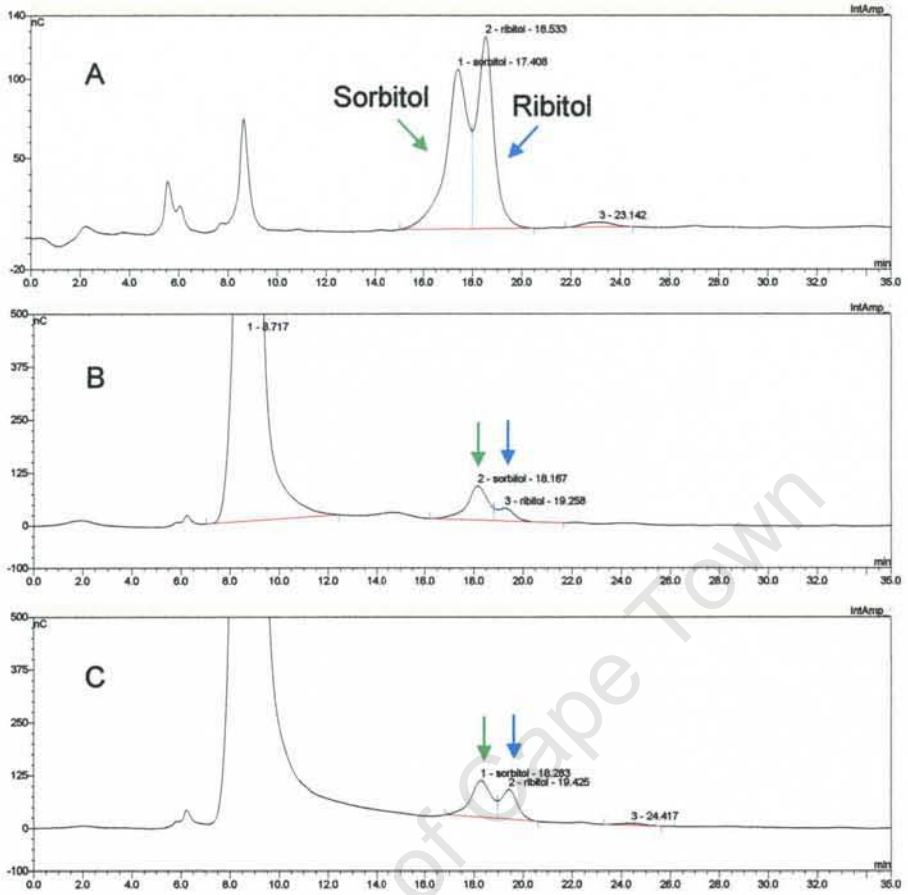

Fig 5.16: *HPAEC-PAD chromatograms for total (A) and free saccharide for PentaL/**ALP** (B) and **PentaH/ALP** (C). Sorbitol and ribitol peaks are indicated by the green and blue arrows respectively.*

The chromatograms are much cleaner than those obtained for the pentavalent vaccine formulated with sucrose excipient. Column performance remained a major challenge with the HPAEC-PAD method. Over time, sites on the column can became blocked by contaminants. This led to reduced retention times and peak overlap. The ionic strength of NaOH was lowered to compensate for this. Sorbitol and ribitol eluted at 17.5 and 18.5 min respectively. The peak for the Tris buffer was detected near 9 min but did not interfere with the analysis of Hib. Use of sorbitol as an internal standard permitted correction of the ribitol concentration. The total saccharide peak (A) corresponds to 39.2±2 µg/ml saccharide. Free saccharide analysis for **PentaL/ALP** (B) and **PentaH/ALP** (C) yielded 2.2 and 22.9 % free saccharide respectively. The % free saccharide values obtained for **PentaL/ALP** and **PentaH/ALP** in the present study was similar to those determined by the manufacturer (0 % and 16.5 % respectively using the

DOC/HCl method and ribose assay) in the monovalent vaccine and indicated good free saccharide recovery in the two pentavalent formulations. However, the fact that the UF method gave slightly higher free saccharide values than the DOC/HCl method may be an indication that free saccharide is underestimated by the DOC/HCl method. These results also confirmed that without interference from sucrose, the free saccharide assay can be used to measure low levels of free saccharide and detect differences in the amount of free saccharide present in combination vaccines containing adjuvant. This investigation also highlighted that some challenges associated with the physicochemical analysis of conjugate vaccines are formulation specific.

5.7.2 Investigation of fucose as an alternative internal standard

Overlapping of the sorbitol and ribitol peaks made it necessary to investigate the use of an alternative internal standard. The hexose deoxy sugar fucose was selected because it has successfully been used as an internal standard for the quantitative determination of saccharides by high performance liquid chromatography[40, 41].

For this study a local vaccine manufacturer supplied a monovalent Hib-TT-**G** (20 µg/ml) and a pentavalent vaccine (**Penta**) formulated with aluminium phosphate adjuvant (initial concentration of 0.95 µg/ml provided by the supplier was diluted to 20 µg/ml). Extraction of free PRP in the adjuvanted sample was performed using **Buffer 2** followed by centrifugation for 10 min at 5 000 rpm and removal of the supernatant layer for analysis. Free saccharide was separated using the UF method described in section 4.3.2. All samples were spiked with 25 µg of the internal standard fucose after the hydrolysis and neutralisation steps and HPAEC-PAD was used for saccharide quantification. Ribitol peak areas were corrected from the averaged peak areas of the internal standard fucose. The HPAEC-PAD chromatograms for total and free saccharide for Hib-TT-**G** (Left panel) and **Penta** (Right panel) are displayed in Fig 5.17.

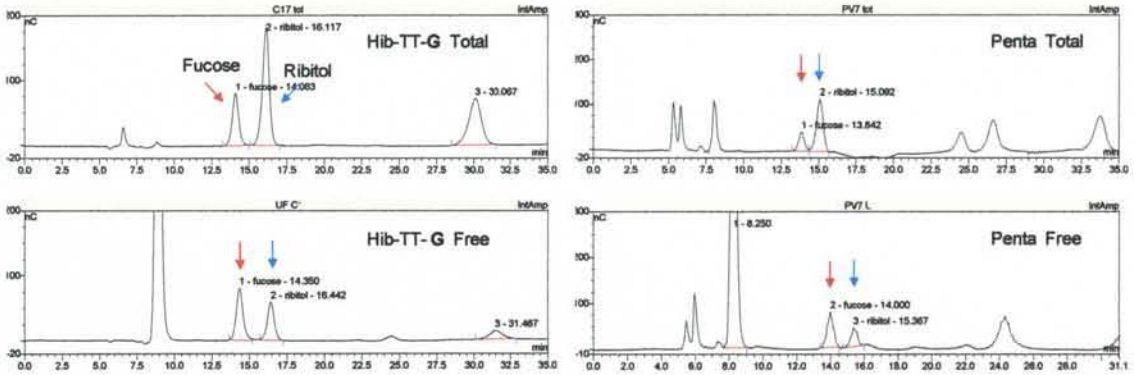

Fig 5.17: *HPAEC-PAD chromatograms for total and free saccharide for Hib-TT-**G** (Left panel) and **Penta** (Right panel). Fucose and ribitol peaks are indicated by the red and blue arrows respectively.*

In the Hib-TT-**G** chromatograms for total and free (left panel), fucose and ribitol eluted separately at approximately 14 and 16 minutes respectively. Therefore, the two peaks could be integrated separately. The amount of total saccharide was 19.5 µg/ml and the percentage of free saccharide was 7.8 %. For the adjuvanted pentavalent sample (right panel), fucose and ribitol eluted at approximately 14 and 15 min respectively and could therefore be integrated separately. Analysis of the pentavalent sample yielded 17.1 µg/ml PRP and 15.2 % free saccharide. In section 5.7, column deterioration was a problem and contributed to the incomplete resolution of the sorbitol and ribitol peaks. The results from this preliminary study were promising because separation of fucose and ribitol was achieved on the same column but spike recovery experiments in both the monovalent and pentavalent formulations would be required to confirm the use of fucose as an internal standard.

5.7.3 Investigating two buffers for DOC/HCl analysis

In adjuvanted vaccines, both the amount of adsorbed antigen and the strength of the adsorption force can be affected by the type of buffer used as diluent[32]. The DOC/HCl method has consistently yielded lower free saccharide values compared to the UF method. This experiment was performed to determine whether the amount of free saccharide recovered would vary as a function of ionic strength.

Hib-TT-**G** provided by the manufacturer was used to prepare separate samples diluted to 100 µg/ml using either MilliQ water, 0.15 M saline or **Buffer 2** (prepared in duplicate).

To determine the separation efficiency, some samples were spiked separately with 28 µg of an activated PRP intermediate (PRP-ADH). The DOC/HCl method described in section 4.3.2 was used for separation of free saccharide in the samples and saccharide quantification was performed using the ribose assay described in section 5.3.2. The amount of free saccharide obtained for the different samples are presented in Table 5.6.

Table 5.6: % free saccharide results using DOC/HCl and ribose assay for Hib-TT-**G** with spike recovery

Conjugate	% free	% recovery
Hib-TT-**G** (dil in MilliQ H_2O)	<1	-
Hib-TT-**G** (dil in 0.15M Saline)	11.7	-
Hib-TT-**G** (dil in PBS)	17	-
Hib-TT-**G** + 28 % spike (dil in MilliQ H_2O)	0	47
Hib-TT-**G** + 28 % spike (dil in 0.15M Saline)	18.3	99.6
Hib-TT-**G** + 28 % spike (dil in PBS)	18.2	96.9

The amount of free saccharide in the vaccine ranged from <1 % to 17 % depending on whether MilliQ water, 0.15 M saline or PBS (**Buffer 2**) was used as diluent. This suggests that the type of buffer used as diluent affects the recovery of free saccharide, an observation that has been noted by other researchers. For example, carrageenans are sulphated polysaccharides and ι-carrageenan can form an electrostatic complex with bovine serum albumin (BSA) in aqueous solution at low ionic strength and pH ≤ 7. This interaction becomes stronger at pH 6 but is dissociated in 100 mM NaCl[45]. Association of free saccharide with the conjugate can be interrupted by increasing the ionic strength of the buffer. This was achieved in the present study with 0.15 M saline or **Buffer 2** (99.6 and 96.9 % recovery respectively). Thus in future studies, either 0.15 M saline or **Buffer 2** should be used as diluents to enhance PRP recovery when the DOC/HCl method is used for free saccharide separation.

5.7.4 Investigating the use of membranes with 30, 50 and 100 kDa molecular weight cut-off for ultrafiltration (UF)

The UF method physically separates free saccharide (which is small enough to pass through pores in the membrane) from the conjugate (which is too large to cross the membrane and is retained on it). If the pores in the UF membrane are too small, they could get blocked by the vaccine components and saccharide recovery would be low.

However, if the pores are large enough to allow conjugated saccharide to pass through, then erroneously elevated free saccharide values would be obtained. In previous experiments, a membrane with a 100 kDa cut-off was chosen based on the size of the conjugate. The molecular weight of TT alone is 150 kDa therefore both TT and the conjugate were expected to be retained on the membrane with a 100 kDa molecular weight cut-off. However, data obtained in sections 5.5.4 and 5.5.5 suggested that the present UF protocol may overestimate the amount of free saccharide. The use of a UF membrane with a 30 kDa molecular weight cut-off has been reported[17]. Thus, the present study was undertaken to investigate PRP and TT recovery after passage through UF membranes with 30, 50 and 100 kDa molecular weight cut-off.

Samples containing 100 µg/ml of Hib-TT-**G** in 0.15 M saline were prepared and spiked separately with either 40 µg activated PRP (PRP-AH) or 50 µg TT. Free saccharide was separated from bound using UF (30, 50 and 100 kDa cut-off). HPAEC-PAD was used for quantification of free saccharide and the protein content determined using the BCA assay (procedure described in section 2.2.5). A summary of the results is presented in Table 5.7.

Table 5.7: Results for ultrafiltration experiments with spike recovery

Sample	PRP (µg/ml)	TT-spike (µg)	% free PRP	% PRP recovery	% TT in filtrate
Hib-TT-**G** (no UF)	100	-	-	-	-
Hib-TT-**G** + TT (30 kDa)	100	50	ND*	ND*	1.64
Hib-TT-**G** (30 kDa)	100	-	0	-	ND*
Hib-TT-**G** + PRP-AH (30 kDa)	140	-	0	0	0.97
Hib-TT-**G** + TT (50 kDa)	100	50	ND*	ND*	4.51
Hib-TT-G (50 kDa)	100	-	11.9	-	ND*
Hib-TT-G + PRP-AH (50 kDa)	140	-	50.6	98	ND*
Hib-TT-**G** + TT (100 kDa)	100	50	ND*	ND*	13.0
Hib-TT-**G** (100 kDa)	107	-	13.4	-	ND*
Hib-TT-**G** + PRP-AH (100 kDa)	140	-	48.7	97	ND*

*ND = Not Determined

No free saccharide was detected in the filtrate when the membrane with a 30 kDa molecular weight cut-off was used, even after spiking the sample with 40 µg PRP. This suggests that free saccharide was retained by the membrane. The fact that <2 % protein was detected in the filtrate (even after spiking with 50 µg TT) suggests that it may

contain amino acid chains and not TT. This could be confirmed using sodium docecyl sulphate (SDS)-polyacrylamide electrophoresis (PAGE) to analyse the filtrate.

PRP recovery was high for spiked samples when the 50 and 100 kDa membranes were used (98 and 97 % respectively). Moreover, the amount of free saccharide detected using the 50 and 100 kDa membranes was comparable (11.9 and 13.4 % respectively) and although the small amount of protein detected in the filtrate when both membranes were used is probably a fragment of TT, the 50 kDa membrane is preferable because it permitted less protein through. The BCA assay indicates the presence of protein in the filtrate. Further investigation would be required to confirm whether this is an artefact due to the presence of a reducing agent in the filtrate or actually due to protein such as a fragment of TT (using SDS-PAGE for example).

The data obtained showed that the 50 kDa membrane can be employed for this Hib-TT vaccine. Ultrafiltration using the 50 kDa membrane gave low protein (<5 %), good spike recovery and comparable free saccharide to the 100 kDa membrane. Ultrafiltration has the added advantage of sample concentration not possible with DOC/HCl. However, the choice of membrane will be vaccine specific.

5.7.5 Method validation and statistical analysis

Analytical method validation is a process of performing several tests designed to verify that an analytical test system is suitable for its intended purpose and is capable of providing useful and reliable analytical data (Fig 5.18)[46]. A validation study involves testing multiple attributes of a method (including accuracy, precision, specificity, limit of detection, limit of quantification, linearity and range, ruggedness and robustness) to determine that it can provide useful and trustworthy data when used routinely[47].

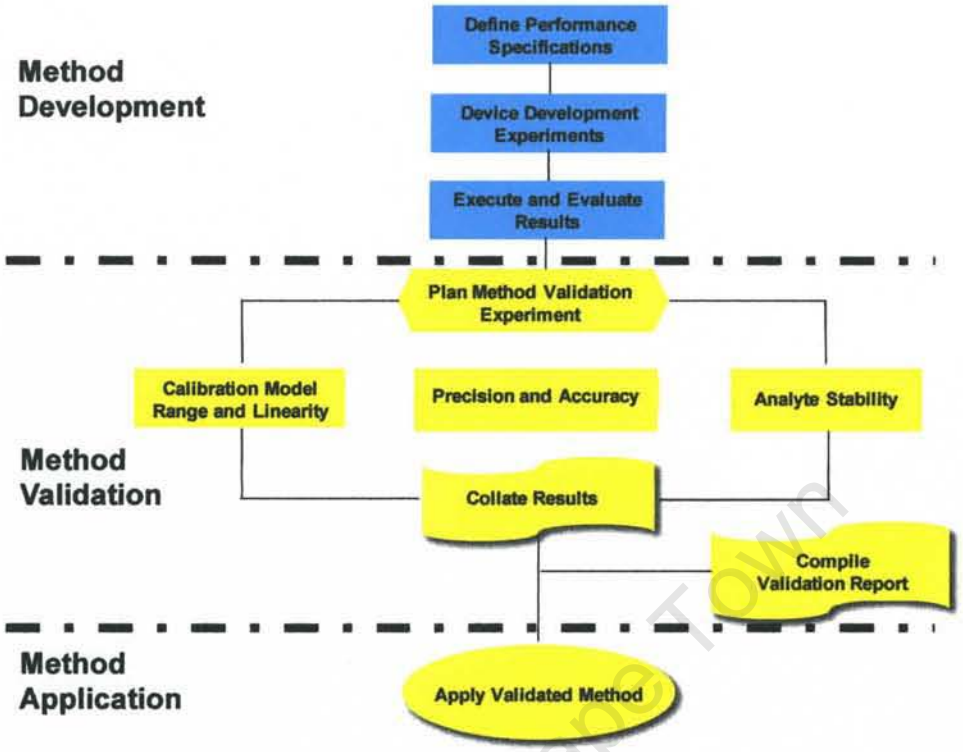

Fig 5.18: *Method validation processes*[49]

Vaccine samples provided by a local vaccine manufacturer for the present study were still in the developmental stage and contained highly variable amounts of free saccharide and in some cases only a limited volume of sample was available for performing the analyses. Thus, the free saccharide assay was not validated completely however a number of key performance parameters have been established which will aid the validation process[47]. For example, the limit of detection was determined to be 1 µg/ml. In addition, the HPAEC-PAD method can be used for PRP quantification even in combination vaccines where other antigens are present. Moreover the internal standards sorbitol (or possibly fucose) can be used to account for changes in ribitol concentration during the analysis. Spike recovery experiments were used to demonstrate the robustness of the free saccharide assay, another key parameter required for validation of the method[47]. With these parameters in place, future studies will focus on completing validation of the free saccharide assay. Furthermore, statistical analysis of method validation data will be performed to demonstrate the validity of the method[48].

5.8 Conclusion

The objective of this study was to develop the total and free saccharide assay for analysing the integrity and stability of conjugate vaccines. The assay was developed (in chapter 4) using Mn A conjugate vaccines as a model compound and then applied to different Hib formulations.

Free saccharide and conjugate were separated by selective precipitation of conjugate using DOC/HCl or UF (100 kDa membrane and later a 30 kDa membrane). When 0.09 % NaCl was used as diluent, the DOC/HCl method underestimated the amount of free saccharide especially in pentavalent vaccines formulated with adjuvant. Further investigation revealed that free saccharide recovery could be improved by using a buffer with a higher ionic strength such as 0.15 M saline or PBS (**Buffer 2**).

The traditional colorimetric assays for phosphorus and ribose were investigated for quantification of saccharide. The presence of sucrose and thiomersal were found to interfere with saccharide quantification when the phosphate assay was used. As a result, application of this assay was limited to vaccines formulated without sucrose and thiomersal and which did not contain phosphate buffer. Hib analysis using the ribose assay worked well for concentrated samples, but dilute samples yielded low OD values which were less reliable because they contained a higher margin of error.

Colorimetric methods cannot be applied to analyse Hib in combination vaccines due to interference from the DTP component. Therefore, a method based on acid hydrolysis of Hib to ribitol, separation on a CarboPac MA 1 column and quantification by HPAEC-PAD was developed and applied to various Hib formulations. Addition of sorbitol as the internal standard to each sample after hydrolysis enabled determination of the corrected ribitol concentration. Since sorbitol was present at a constant amount, it was used to account for changes in sample concentration during preparation for chromatography and to compensate for changes in the chromatographic system such as detector sensitivity. Good recovery from spiked samples proved that this method could detect varying concentrations of Hib saccharide in non-adjuvanted mono- and pentavalent vaccines. Fucose was later investigated as an alternative internal standard to sorbitol. The free saccharide assay could possibly be further improved by using a second internal standard to compensate for the separation and filtration steps prior to hydrolysis.

Monovalent vaccine samples formulated with ALH, ALP and Pheroid™ adjuvants were analysed using the free saccharide assay to evaluate their stability and integrity. Elution of antigens from all three adjuvants was possible using PBS (**Buffer 2**) at pH 7.5. Free saccharide desorption with **Buffer 2** was much easier in formulations containing ALP but was not as efficient in ALH-containing formulations. In adjuvanted vaccines, use of the DOC/HCl method underestimated the amount of free saccharide present and UF (100 kDa molecular weight cut-off) may overestimate it. Further investigation revealed the presence of a small amount of protein in the filtrate (of the unadjuvanted samples tested). Future studies using SDS-PAGE would be required to determine whether the protein is indeed TT or a fragment thereof. In addition, interference studies should also be conducted to ensure that vaccine excipients (such as sucrose) do not interfere with the BCA assay (and yield a false positive result). Thus, a comparison of the BCA and Bradford assay results on the filtrate are recommended for future studies.

An accelerated thermal stability study was conducted on pentavalent vaccines formulated with ALH, ALP or Pheroid™ (i.e **Penta/ALH**, **Penta/ALP** and **Penta/Pheroid™** respectively) and containing sucrose excipient in order to determine the quality of the vaccines during storage at 4, 25 and 40 °C. Due to severe interference from the large amount of sucrose in these formulations, conclusions from this study were based on the general trends observed. The control vaccine (**Penta**) and **Penta/ALP** were generally stable at low temperatures (4 and 25 °C). **Penta/ALH** was least stable at all temperatures and the results suggested that ALH catalyses hydrolysis of the phosphodiester bond in the PRP chain. Unlike the monovalent vaccine, use of PBS (**Buffer 2**) was unsuitable for free saccharide extraction in the **Penta/Pheroid™** formulation. In all samples, storage of vaccines at 40 °C resulted in the generation of large amounts of free saccharide after 5 weeks. In the control pentavalent vaccine and aluminium phosphate-adjuvanted vaccine, the finding that the free saccharide assay could detect increasing amounts of free saccharide generated showed the potential of this method for these formulations.

Interference from sucrose was found to be formulation specific because when the free saccharide assay was conducted on a pentavalent vaccine formulated with aluminium phosphate but without sucrose excipient, good results could be achieved by HPAEC-PAD. The free saccharide assay was subsequently applied to two aluminium phosphate-adjuvanted pentavalent vaccines **PentaL/ALP** and **PentaH/ALP**, formulated

without sucrose. The monovalent Hib-TT vaccines used to prepare **PentaL/ALP** and **PentaH/ALP** contained 0 % and 16.5 % free saccharide respectively (as determined by the manufacturer using the DOC/HCl method). Free saccharide was extracted from the adjuvant using **Buffer 2**, separated by UF and quantified by use of the HPAEC-PAD method. Good free saccharide recovery was obtained from the pentavalent formulations because the % free saccharide values obtained (2.2 % and 22.9 % for **PentaL/ALP** and **PentaH/ALP** respectively) were similar to those in the monovalent vaccines. This confirmed that in the absence of interference from sucrose, the free saccharide assay can successfully be used to measure low levels of free saccharide. Hence, success of the free saccharide assay was found to be formulation specific. Since these were the last batches of samples to be analysed, severe column degradation had occurred with loss of separation efficiency. The free saccharide assay could be improved by using fucose as an internal standard instead of ribitol since the fucose peak did not overlap with that of ribitol. In addition, the use of a high ionic strength buffer such as 0.15 M saline or PBS (**Buffer 2**) enabled improved free saccharide recovery during the DOC/HCl assay by reducing electrostatic interactions. For this vaccine ultrafiltration with a 50 kDa membrane gave low protein concentration in the filtrate (<5 %), good free saccharide recovery and comparable free saccharide to the 100 kDa membrane.

A complete validation of the free saccharide assay is planned for future studies using ICH (International Conference on Harmonisation) guidelines. Key parameters which will be investigated include accuracy, precision, limit of quantification, linearity and range, ruggedness and robustness.

5.9 References

1. Capiau C. P. J., Hoet B, Bogaerts H, Andre FE, Development and clinical testing of multivalent vaccines based on a diphtheria-tetanus-acellular pertussis vaccine: difficulties encountered and lessons learned. *Vaccine* 2003;**21**:2273-87.

2. Andre, F. E., Development and clinical application of new polyvalent combined paediatric vaccines. *Vaccine* 1999;**17**:1620-7.

3. Ellis, R. W., Development of combination vaccines. *Vaccine* 1999;**17**:1635-42.

4. Plotkin, S. A., Cadoz, M., The acellular pertussis vaccine trials: an interpretation. *Pediatr Inf Dis J* 1997;**16**:508-17.

5. Prevention of poliomyelitis: recommendations for use of only inactivated poliovirus vaccine for routine immunization. Committee on Infectious Diseases. American Academy of Pediatrics. *Pediatrics* 1999;**104**:1404–6.

6. Ganoff D. M., Anderson E. L., et. al. Differences in the immunogenicity of three *Haemophilus influenzae* type b conjugate vaccines in infants. *J Pediatr* 1992;**121**:187-94.

7. Global Programme for Vaccines and Immunization (GPV). The WHO position paper on *Haemophilus influenzae* type b conjugate vaccines. *Wkly Epidemiol Rec* 1998;**73**:64-8.

8. Peltola H, et al. *Haemophilus influenzae* type b capsular polysaccharide vaccine in children: a double-blind field study of 100 000 vaccines 3 month to 5 years of age in Finland. *Pediatrics* 1977;**60**:730–7.

9. http://www.doh.gov.za/programmes/index.html. Accessed 26 March 2008.

10. Bell, F., Heath, P., et al. Effect of combination with acellular pertussis, diphtheria, tetanus vaccine on antibody response to Hib vaccine (PRP-T). *Vaccine* 1998;**16**:637-42.

11. Jones, I. G., Tyrrell, H., et. al. Randomised controlled trial of combined diphtheria, tetanus, whole-cell pertussis vaccine administered in the same syringe and separately with *Haemophilus influenzae* type b vaccine at two, three and four months of age. *Vaccine* 1998;**16**:109-13.

12. Win, K. M., Aye, M., et al. Comparison of separate and mixed administrations of DTPw-HBV and Hib vaccines: immunogenicity and reactogenicity profiles. *Int J Infect Dis* 1997;**2**:79-84.

13. Sesardic, D. and Dobbelaer, R., European Union regulatory developments for new vaccine adjuvants and delivery systems. *Vaccine* 2004;**22**:2452-6.

14. Cuervo, M. L., Perez, L. R., et al., Relationships among physico-chemical and biological tests for a synthetic Hib-TT conjugate vaccine. *Vaccine* 2007;**25**:194-200.

15. Sesardic, D., Requirements for valid alternative assays for testing of biological therapeutic agents. *Dev Biol Stand* 1996;**86**:311-8.

16. WHO Expert Committee on Biological Standardization. Forty-ninth report. *World Health Organ Tech Rep Ser* 2000;**897**:i-vi, 1-106.

17. Bardotti, A., Ravenscroft, N., et al., Quantitative determination of saccharide in Haemophilus influenzae type b glycoconjugate vaccines, alone and in combination with DPT, by use of high-performance anion-exchange chromatography with pulsed amperometric detection. *Vaccine* 2000;**18**:1982-93.

18. Sturgess, A. W., Rush, K., et al., Haemophilus influenzae type b conjugate vaccine stability: catalytic depolymerization of PRP in the presence of aluminum hydroxide. *Vaccine* 1999;**17**:1169-78.

19. Ip, C. C., Manam, V., et al., Carbohydrate composition analysis of bacterial polysaccharides: optimised acid hydrolysis conditions for HPAEC-PAD. *Anal Biochem* 1992;**142**;58-67.

20. Lei, Q. P., Lamb, D. H., et al., Quantitation of low level unconjugated polysaccharide in tetanus toxoid-conjugate vaccine by HPAEC/PAD following rapid separation by deoxycholate/HCl. *J Pharm Biomed Anal* 2000;**21**:1087-91.

21. Tsai, C. M., Gu, X. X., et al., Quantification of polysaccharide in Haemophilus influenzae type b conjugate and polysaccharide vaccines by high-performance anion-exchange chromatography with pulsed amperometric detection. *Vaccine* 1994;**12**:700-6.

22. Ho, M. M., Mawas, F., et al., Physico-chemical and immunological examination of the thermal stability of tetanus toxoid conjugate vaccines. *Vaccine* 2002;**20**:3509-22.

23. Mawas, F., Bolgiano, B., et al., Evaluation of the saccharide content and stability of the first WHO international standard for *Haemophilus influenzae* b capsular polysaccharide. *Biologicals* 2007;**35**:235-45.

24. Ashwell, G., Colorimetric analysis of sugars. *Methods Enzymol* 1957;**3**:73-105.

25. Monsigny, M., Petit, C., et al., Colorimetric determination of neutral sugars by a resorcinol sulfuric acid micromethod. *Anal Biochem* 1988;**175**:525-30.

26. Skoog, D. A., West, D. M., et al., *Analytical Chemistry: An Introduction*, 7th edition, Sauder College, 1996.

27. Belfast, M., Lu, R., et al., A practical approach to optimization and validation of a HPLC assay for analysis of polyribosyl-ribitol phosphate in complex combination vaccines. *J Chromatogr B Analyt Technol Biomed Life Sci* 2006;**832**:208-15.

28. Turula, V. E., Kim, J., et al., An integrity assay for a meningococcal type B conjugate vaccine. *Anal Biochem* 2004;**327**:261-70.

29. Rinella, J. V. Jnr., White J. L., et. al., Effect of pH on the elution of model antigens from aluminium-containing adjuvants. *J Colloid Interf Sci* 1998;**205**:161-5.

30. Rinella, J. V. Jnr., White J. L., et. al., Effect of anions on model aluminium-containing adjuvant vaccines. *J Colloids Interf Sci* 1995;**172**:121.

31. Matheis, W., Zott, A., et. al. The role of the adsorption process for production and control combined adsorbed vaccines. *Vaccine* 2002;**20**:67-73.

32. Jendrek, S., Little, S. F., Hem, S., et al., Evaluation of the compatibility of a second generation recombinant anthrax vaccine with aluminium-containing adjuvants. *Vaccine* 2003;**21**:3011-18.

33. Heimlich, J., M., Regnier, F., E., The in vitro displacement of adsorbed model antigens from aluminium containing adjuvants by interstitial proteins. *Vaccine* 1999;**17**:2873-81.

34. Grobler, A., Composition in the form of a microemulsion containing free fatty acids and/or free fatty acid derivatives. 2007, North West University: South Africa.

35. Opawale, F. O. and Burgess, D. J., Influence of Interfacial Properties of Lipophilic Surfactants on Water-in-Oil Emulsion Stability. *J Colloid Interface Sci* 1998;**197**:142-50.

36. Product manual for CarboPac® MA1, PA1, PA10, PA100. Available at http://www.dionex.com/en-us/webdocs/4375_31824-07-Manual-Column-CP-Combined-V27.pdf. Accessed on 28 September 2009.

37. Wong, K. H., Barrera, O., et al., Standardisation and control of meningococcal vaccines, group A and group C polysaccharides, *J Biol Stand* 1977;**5**:197-215.

38. Claesson, B. A., Trollfors, B., et al. Clinical and immunologic responses to the capsular polysaccharide of *Haemophilus influenzae* type B alone or conjugated to tetanus toxoid in 18- to 23-month-old children. *J Pediatr* 1988;**112**:695-702.

39. Kim, J., S., Laskowich, E., R., et. al. Determination of saccharide content in pneumococcal polysaccharides and conjugate vaccines by GC-MSD. *Anal Biochem* 2005;**347**:262-74.

40. Eberendu, A. R., Booth, C., Luta, G., et al., Quantitative determination of saccharides in dietary glyconutritional products by anion-exchange liquid chromatography with integrated pulsed amperometric detection. *J AOAC* Int 2005;**88**:998-1007.

41. Aghazadeh-Habashi, A., Carran, J., Anastassiades, T., et al., High performance liquid chromatographic determination of N-butyryl glucosamine in rat plasma. *J Chromatogr B Analyt Technol Biomed Life Sci* 2005;**819**:91-6.

42. Plumb, J. E., Yost, S. E., Molecular size characterization of *Haemophilus influenza* type b polysaccharide-protein conjugate vaccines. *Vaccine* 1996;**14**:300-404.

43. von Hunolstein, C., Parisi, L., Recchia, S., A routne high-performance size-exclusion chromatography to determine molecular size distribution of *Haemophilus influenza* type b conjugate vaccines. *Vaccine* 1999;**17**:118-25.

44. Bolgiano, B., Mawas, F., Burkin, K., et al., A retrospective study on the quality of *Haemophilus influenzae* type b vaccines used in the UK between 1996 and 2004. *Hum Vaccine* 2007;**3**:176-82.

45. Dickinson, E., Pawlowsky, K., Effect of ι-carrageenan on flocculation, creaming and rheology of a protein-stabilised emulsion. *J Agric Food Chem* 1997;**45**:3799-3806.

46. http://www.asi-rtp.com/method_validation.html

47. http://www.boreal-laser.com/docs/HFISOk.pdf

48. http://www.labcompliance.de/documents/FDA/FDA-Others/Laboratory/f-505-method-validation-draft.pdf

CHAPTER 6

SUMMARY, DISCUSION, CONCLUSION AND FUTURE OUTLOOK

Routine administration of Hib conjugate vaccine to infants provides protection against invasive disease caused by *Haemophilus influenzae* type b[1]. A local vaccine manufacturer is in the process of developing a combined tetravalent DTP-HBV as well as a liquid pentavalent DTP-HBV-Hib vaccine. The development and application of appropriate physicochemical methods for conducting quality control of these complex products were required and provided motivation for this study.

Most combination vaccines are formulated with aluminium-containing adjuvants which serve to enhance the immune response to the antigen[2, 3]. However, aluminium hydroxide has been found to catalyse the hydrolysis of PRP when added to Hib conjugate vaccines[4]. Although this can be circumvented by the use of aluminium phosphate, there is a need for new adjuvants that elicit broader immune responses. A patented fatty acid-based formulation containing nitrous oxide results in a micro-emulsion (Pheroid™) which has shown potential for use as an adjuvant for viral vaccines and may also be used for bacterial vaccines. Physicochemical analysis of this promising adjuvant by NMR spectroscopy and Coulter Counter was undertaken (Chapter 3). NMR spectroscopy provided a structural fingerprint for Pheroid™ formulations and indicated the relative proportions of the major components but the method was invasive because it required removal of the aqueous phase. Nevertheless, the NMR spectroscopy presented in this thesis can be used routinely to monitor the quality of Pheroid™ raw materials and to evaluate the final formulation to ensure batch-to-batch consistency. Evaluation of the particle size distribution in Pheroid™ was performed using a Coulter Counter. The average size distribution in the two formulations studied was similar and ranged between 5-12 µm. Antigen encapsulation in Pheroid™ would enable protection from degradation, targeted delivery and controlled release, thus enhancing its immune response. Indeed, the engineering of nanoparticles for use in nasal (to induce mucosal immunity) and transcutaneous vaccines (to target immature dendritic cells found in high density in the epidermis and dermis of the skin) is a cutting-edge area of research in which immunogenicity is enhanced by targeted delivery of antigens which facilitates lymphatic uptake[5].

A non-invasive NMR method which enables analysis of the intact emulsion by using pulsed field gradient (PFG) techniques to measure the particle size distribution of the

emulsion should be investigated because it has the potential of replacing the Coulter Counter method[6]. Acoustic and electroacoustic spectroscopies are two new techniques that can be used to investigate the particle size distribution and calculate the zeta potential of emulsion particles[7, 8]. These new non-invasive techniques will also be applied to the study of Pheroid™ in future studies. It has been suggested that adjuvant action results from a depot effect by prolonging the duration of the interaction between antigen and cells, and thus is related to the antigen-releasing properties of emulsion adjuvants[9]. Future physicochemical studies on Pheroid™ (e.g. conductivity, viscosity, surface charge) should aim to clarify the physicochemical basis or molecular reasons for its adjuvant activity. Such studies usually include analysis of cell death by the emulsion adjuvant *in vitro* because cell apoptosis is an important factor for induction of immunogenicity by emulsion aduvants[10]. This is followed by an assessment of antibody response in animal models after subcutaneous (and possibly intranal) immunisation with the antigen plus adjuvant using enzyme linked immunosorbent assay (ELISA).

The use of modern physicochemical methods for the assessment of glycoconjugate vaccines is necessary because traditional assays using live animals do not correlate well with immunogenicity in humans. The primary focus of this thesis was the application of appropriate physicochemical procedures for evaluation of the locally manufactured Hib vaccine alone and when in combination with DTP-HBV-Hib. In the absence of a suitable Hib conjugate, model compounds such as HSA, PsA and Mn A-TT were used to investigate methods of free saccharide separation namely SPE, DOC/HCl and UF (Chapter 4). The SPE cartridge was selected to retain the conjugated saccharide while the free saccharide passed through as eluent. At physiological pH, the binding capacity was low and so this method was not investigated further. The DOC/HCl method underestimated the amount of free saccharide. This problem was initially thought to be circumvented by use of the UF method because the ultrafiltration membrane could be washed to ensure maximum recovery of free saccharide. Although the free saccharide-containing filtrate was diluted due to washing of the filter, it could be concentrated using a speed-vac system consisting of a centrifuge, refrigerated vapour trap and vacuum pump prior to hydrolysis and chromatography. Saccharide quantification was performed using a colorimetric assay for phosphorus as well as the more sophisticated HPAEC-PAD method for the monomer (mannosamine-6-phosphate from acid hydrolysis). The HPAEC-PAD method permitted quantification of free saccharide at low levels and afforded higher specificity and sensitivity for free saccharide analysis.

In the absence of appropriate vaccine intermediates, validation of the free saccharide assay was not possible. However, an accelerated stability study was conducted to evaluate both the stability of the vaccine and the performance of the free saccharide assay. Mn A-TT conjugate samples were stored at 25 and 40 °C for 5 weeks. Quantification of the amount of free saccharide in these samples by the phosphate and HPAEC-PAD methods after separation using the DOC/HCl and UF methods showed little increase in the % free saccharide for the conjugate stored at 25 °C and a substantial increase in free saccharide following storage at 40 °C for 5 weeks. As part of the accelerated stability study, changes in the molecular size distribution of the conjugate induced by exposure to elevated temperatures was monitored by HPSEC-UV on a Waters Ultrahydrogel 2000A column. The results showed that Mn A-TT remained stable at 25 °C, however when kept at 40 °C, the chromatographic profile changed dramatically after 3 weeks and supported the free saccharide assay results determined by HPAEC-PAD and use of DOC/HCl and UF. The HPSEC-UV method was limited in that it provided no quantitative indication of the effect of elevated temperatures on the amount of free saccharide generated. Inclusion of a refractive index detector in future studies would enable detection of the free saccharide generated. The results of the study agreed with previously published reports which demonstrated the thermal stability of Mn A conjugates at 4 °C but degradation ensued following incubation at 37 °C or higher[11, 12].

Induction of an immune response by conjugate vaccines occurs when pathogen-associated molecular patterns (PAMPs) contained in the vaccine antigens are recognised by pattern recognition receptors (PRRs) such as toll-like receptors on dendritic cells and monocytes. Binding of an antigen to its receptor triggers activation of dendritic cells and monocytes, which modifies the expression of receptors on their surfaces and induces their migration along lymphatic vessels to the draining lymph nodes or spleen where activation of T and B lymphocytes takes place. Thermal degradation of vaccines results in the destruction or alteration of the PAMP regions and therefore little or no binding to PRRs. Thus, dendritic cells remain immature and upon contact with naive T cells, the T cells do not differentiate into effectors but into regulatory CD4+ T cells which maintain immune tolerance[13, 14].

It was concluded from this investigation that free saccharide separation by UF and detection by HPAEC-PAD gave more reliable results because the HPAEC-PAD method

is specific for M6P quantification and has a higher sensitivity than the phosphate assay. However, further investigation of the UF method was necessary to ensure that the conjugate was not passing through the membrane and yielding erroneously high free saccharide values.

The free saccharide assay was subsequently applied to investigate the potency of the Hib component in monovalent and pentavalent vaccines. Separation of free saccharide from bound was achieved by the DOC/HCl and UF methods followed by quantification using the phosphate and ribose colorimetric assays and HPAEC-PAD analysis of the ribitol component (released by acid hydrolysis) (Chapter 5). Use of the phosphate assay was limited because the presence of sucrose (added as a stabiliser) and thiomersal (added as a preservative) interfered with saccharide quantification. As a result, application of this assay was to vaccines formulated without sucrose and thiomersal and which did not contain phosphate buffer. Application of the ribose assay to Hib analysis in concentrated samples was possible, but dilute samples yielded low OD values which were less reliable because they contained a higher margin of error. The HPAEC-PAD method proved to be sensitive and specific and with the use of an internal standard, potentially applicable to the analysis of Hib in both monovalent and combination vaccines. Glucose-6-phosphate and glucose-1-phosphate have been used by other researchers as internal standards but for the quantification of Hib saccharide after base hydrolysis. Sorbitol (and later fucose) was found to be a suitable internal standard because it was stable and measurable under the conditions used but eluted at a different retention time from ribitol. It could therefore be used to account for changes in sample concentration during preparation for chromatography and to compensate for changes in the chromatographic system such as detector sensitivity. The Hib vaccine available for most of this study was formulated with sucrose (85 000 µg sucrose: 20 µg). The presence of such a large amount of sucrose severely interfered with ribitol detection and column degradation may have been facilitated by residual amino acids in the samples after hydrolysis. Column deterioration in turn caused the peaks for ribitol and sorbitol to overlap slightly which made accurate integration of small peaks difficult. This problem could be circumvented by using sucrose-free samples and fucose as an internal standard.

A review of the literature revealed two common methods by which adsorbed antigens could be released from the adjuvant. The first of these was the dissolution of ALH and

ALP in either 10 % sodium citrate or NaOH respectively[4]. The former was found to be ineffective in dissolving ALH. The latter was effective at NaOH concentrations ≥ 500 mM but would not be suitable for routine analysis of Hib because the harsh alkaline conditions would induce hydrolysis of the PRP, resulting in an erroneously high free saccharide concentration. A second method for elution of antigen was the use of the phosphate anion[15]. In theory, the phosphate anion specifically adsorbs to ALH and lowers its isoelectric point (IP) causing the surface charge of ALH to change from positive to negative. Consequently, electrostatic repulsive forces between the negatively charged adjuvant and the negatively charged antigen results in elution. Adsorption of additional phosphate anions by ALP adjuvant also reduces its IP and increases its negative surface charge thus resulting in increased electrostatic repulsion with a negatively charged antigen. Free saccharide desorption with PBS (**Buffer 2**) was much easier in formulations containing ALP but was not as efficient in ALH containing formulations. Preliminary results also suggested that PBS could potentially be used for saccharide recovery in Pheroid™-adjuvanted samples and the mechanism by which this takes place merits further investigation in future studies.

The present study investigated the applicability of the free saccharide assay to the analysis of Hib in four pentavalent formulations containing sucrose excipient: the pentavalent formulated without adjuvant (Penta) and with ALH, ALP and Pheroid™. The samples were stored at 4, 25 and 40 °C for 5 weeks. Accurate quantification of ribitol in these formulations was complicated by interference from sucrose. Free saccharide extraction by PBS (**Buffer 2**) was effective in formulations containing ALP and difficult when ALH or Pheroid™ was used. Therefore, general conclusions were derived, based on the results obtained in the control (**Penta**) and **Penta/ALP** formulations. Both **Penta** and **Penta/ALP** appeared to be stable at 4 °C for 5 weeks. The **Penta** control appeared more stable (no free saccharide detected over 5 weeks) than **Penta/ALP** (35 % and 52 % free saccharide detected at 2 and 5 weeks respectively) when the vaccines were stored at 25 °C. After storage for 2 and 5 weeks at 40 °C, both **Penta** and **Penta/ALP** formulations showed a large increase in % free saccharide. The immunogenicity of Hib conjugate vaccines which have been subjected to adverse conditions depends upon the depolymerisation of the attached saccharide and the nature of the carrier protein. TT conjugates have been reported to have a higher thermal stability than conjugates prepared using CRM_{197}[16]. Published studies have demonstrated that carrier protein conformational changes resulting from storage under adverse conditions did not affect

the immunogenicity to PRP in laboratory animals unless associated with loss of bound saccharide presumably because the carrier protein retains continuous T-helper cell epitopes which are unaffected by conformational changes. Real time stability studies have demonstrated the stability of lyophilised vaccines to extend past their licensed expiry dates by up to 6 years while liquid formulations are less stable[16]. However, the advantage of a liquid formulation is that the logistical requirements and the number of clinical manipulations required prior to obtaining a preparation suitable for administration are significantly reduced. Real time stability studies on the bulk and final fill formulations of the locally manufactured DTP-HBV-Hib is likely to confirm that the formulation is stable (and immunogenic) at 4 °C for at least two years.

A number of experiments were conducted to investigate different ways in which the free saccharide assay could be improved. In the first experiment the free saccharide assay was applied to two aluminium phosphate-adjuvanted pentavalent vaccines **PentaL/ALP** and **PentaH/ALP**, formulated *without sucrose*. The monovalent Hib-TT vaccines used to prepare **PentaL/ALP** and **PentaH/ALP** contained 0 % and 16.5 % free saccharide respectively (as determined by the manufacturer using the DOC/HCl method). Free saccharide was extracted from the adjuvant using phosphate buffer, separated by UF and quantified by use of the HPAEC-PAD method. Good free saccharide recovery was obtained from the pentavalent formulations because the % free saccharide values obtained (2.2 and 22.9 % for **PentaL/ALP** and **PentaH/ALP** respectively) were similar to those in the monovalent vaccines. This confirmed that in the absence of interference from sucrose, the free saccharide assay can successfully be used to measure low levels of free saccharide. Hence, success of the free saccharide assay was found to be formulation specific.

The search for a better internal standard to sorbitol was necessitated by the overlapping of the sorbitol and ribitol peaks. Fucose had successfully been used as an internal standard for the quantitative determination of saccharides by high performance liquid chromatography and was therefore investigated as an alternative internal standard to sorbitol[17, 18]. The HPAEC-PAD chromatograms showed complete separation of the fucose and ribitol peaks. Therefore, they could be integrated separately. Spike recovery experiments will be conducted in future studies to optimise the use of fucose as an internal standard.

An important observation was that free saccharide recovery using the DOC/HCl method is affected by the type of buffer used as diluent. Electrostatic interaction of free saccharide with the conjugate could be interrupted by increasing the ionic strength of the diluent. The use of either PBS (**Buffer 2**) or 0.15M saline yielded good free saccharide recovery when the DOC/HCl method was used.

Ultrafiltration using a membrane with a 30 kDa molecular weight cut-off has been used for the separation of free saccharide in conjugate vaccines. Selection of a membrane with a 100 kDa molecular weight cut-off for the present study was based on the size of the conjugate (thought to be >100 kDa because TT alone is 150 kDa). In addition, the choice of this molecular weight cut-off was supported by the fact that the vaccine manufacturing process includes diafiltration using a 100 kDa membrane for conjugate purification. Analysis of the filtrate from three different membranes (30, 50 and 10 kDa), using the BCA assay, showed the presence of a small amount of protein – probably a fragment of TT. However, further investigation by SDS-PAGE for example would be required to confirm this. Filtrate from the membrane with a molecular weight cut-off of 30 kDa contained no free saccharide even when the samples were spiked with free saccharide. This suggests that the membrane pore size was too small and so free saccharide was retained on the membrane. The 50 kDa membrane is recommended for future studies because not only did it give a low concentration of protein in the filtrate (<5 %) but also good free saccharide spike recovery as well as comparable free saccharide to the 100 kDa membrane.

The HPAEC-PAD method could replace colorimetric assays for the analysis of Hib vaccines but a complete validation of the free saccharide assay using ICH ((International Conference on Harmonisation)) guidelines would be required in future studies. This includes accuracy, precision, specificity, limit of detection, limit of quantification, linearity and range, ruggedness and robustness.

Consideration of all of the afore-mentioned results shows that this thesis has provided background for the development of some very important methods for determining the free saccharide content of unadjuvanted and adjuvanted conjugate vaccines. Further studies could investigate the use of two internal standards to compensate for ribitol lost during separation, filtration and hydrolysis. Both the UF and DOC/HCl methods are recommended for routine application of the free saccharide assay to monovalent and

combination Hib vaccines. ALP is recommended over ALH for use in Hib vaccines for two reasons. Firstly, it does not catalyse depolymerisation of the Hib polysaccharide; and secondly, electrostatic repulsion with the negatively charged PRP moiety facilitates free saccharide recovery in the presence of the phosphate anion. Future studies could also investigate suitable buffers and conditions for the recovery of PRP from Pheroid™. In addition, data obtained from physicochemical analyses will be validated against immunogenicity studies in animal models.

6.1 References

1. Eskola, J., Kayhty, H., Early immunization with conjugate vaccines. *Vaccine* 1998;**16**:1433-8.

2. Gupta, R. K., Siber, G. R., Adjuvants for human vaccines--current status, problems and future prospects. Vaccine 1995;13:1263-76. *Vaccine* 1995;**13**:1263-76.

3. Marciani DJ., Vaccine adjuvants: role and mechanisms of action in vaccine immunogenicity. *Drug Discov Today* 2003;**8**:934-43.

4. Belfast, M., Lu, R., et al., A practical approach to optimization and validation of a HPLC assay for analysis of polyribosyl-ribitol phosphate in complex combination vaccines. *J Chromatogr B Analyt Technol Biomed Life Sci* 2006;**832**:208-15.

5. Csaba, N., Garcia-Fuentes, M., et al., Nanoparticles for nasal vaccination. Adv Drug Deliv Rev 2009;61:140-57.

6. Johns, M. L., NMR studies of emulsions. *Curr Opin Colloid Interfaces Sci* 2009;**14**:178-83.

7. Dukhin, A. S., Goetz, P. J., et al., Acoustic and electroacoustic spectroscopy. *Colloids Surf A Physicochem Eng Asp* 2000;**173**:127-58.

8. Dukhin, A. S., New developments in acoustic and electroacoustic spectroscopy for characterising concentrated dispersions. *Colloids Surf A Physicochem Eng Asp* 2001;**192**:267-306.

9. Verdier, F., Burnett, R., et al., Aluminium assay and evaluation of the local reaction at several time points after intramuscular administration of aluminium containing vaccines in the Cynomolgus monkey. *Vaccine* 2005;**23**:1359-67.

10. Yang, Y-W., Wei, A-C., et al., The immunogenicity-enhancing effect of emulsion vaccine adjuvants is independent of the dispersion type and antigen release rate

– a visit of the role of hydrophile-lipophile balance (HBL) value. *Vaccine* 2005;**23**:2665-75.

11. Lei, Q. P., Shannon, R.K., et al., Quantification of free polysaccharide in meningococcal polysaccharide-diphtheria toxoid conjugate vaccines, In *Physico-Chemical procedures for the characterization of vaccines*, Brown, F., Corbel, M., et al., Editors. 2000, Karger. Basel. pp. 259-64.

12. von Hunolstein, C., Parisi, L., et al. Simple and rapid technique for monitoring the quality of meningococcal polysaccharides by high performance size-exclusion chromatography. *J Biochem Biophys Methods* 2003;**56**:291-6.

13. Marciani DJ., Vaccine adjuvants: role and mechanisms of action in vaccine immunogenicity. *Drug Discov Today* 2003;**8**:934-43.

14. Medzhitov, R., Janeway, C., Innate immunity. *NEJM* 2000;**343**:338-344.

15. Rinella, J. V. Jnr., White J. L., et. al., Effect of anions on model aluminium-containing adjuvant vaccines. *J Colloids Interf Sci* 1995;**172**:121.

16. Ho, M. M., Mawas, F., et al., Physico-chemical and immunological examination of the thermal stability of tetanus toxoid conjugate vaccines. *Vaccine* 2002;**20**:3509-22.

17. Eberendu, A. R., Booth, C., Luta, G., et al., Quantitative determination of saccharides in dietary glyconutritional products by anion-exchange liquid chromatography with integrated pulsed amperometric detection. *J AOAC* Int 2005;**88**:998-1007.

18. Aghazadeh-Habashi, A., Carran, J., Anastassiades, T., et al., High performance liquid chromatographic determination of N-butyryl glucosamine in rat plasma. *J Chromatogr B Analyt Technol Biomed Life Sci* 2005;**819**:91-6.